AD/A-002 310

DEVELOPMENT OF STATISTICAL FATIGUE FAILURE CHARACTERISTICS OF 0.125-INCH 2024-T3 ALUMINUM UNDER SIMULATED FLIGHT-BY-FLIGHT LOADING

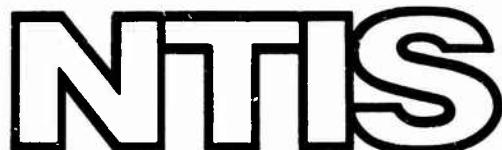J. P. Butler, et al

Boeing Commercial Airplane Company

Prepared for:

Air Force Materials Laboratory

July 1974

REPORT DOCUMENTATION PAGE		READ INSTRUCTIONS BEFORE COMPLETING FORM
1. REPORT NUMBER AFML-TR-74-124	2. GOVT ACCESSION NO.	3. RECIPIENT'S CATALOG NUMBER AD/A-002310
4. TITLE *(and Subtitle)* DEVELOPMENT OF STATISTICAL FATIGUE FAILURE CHARACTERISTICS OF 0.125-INCH 2024-T3 ALUMINUM UNDER SIMULATED FLIGHT-BY-FLIGHT LOADING		5. TYPE OF REPORT & PERIOD COVERED Final Report August 1972-March 1974
		6. PERFORMING ORG. REPORT NUMBER
7. AUTHOR(s) J. P. Butler, D. A. Rees		8. CONTRACT OR GRANT NUMBER(s) F33615-72-C-2003
9. PERFORMING ORGANIZATION NAME AND ADDRESS Boeing Commercial Airplane Company P.O. Box 3707 Seattle, Washington 98124		10. PROGRAM ELEMENT, PROJECT, TASK AREA & WORK UNIT NUMBERS Proj. 7351 Metallic Materials Task 735106 Behavior of Metals
11. CONTROLLING OFFICE NAME AND ADDRESS Air Force Materials Laboratory (AFML/LLN) Air Force Systems Command Wright-Patterson Air Force Base, Ohio 45433		12. REPORT DATE July 1974
		13. NUMBER OF PAGES
14. MONITORING AGENCY NAME & ADDRESS*(if different from Controlling Office)*		15. SECURITY CLASS. *(of this report)* Unclassified
		15a. DECLASSIFICATION/DOWNGRADING SCHEDULE

16. DISTRIBUTION STATEMENT *(of this Report)*

Approved for public release; distribution unlimited.

17. DISTRIBUTION STATEMENT *(of the abstract entered in Block 20, if different from Report)*

19. KEY WORDS *(Continue on reverse side if necessary and identify by block number)*

Reliability	Shape parameter (distribution)	Spectrum testing
Fatigue scatter	Scale parameter (distribution)	Flight-by-flight fatigue test
Mean life	Maximum likelihood estimate	Weibull distribution
Characteristic life	Fatigue variability	Log-Normal distribution

20. ABSTRACT *(Continue on reverse side if necessary and identify by block number)*

Thirty-two unique multidetail specimens were tested to develop a data base for investigating the statistical materials/structures fatigue failure characteristics of 2024-T3 aluminum alloy in the form of 0.225-in.-thick sheet. Twelve of these specimens were 36 by 120 inches in size and contained a central, 10-row, 11-column matrix of 110 open holes at a regular spacing providing a similar and independent local stress-field exposure at each detail. The remaining 20 specimens were 10 by 65 inches in size and contained a central, 10-row, 2-column matrix of 20 details which were open holes, filled holes, or one of two levels of load transfer at fasteners, with the load transfer accomplished by double shear through local

DD FORM
1 JAN 73 **1473** EDITION OF 1 NOV 65 IS OBSOLETE

doubler straps with a fastener in each end of the straps. A limited sampling of three heats of material was included in the program. Also a 95% relative humidity (RH) ambient environment was applied to two of the open-hole, 20-detail specimens. The test loading was a random-load, flight-by-flight loading block spectrum repeated to obtain crack initiation. Six different basic spectra, representative of cargo/transport or gust load flights, were applied to the specimens. Two of the gust load and two of the maneuver load spectra contained five flights of 30 load cycles, while one each of the gust and maneuver load spectra contained 10 flights of 15 load cycles. Columnar buckling restraint against compressive loading was provided for both sizes of specimen by welded fixtures which sandwiched the specimen. Lubrication was applied to the bearing support surfaces. Fatigue crack initiation was detected and controlled to a nominal crack length of about 0.04 in. from the edge of the hole by a painted crack detection circuit system. After detection of crack initiation, each hole was restored to an undamaged state by oversizing and coldworking. A statistical analysis of the data by previously developed maximum likelihood methods is presented for both scale and shape parameters of the log-normal and two-parameter Weibull distributions. The variability of the fatigue data, as defined by the shape parameters, is somewhat less than that established in a previous review of fatigue scatter. Also the Weibull distribution generally predicts a conservative estimate of the early failure initiation times, with the degree of conservatism depending on selected reliability level.
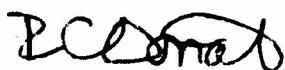
NOTICE
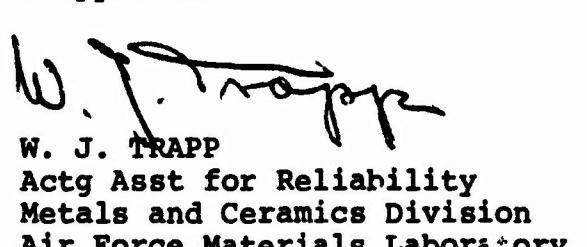
When Government drawings, specifications, or other data are used for any purpose other than in connection with a definite related Government procurement operation, the United States Government thereby incurs no responsibility nor any obligation whatsoever; and the fact that the Government may have formulated, furnished, or in any way supplied the said drawings, spcifications, or other data, is not to be regarded by implication or otherwise as in any manner licensing the holder or any any other person or corporation, or conveying any rights or permission to manufacture, use, or sell any patented invention that may in any way be related thereto.

This report has been reviewed and is approved.

R. C. DONAT
Project Engineer
Metals Behavior Branch
Metals and Ceramics Division
Air Force Materials Laboratory

W. J. TRAPP
Actg Asst for Reliability
Metals and Ceramics Division
Air Force Materials Laboratory

Copies of this report should not be returned unless return is required by security considerations, contractual obligations, or notice on a specific document.

FOREWORD

The research work reported herein was conducted at the Boeing Commercial Airplane Company, P.O. Box 3707, Seattle, Washington, for the Metals and Ceramics Division, Air Force Materials Laboratory, Air Force Systems Command, Wright-Patterson Air Force Base, Ohio, under contract F33615-72-C-2003. The contract was initiated under project 7351, "Metallic Materials," task 735106, "Behavior of Metals," with Mr. R. C. Donat (AFML/ LLN) acting as project engineer.

The research program was performed by the Boeing Commercial Airplane Company, structures technology staff, stress research group, fail-safe and fatigue section with Mr. J. P. Butler acting as program manager and principal investigator. Work began 1 August 1972, and the experimental work was completed in December 1973. This technical report was submitted by the authors in March 1974.

The experimental work was done in the structural test laboratories of the Boeing Commercial Airplane Company by the Materials Laboratory Fatigue and Fracture Group under Mr. W. B. King, supervisor, and Mr. W. C. Larson, group lead engineer. Mr. D. A. Rees was the principal test engineer and directed the test work. Assisting Mr. Rees in the test work were Messrs. P. L. Malland and J. A. Gertis, while Mr. B. Taylor assisted in the initial design of the buckling restraint fixtures. Mr. C. D. Czajka was the principal instrumentation engineer and test machine operator. He was assisted by Messrs. D. P. Nordstrand and R. A. Sager during this phase of the work.

CONTENTS

ILLUSTRATIONS

ILLUSTRATIONS (Continued)

TABLES

TABLES (Concluded)

SECTION I

INTRODUCTION

The design of an effective and reliable or durable aircraft structural system is influenced by several considerations. Material selection is one of the initial and primary elements in this structural design process. In its structural form, a material must resist the effects of not only the envelope of maximum loads, but also the total cumulative exposure to the variable loads during the service life of the structure. Superimposed on these strength and fatigue requirements is the calendar time effect of environmental exposure, causing corrosion and/or embrittlement peculiar to the specific alloy system. However, the chief detriment to the structural integrity and reliability of an aircraft structural system is the unanticipated or premature initiation of fatigue damage, regardless of whether such damage originates from the local environmental physical effects, or from the localized, highly stressed areas at cutouts or holes, sectional changes, joints or joint fastener locations, in response to a mechanical loading environment. This early appearance of fatigue-crack initiation presents, at best, an added and often burdensome maintenance task to the operator. Furthermore, without the aid of fail-safe or damage-tolerant structural design, this early or unexpected fatigue damage initiation may reduce structural integrity and create structural safety problems leading to loss of the structure and aircraft.

Although inadvertent or extraneous transgressions in the many-faceted and often monumental task of structural design and fabrication do play a significant part in the actual fatigue performance of structures, it should be clearly evident that recognition of the potential variation or scatter in the fatigue performance of real materials and their structures can reduce or forestall the impact of early fatigue damage regardless of its origins. The application of reliability analysis technology to resolve the problems of fatigue variability is a logical step. An exploratory development of such an approach is reported in reference 1. That study pointed out the need for defining the variability in terms of some functional form, identifying the scatter in fatigue performance, as measured by time (i.e., cycles) to fatigue crack initiation, in an analytical distributional form. This approach is particularly important and even necessary if the first and next few likely cases of crack initiation are the focal point for measuring the fatigue performance of a group of parts or a fleet of aircraft.

Ordinarily, the evaluation of fatigue performance relies on identifying the median or average behavior and applying a scatter factor to obtain a likely or "predictable" operational life without significant and/or damaging fatigue crack initiation in a detail. Alternately, the arbitrary least of scatter in a test group or a probabilistic level of fatigue performance, defined by an assumed distribution, may be used. However, these approaches do not identify the likelihood of the first or early initiation within a fleet as specifically investigated in reference 1. In practice, the collection of a sufficient quantity of fatigue performance data to identify the distributional form of the scatter has been considered an economically and calendar timewise impossible task during the vital design and initial, definitive production stage of an aircraft. Thus, the assessment of the statistical fatigue failure characteristics of material/structures in distributional form potentially has serious limitations. Practical considerations force limited testing that can only guide identification of the central tendency or scale parameter of a distribution. Controlling the impact of the

1

first or early failure in a fleet of aircraft, or the equivalent large group of identical details under the same loading environment, requires testing quantities to at least the extent which includes the desired level of probabilistic performance. Of course, testing to this extent also provides a capability for selecting the specific distributional function and its shape parameter for identifying extremal behavior in fatigue.

Two candidate distributions more widely used in the description of fatigue variability are the log-normal and the two-parameter Weibull distributions. While the behavior of both of these distributions is similar for levels of fatigue performance exceeded by 95% or less of the population, the extremal behavior of the two distributions is significantly different. The Weibull distribution appears to recognize extremal behavior and central characteristics more representatively than the log-normal (ref. 1). In a feasibility study reported in reference 2, the application of a unique, multidetail fatigue test specimen was explored for aid in the selection of a basic distribution representative of extremal fatigue scatter. By using a simple hole in a sheet as a structural element, and a large sheet with an array of such holes, each structurally independent by virtue of placement, a single test specimen provides a simulation of a fleet or group of parts. The transposition of the simple open-hole detail to real and complex configurations of monolithic and built-up configurations rarely relies on accepting that the local stress environment is the prime initiator of fatigue damage, and that local stresses can be related through stress analysis procedures. In summary, this multidetail specimen has a potential for providing guidance in distribution selection for a reliability analysis approach to fatigue performance assurance. In a single test, sufficient extremal and central data are gained to relate both regions of a distribution function.

Accordingly, the objective of this research is the development of a 2024-T3 aluminum alloy data base to guide the selection or identification of a distribution function that satisfactorily represents fatigue variability. The fatigue performance will be checked in a flight-by-flight loading environment in contrast to the constant amplitude testing accomplished in the feasibility study (ref. 2). Additionally, some specimens having other structural details, such as the fastener-filled hole and load transfer, are tested to explore in depth the nature of fatigue variability.

2

SECTION II

TEST PROGRAM

Because of the phenomenalistic nature of fatigue performance and its variability, the selection of the more appropriate distribution function in a reliability analysis scheme must rely upon both central and extremal characteristics of a sufficiently large data base to make that decision with any degree of certainty. Taking advantage of the background experience reported in the feasibility study (ref. 2), this developmental test program initiated plans for a data base that will obtain initial sequential data or order-statistical data for a number of sets of structural details, represented by the stress field of an open-hole or fastener-containing structure, under a controlled fatigue loading environment. The loading environment included six arbitrary flight-by-flight loading spectra for application to the two differently sized specimens to add further realism to the loading as compared to constant amplitude testing.

A total of 12 large and 20 small specimens of 0.125-in. bare 2024-T3 aluminum alloy sheet make up the test plan. The smaller specimens include six open-hole specimens, two fastener-filled specimens and two each of two different levels of load transfer. A limited amount of strain gaging was planned to detect any obvious irregularities in the stress distribution in the basic types of specimens. Details of the program are summarized in tables 1 and 2 while the test specimens are illustrated in figures 1 and 2 and are described subsequently in more detail. Three heats of material were used to fabricate the specimens. Chemistry and mechanical properties of the specific test material are given in table 3.

The definition of fatigue crack initiation on these multidetail specimens is controlled by a Boeing-developed crack-monitoring system that uses a conductive paint crack detection circuit. The circuit is carefully placed within 0.030 in. of the edge of the open hole or within 0.050 in. of the other details at the general area of the net section to intercept the crack tip. The local strain of the crack tip fractures the painted circuit and actuates a warning system and shutdown of the fatigue test machine. Both faces of the test specimen have the crack detection circuit installed for each column of holes to detect crack initiation at four locations on each hole (i.e., two faces and two sides of the detail). The specific location of a cracked detection circuit was accomplished with a continuity meter check followed by a local dye penetrant inspection and visual inspection. An overall view of the crack detection circuitry on a large panel is shown in figure 3 while figure 4 is a closeup view. Figure 5 illustrates the four types of usage simulation specimens while figure 6 provides a closeup of the crack detection circuit on an open-hole type of specimen.

With detection of a crack on an open-hole specimen, the hole is oversized to 0.375-in. diameter and coldworked to assure inactivation of that hole as a future crack site. The spacing of the open holes is sufficient to avoid significant stress field interference with adjacent holes after the oversizing treatment. In the large 110-detail specimens, testing was continued to initiate cracks in at least 10% to 20% of the total exposed holes. Actually, two of these specimens were carried to 61 and 56 failures, while in the remainder 16 to 24 cracked holes were developed.

3

Meeting the requirement for flight-by-flight testing in this program is keyed to the capability to stabilize the large flat sheets of either size of specimen for compressive loads such as may be encountered in the ground-air-ground transition of wing lower surfaces. For economic reasons, a simple, rigid, welded frame of structural steel accomplishes the stabilizing action. For the large panels, a 0.19- by 4- by 12-in. rectangular tube is the basic frame of the fixture. A local reinforcement, a 0.19- by 3- by 10-in. rectangular tube, is added to the central test area to increase torsional rigidity of the large frame. The smaller specimen fixture has a frame of 0.375- by 6- by 4-in. rectangular tubing. For both fixtures the columnar supports are 0.5- by 2-in. bars welded to the frame and intermediate supports. A stabilizing stress relief was given to the welded assembly before machining to a plane through the stabilizing-bar contact surface. A teflon coating is baked on each stabilizing support bar to reduce friction. This coating was refurbished during the test by an onsite spray coat of a teflon solution. The fixture, in two parts, clamps the specimen between the two halves. Shimming provides optimally a net to about 0.001-in. clearance for the test specimen, but actual local fit-up is dependent on basic specimen thickness variation. Particular care is taken in the fit-up process to assure that load transfer from the specimen by friction at the fixture contact surfaces is negligible. The fixture is fixed in the test machine at the static head (i.e., upper head) and has sufficient overall clearance to avoid bottoming out at the dynamic head under compressive loadings nominally expected. Figures 7 through 13 show the test fixtures and general machine setup. A closeup of the large structural simulation specimen is given in figure 14. Figure 15 provides an overall view of the test setup for a large panel and the tool used to pull the coldworking mandrel through the oversized hole.

A check of the influence of humidity on crack initiation is also part of the test program. Two open-hole types of the usage simulation specimen configuration (fig. 2a) are tested. A plexiglass environmental chamber, enclosing both the specimen and stabilizing fixture, is used to contain a 95% relative humidity (RH). That level of RH is obtained by passing throttled plant air through a series of two plastic jars (of 6.5- and 2.0-gal capacity) filled with tap water and into the environmental chamber enclosure. By introducing this air into three locations on each side of the specimen within the chamber, the desired physical environment was obtained. Incidentally, only the open-hole specimens were tested under this moist atmosphere since the other specimens by nature of their design did not allow ready exposure of the specimen stress concentration area to the ambient environment. Figure 16 is an overall view of the environmental control setup and test machine.

The flight-by-flight loading spectra are of two types. One reflects a cargo/transport or gust load experience. The other spectrum simulates a fighter or maneuver load experience. In brief, these loadings were generated by assuming a typical flight load profile, selecting the pertinent loading exceedance data from the literature, using a nominal load stress response for the structure, choosing an arbitrary S/N curve representative of typical structures, and applying the Palmgren-Miner cumulative damage rule to condense the expected loadings to the simplified test loads. Two of the three loading spectra of each type of loading have five flights with 30 flight load cycles and three ground load cycles per flight. These spectra differ only in load level. The third spectrum type (i.e., spectra A-2 or B-2) utilizes the same loading content of the five-flight, more severe loading (i.e., spectra A-1 or B-1), but introduces ground loading cycles at each flight midpoint to develop a ten-flight spectrum of identical total load content except for the added ground load cycles. The gust load spectrum

4

contains seven levels of cyclic flight loads while the maneuver load spectrum contains four levels. Tables 4 through 21 present the stress levels and test loads for the program. Figures 17 through 19 graphically compare and summarize the loading content of the two types of spectra. Actual test loading sequence was generated by simply selecting five sequences of the basic 30-cycle flight through use of a random number table. The final result, a five- or ten-flight random loading block, was repeated as necessary to initiate cracks. Figures 20 through 25 show the gust and maneuver spectra.

The test loads were applied by an Electro Mechanical Research (EMR) Programmed Fatigue Testing Machine. This machine has a 150,000-lb maximum capacity at a frequency of 0.5 to 20 Hz. Testing in this program was nominally performed at 5 Hz. The machine can accommodate specimens up to 180-in. overall length. The machine operates on the hydraulic servovalve closed-loop principle. Random loading is accomplished by use of a seven-track digital magnetic tape programmer. The constant amplitude and programmed loads approximate a square wave at low frequencies and a reversed exponential wave at high frequencies by nature of the system. Programmed loads for this machine must be introduced at the nearest 300-lb equivalent of the selected stress. Overload stops on the machine were set to provide about 0.010-in. clearance at the maximum load of each type of spectra. Tensile loads were applied and zeroed three times while compression loads were applied and zeroed twice.

SECTION III

TEST SPECIMENS

The test specimen design of this program is a development of a feasibility study summarized in reference 2. The large open-hole structural simulation specimen, as described in figure 1, has an overall width dimension of 36 in. and a length of 120 in. These dimensions were primarily selected to be compatible with available standard sheet widths of other structural alloy systems, like titanium and steel. This configuration provides a 110-detail test section that has an increased relative distance between the rigid grip of the test machine and the array of open holes, as compared to those of reference 2.

A further extension to the multidetail specimen concept is the introduction of other types of structural details. Fatigue performance of filled-hole and load-transfer structural details are developed to broaden the data base for ultimate reference in identifying the more likely distribution function reflecting fatigue damage initiation variability. The added complexity of these additional types of structural details forces the size of the specimens to a 20-detail configuration. Figure 2 describes these smaller specimens in detail. The load transfer is introduced by adding doubler straps on both sides of the basic specimen and fastening with a single fastener in each end. Varying the distance between end fasteners tends to increase the load transfer by the strap while yet providing a specimen with symmetry (i.e., double shear). Because of the nature of these more complex specimens as identified in figures 2b, 2c, and 2d, it is evident that detail crack sizes at detection are sufficiently long to cause interactions with the adjacent details. Hence, a single failure per specimen is the estimated limit of these particular structural details, and a multiplicity of test specimens are necessary to provide statistically useful extremal data. All of the specimens had their bonded end doublers grit-blasted to improve friction between the test specimen and the test machine grips. Load transfer at the grips is obtained by high clamp-up of the grip bolts which pass through clearance holes in the specimens.

All holes had tool exit burrs removed by use of 600-grit abrasive paper backed by a flat steel block and longitudinal action parallel to the columns of holes. Burr removal has been found necessary to assure deposition of the crack detection circuit at the desired 0.030-in. distance from hole edge in the open-hole specimens. Normal fabrication practice for individual parts would deburr holes by chamfering. In assemblies of aluminum alloy skin-stiffener structure, tooling, hole-drilling practice, and subsequent clamp-up by the fasteners seems to reduce the influence of burrs as found in these specimens. The hole-installation procedure is accomplished on a numerically controlled drilling machine with four panels stack drilled and reamed at one time.

Strain gages are installed at a 4-in. distance from upper and first row fasteners and at midsection of the specimen to explore buckling restraint fixture installation effects on load distribution within typical specimen types. The gages were installed on both open-hole type of configurations (figs. 1 and 2a) and the two load transfer specimens (figs. 2c and 2d). A typical filled-hole specimen was not instrumented because of its close similarity to the open-hole specimen. For instance, the hole filling qualities would be most effective under the compressive loads, but these at best are a fraction of the tensile loads. Under tensile

7

Preceding page blank

loads, the lateral hole-propping effect of the close tolerance fasteners, as in figure 2b, does not override the hole discontinuity; hence, no strain measurements were made on this specimen. The strain gages themselves are a 0.25-in. grid (micromeasurements type WA13-250-BA-350). A typical strain gage installation may be noted in figures 3 and 4.

SECTION IV

TEST RESULTS

Static strain measurements taken on all the representative specimens are summarized in tables 22 through 29. Graphic presentations of these results are shown in figures 26 and 27 for the large panel (fig. 1). Data with and without the buckling restraint fixture in place are se$_t$ arately shown. Figures 43 through 47 present the measured strain for the smaller figure 2 specimens having the open-hole and the two-load transfer types of configurations.

A summary of the fatigue test results for the figure 1 type of specimens is shown in table 30. Each of the four specimens has the material heat, the ambient physical environment (e.g., laboratory air), the test spectrum, the crack initiation sequence, location and size information, plus both the total load points and equivalent cycles to crack detection. Hole position is identified by column and row designations given in figure 28. The cyclic load data is counted by the test machine in terms of load points representing the successive maximum and minimum of any one cycle. Thus, cycles are derived by merely dividing load points by a factor of two for the A-1, A-3, B-1, and B-3 spectra. The ten-flight A-2 and B-2 spectra had zero load level introduced between the transition from the last flight-load point and the following maximum ground-load level. Hence, the equivalence between load points and load cycles in these two spectra is a factor slightly greater than two (i.e., 370 load points represents each ten-flight spectrum of 180 load cycles). Sketches illustrating the dispersion of the initiated crack locations in these twelve large panels are presented as figures 29 through 40. As a matter of reference, similar charts are presented as figures 41 and 42 for the two multidetail panels reported in reference 2. Tables 31, 32, and 33 duplicate the pertinent test data of the two test panels and the single-hole specimens of reference 2.

A summary of the fatigue test results for the twenty figure 2 types of specimens is presented in table 34. Strain measurements are plotted in figures 43 through 50. Identification of the crack locations is given in figure 51. In figures 52 through 60, sketches of crack locations, detected after disassembly, are shown for the fastener containing types of figure 2 specimens. Photographs of fluorescent penetrant inspection results on a typical figure 2 specimen (2A11) are included as part of figure 55.

In figures 61 through 84, probability plots are shown for both the log-normal and two-parameter Weibull distributions. Plotting positions (ref. 3) for each initiated crack were simply determined by the ratio of n/(N+1), where n is the order of detection of each detected crack, and N is the total number of test details in each specimen. The solid straight line in these curves is located by the maximum likelihood estimate (MLE) technique reported in reference 1. A comparison is also shown of the fixed-shape-parameter fit of the data. Similar data is presented for the two constant amplitude tested panels (ref. 2), but with the additional results of the comparable single-hole specimens of that program.

A comparison is made in table 35 of the MLE distribution parameters and the bounds of the shape parameters for the 12 large panels of this test program plus the two panels and single-hole specimens of the reference 2 feasibility study program. The parameter

calculations were made considering the data in terms of the face of origin of the initiated fatigue crack as well as the total failures. Failure face origin was established by the location and size of the crack. Where cracks penetrated through the specimen, the face having the longer crack, or having a crack at both sides of the hole on one face as well as a through crack on one side of the hole, was established as the origin face. Where no discernible difference in length on either face was noted for through cracks, the crack was arbitrarily identified as originating on the tool exit face. In tables 36 through 39, the calculated and test ordered statistical failure characteristics are shown for the first five failures on each figure 1 test panel, as well as the two panels and single-hole specimens of reference 2. The results consider a 0.50 reliability level for the selected number of specimens, a 0.50 reliability level with a 0.95 confidence, and a 0.90 and 0.95 reliability level with no confidence level. These ordered-failure results are presented for only the total number of failures (i.e., the number of holes detected with valid cracks).

SECTION V

DISCUSSION OF TEST RESULTS

While no static test properties were performed on the 2024-T3 aluminum alloy sheet material as part of this program, the mechanical property test data supplied by the vendors indicate the material did meet specification standards. Furthermore, there is an observable but not a really significant variation in the properties for each heat.

The behavior of the test specimens, as indicated by the measured static strain data plotted in figures 26, 27, and 43 through 47, seems to indicate satisfactory response in the presence of the buckling restraint fixture. The response appears linear over the range of strain measurements. Although there is some departure from the equivalence of the measured and applied strains, this difference is believed reasonable. For instance, the open-hole specimens indicate a slight dropping off of measured stress. This is more so for the figure 2a specimen than the figure 1 specimen. This could probably be attributed to the shunting of stress away from the column of holes due to the discontinuity of the hole. In the case of the slightly larger hole and closer spaced strain gage in the figure 2a specimen, this difference is a bit more pronounced. However, the actual magnitude of the difference is slight and approaches the ordinary limits of strain gage readability. The influence of structural detail is more obvious in the case of the load transfer straps, as observed in a comparison of figures 47, 48, and 50. The load transfer straps appear to draw panel load to their line of action as indicated by the higher measured strains, and compared to the expected equivalent strain of uniform loading. Furthermore, the longer straps appear to attract more load as may be inferred by examining figures 46 and 47. It appears that the buckling restraint fixtures do function to control the out-of-plane bending of the specimens of both sizes. Likewise, no in-plane bending is observable; however, the flexural rigidity of the specimens is likely to mask any such effect if at all present, because of the careful attention to specimen lateral alignment in the test grips. It also appears that friction between the specimen and test fixture is not significant, or at least not detectable by the strain measurements.

The observed performance of both test buckling restraint fixtures appeared quite promising under the dynamic loads and the flight-by-flight loading exposures. The test panels performed without any observable buckling between the supports. It is believed that the fixtures function satisfactorily and can provide responsive flight-by-flight testing.

The crack detection circuitry functioned satisfactorily. The fatigue cracks were detected at a consistent length, but apparently not quite to the precision found in the feasibility study reported in reference 2. However, the results are considered far more consistent than what has been observed in service results on actual structures, and they should provide a good data base for further development of reliability analysis technology. Looking at the summary of data found in table 30, there is no pronounced or obvious difference in crack initiation sites with respect to tool entry or exit face of the specimens of the figure 1 configuration. A review of the location of crack origins, as illustrated in figures

11

29 through 42, indicate a rather random dispersion of the crack locations, even in the case of specimen A3 in which 61 crack initiation sites were obtained.

Accordingly, the painted crack detection circuitry performed adequately on both sizes of specimens. However, under the 95% RH conditions, circuit performance for the figure 2A specimens was suspected sufficiently to replace the painted circuitry with crack wires. Even this change was found to be inadequate and detection had to resort to visual examination through the plexiglass environmental chamber, with the presence of the wire circuit being a detriment. Without a developmental program on this type of crack detection circuitry (i.e., either painted or wire), it appears that visual observation must be relied upon. Furthermore, the precision of visual detection under the environmental controls of humidity may not be adequate to obtain a satisfactory data base. It is thought that simpler tests could resolve the likely effects of humidity and fatigue crack initiation unless further developmental work is accomplished on the circuitry. In the case of 2024-T3 material, other programs described in the literature (i.e., crack propagation) indicate less or negligible effect of this humid environment as compared to the conventional 7000 series of aluminum alloys (particularly 7075 and 7178). Accordingly, in the current program it is suggested that reliance be made on visual detection of the bare specimens without the camouflaging effect of the primer and circuit. As can be observed from the test data in table 34, the RH tests did not produce any significant cyclic effect, except for specimen 2A4. This figure 2a configuration was found with a number of cracks not observed through the environmental chamber walls with the associated ambient environmental test conditions.

Examination of the crack initiation data for the structural simulation specimens (fig. 1), as presented in figures 61 through 88, seems to point out several interesting features. First, the test data in most of the cases exhibits a scatter, as indicated by the shape parameter, less than the values deduced in reference 1 (i.e., 0.14 for the log-normal and 4.00 for the Weibull distribution). The results for specimen A4 indicate a greater likely scatter. The extremal replication of data by both the log-normal and Weibull distributions is not precise in any of the cases.

One factor, particularly in the case of specimen A4, possibly dictating fatigue response may be alloy heat differences, although the figure 2a specimens (i.e., open hole) did not demonstrate any similar significant behavior. Of course, the latter specimens provide a single reference point in the 5% failure region, while the figure 1 specimens expand the sampling scale to less than 1%. Possibly the difficulties or limitations of sampling, and the coincident need for sampling to define fatigue behavior confidently in the extremal range, play a part in formulating these observations. Additional testing quantities should provide a better data base that can add more guidance to the selection of the distribution.

In an analytical examination of the data, compiled in tables 36 through 39, the comparison of the actual test data for one through five failures (i.e., initiated cracks) is made with that predicted from the data by a MLE-analysis and assumed fixed-shape parameters for the two distributions fitted to the test data. Obviously, the MLE-based data certainly seems to compare favorably with the test data over the range of considered failures

for an assessment based on the sample lot or "fleet" size of 110 details and a 0.50 reliability based on the estimated test mean or characteristic life. Reliability levels of 0.90 and 0.95 expectedly indicate more conservatism in scale estimates. Under the assumption of fixed-shape parameters, all levels of reliability provide more conservative estimates relative to the actual test data. Furthermore, the Weibull distribution exhibits an appreciably greater relative reduction in fatigue performance than the log-normal distribution.

Extending this analysis to include a 0.95 level of confidence at 0.50 reliability shows a similar response to the influence of reliability level. Examining all of the summarized data in tables 36 through 39 still indicates a somewhat acceptable comparison between test values, and the 0.50 reliability based on the 110-detail sample lot per specimen. However, the demand for increased reliabilities of 0.90 and 0.95 leads to further conservative differences between the test and estimated values. In all of these cases the Weibull distribution provides the more conservative estimate.

In table 35, a summary of the estimated scale and shape parameters is compiled for all tested specimens of the figure 1 configuration. Essentially similar observations on the central characteristic parameter (scale or location parameter) are observed as found in the analysis of the extremal data. With fixed-shape parameters the nominal Weibull characteristic life is greater than those of the log-normal distribution, as can be noted in comparing figures 61 through 84. In contrast, the MLE estimates of the nominal central value from the test data indicate a "relatively" close correlation in magnitude of the mean life and characteristic life for the two distributions. The Weibull distribution indicates slightly lower values in all but test specimen A3, where the reverse trend is found, although that specimen had 61 holes with crack origins. Accordingly, this infers a likely difference in prediction of the median life by the two distributions in all but this latter test case. Adding a requirement of a 0.95 level of confidence only reinforces the observation that the MLE estimates of the scale parameters (i.e., the mean or characteristic life) are very similar for both distributions and each panel.

As to the shape parameter, table 35 shows that distributions fit the data with nominal values (MLE), indicating less scatter than that proposed in reference 1 except in the case of specimen A4. This same observation is demonstrated in an examination of the plots in figures 61 through 84. Looking at the 2%/98% and 5%/95% bounds on the estimated shape factor, specimen A4 indicates both distributions provide estimates indicating sampling from a population that has the 0.14 or 4.00 shape parameter.

Specimens A2, A8, A12, and panel one (ref. 2) also indicate a relationship to these assumed values for the log-normal distribution alone. The shape parameter for all of the panels indicates less variability in scatter as suggested by $\alpha = 4.00$ or $\sigma = 0.14$. At the moment, however, this result is suggested to be a problem of limited sampling, and further examination of the data by advanced classes of distributions is recommended.

13
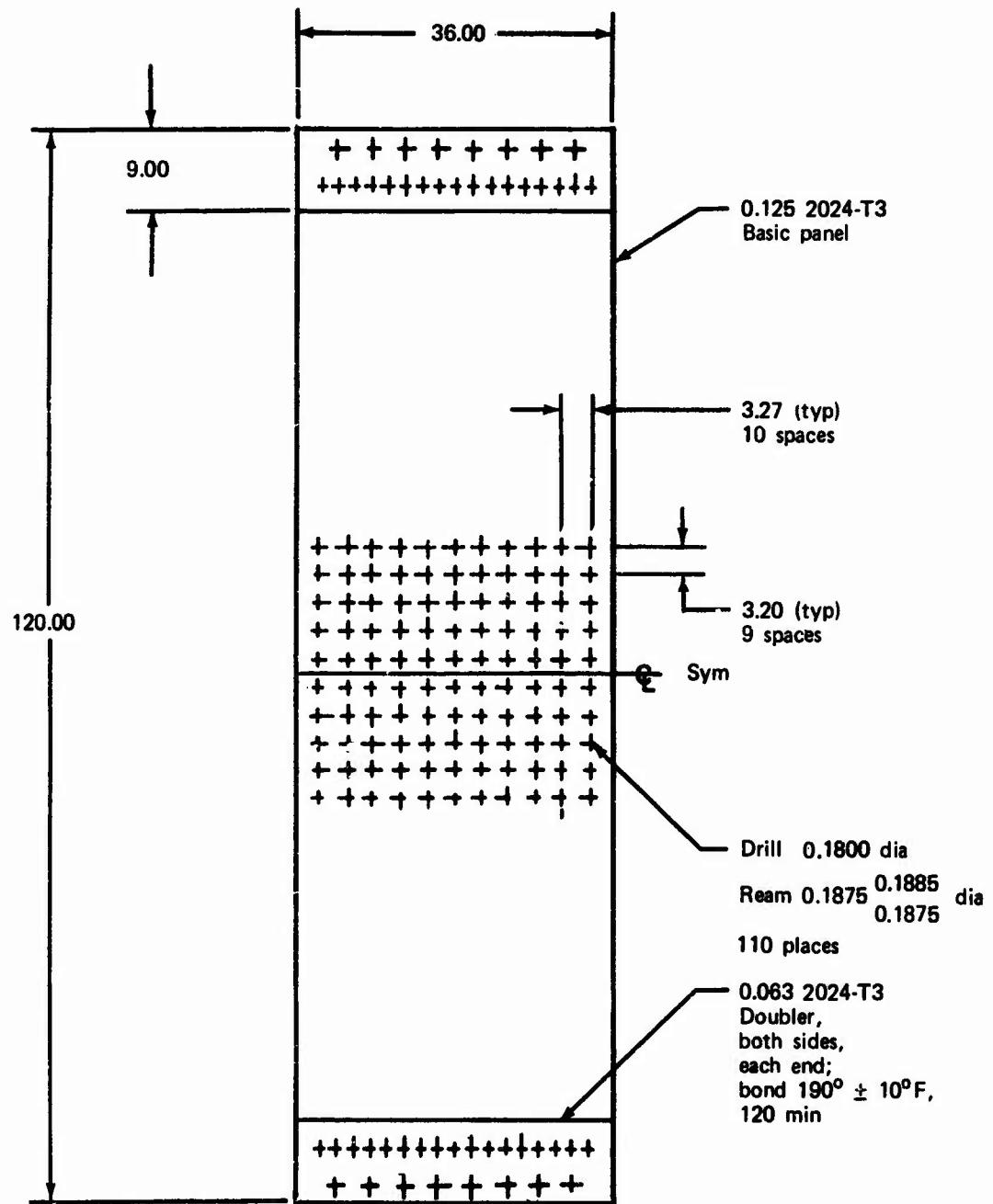
SECTION VI

CONCLUSIONS

In summary, several conclusions and recommendations can be developed from the testing of this program. These are essentially as follows:

a. The test program itself, utilizing the buckling restraint fixtures, can produce flight-by-flight fatigue crack initiation data for definition of material/structure statistical failure characteristics.

b. The open-hole specimen is the more effective costwise specimen in providing both extremal and central type of data. Testing was successfully accomplished on two specimens with 61 and 56 out of their 110 open-hole details.

c. The use of the Boeing previously developed painted crack detection circuit system is believed to be a simple and effective means to provide consistent fatigue crack initiation data from a multidetail specimen in a typical ambient laboratory environment. High humidity conditions (95% RH) are currently too severe for the functioning of the system.

d. The fatigue performance of the 110-detail structural simulation specimens and the 20-detail usage simulation specimens provide a fatigue statistical response comparable to actual structures.

e. Fatigue crack origin site as to tool entry or exit face does not appear to occur significantly on one face or the other in the specimens tested in this program.

f. The test results of this program have not demonstrated an obvious advantage for either the log-normal or Weibull distribution in simulation of the test. However, the Weibull distribution does demonstrate the expected more conservative representation of extremal data. This effect becomes more pronounced as higher levels of reliability are selected.

g. Fatigue crack initiation in the fastener-filled and load-transfer types of 20-detail test specimens was found to originate at fretting sites away from the net section area of the hole itself. This behavior simulates the behavior of joined operational structures.

It is recommended that further study of this data be accomplished, particularly in regard to the choice of an advanced class of distributions for replication of statistical behavior.

15   **Preceding page blank**

Dimensions in inches

Figure 1.—Structural Simulation Test Specimen Configuration

Preceding page blank
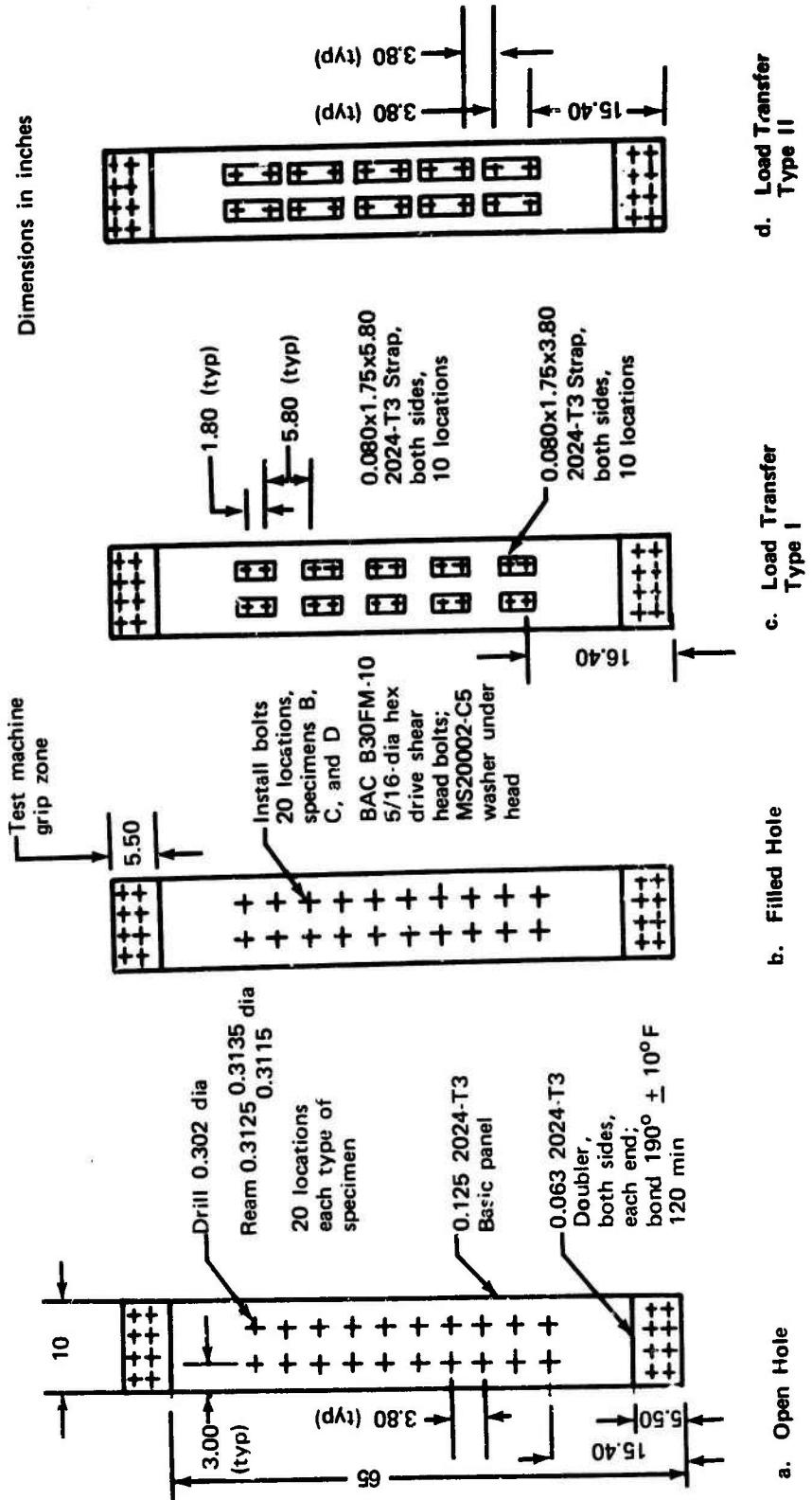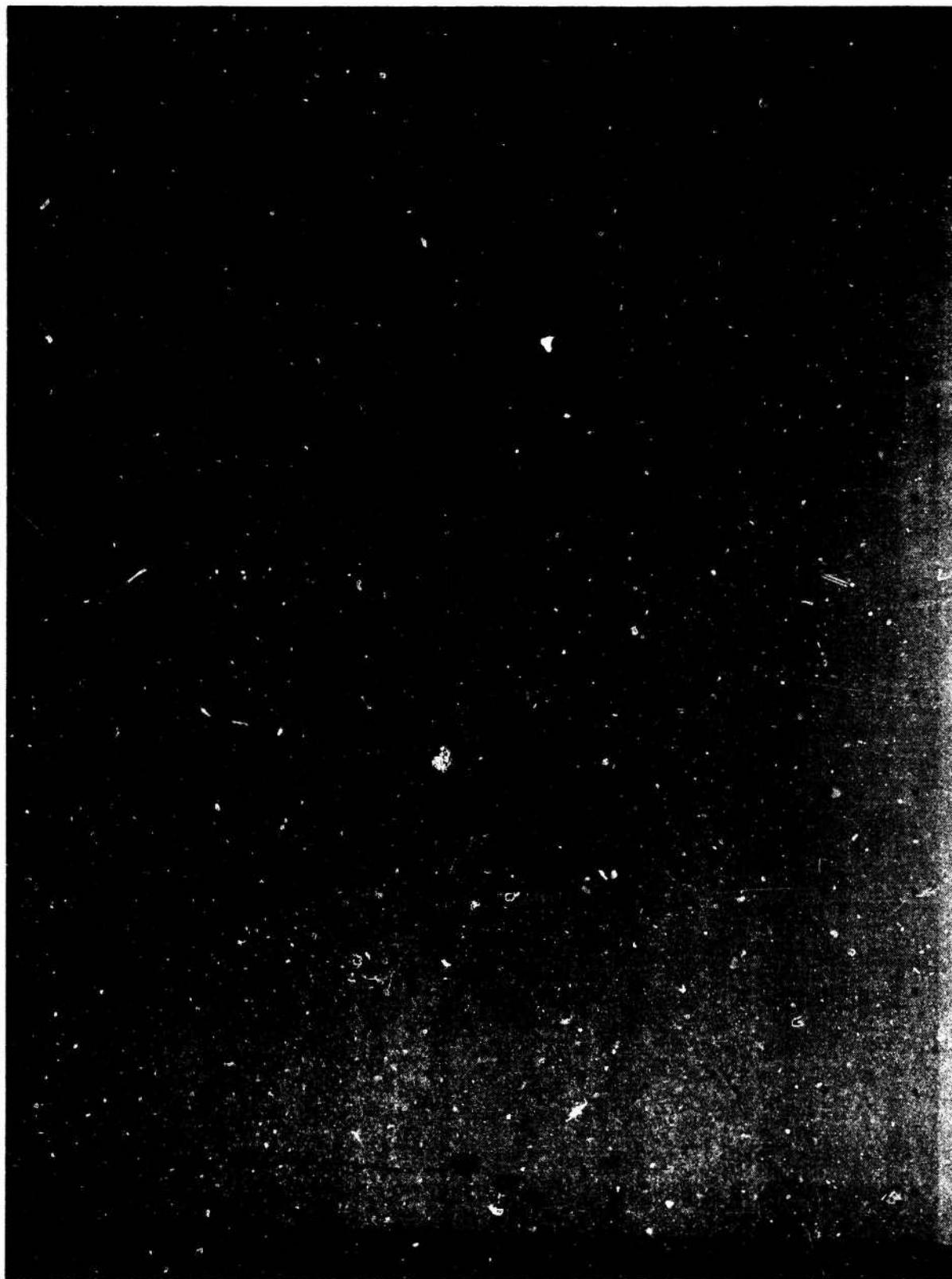
Figure 2.—*Usage Simulation Test Specimen Configurations*

Dimensions in inches

a. Open Hole

Drill 0.302 dia
Ream 0.3125 dia
0.3135
0.3115

20 locations each type of specimen

0.125 2024-T3 Basic panel

0.063 2024-T3 Doubler, both sides, each end; bond 190° ± 10°F 120 min

10

3.00 (typ)

3.80 (typ)

15.40

5.50

65

b. Filled Hole

Test machine grip zone

5.50

Install bolts 20 locations, specimens B, C, and D

BAC B30FM-10 5/16-dia hex drive shear head bolts; MS20002-C5 washer under head

c. Load Transfer Type I

1.80 (typ)

5.80 (typ)

0.080x1.75x5.80 2024-T3 Strap, both sides, 10 locations

0.080x1.75x3.80 2024-T3 Strap, both sides, 10 locations

16.40

d. Load Transfer Type II

3.80 (typ)

3.80 (typ)

15.40

18

Figure 3. View of Strain Gage and Crack Detection Circuit on Structural Simulation Test Specimen

19
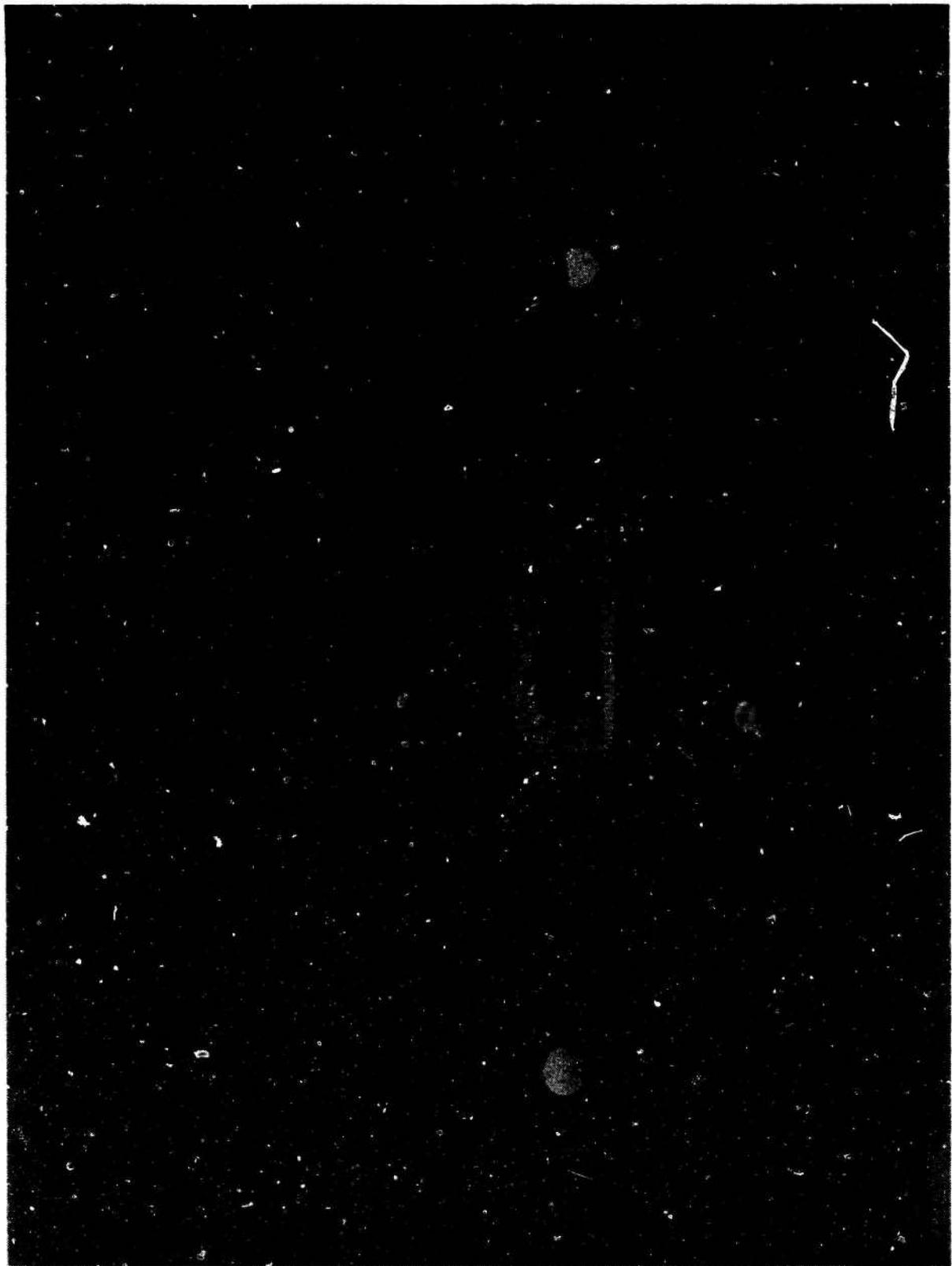
Figure 4.—Closeup of Strain Gage and Crack Detection Circuit on Structural Simulation Test Specimen
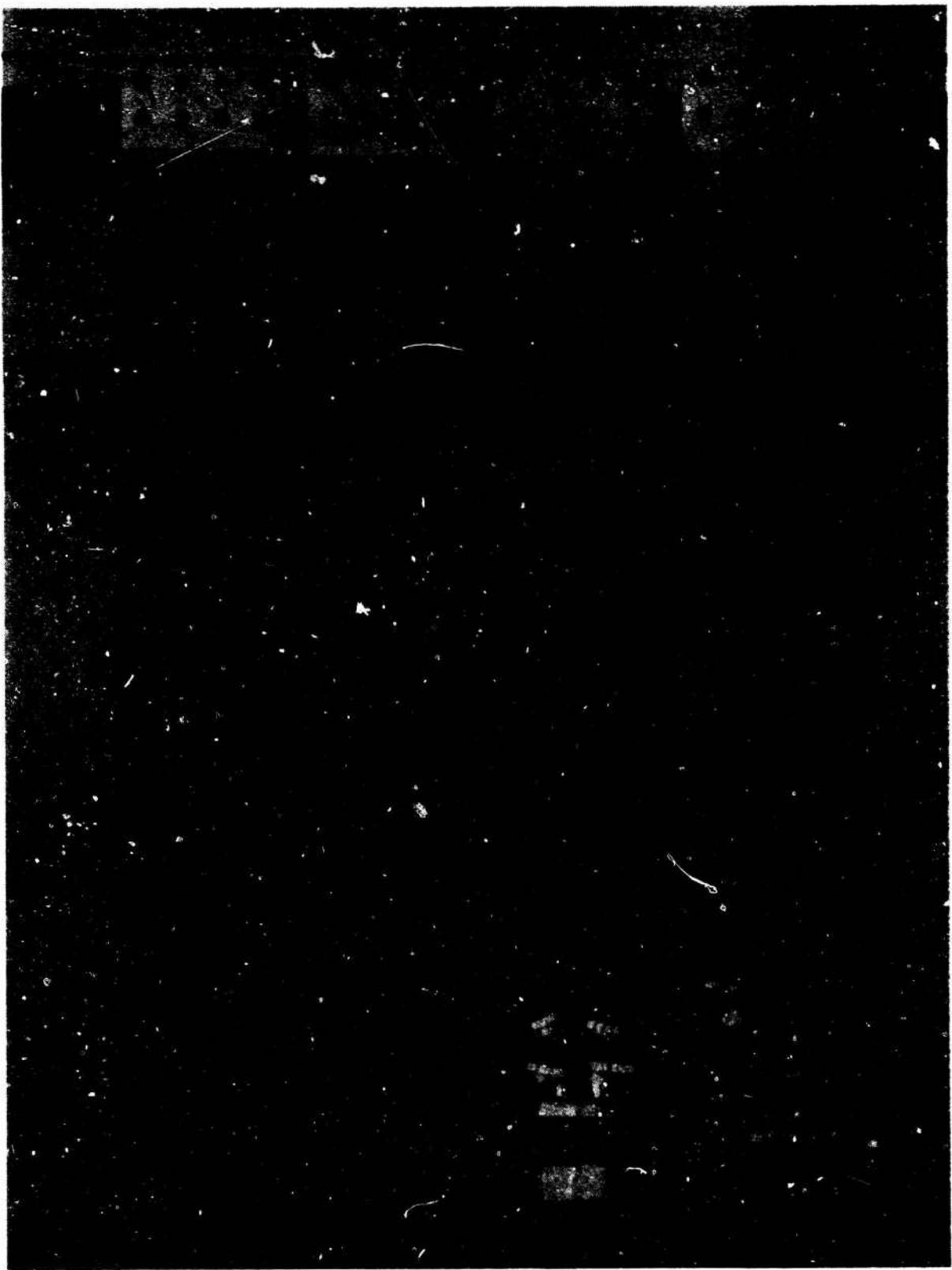
Figure 5.-- Typical Usage Simulation Test Specimens
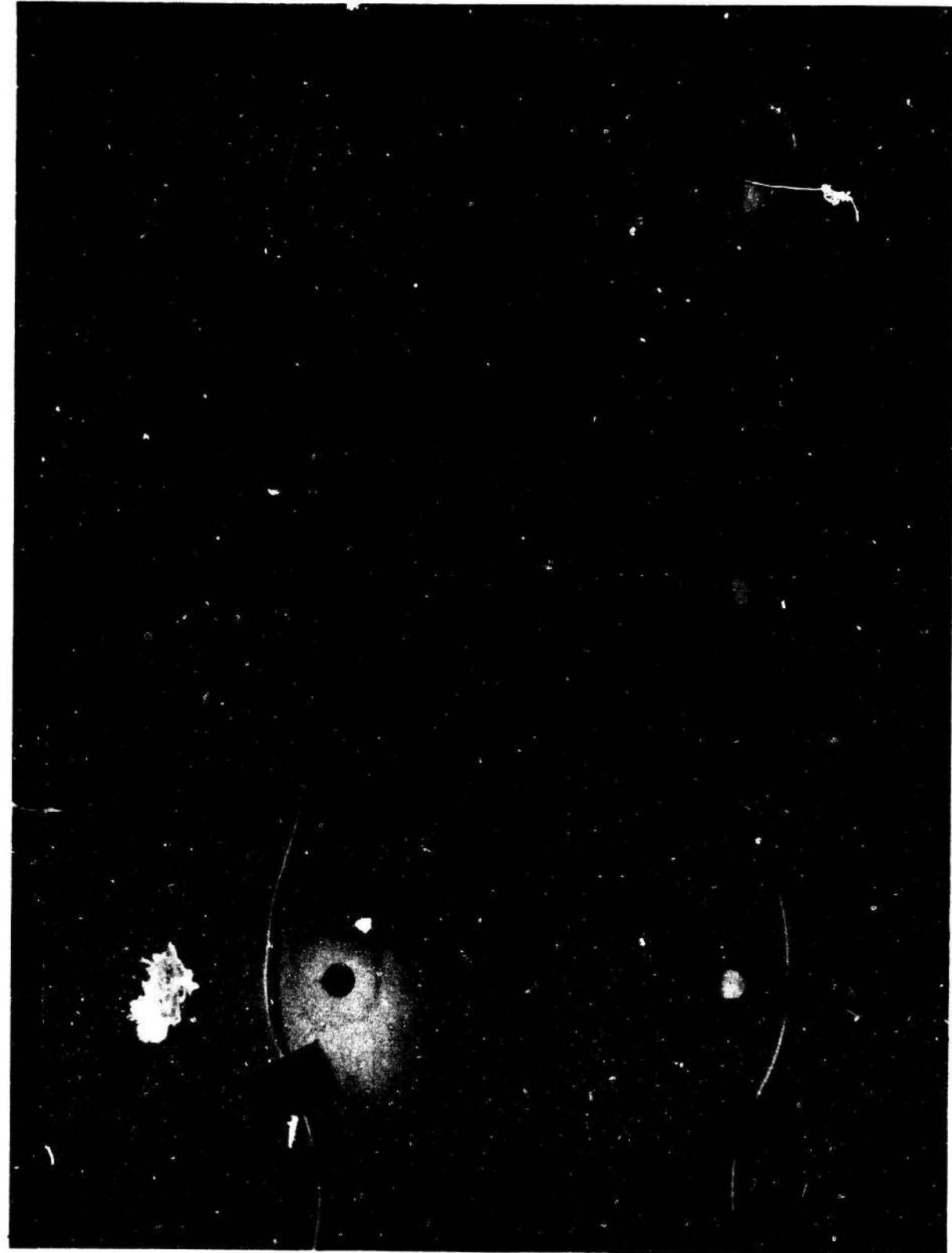
Figure 6. — Closeup of Painted Crack Detection Circuit on Open Hole Usage Simulation Specimen
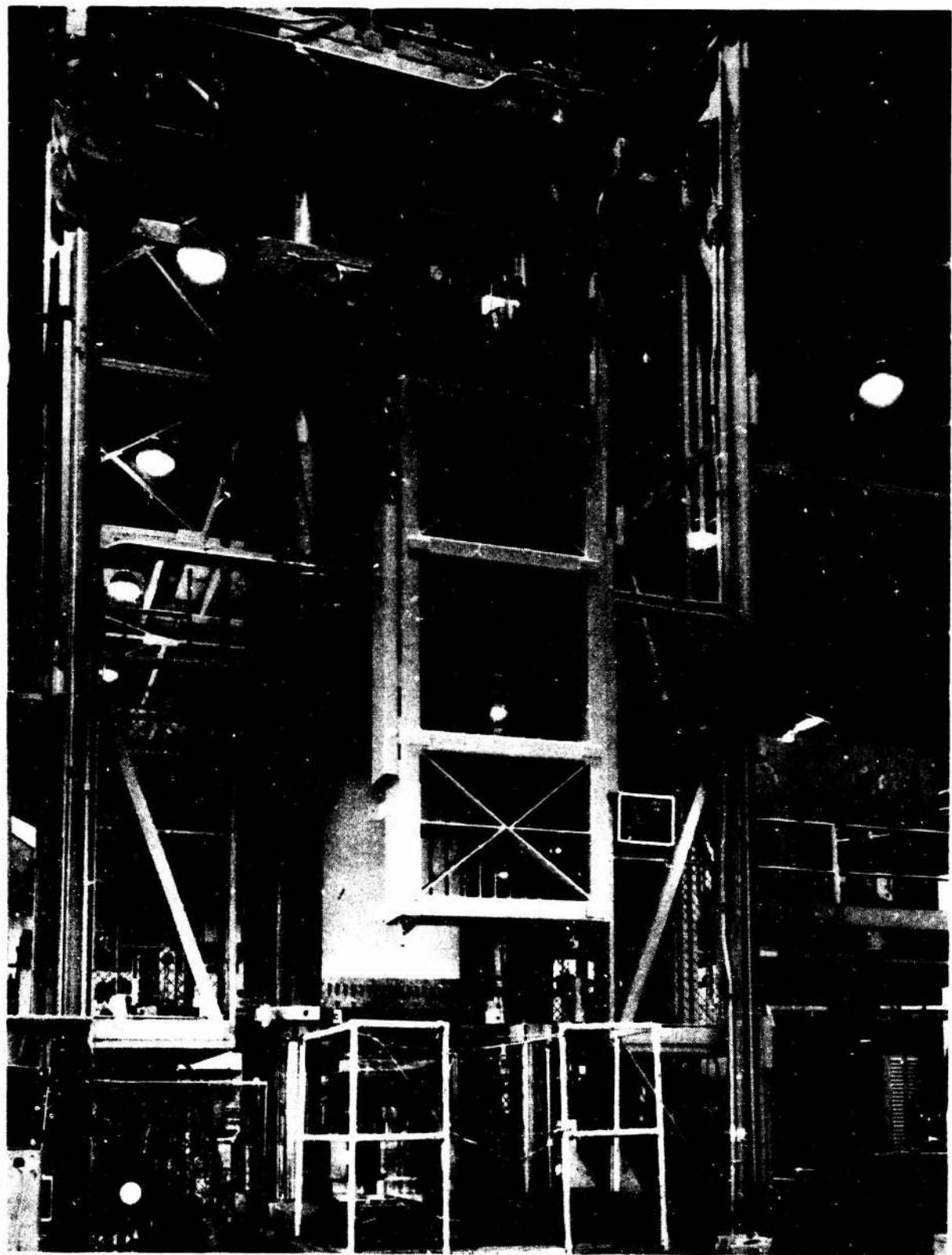
Figure 7.– Rear View of Buckling Restraint Fixture Ready for Positioning on Structural
Simulation Test Specimen

23

Figure 8. – *Bearing Face of Buckling Restraint Fixture for Structural Simulation Test Specimens*
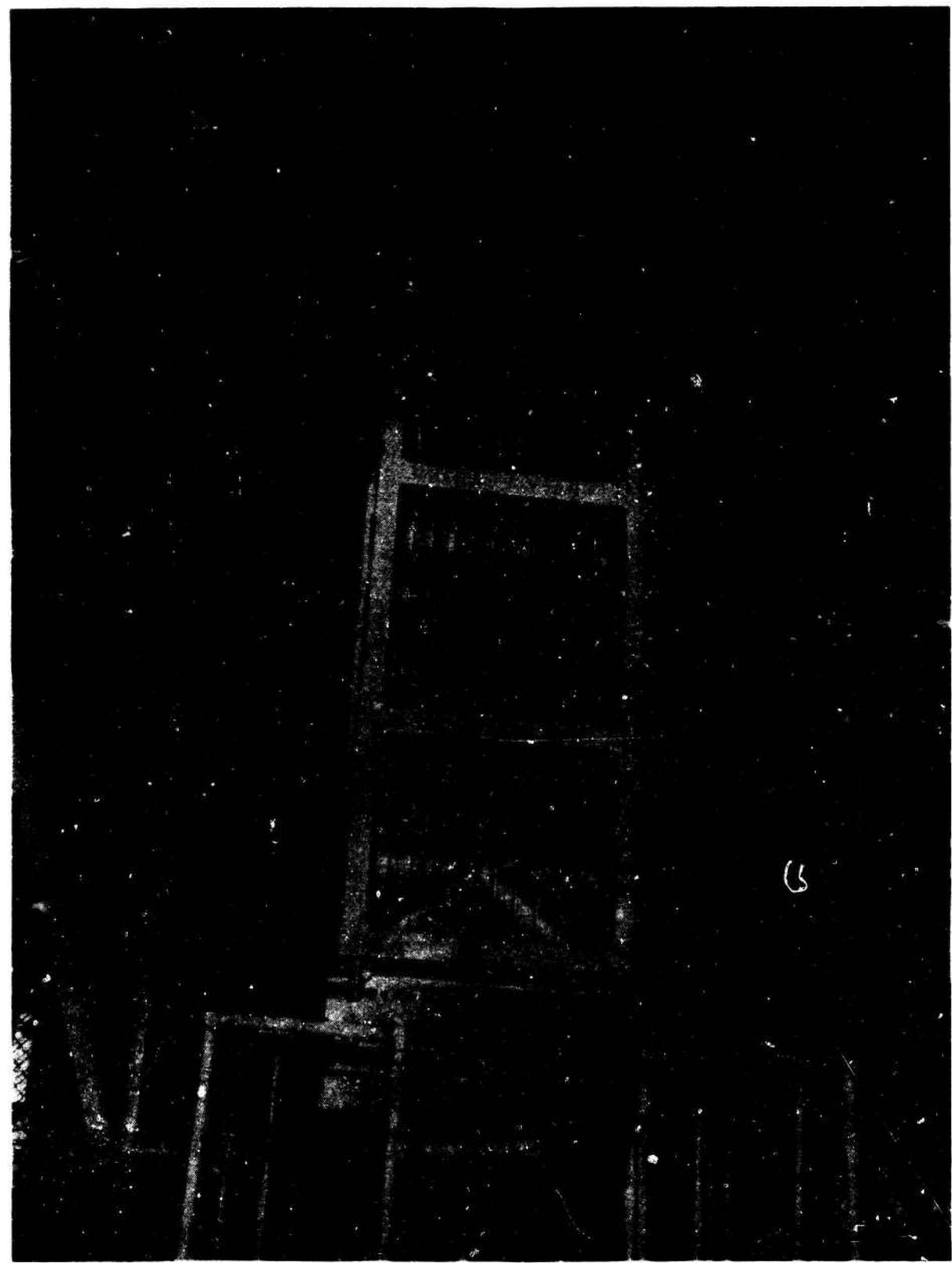
Figure 9. – Buckling Restraint Fixture Assembled on Structural Simulation Test Specimen in Fatigue Test Machine
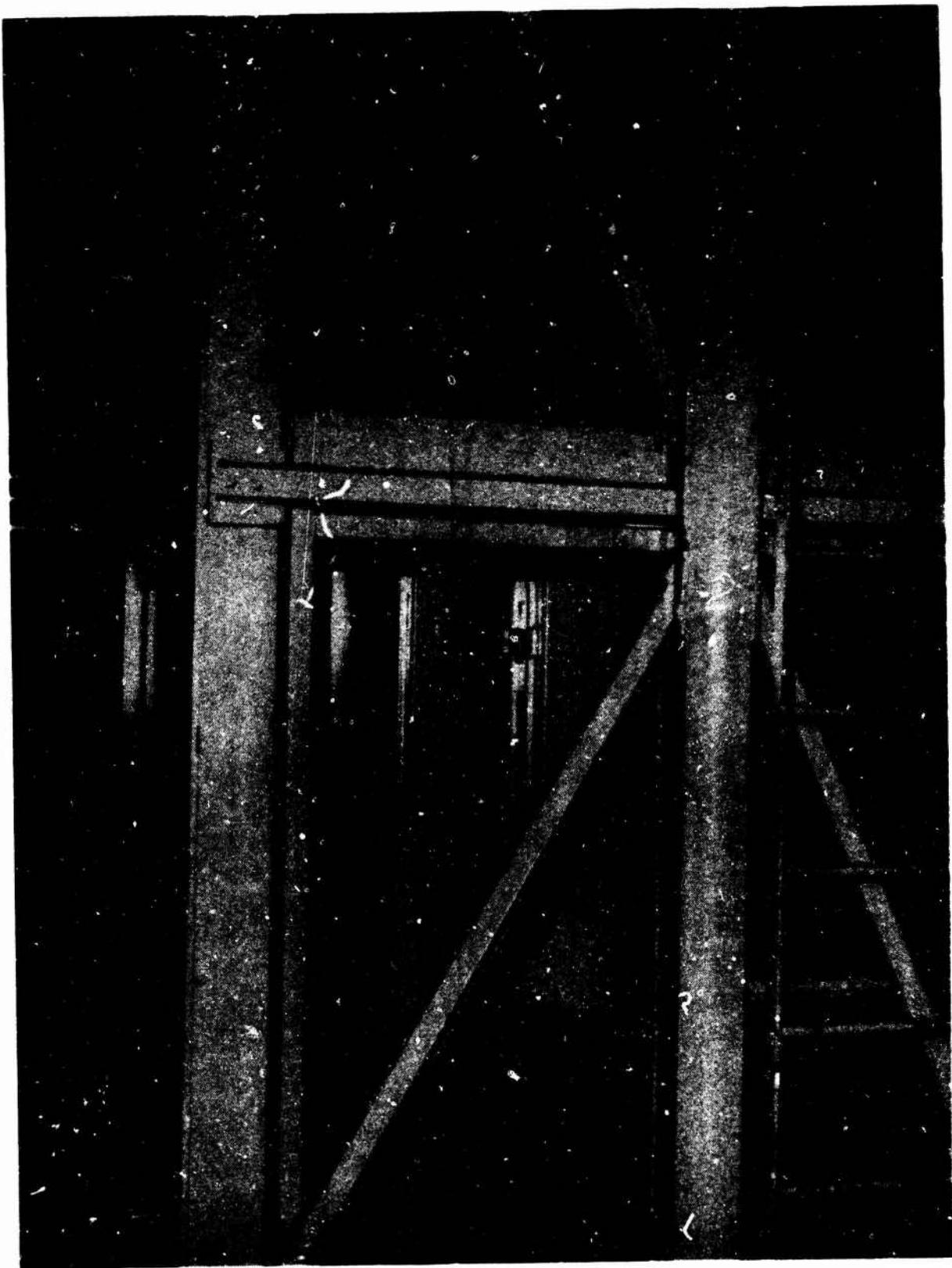
Figure 10.—Side View of Assembled Buckling Restraint Fixture on Structural Simulation Test Specimen in Fatigue Test Machine
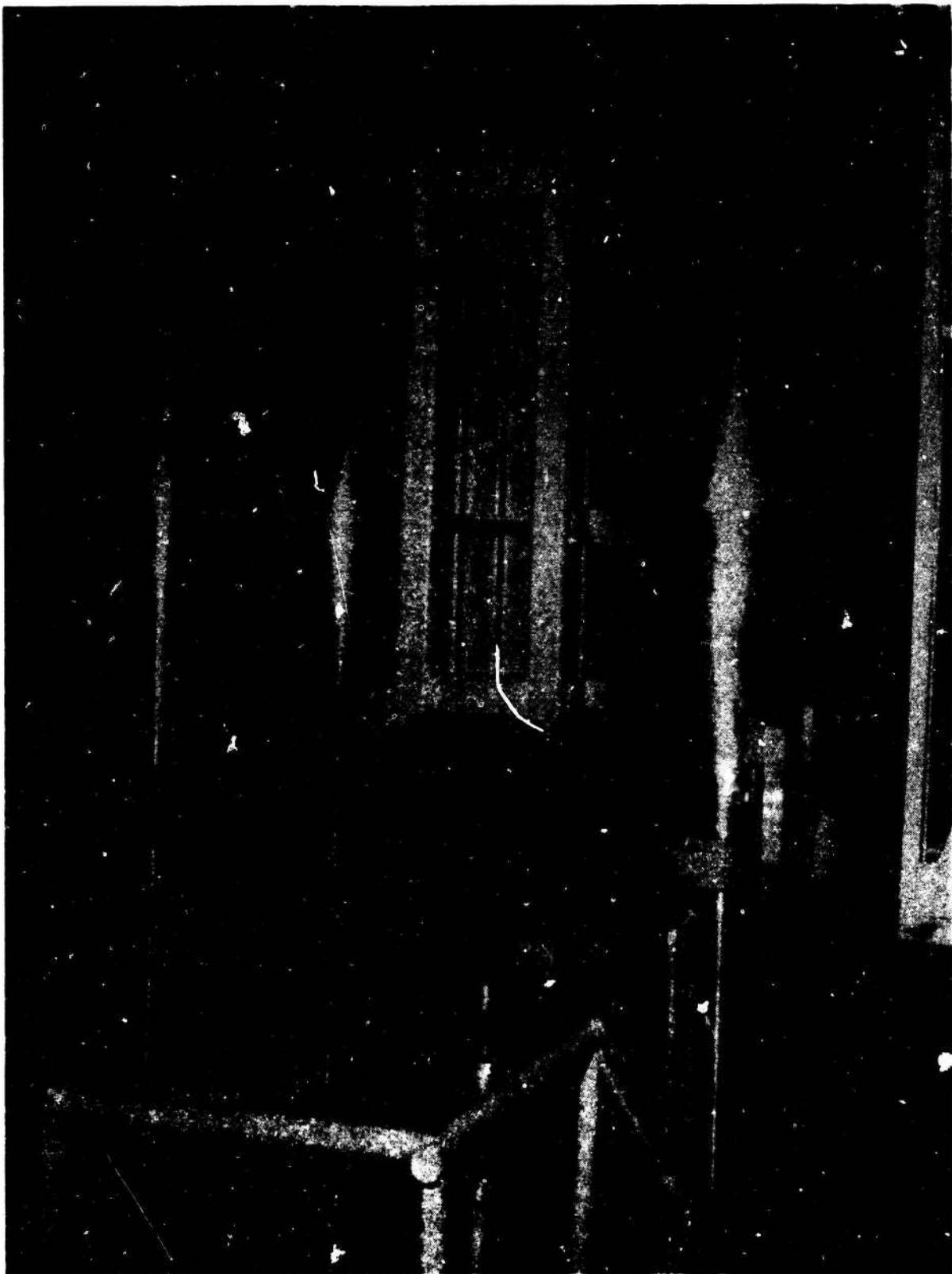
Figure 11.--Buckling Restraint Jig Installed on a Usage Simulation Specimen in 150,000-Lb EMR Fatigue Test Machine

27
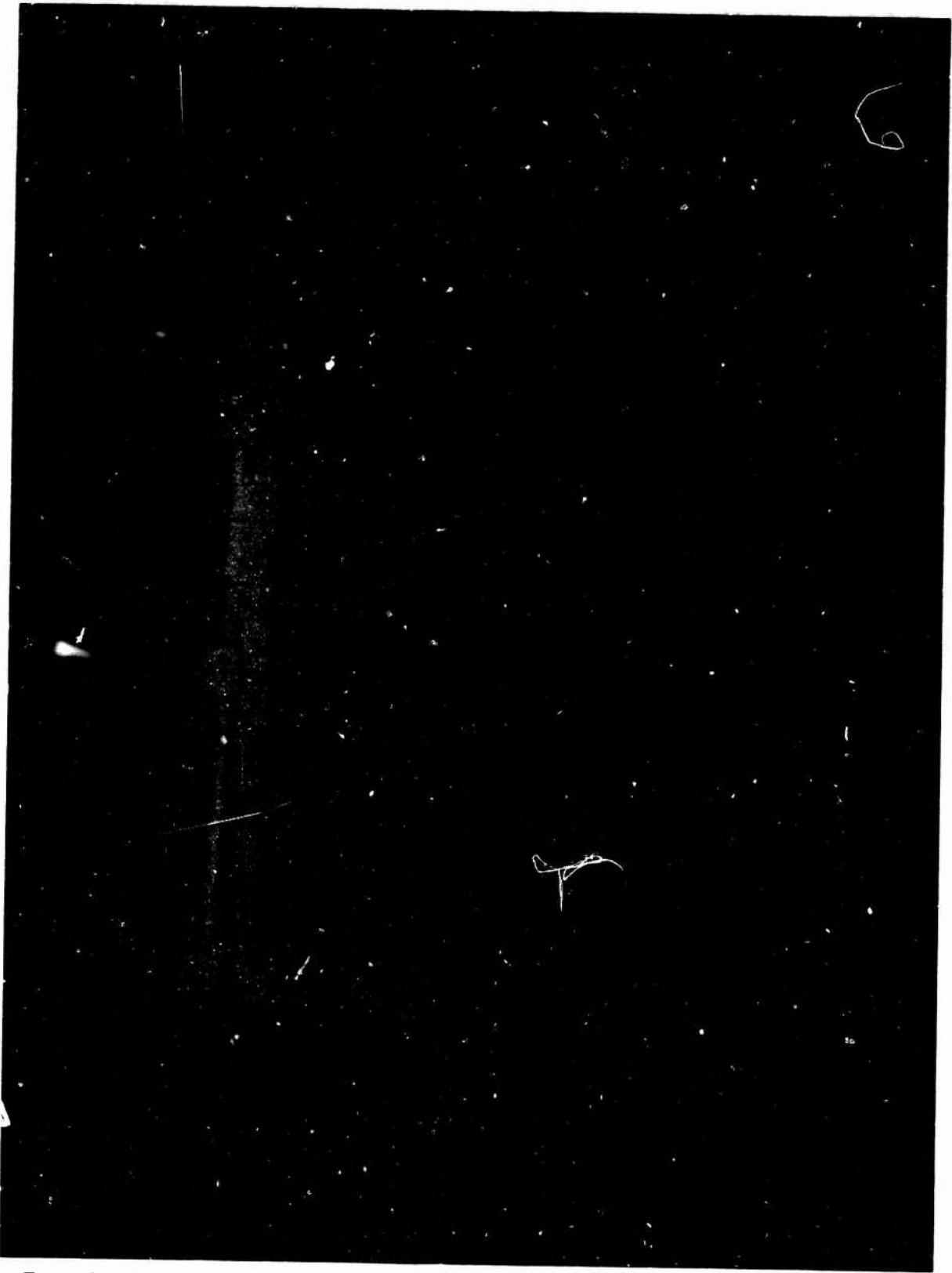
Figure 12.—One Stabilizing Face of the Buckling Restraint Jig for Usage Simulation Specimens
Suspended From Rail Hoist System of 150,000-Lb EMR Fatigue Test Machine
With Installed Panel

28
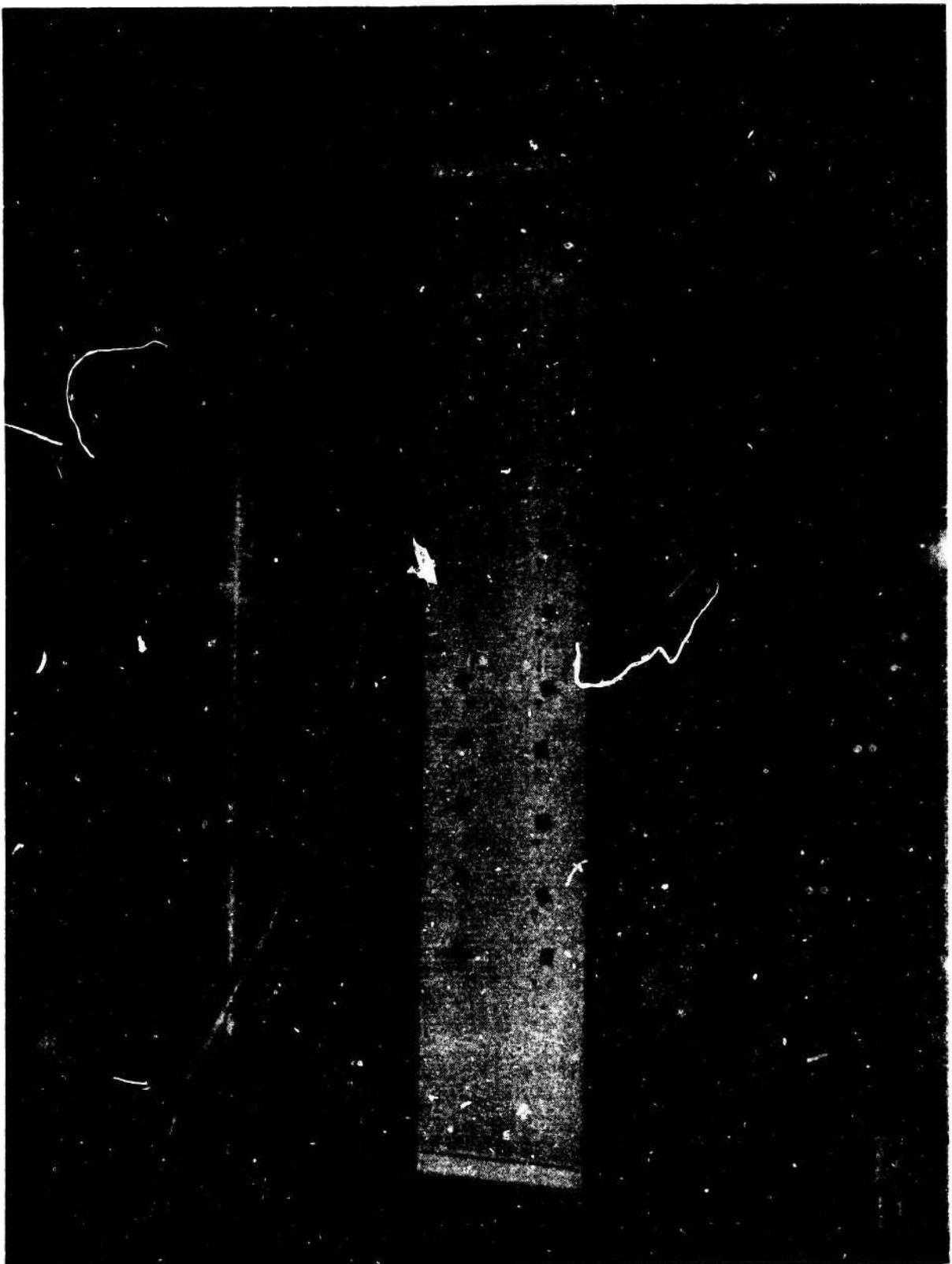
Figure 13. – Usage Simulation Specimen (Open Hole) With Crack Detection Circuit
and Strain Gages (Buckling Restraint Fixture Section in Background)

29
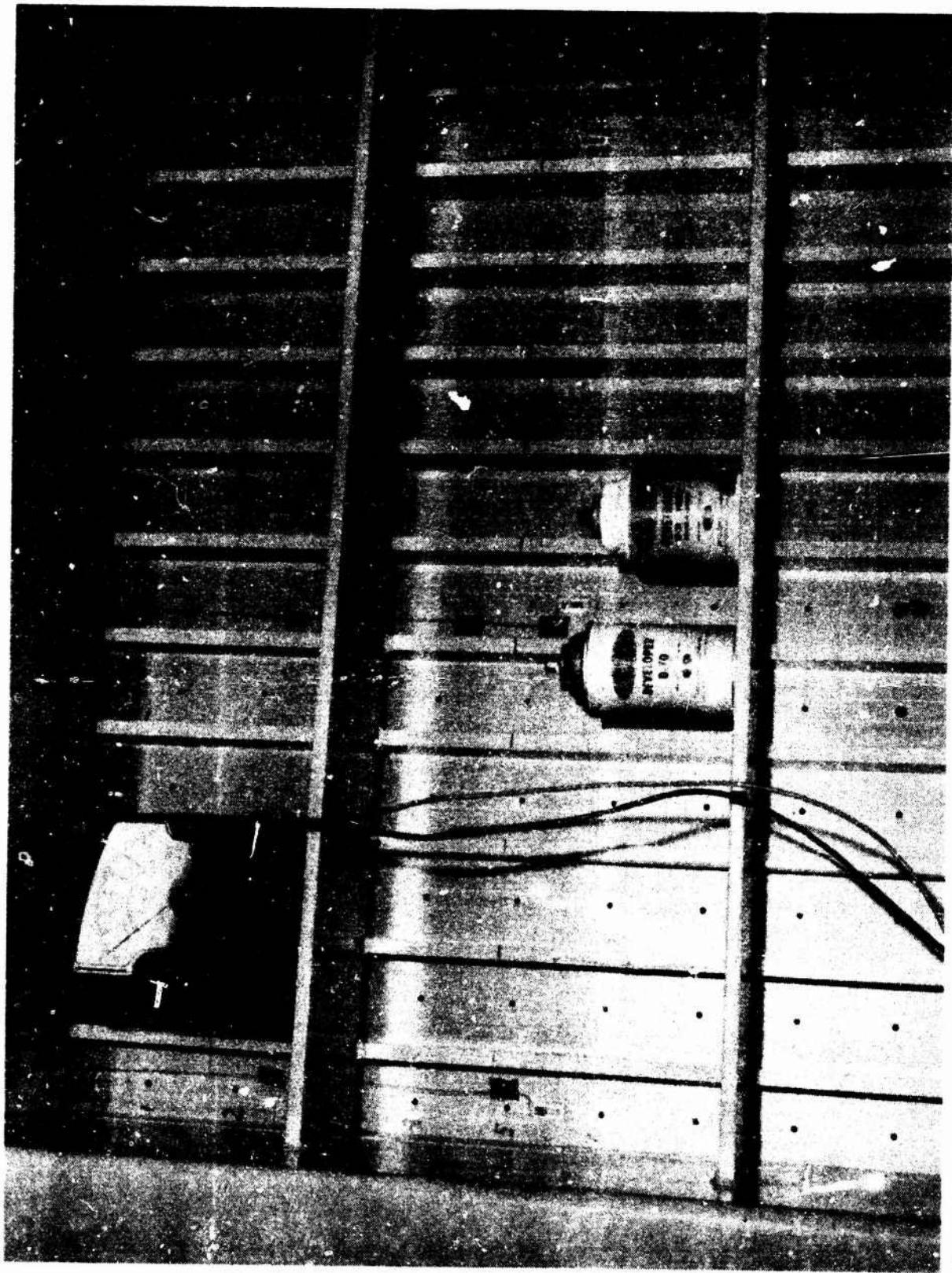
Figure 14. Test Section of Structural Simulation Specimen as Seen Through Buckling Restraint Fixture in Fatigue Test Machine
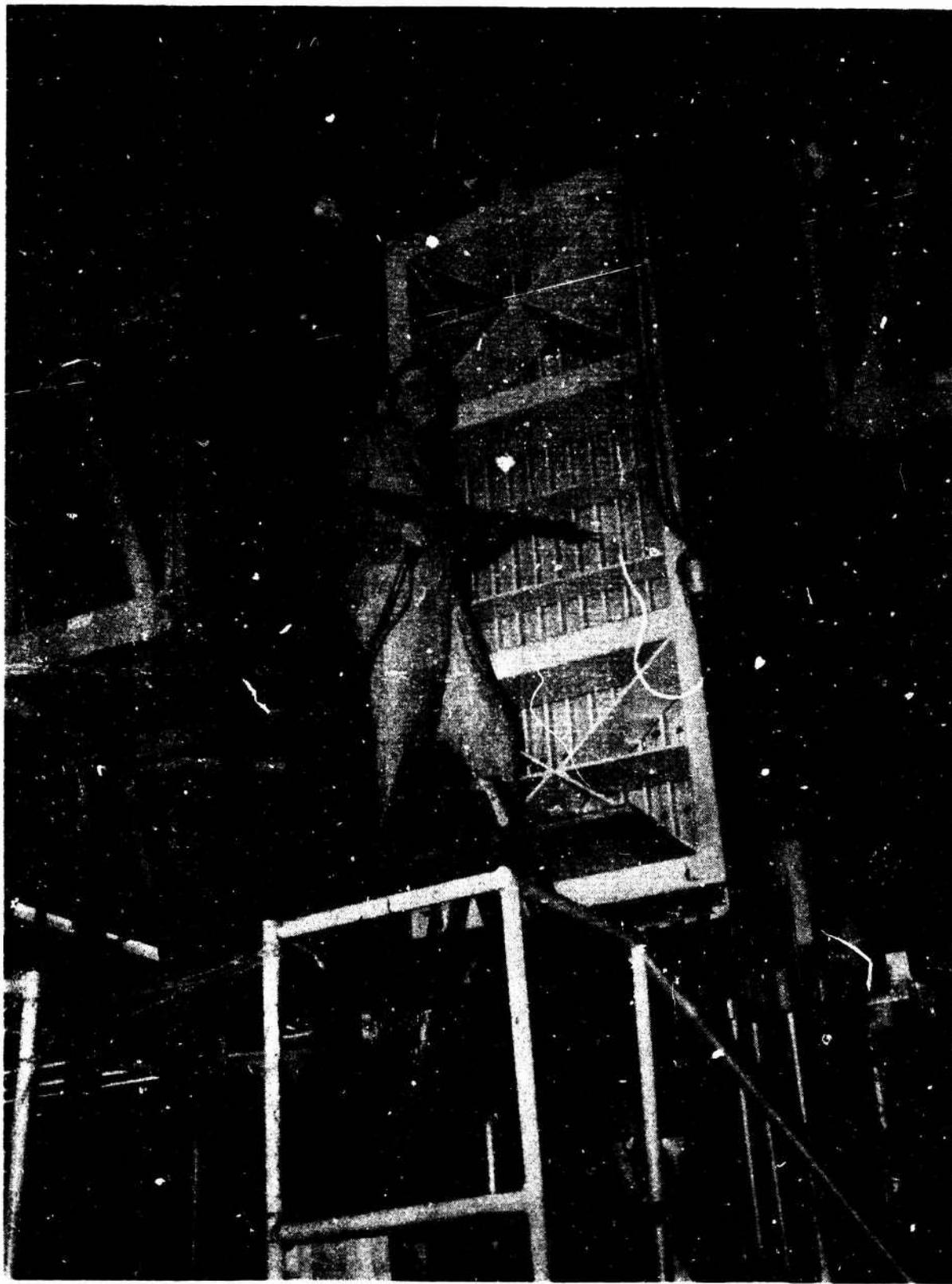
Figure 15.—Hole Cold-Working Tool
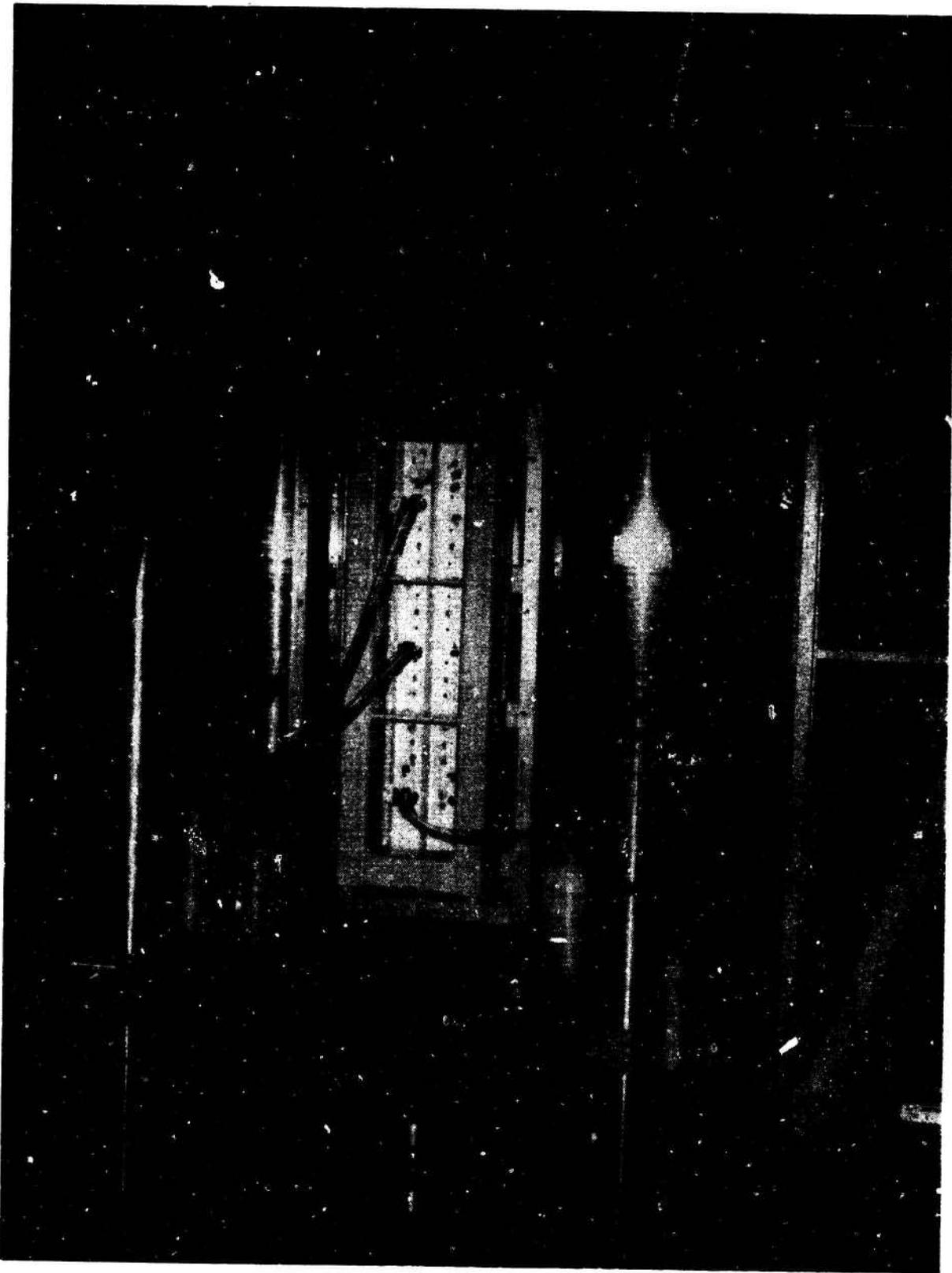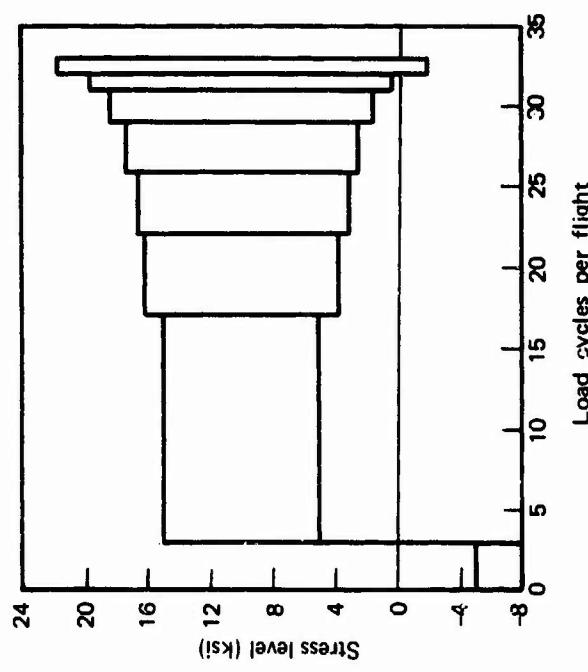
Figure 16.–*Environmental Control Box and System Installed Around Buckling Restraint Fixture and Usage Simulation Specimen in 150,000-Lb EMR Fatigue Test Machine*

Spectrum B-1 Basic Stresses
(Maneuver Loading: Fighter)

a. Spectrum A-1 Basic Stresses
(Gust Loading: Transport)
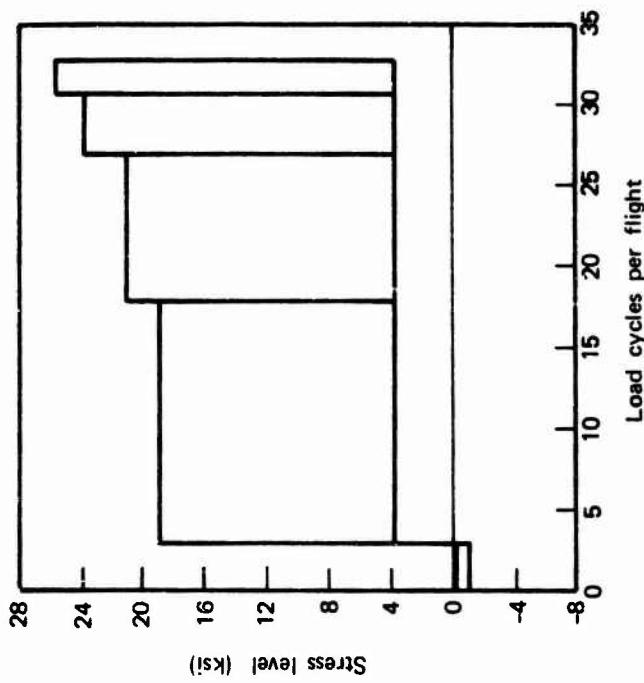
Figure 17.—Basic Fatigue Test Spectrum Loading Content Per Flight for Spectrums A-1 and B-1 for Aluminum Alloy 2024-T3

33

(a) Spectrum A-2 Basic Stress
Gust Loading

(b) Spectrum B-2 Basic Stress
Maneuver Loading
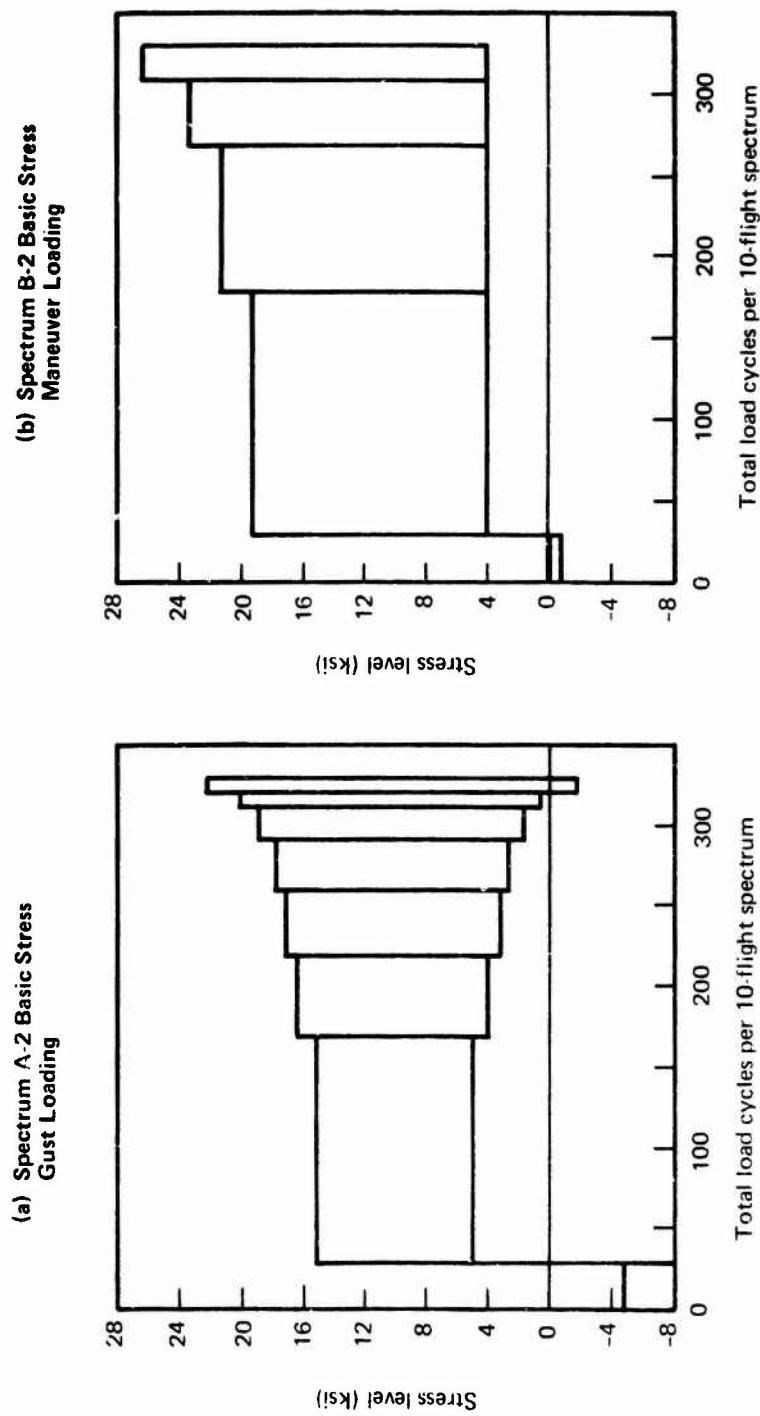
Figure 18. —Basic Fatigue Test Spectrum Loading Content Per 10-Flight Spectrums A-2 and B-2 for Aluminum Alloy 2024-T3

34

(a) Spectrum A-3 Basic Stresses
Gust Loading

(b) Spectrum B-3 Basic Stresses
Maneuver Loading
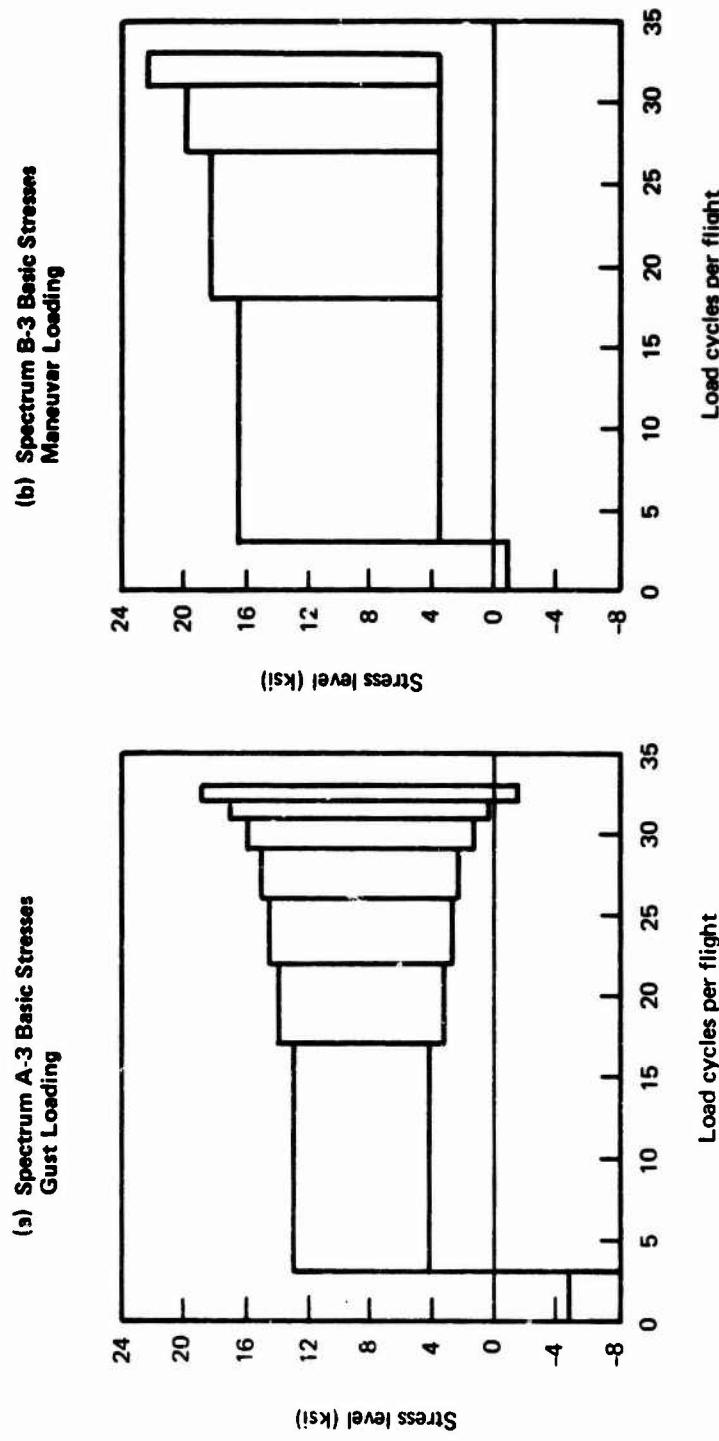
Figure 19. – Basic Fatigue Test Spectrum Loading Content Per Flight for Spectrum A-3 and B-3 for Aluminum Alloy 2024-T3

35
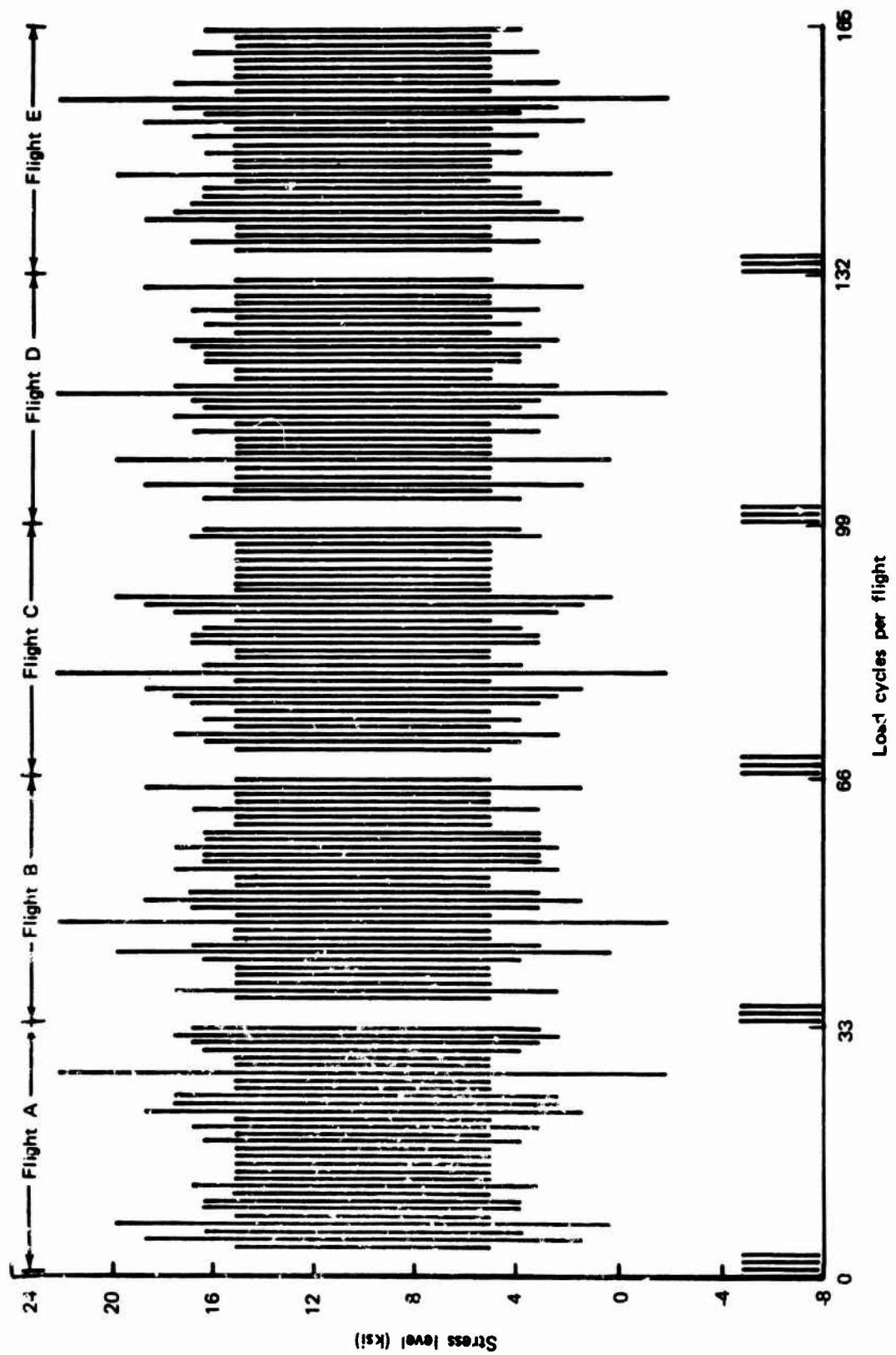
Figure 20.—Basic Test Spectrum A-1 (Five-Flight Gust Load Type)

36
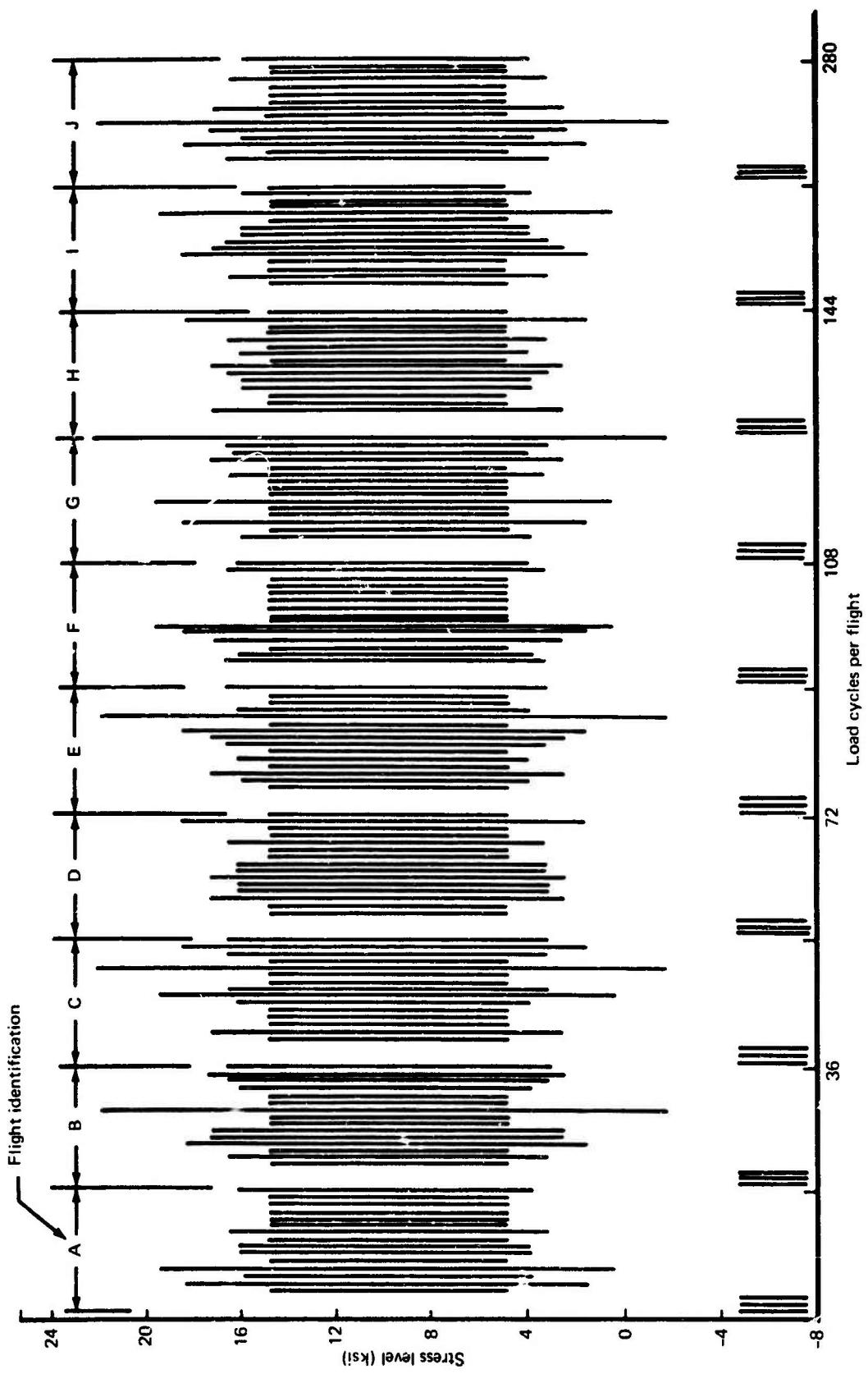
Figure 21.—Basic Test Spectrum A-2 (10-Flight Gust Load Type)

37
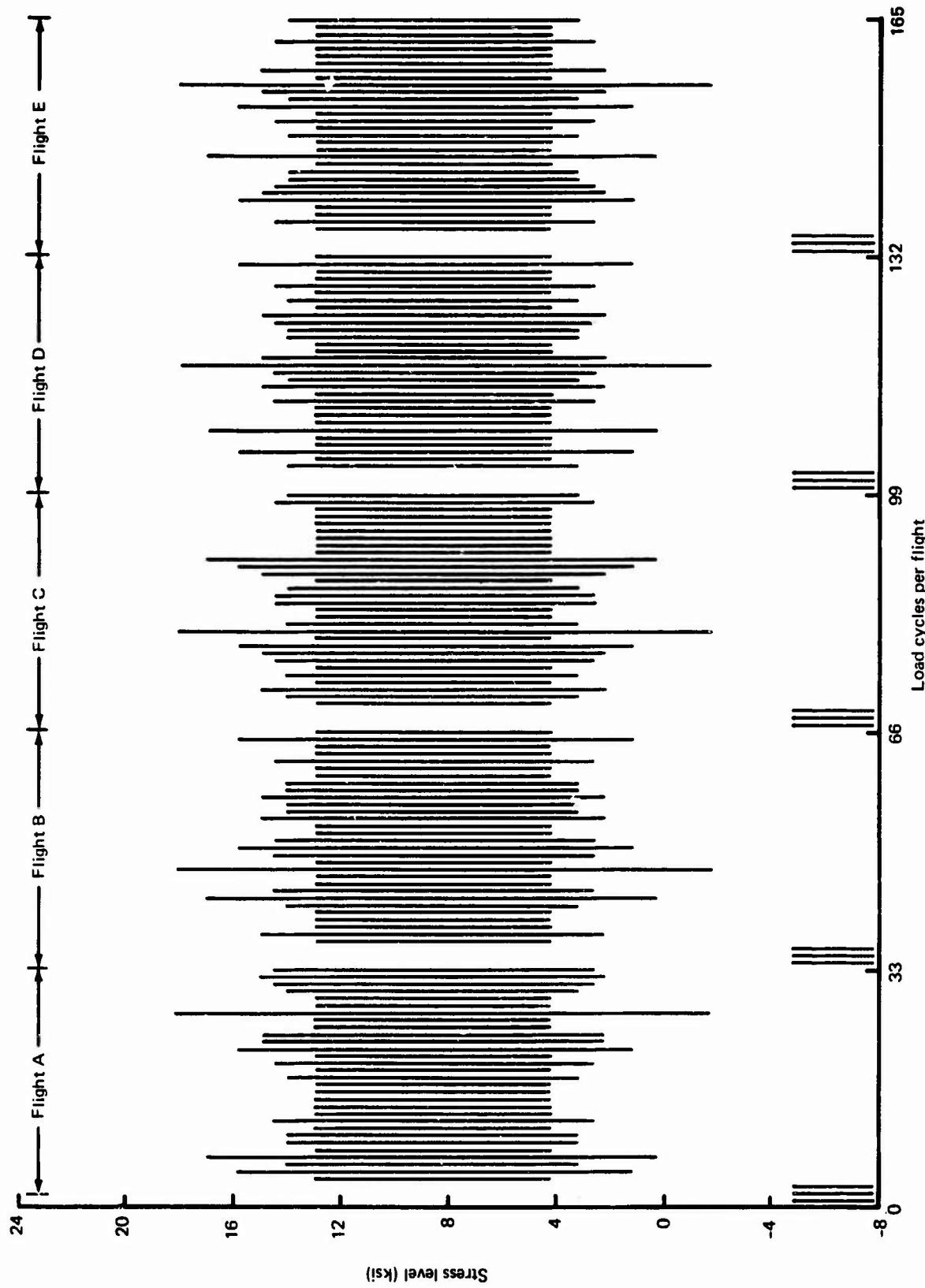
Figure 22.—Basic Test Spectrum A-3 (Reduced Level Five-Flight Gust Load Type)

38
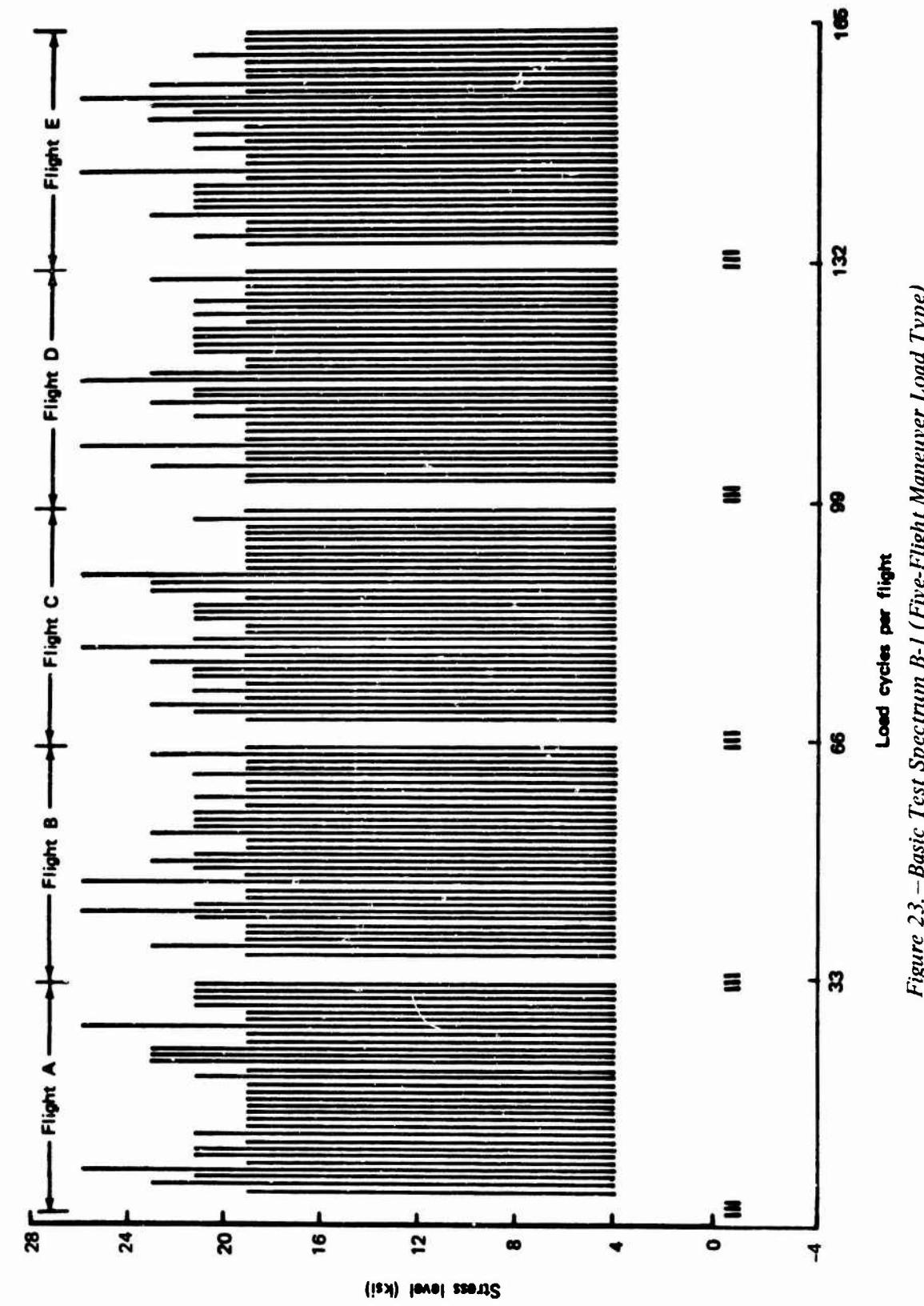
Figure 23. – Basic Test Spectrum B-1 (Five-Flight Maneuver Load Type)
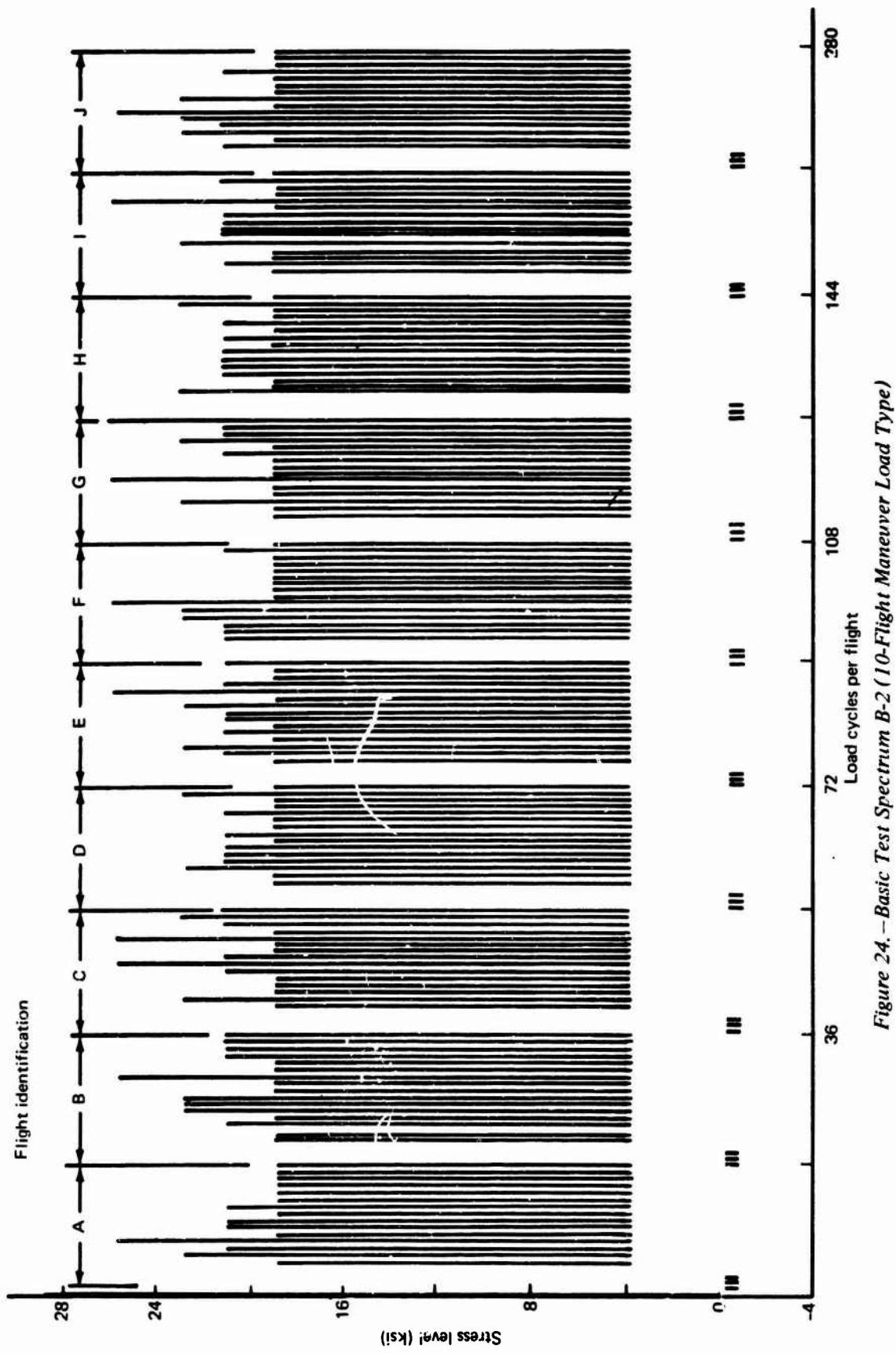
Figure 24. — Basic Test Spectrum B-2 (10-Flight Maneuver Load Type)
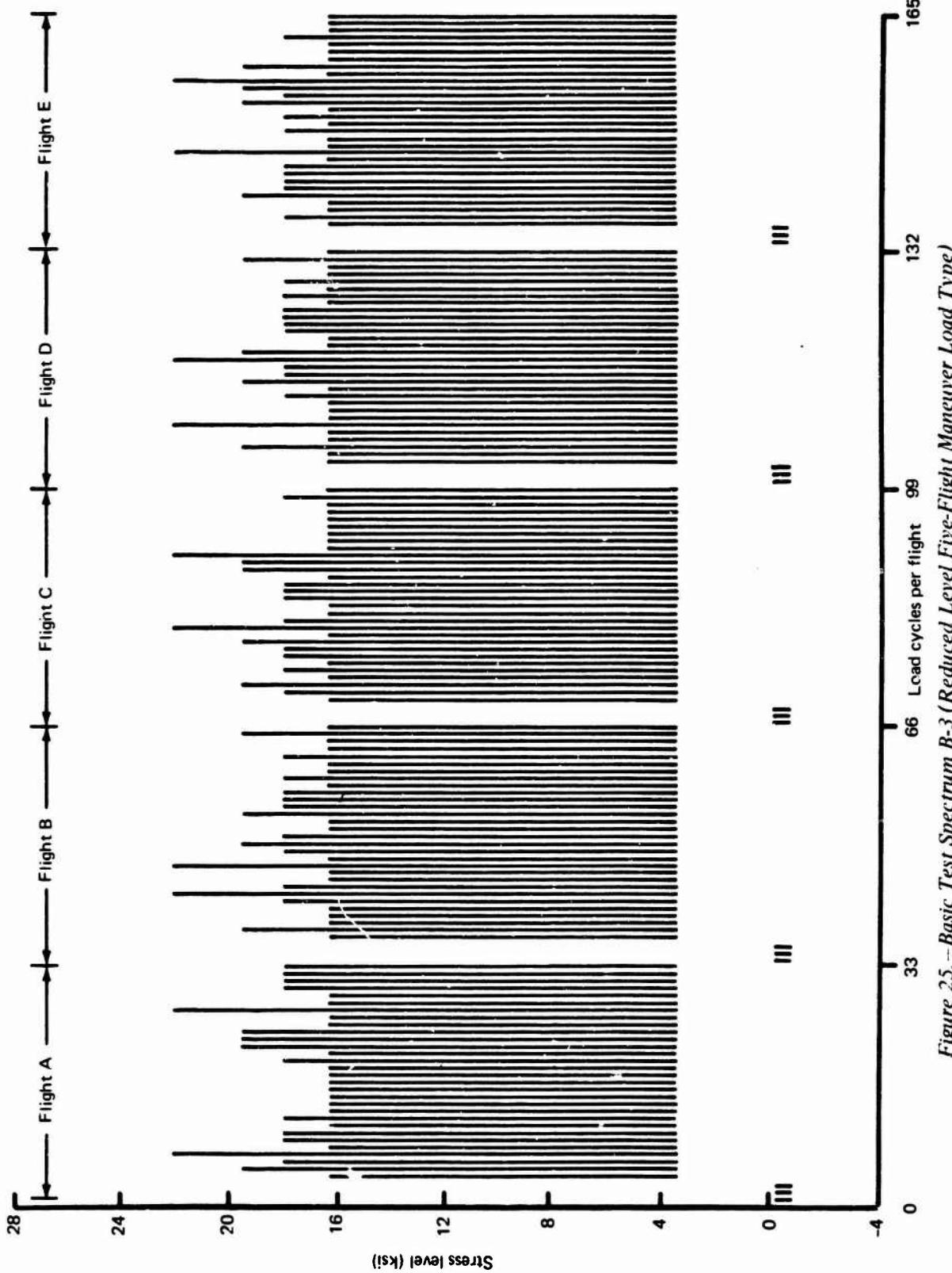
Figure 25. — Basic Test Spectrum B-3 (Reduced Level Five-Flight Maneuver Load Type)

41
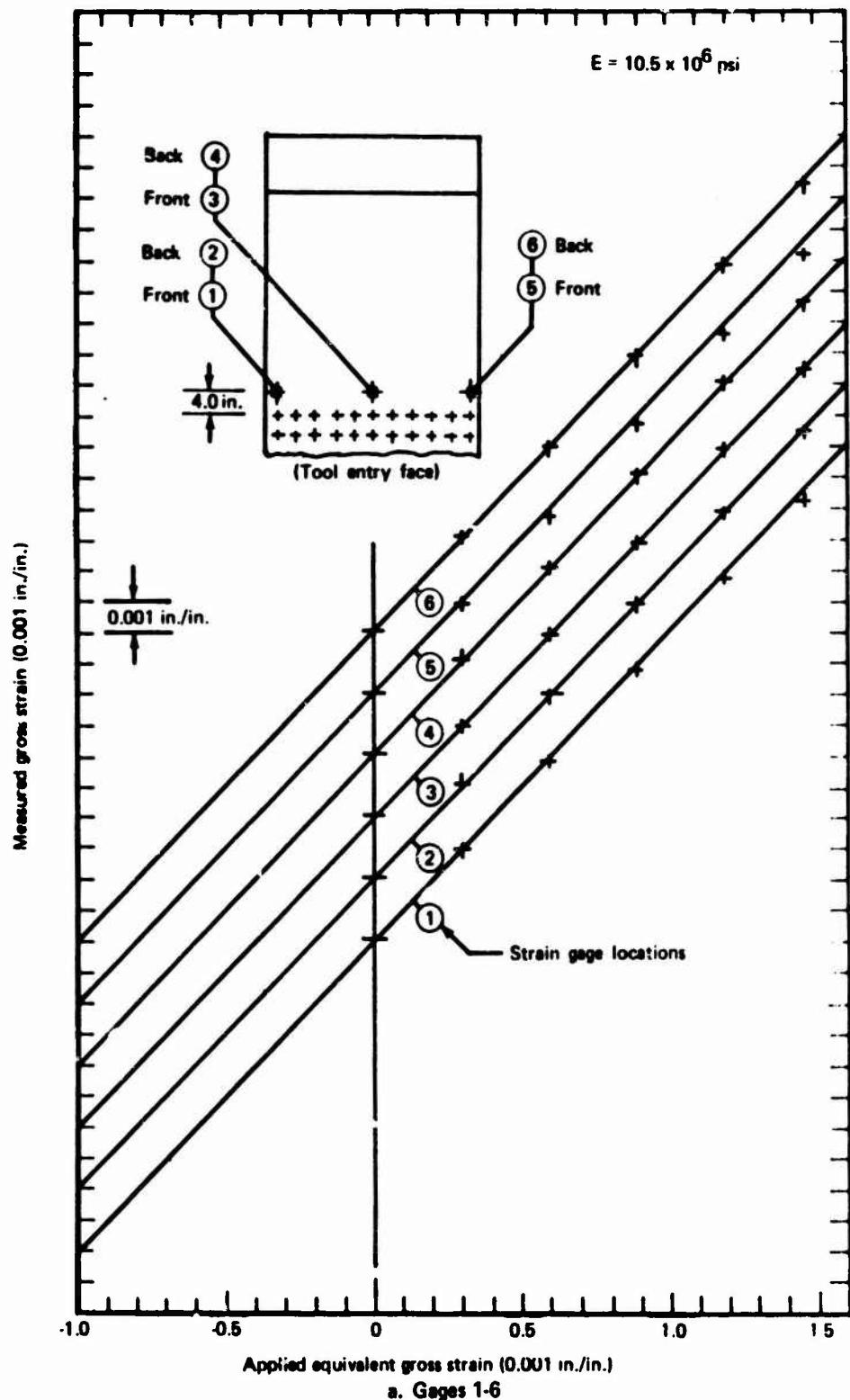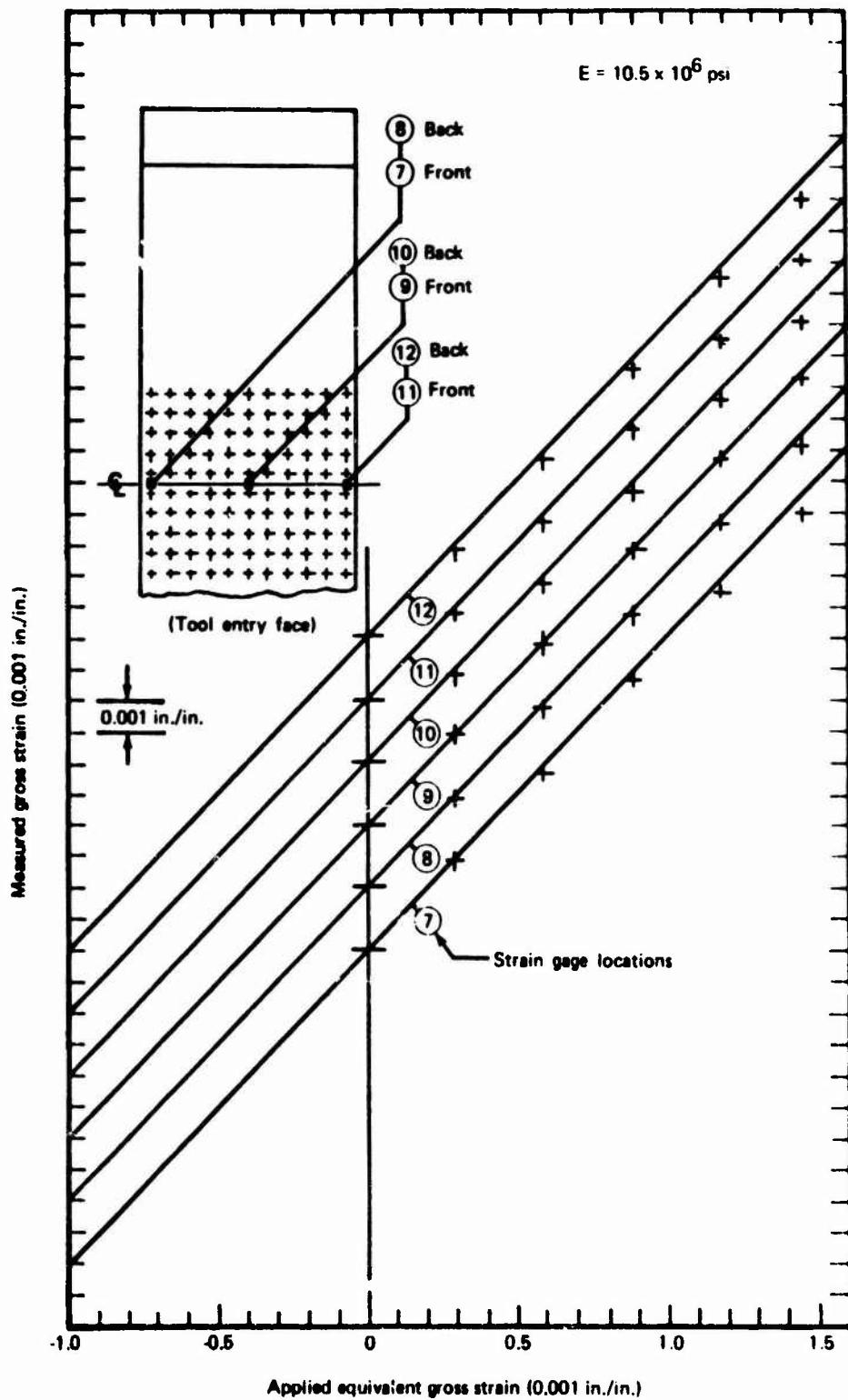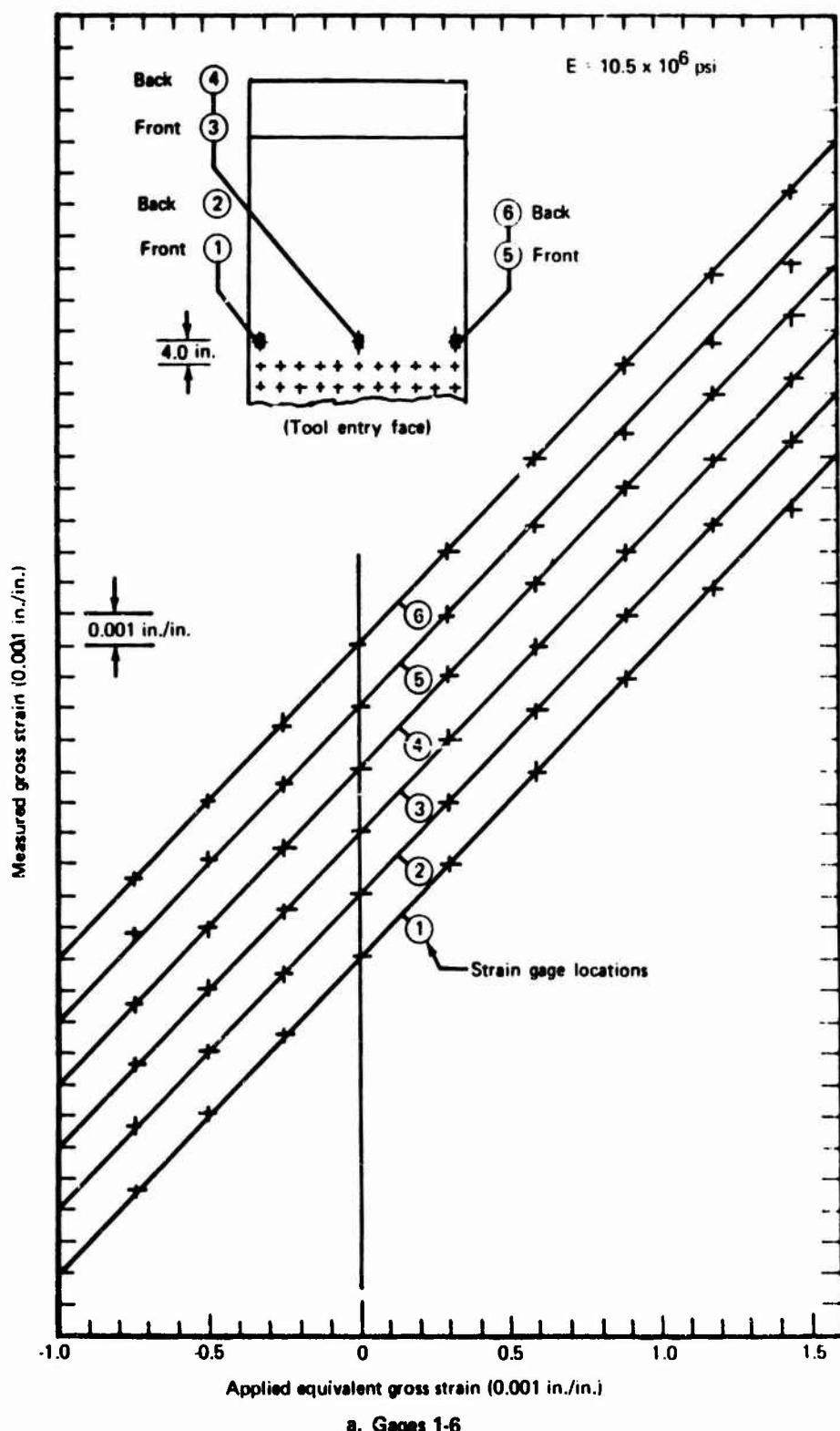
Figure 26. – Comparison of Measured Strains With Applied Equivalent Strains on Structural Simulation Specimen Without Buckling Restraint Fixture

42

b. Gages 7-11

Figure 26.—Concluded

43

Figure 27. — Comparison of Measured Strains With Applied Equivalent Strains on Structural Simulation Specimen With Buckling Restraint Fixture

44

b. Gages 7-11

Figure 27. -Concluded

45
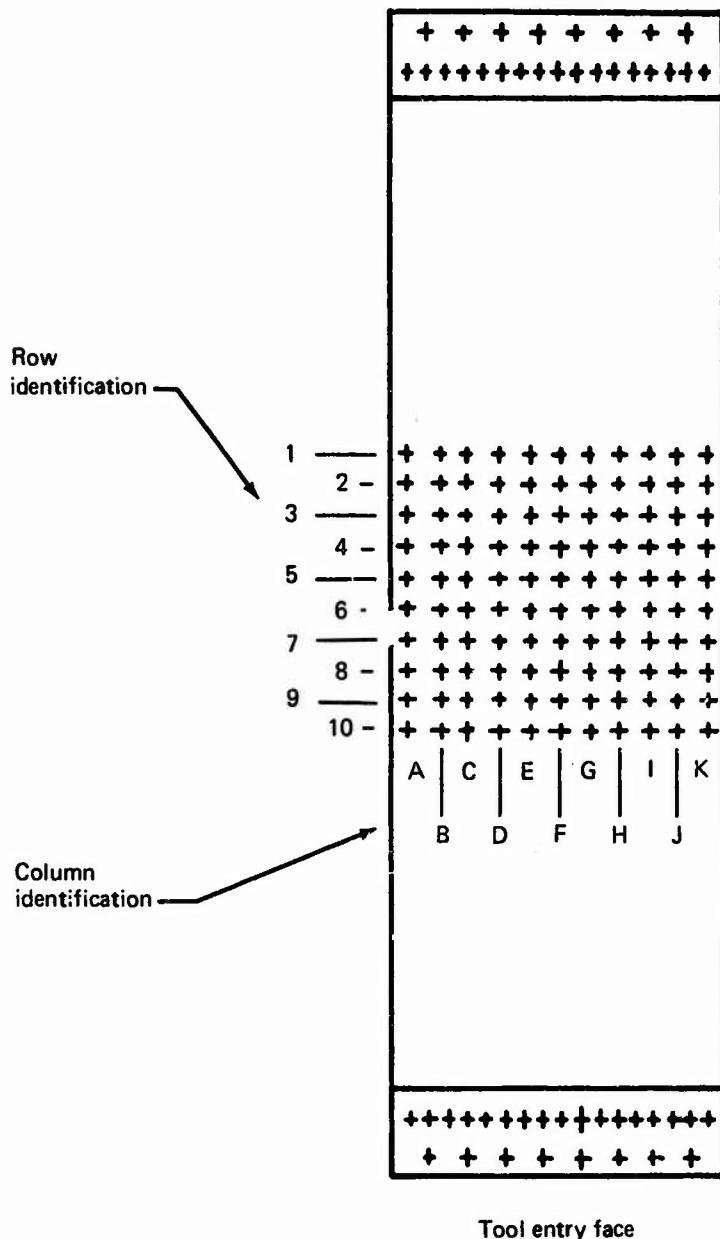
Figure 28.—Identification of Hole Location and Crack Growth Direction in Structural Simulation Test Specimen Configuration

46

Figure 29.—Fatigue Crack Initiation Sites at Holes in Structural Simulation
Specimen A1. (Al. Alloy 2024-T3 Heat A, Test Spectrum A-1)

47

Figure 30.—Fatigue Crack Initiation Sites at Holes in Structural Simulation Specimen A2. (Al. Alloy 2024-T3 Heat A, Test Spectrum A-1)

48

Legend:

● Tool entry face origin
⊗ Tool exit face origin

Note: Superscript numeral is detection sequence
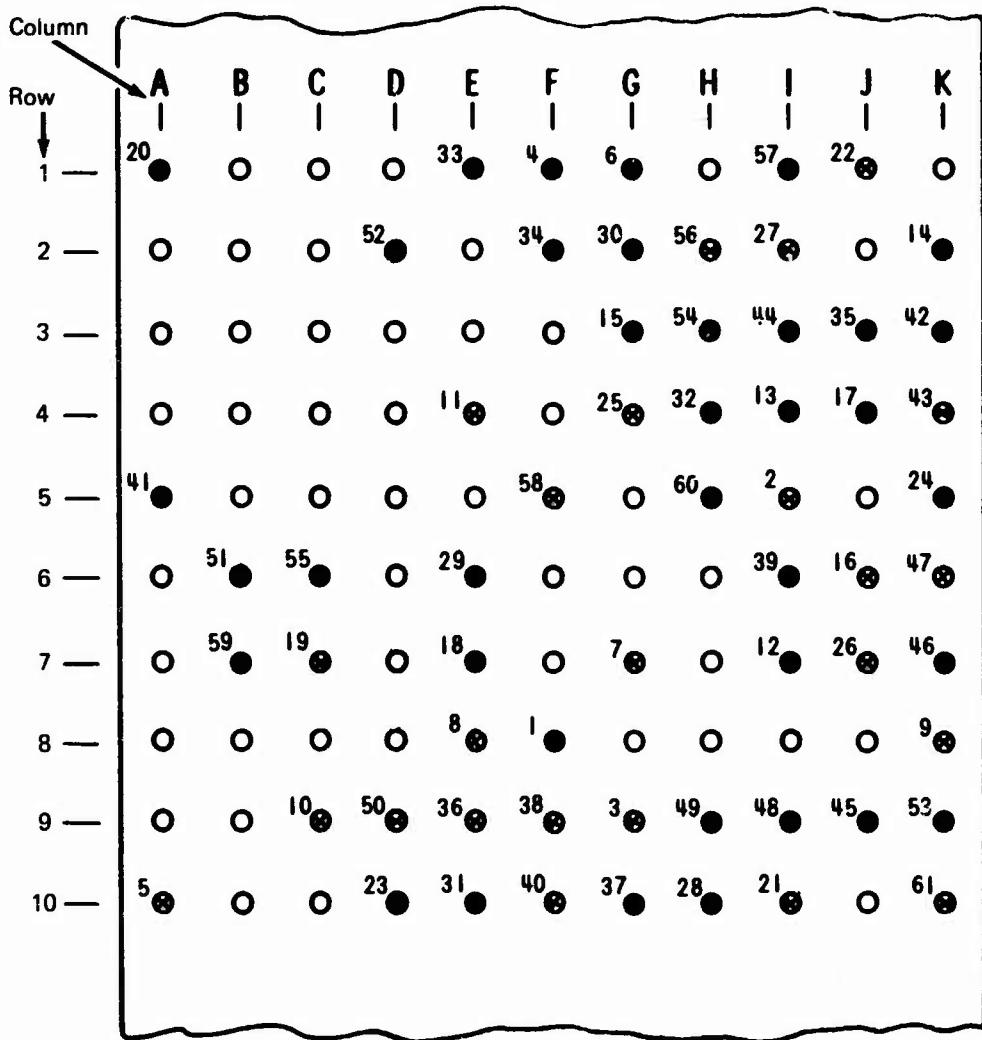
Figure 31.—Fatigue Crack Initiation Sites at Holes in Structural Simulation
Specimen A3. (Al. Alloy 2024-T3 Heat B, Test Spectrum A-1)

Column

Row

	A	B	C	D	E	F	G	H	I	J	K
1	O	O	O	O	^{9}⊗	O	^{11}●	^{13}●	^{4}⊗	^{5}●	^{7}⊗
2	O	O	O	O	O	O	O	O	^{16}●	O	O
3	O	^{3}⊗	O	O	O	O	O	O	O	O	^{12}⊗
4	O	O	O	O	O	O	O	O	O	O	O
5	^{8}●	^{10}●	O	O	O	O	O	O	O	O	O
6	^{15}●	O	O	O	^{6}⊗	O	O	O	O	O	O
7	^{17}⊗	O	O	O	O	O	O	O	O	O	O
8	O	O	O	O	O	O	O	O	O	O	O
9	O	O	O	O	O	O	O	O	O	O	O
10	O	O	^{2}●	^{14}●	O	O	O	O	O	O	^{1}●

Figure 32. - Fatigue Crack Initiation Sites at Holes in Structural Simulation Specimen A4. (Al. Alloy 2024-T3 Heat C, Test Spectrum B-1)

50
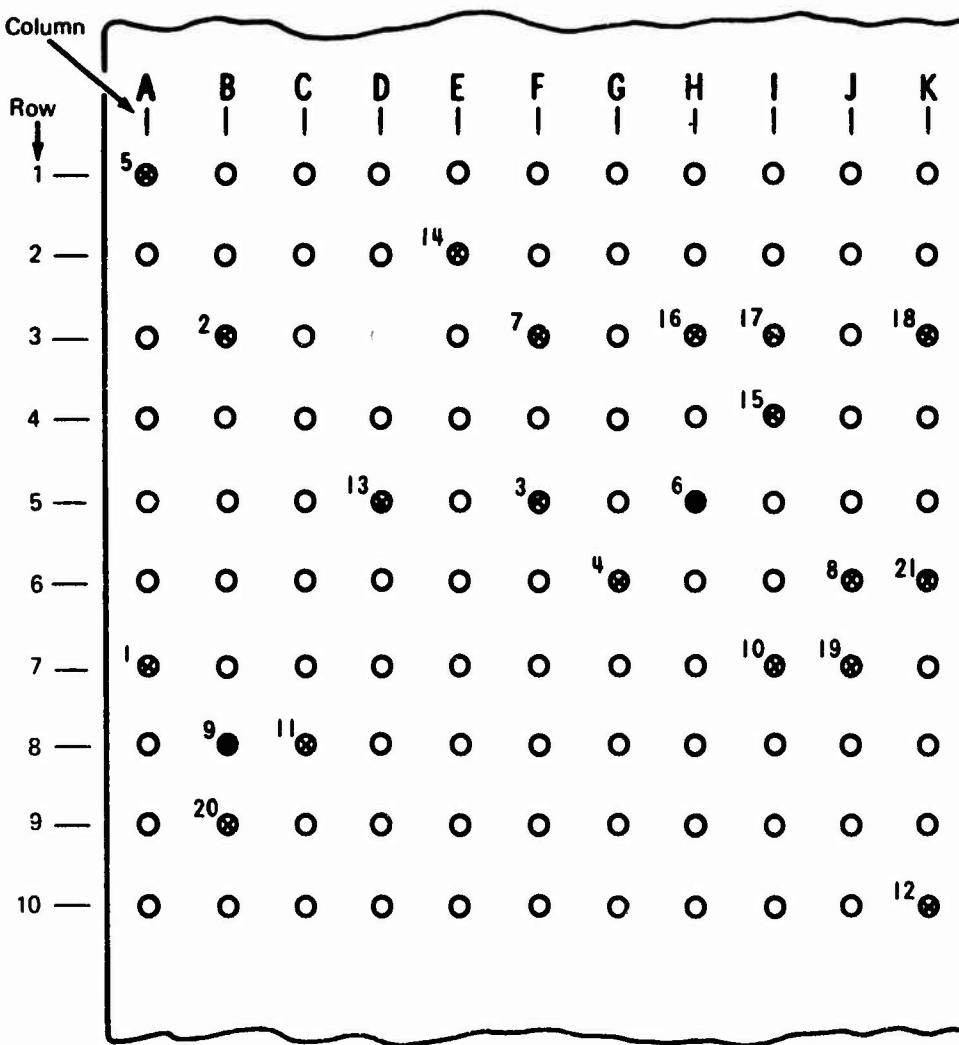
Figure 33. - Fatigue Crack Initiation Sites at Holes in Structural Simulation
Specimen A5. (Al. Alloy 2024-T3 Heat B. Test Spectrum A-1)

51

Figure 34. – Fatigue Crack Initiation Sites at Holes in Structural Simulation
Specimen A6. (Al. Alloy 2024-T3 Heat A, Test Spectrum B-1)

52
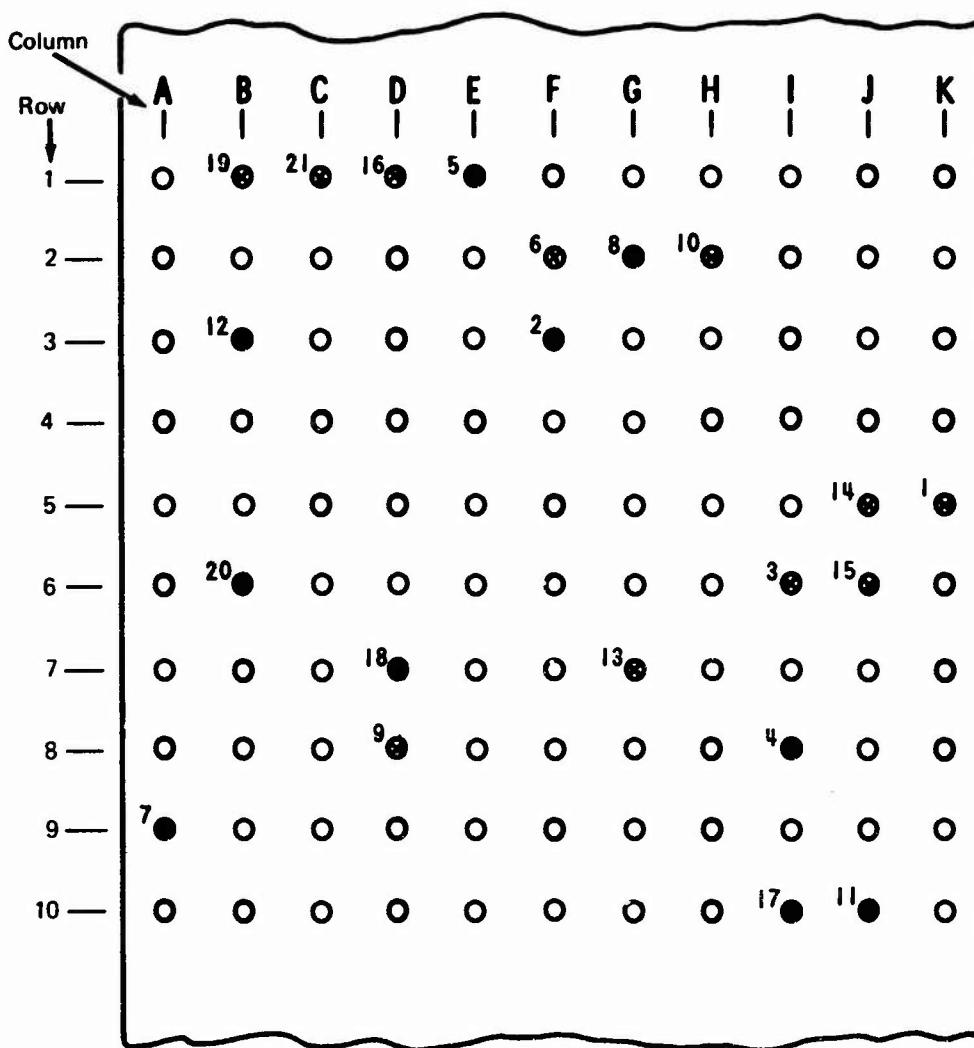
Figure 35. – Fatigue Crack Initiation Sites at Holes in Structural Simulation Specimen A7. (Al. Alloy 2024-T3 Heat A, Test Spectrum A-2)

53
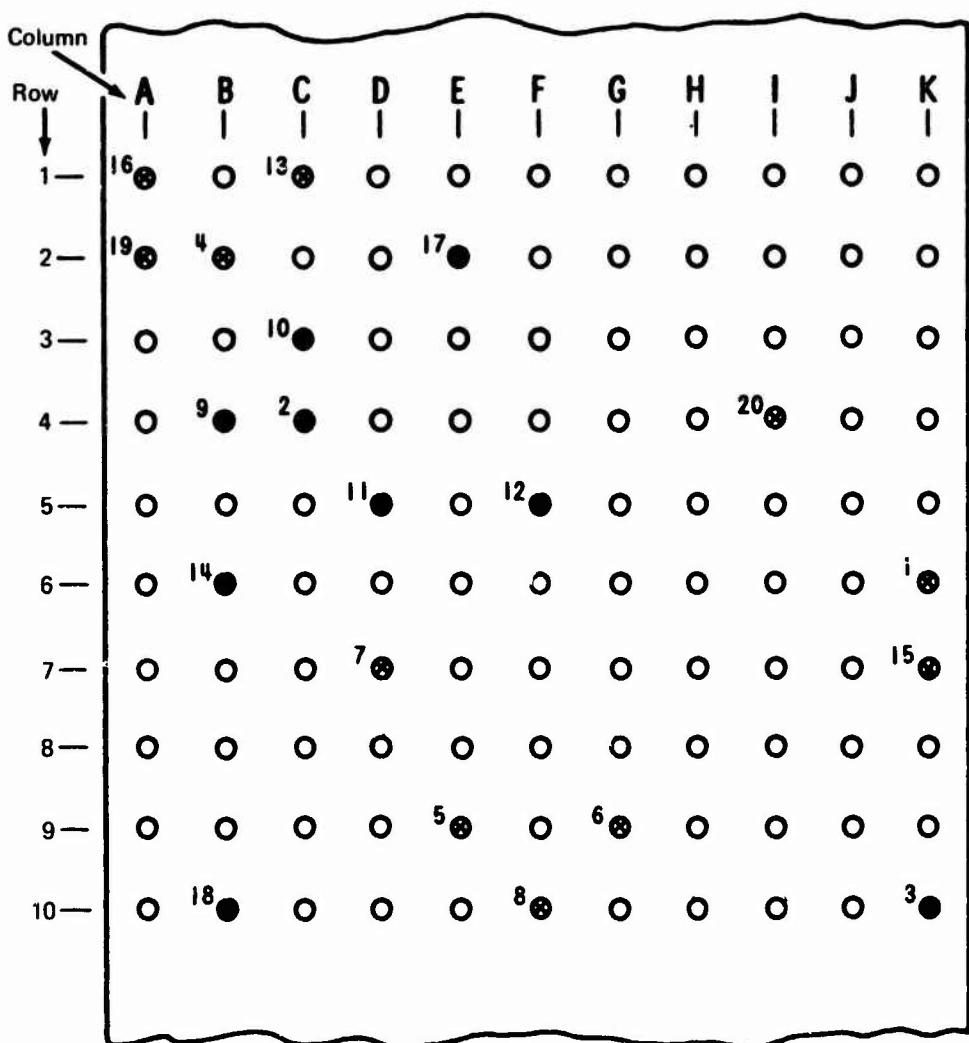
Figure 36. — Fatigue Crack Initiation Sites at Holes in Structural Simulation Specimen A8. (Al. Alloy 2024-T3 Heat A. Test Spectrum B-1)

54

Legend:
- ● Tool entry face origin
- ⊗ Tool exit face origin

Note: Superscript numeral is detection sequence.
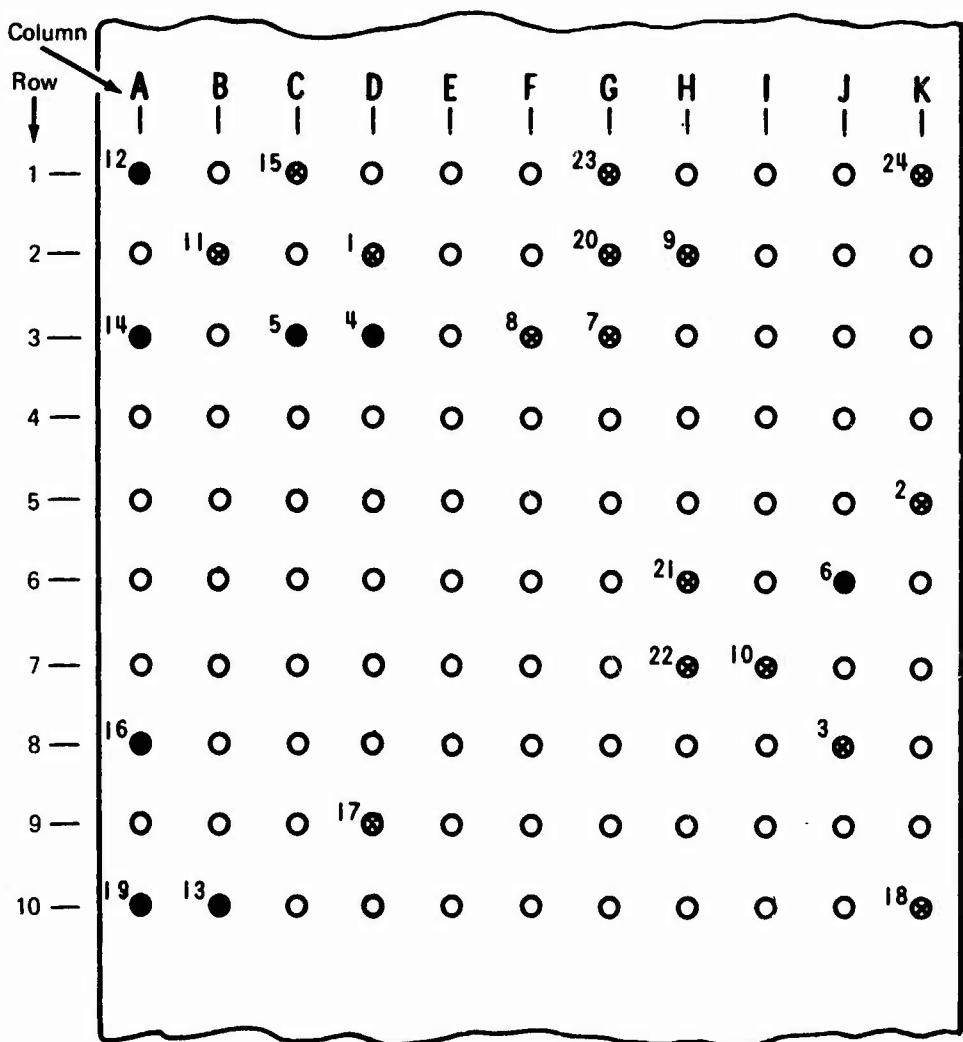
Figure 37. – Fatigue Crack Initiation Sites at Holes in Structural Simulation Specimen A9. (Al. Alloy 2024-T3 Heat A, Test Spectrum B-2)
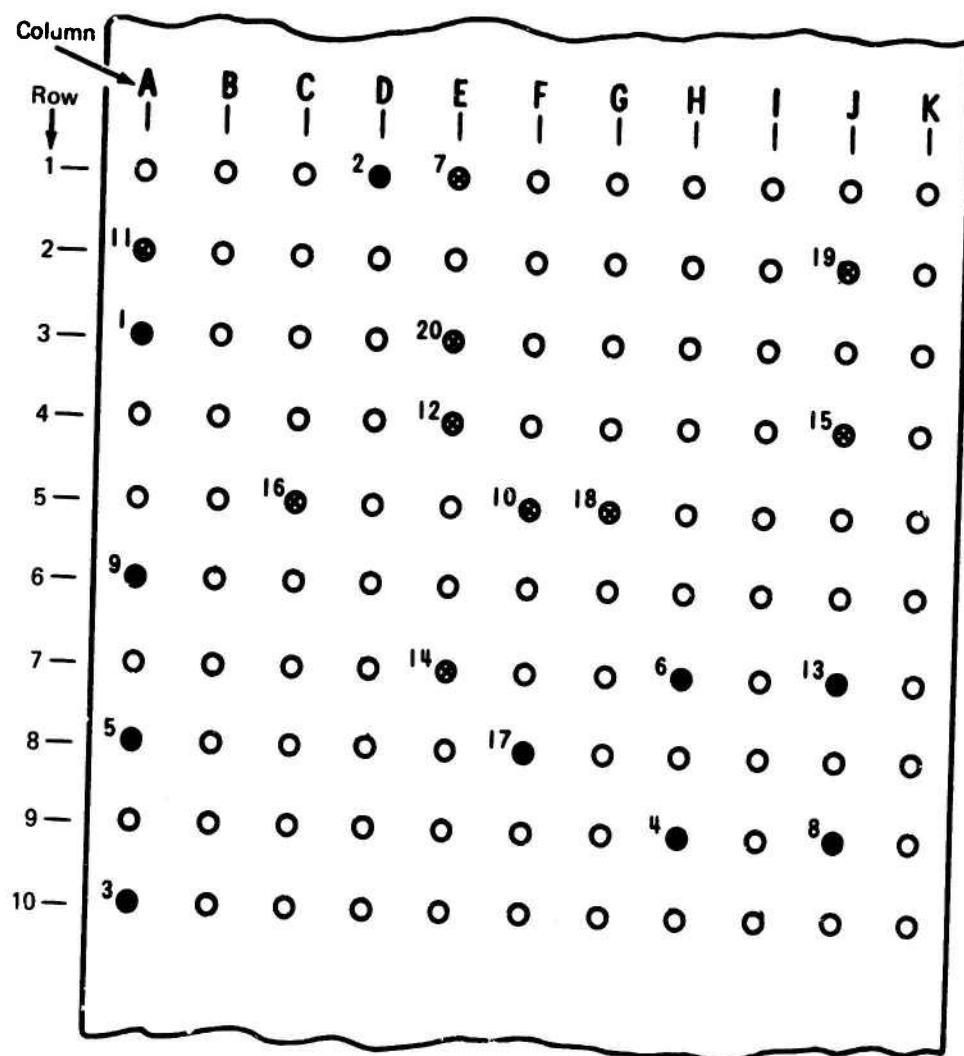
Figure 38.–Fatigue Crack Initiation Sites at Holes in Structural Simulation Specimen A10. (Al. Alloy 2024-T3 Heat A, Test Spectrum A-3)

Legend:
● Tool entry face origin
⊗ Tool exit face origin

Note: Superscript numeral is detection sequence.
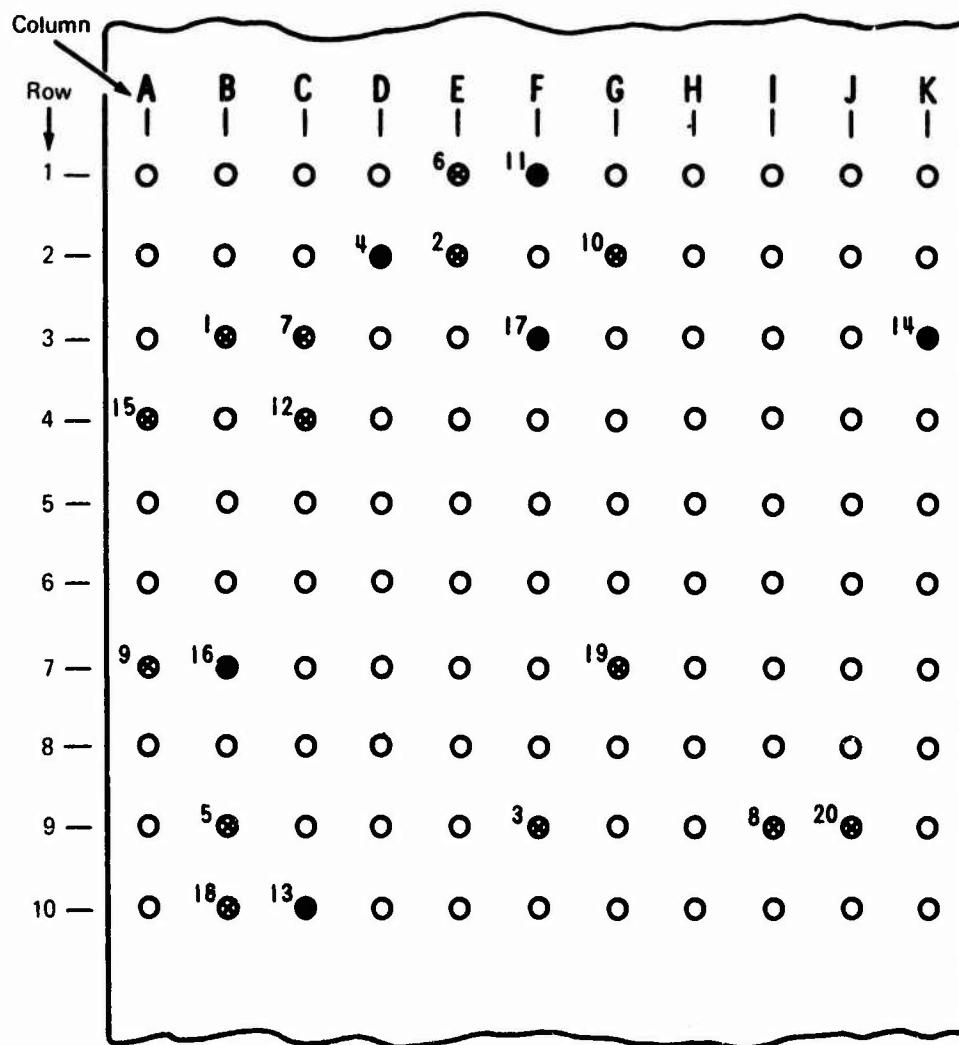
Figure 39. – Fatigue Crack Initiation Sites at Holes in Structural Simulation Specimen A11. (Al. Alloy 2024-T3 Heat A. Test Spectrum B-3)

57

Legend:
● Tool entry face origin
⊗ Tool exit face origin
Note: Superscript numeral is detection sequence.
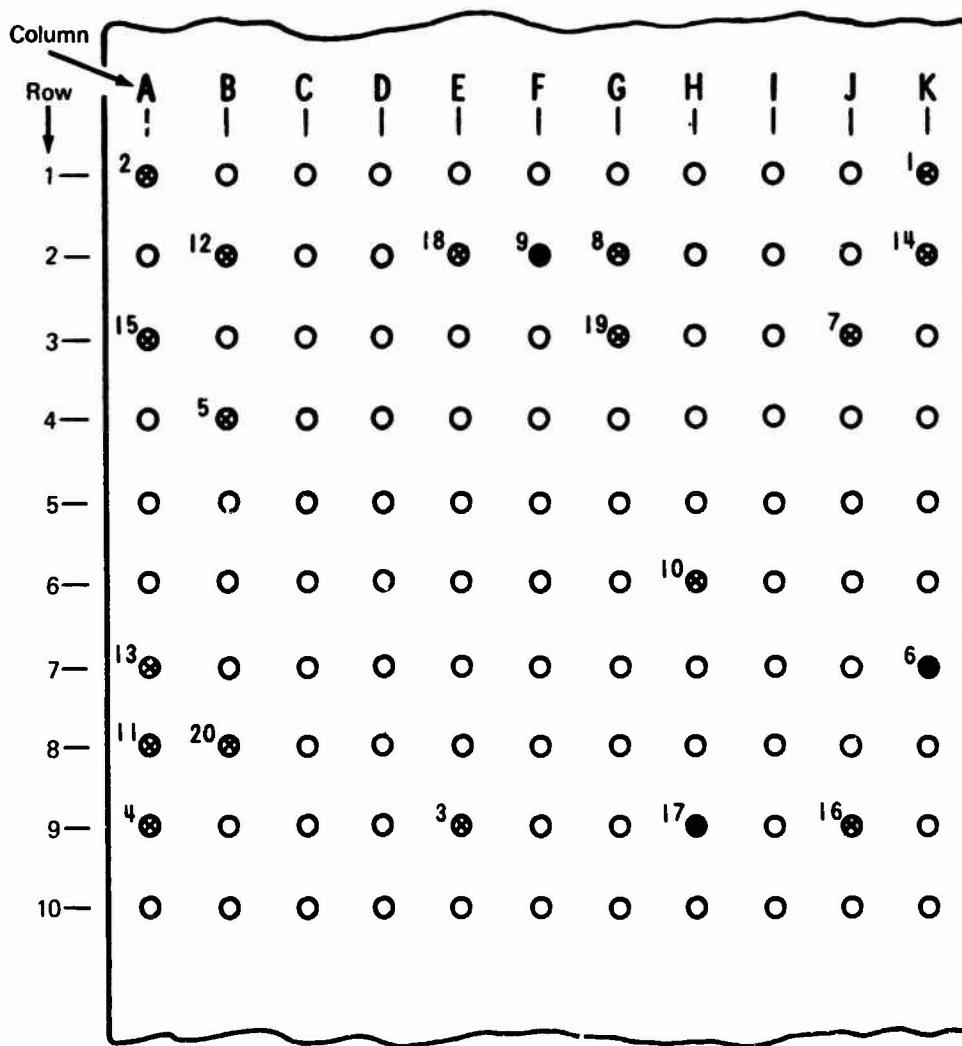
Figure 40.—Fatigue Crack Initiation Sites at Holes in Structural Simulation Specimen A12. (Al. Alloy 2024-T3 Heat C, Test Spectrum A-1)

Legend:

● Tool entry face origin
⊗ Tool exit face origin

Note: Superscript numeral is detection sequence.
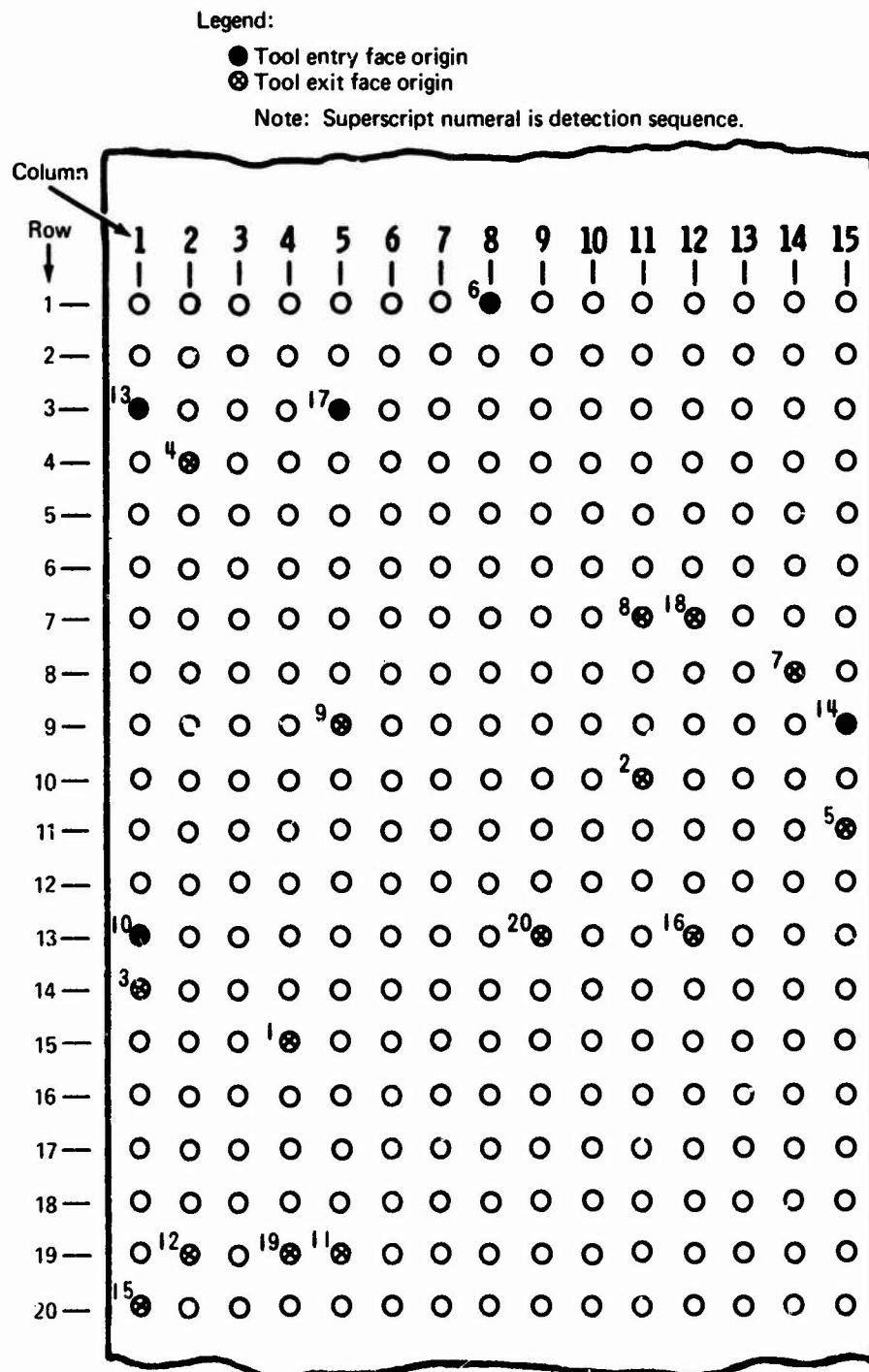
Figure 41.- Fatigue Crack Initiation Sites in Holes of Multihole Panel No. 1, Reference 2 (Al. Alloy 2024-T3 0.125 In. Thick)

59
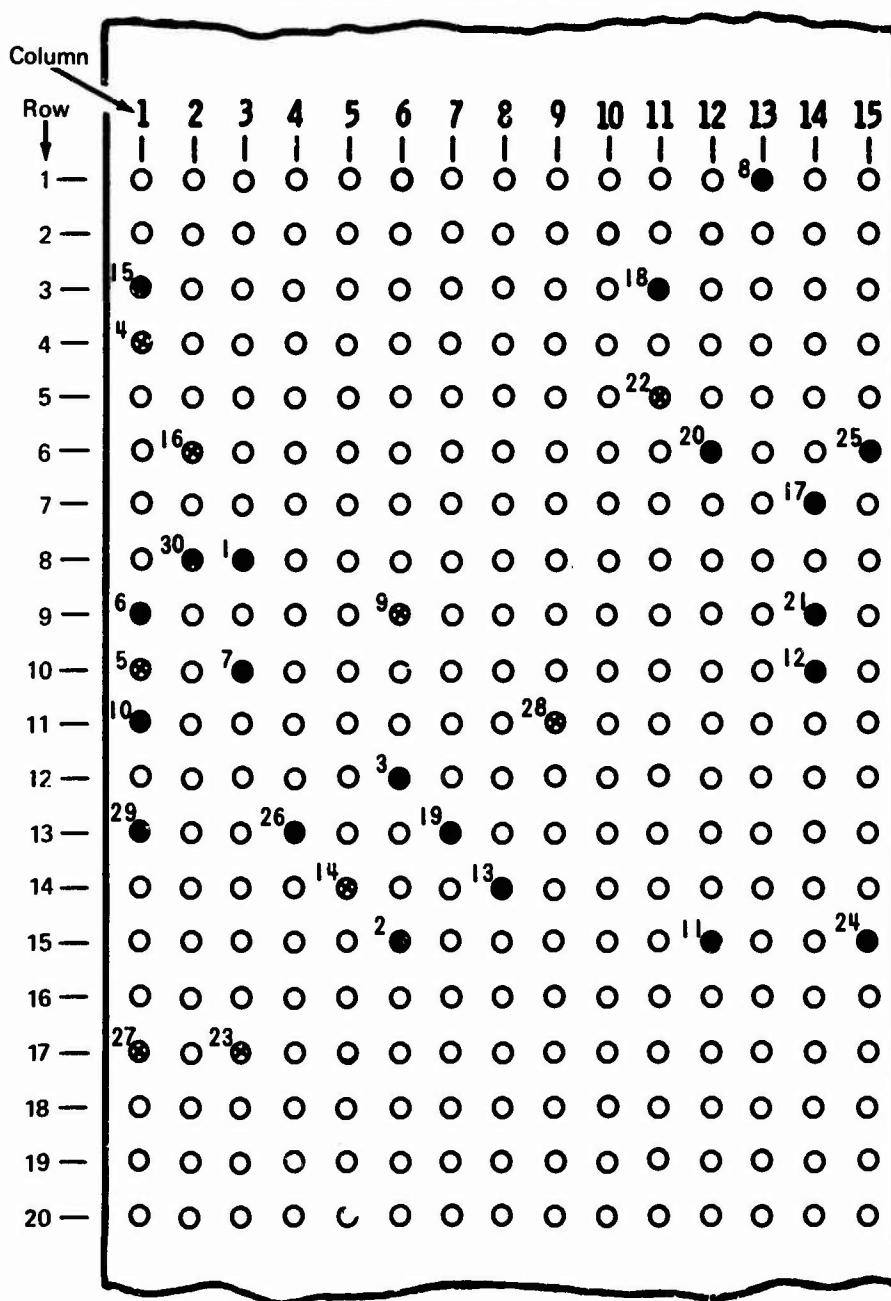
Figure 42.--Fatigue Crack Initiation Sites in Holes of Multihole Panel No. 2, Reference 2. (Al. Alloy 2024-T3, 0.125 In. Thick)
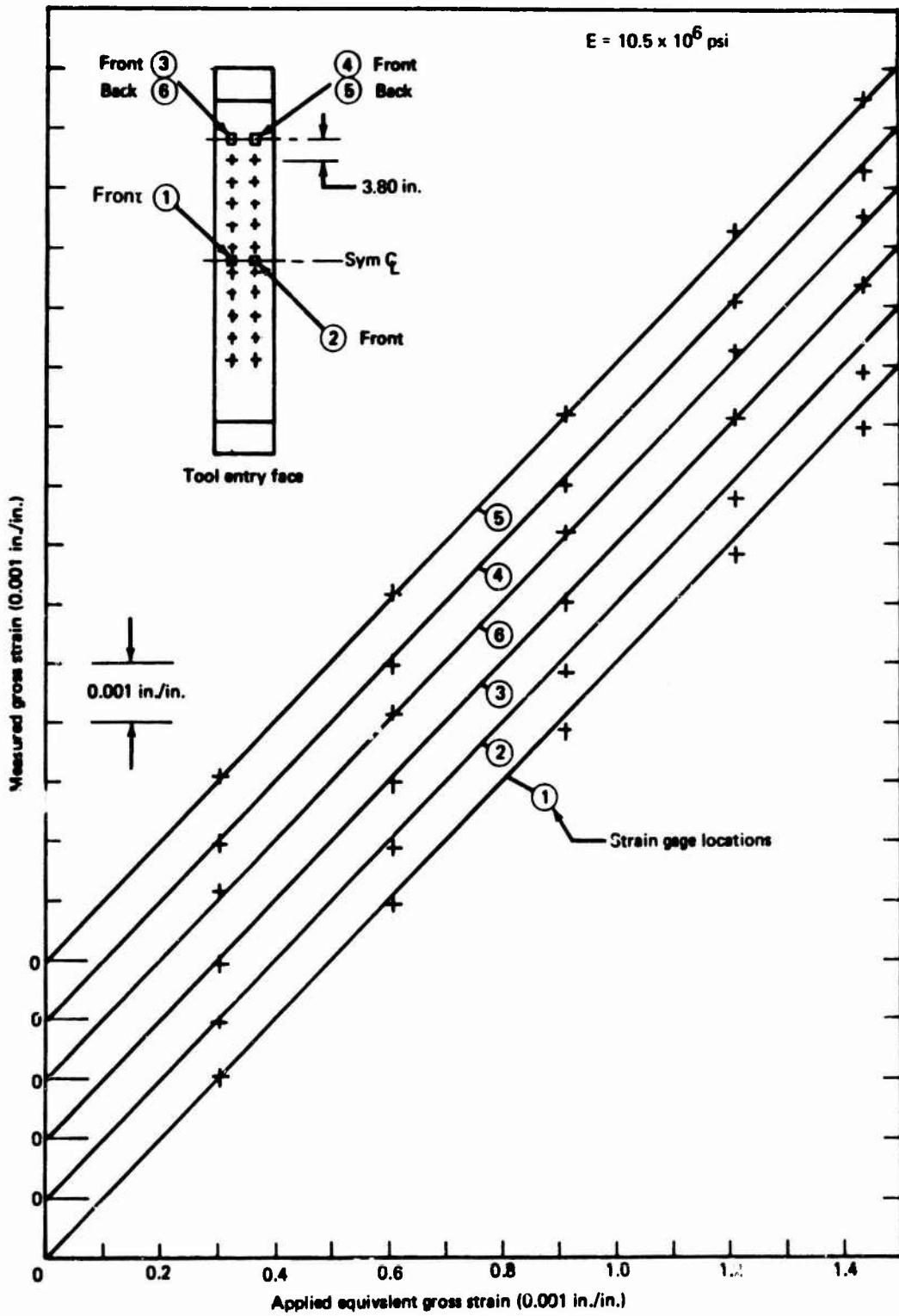
Figure 43 – Comparison of Measured Strains With Applied Equivalent Strains on Usage Simulation Specimen (Fig. 2a, Open Hole) Without Buckling Restraint Fixture

61
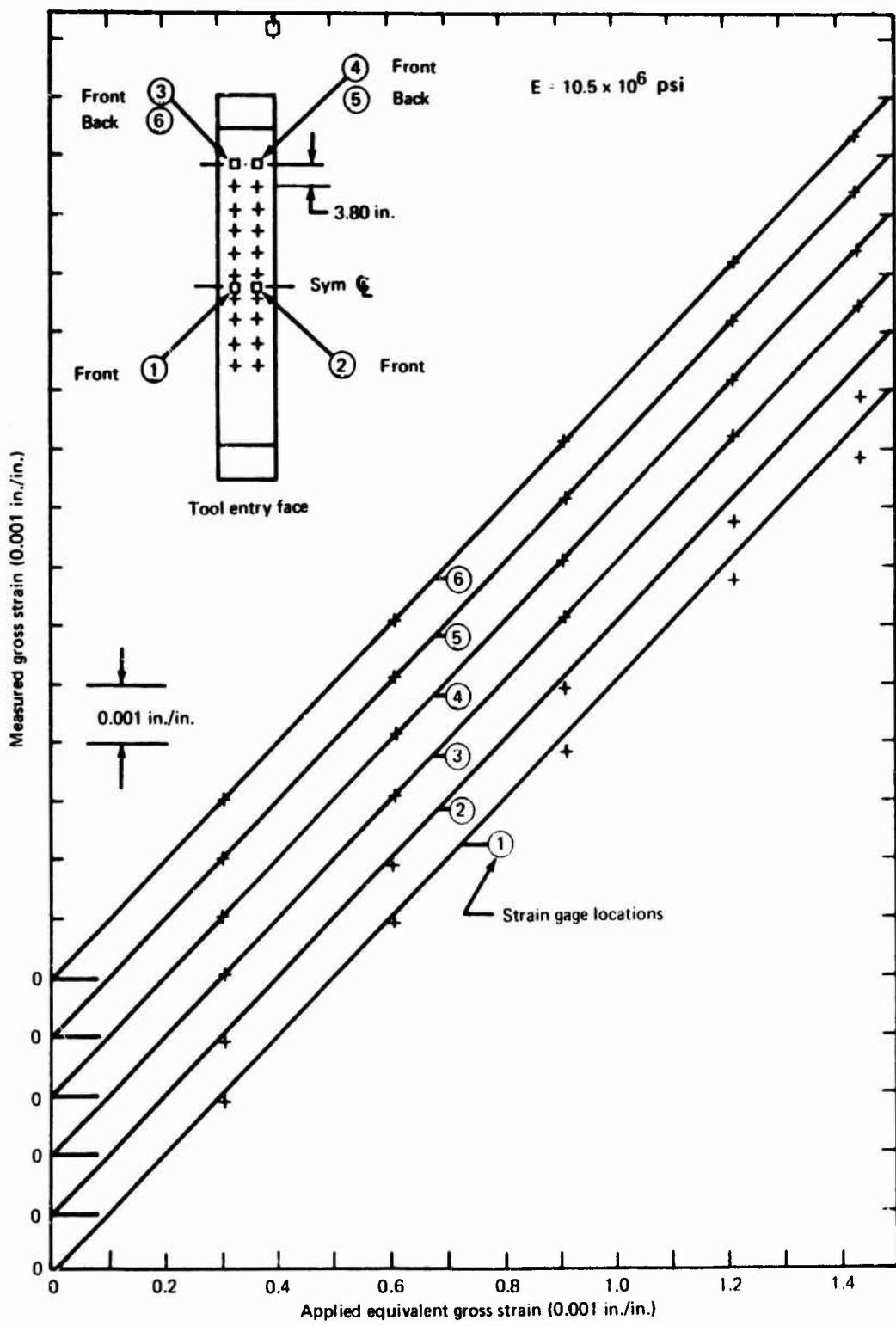
Figure 44. —Comparison of Measured Strains With Applied Equivalent Strains on Usage
Simulation Specimen (Fig. 2a, Open Hole) With Buckling Restraint Fixture

62
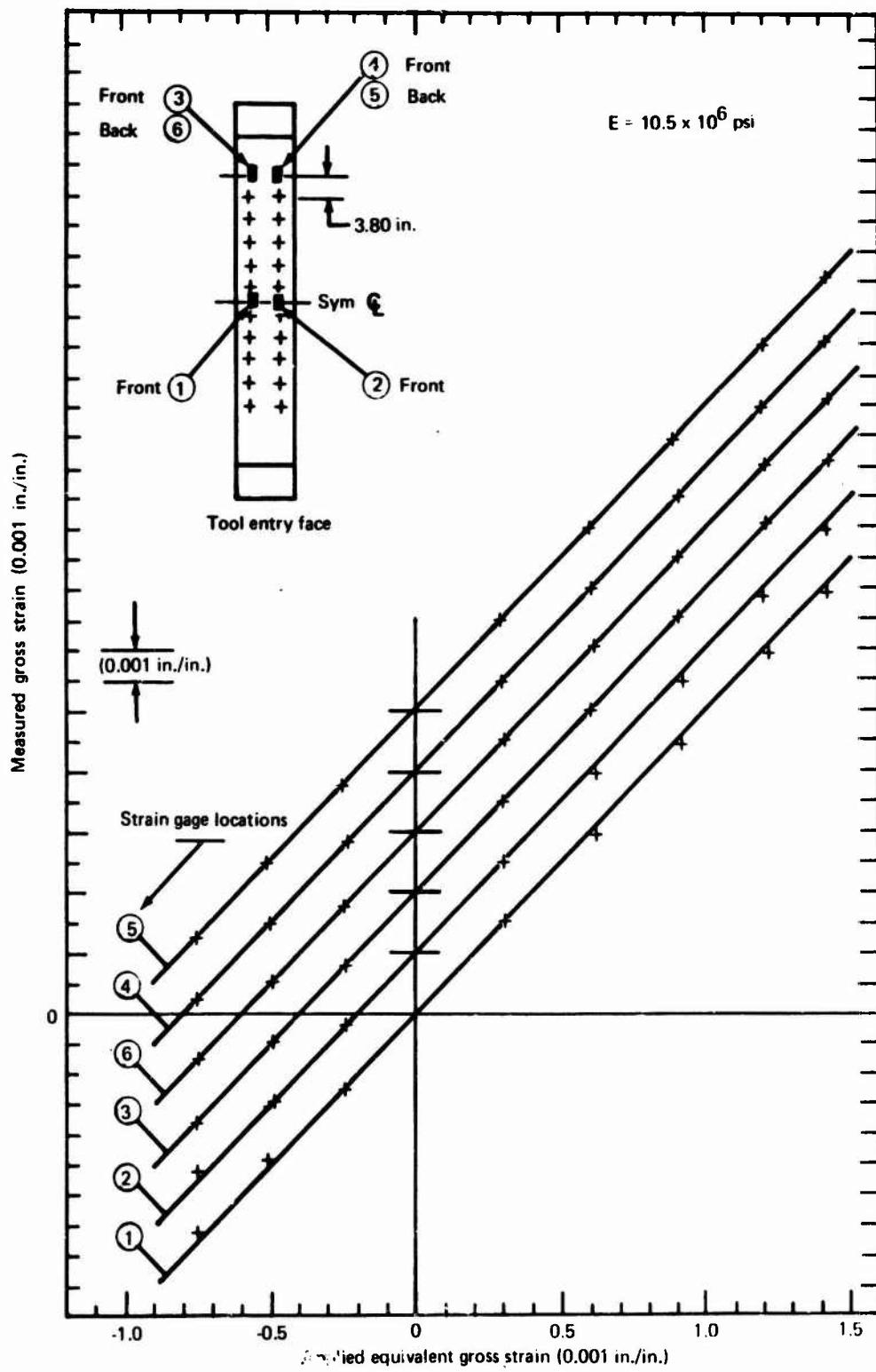
Figure 45. —Comparison of Measured Strains With Applied Equivalent Strains for Usage Simulation Specimen (Fig. 2a, Open Hole) With Buckling Restraint Fixture and Load Reversal

63
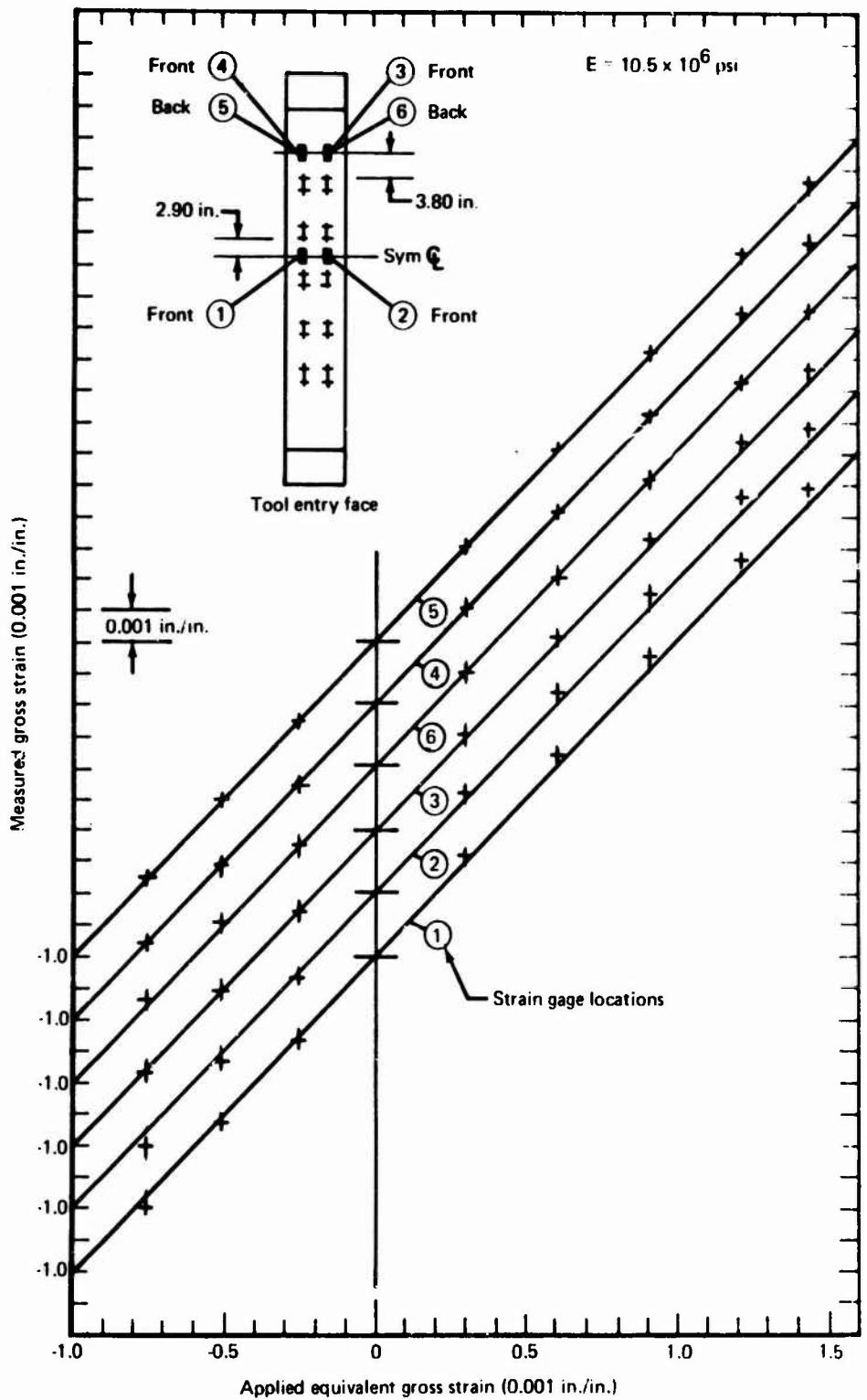
Figure 46. —Comparison of Measured Strains With Applied Equivalent Strains for Usage Simulation Specimen (Fig. 2c, Load Transfer Type I) With Buckling Restraint
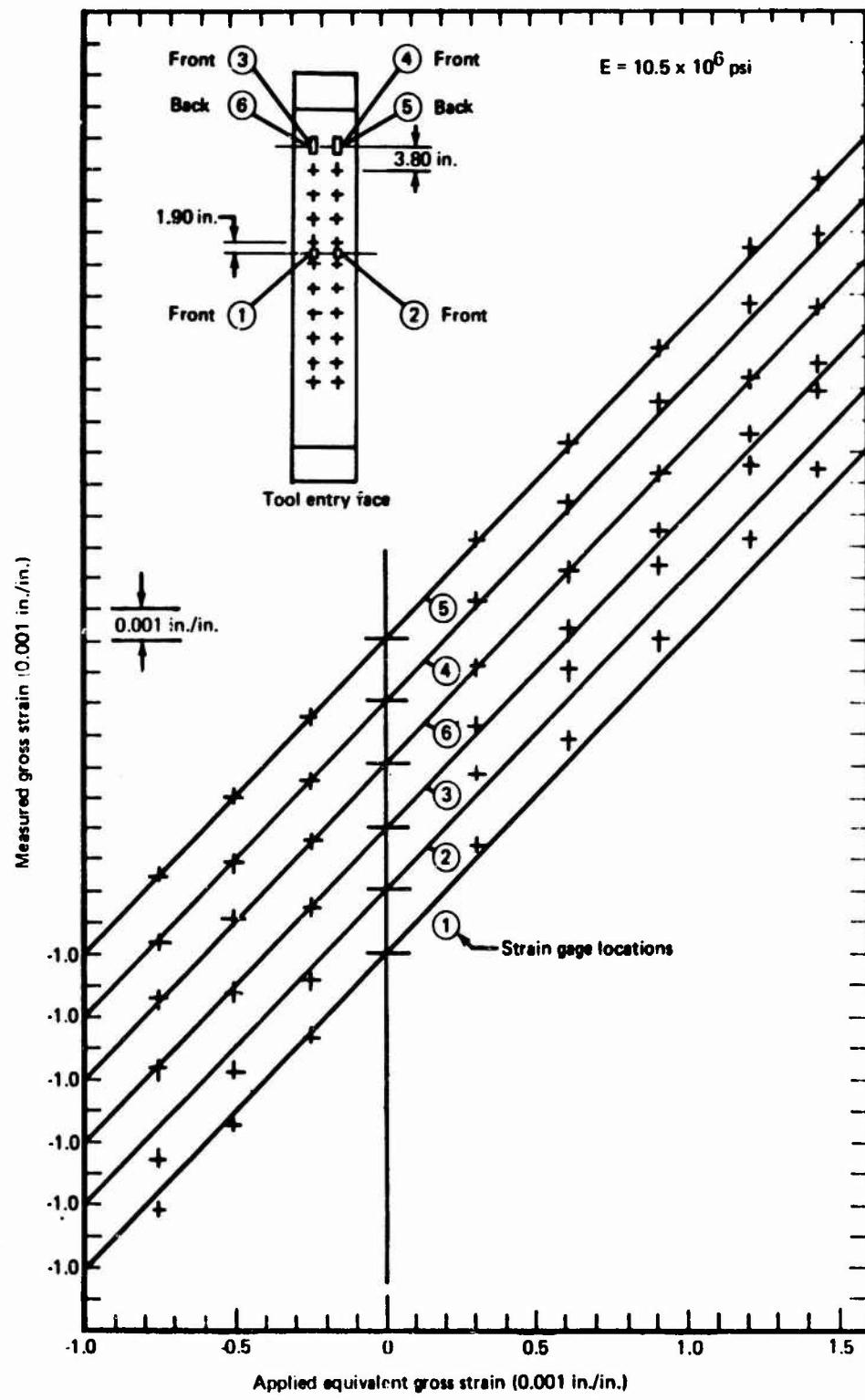
Figure 47. — *Comparison of Measured Strains With Applied Equivalent Strains for Usage Simulation Specimen (Fig. 2d, Load Transfer Type II) With Buckling Restraint*

65
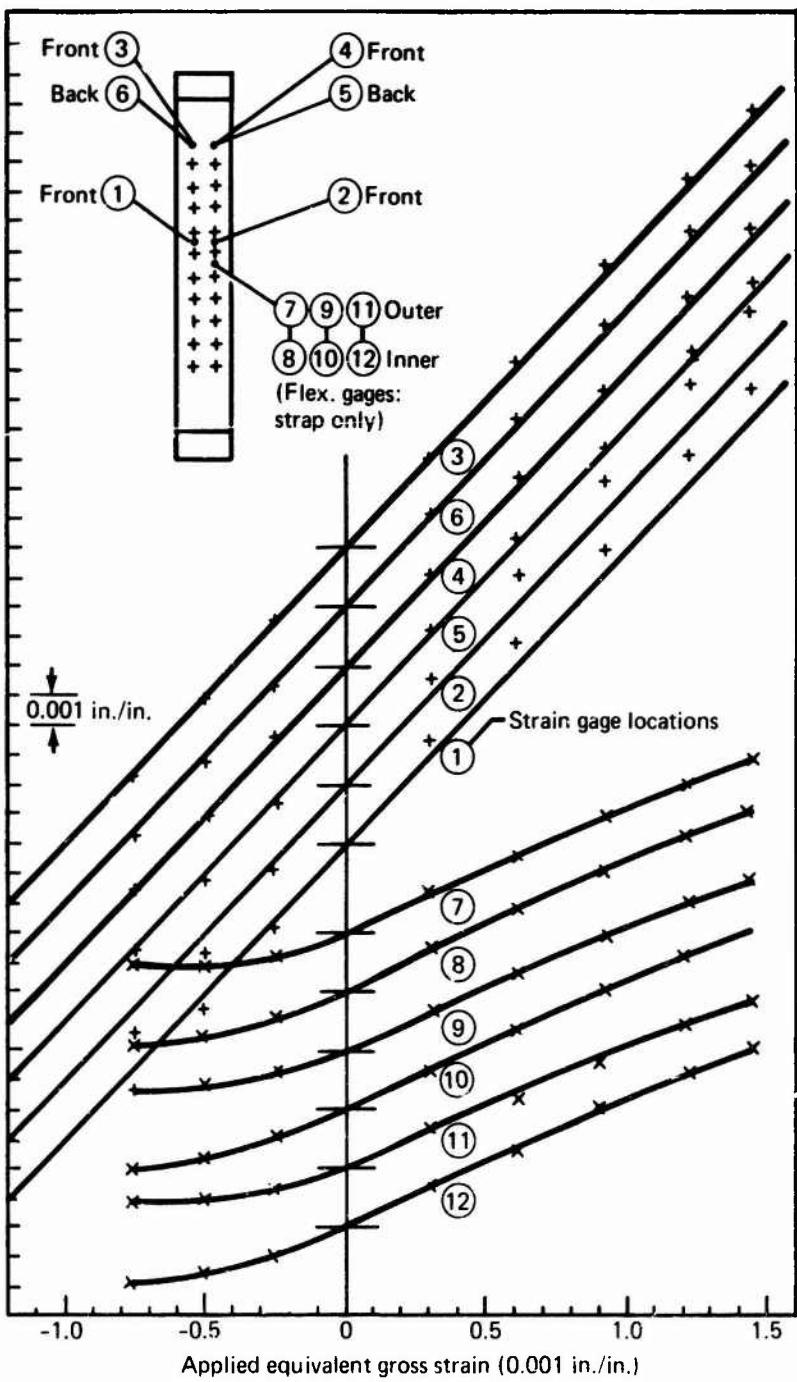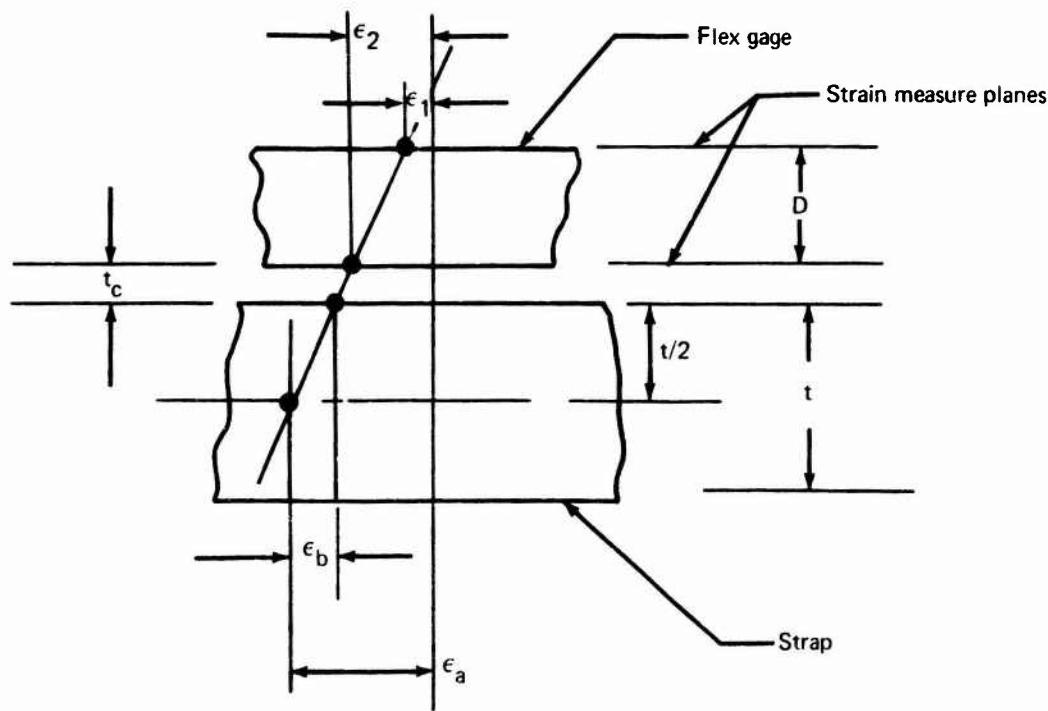
Figure 48. – Comparison of Measured and Applied Equivalent Strains for Basic Sheet and Load Transfer Straps of Usage Simulation Specimen (Fig. 2d) With Buckling Restraint

66

ϵ_1 = strain reading of outer or top gage in flexgage, in./in.

ϵ_2 = strain reading of inner or interface gage in flexgage, in./in.

ϵ_b = calculated bending strain at instrumented or free surface of strap, in./in.

ϵ_a = calculated axial of strap, in./in.

t = thickness of strap, in (0.080 in.)

t_c = estimated thickness of gage adhesive, in. (0.003 in.)

D = distance between gages in flexgage in. (0.021 in. for gages used in this test)

Accordingly, $\epsilon_a = \epsilon_2 - \frac{t}{2D}(\epsilon_1 - \epsilon_2) - \frac{t_c}{D}(\epsilon_1 - \epsilon_2)$ or

$$\epsilon_b = \frac{t}{2D}(\epsilon_1 - \epsilon_2)$$

Figure 49. Estimation of Load Transfer Strains in Loading Straps of Usage Simulation Specimens (Fig. 2d) With Buckling Restraint

67
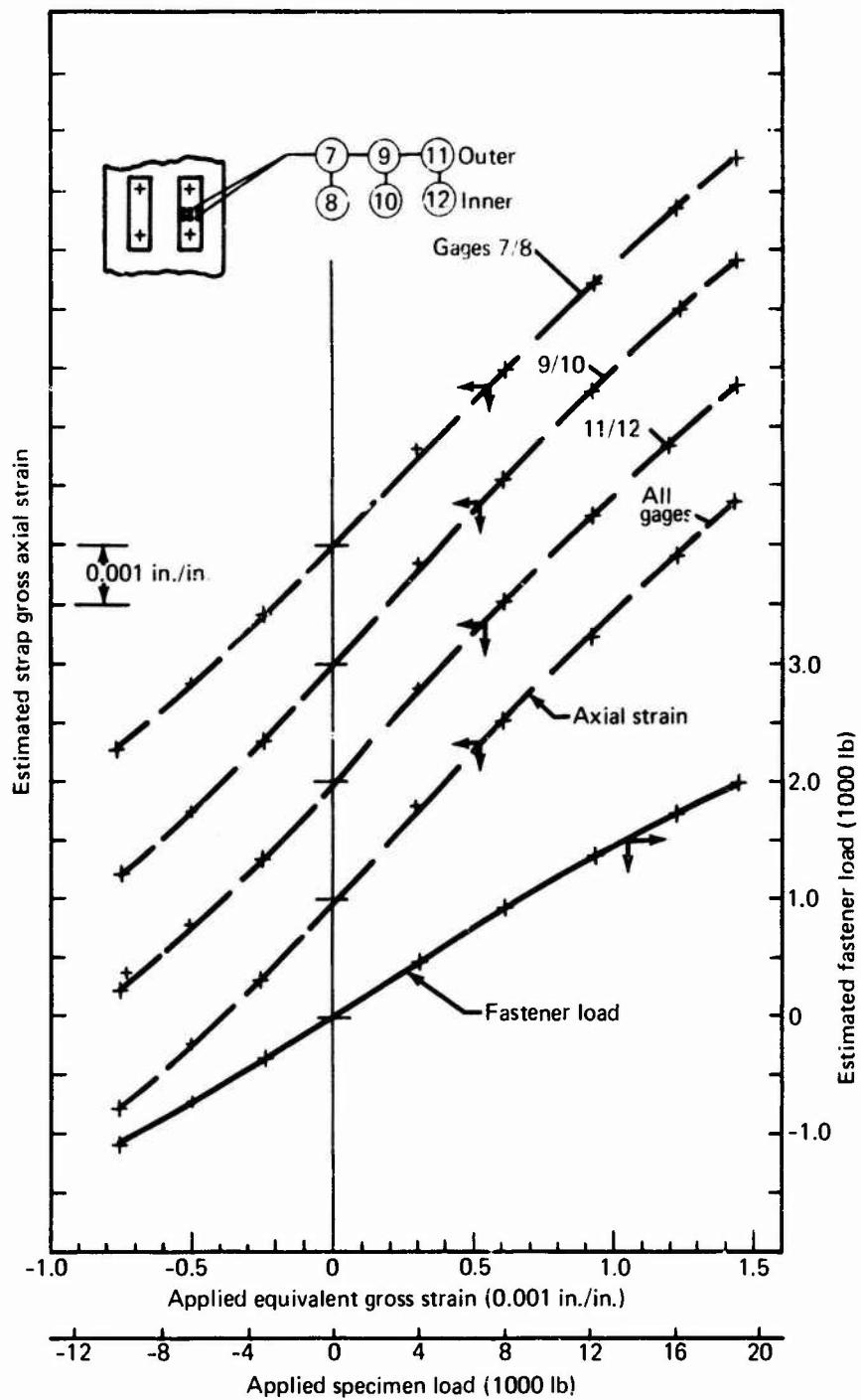
Figure 50.–Calculated Axial Strains and Loads in Load Transfer Straps of Usage Simulation
Specimen (Fig. 2d) With Buckling Restraint

68

Note:

All crack locations are identified as extending to the right or to the left of the open hole or fastener location when viewed looking at the tool entry face of the test specimen.

Up
in
test
machine

Hole or fastener locations, 20 places

Part number location (ref)

Tool Entry Face

Tool Exit Face
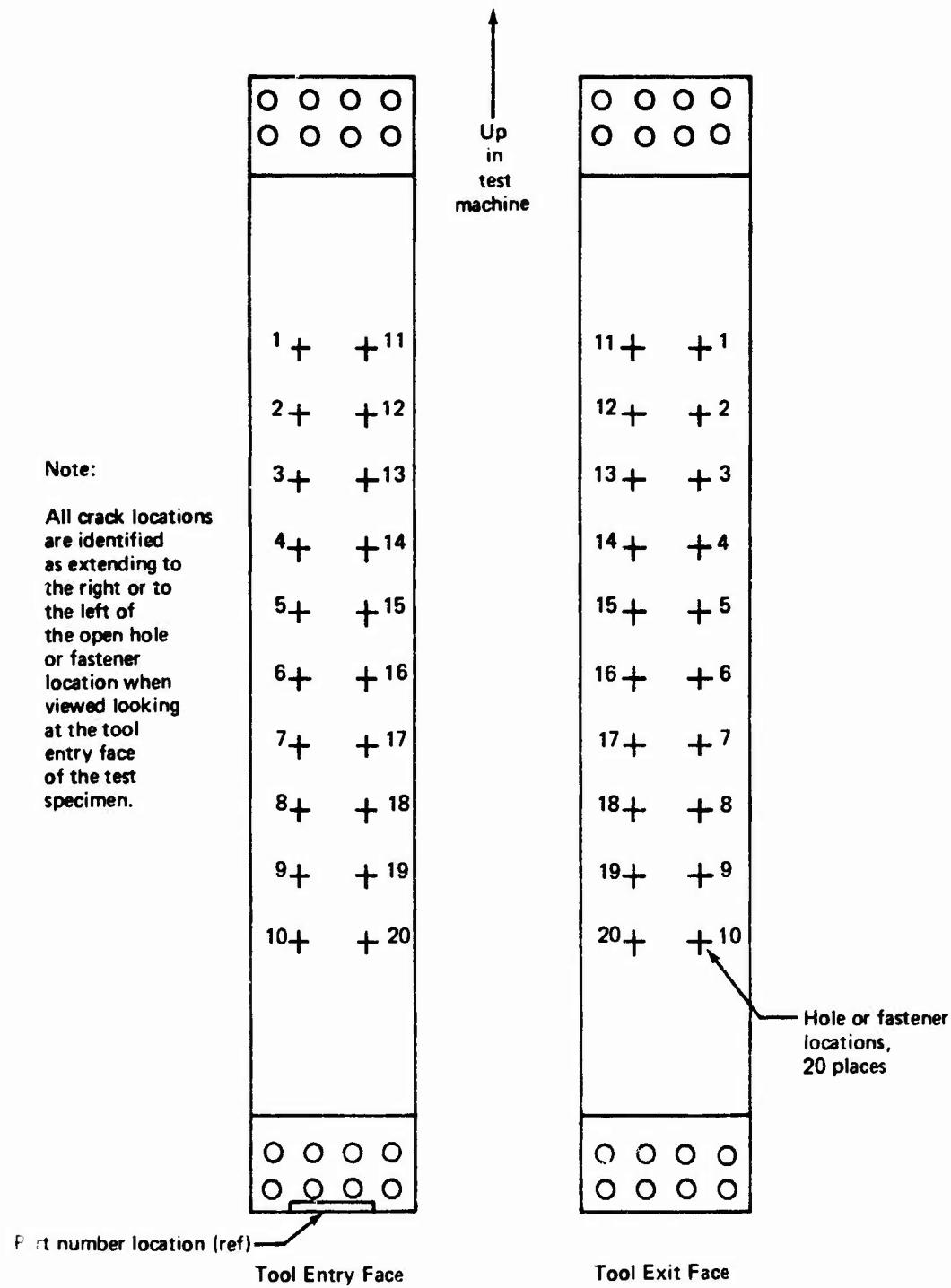
Figure 51. – Identification of Hole or Fastener Location and Crack Growth Direction in Usage Simulation Test Specimen

69

Figure 53.– Fatigue Crack Initiation Sites in Usage Simulation Specimen No. 2A9 (Fig. 2, Load Transfer, Type I) Detected During Testing and After Disassembly
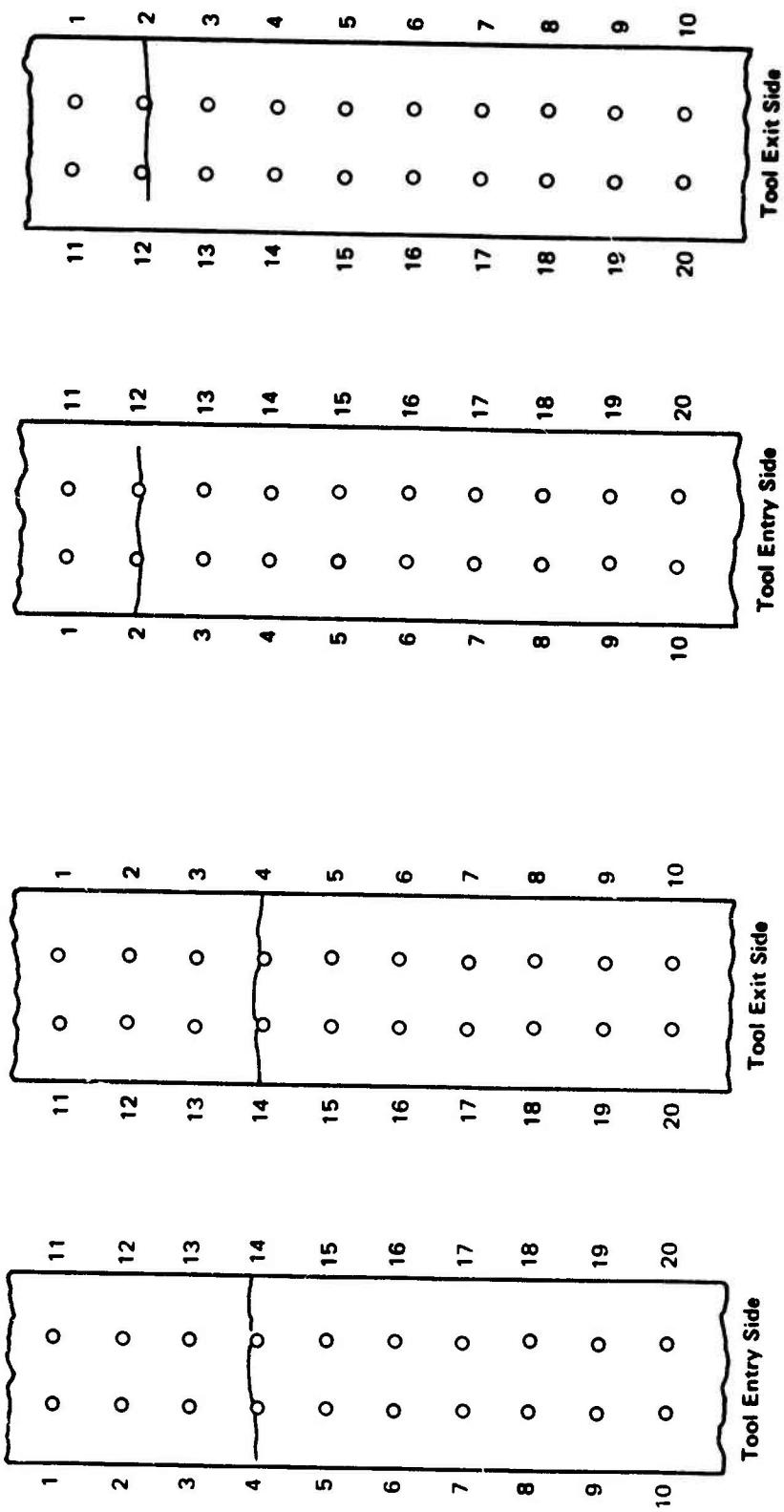
Figure 52.– Fatigue Crack Initiation Sites in Usage Simulation Specimen No. 2A8 (Fig. 2, Filled Hole) Detected During Testing and After Disassembly

70

a. Sketch of Crack Locations on Both Faces of Specimen

*Figure 55.— Fatigue Crack Initiation Sites in Usage
Simulation Specimen No. 2A11 (Fig. 2,
Load Transfer, Type II) Detected During
Testing and After Disassembly*
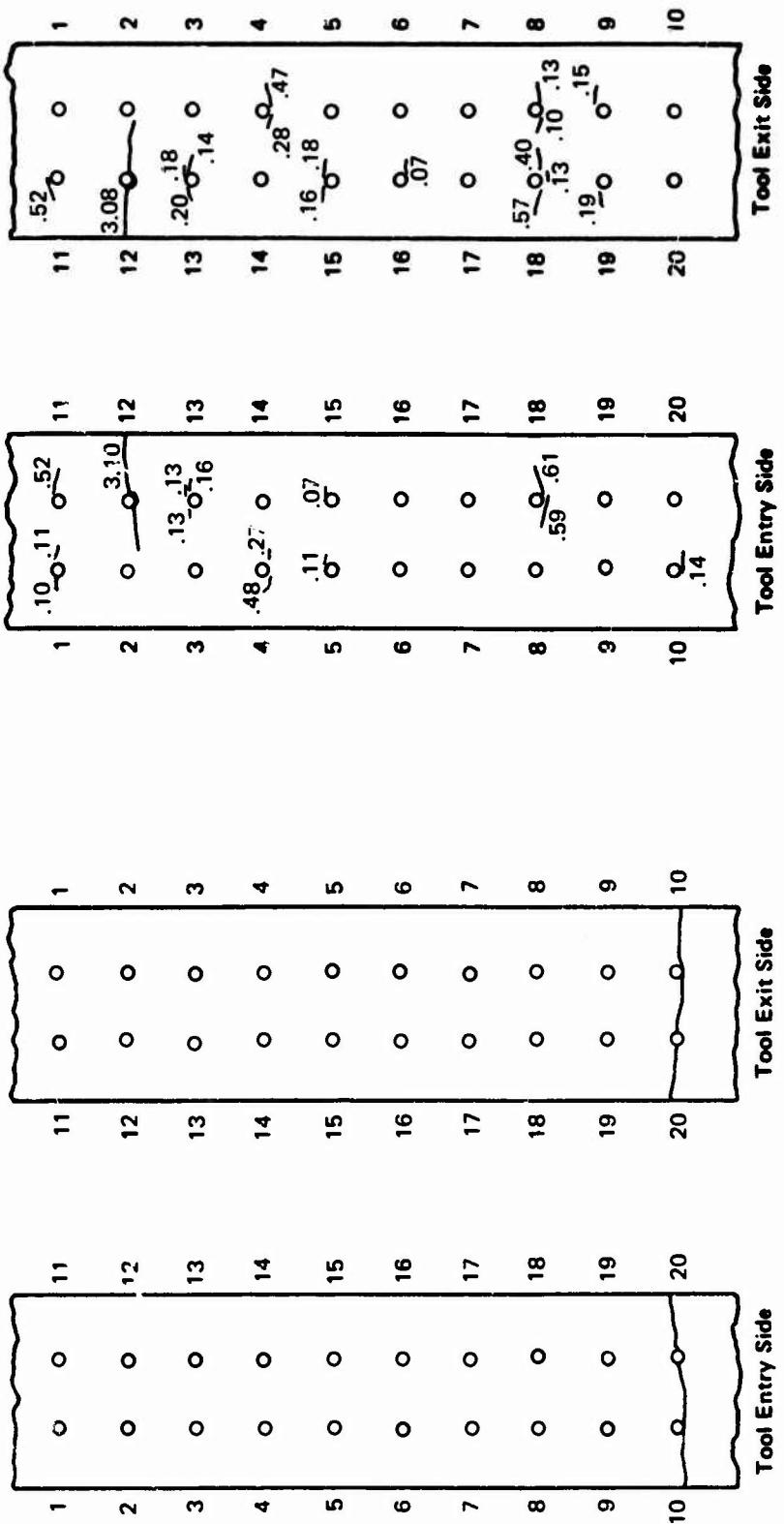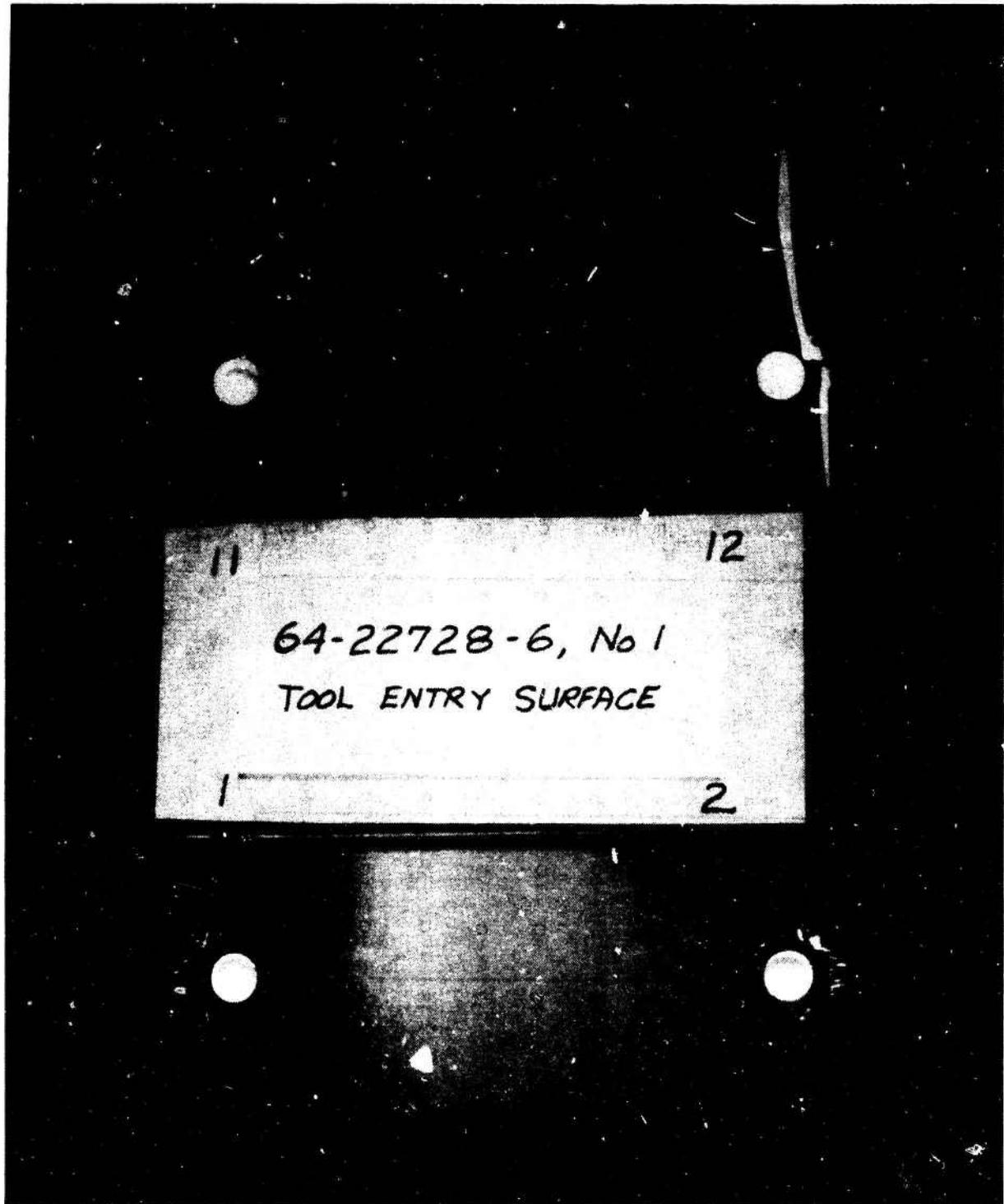
*Figure 54.— Fatigue Crack Initiation Sites in Usage
Simulation Specimen No. 2A10 (Fig. 2,
Load Transfer, Type I) Detected During
Testing and After Disassembly*
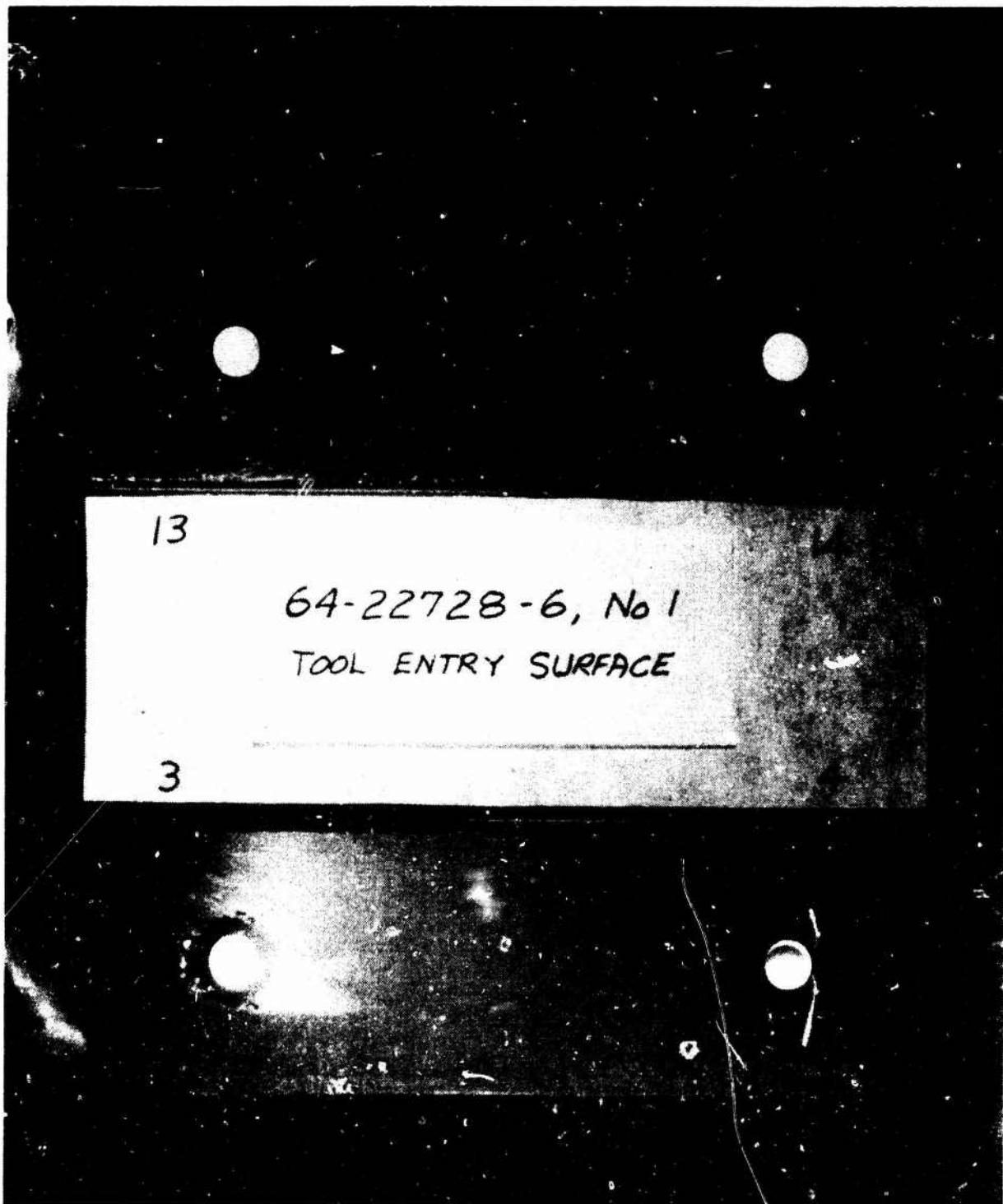
b. Specimen 2A11 Fluorescent Penetrant Identification of Fatigue Cracks and Local Surface Fretting on Tool Entry Curface After Disassembly at Fasteners 1, 2, 11, and 12

Figure 55.–Continued

72

c. Specimen 2A11 Fluorescent Penetrant Identification of Fatigue Cracks and Local Surface Fretting on Tool Exit Surface After Disassembly at Fasteners 1, 2, 11, and 12

Figure 55.—Continued

73
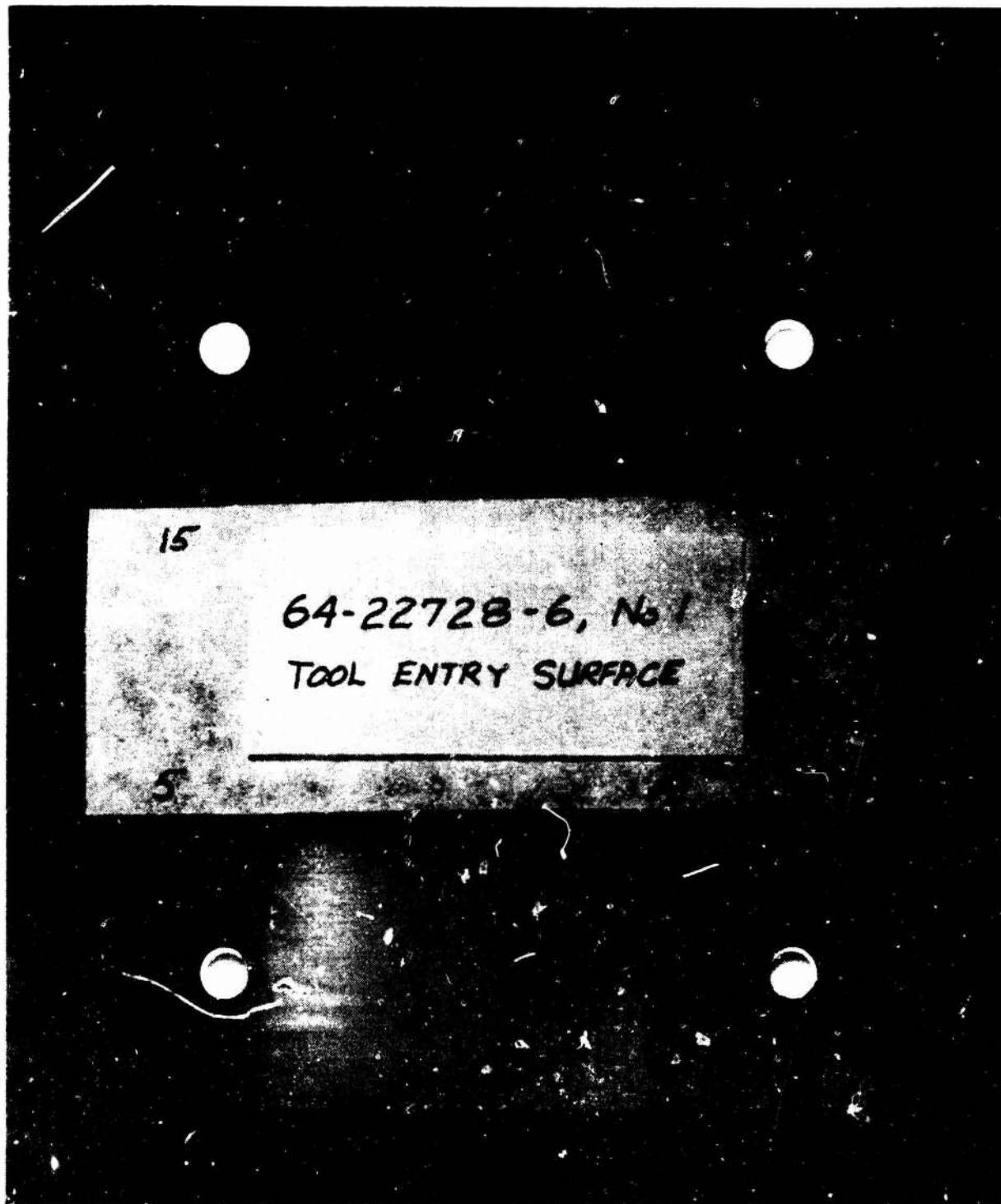
d. Specimen 2A11 Fluorescent Penetrant Identification of Fatigue Cracks and Local Surface Fretting on Tool Entry Surface After Disassembly at Fasteners 3, 4, 13, and 14

Figure 55. — Continued
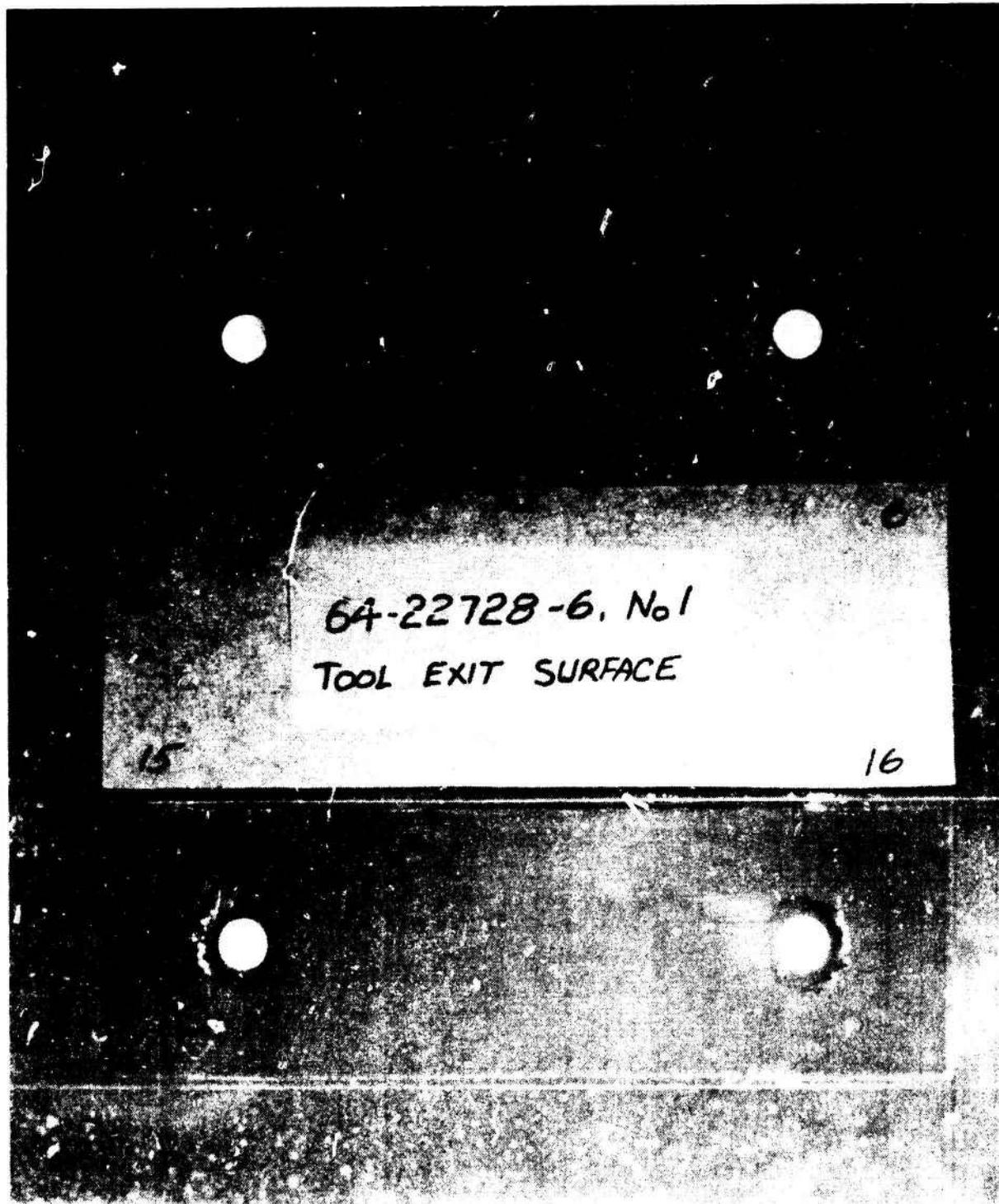
e. Specimen 2A11 Fluorescent Penetrant Identification of Fatigue Cracks and Local Surface Fretting on Tool Exit Surface After Disassembly at Fasteners 3, 4, 13, and 14

Figure 55.--Continued
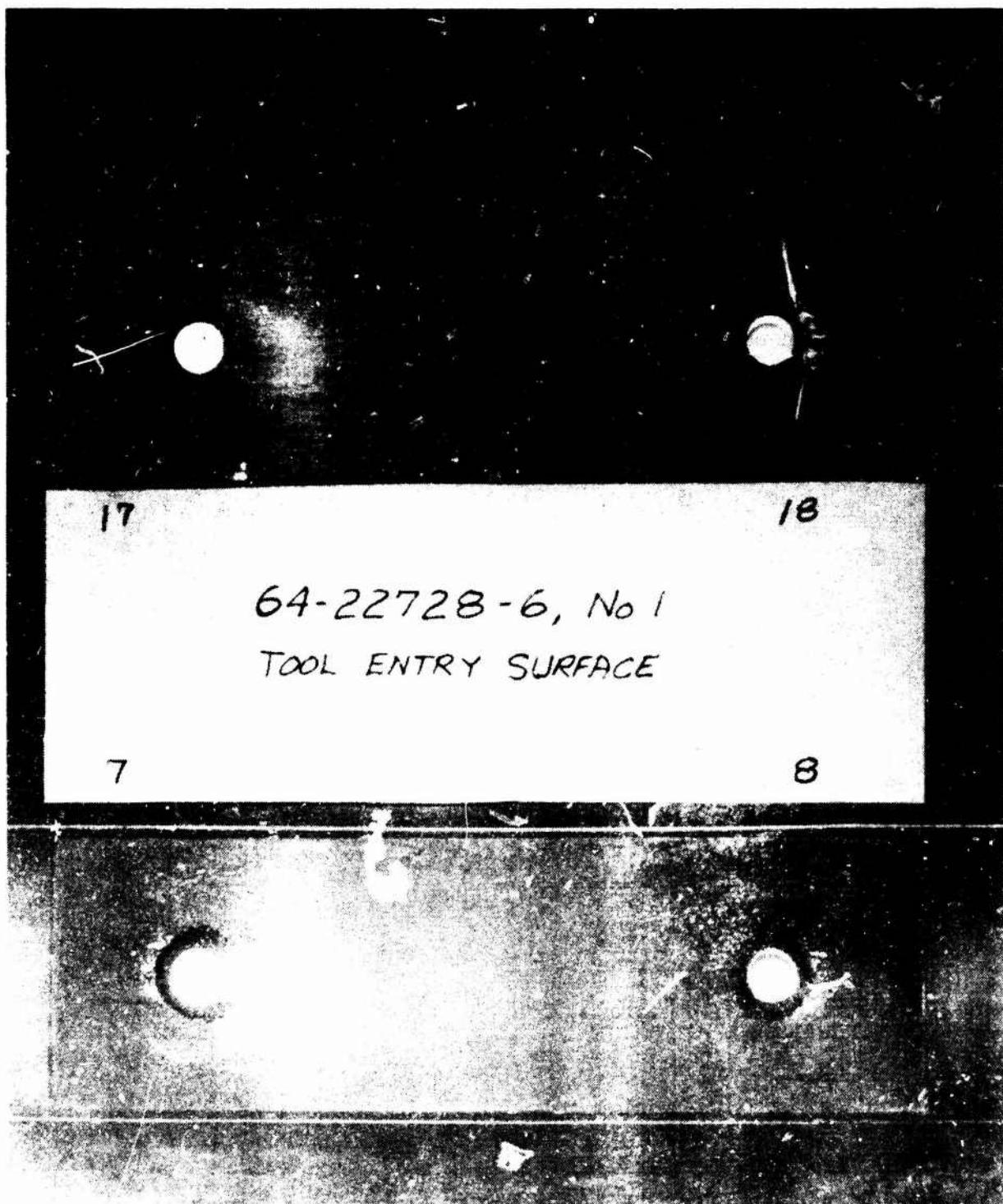
f. Specimen 2A11 Fluorescent Penetrant Identification of Fatigue Cracks and Local Surface Fretting on Tool Entry Surface After Disassembly at Fasteners 5, 6, 15, and 16

Figure 55.--Continued

76
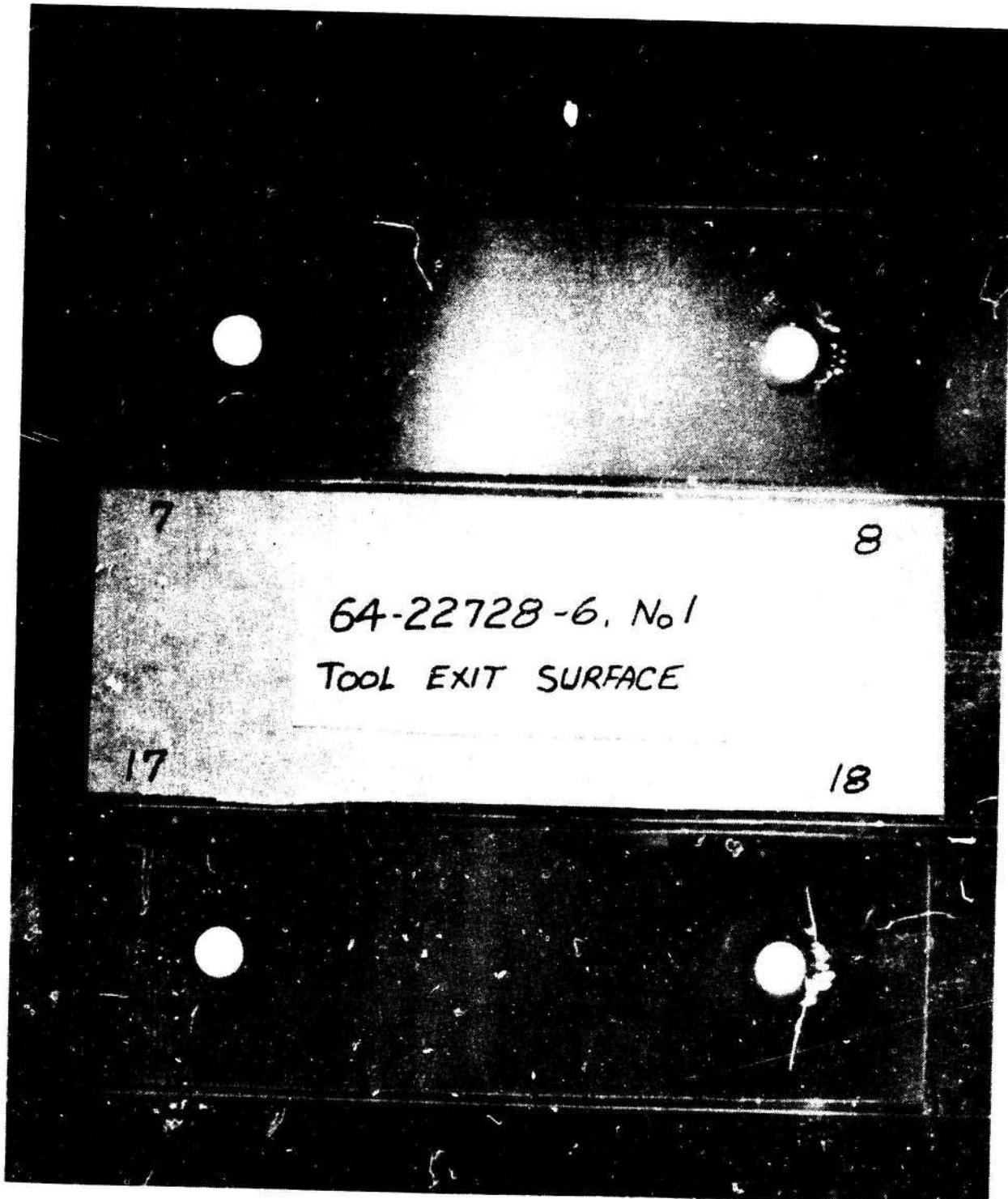
g.   Specimen 2A11 Fluorescent Penetrant Identification of Fatigue Cracks and Local Surface Fretting on Tool Exit Surface After Disassembly at Fasteners 5, 6, 15, and 16

Figure 55.—Continued

77
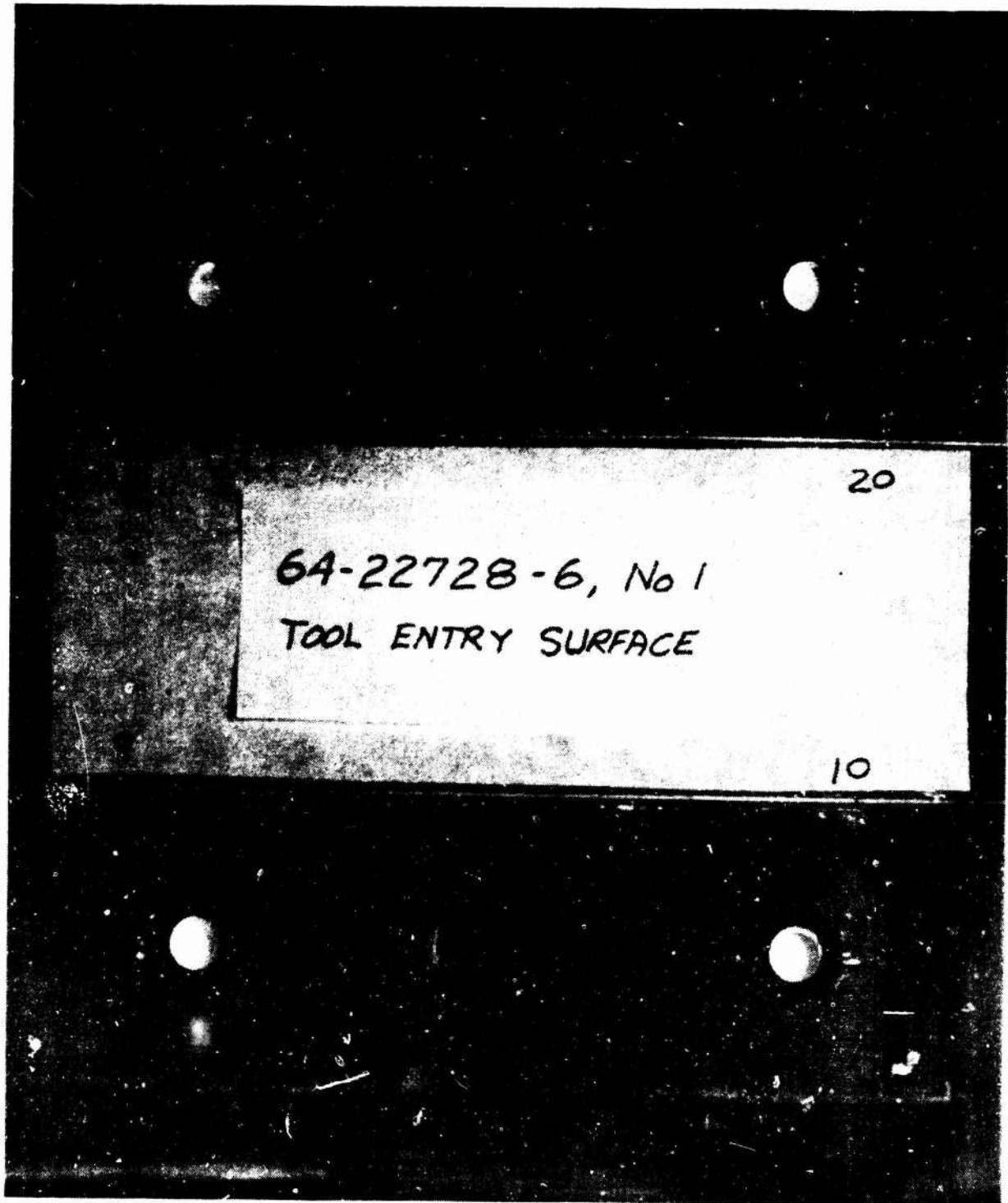
h. Specimen 2A11 Fluorescent Penetrant Identification of Fatigue Cracks and Local Surface Fretting on Tool Entry Surface After Disassembly at Fasteners 7, 8, 17, and 18

Figure 55.—Continued

i. Specimen 2A i1 Fluorescent Penetrant Identification of Fatigue Cracks and Local Surface Fretting on Tool Exit Surface After Disassembly at Fasteners 7, 8, 17, and 18

Figure 55.- Continued

j.   Specimen 2A11 Fluorescent Penetrant Identification of Fatigue Cracks and Local Surface Fretting
     on Tool Entry Surface After Disassembly at Fasteners 9, 10, 19, and 20

Figure 55.– Continued

k. Specimen 2A11 Fluorescent Penetrant Identification of Fatigue Cracks and Local Surface Fretting on Tool Exit Surface After Disassembly at Fasteners 9, 10, 19, and 20

Figure 55.—Concluded

Figure 57.— Fatigue Crack Initiation Sites in Usage Simulation Specimen No. 2A17 (Fig. 2, Load Transfer, Type II) Detected During Testing and After Disassembly
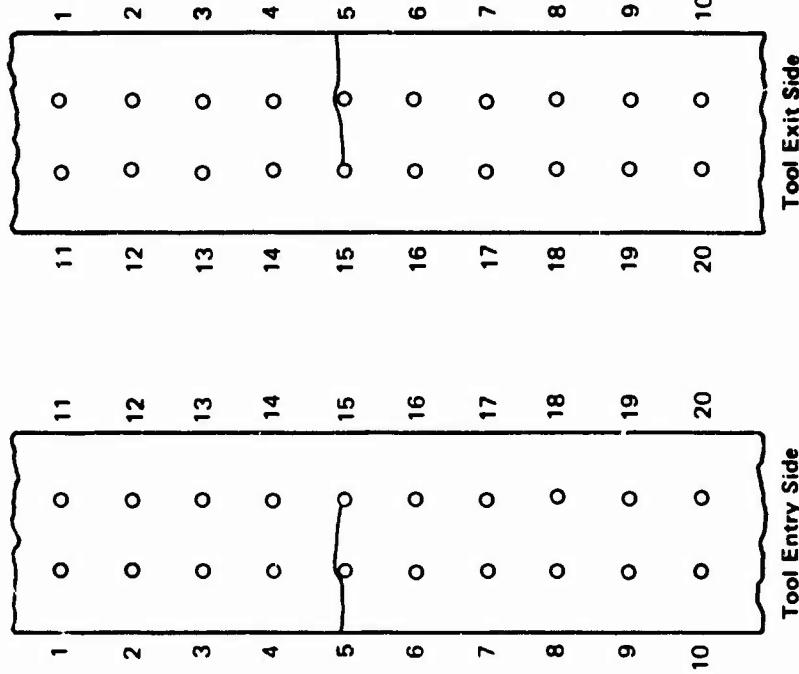
Figure 56.— Fatigue Crack Initiation Sites in Usage Simulation Specimen No. 2A12 (Fig. 2, Load Transfer, Type II) Detected During Testing and After Disassembly

82

Figure 59. – Fatigue Crack Initiation Sites in Usage Simulation Specimen No. 2A19 (Fig. 2, Load Transfer, Type II) Detected During Testing and After Disassembly

Figure 58. – Fatigue Crack Initiation Sites in Usage Simulation Specimen No. 2A18 (Fig. 2, Load Transfer, Type II) Detected During Testing and After Disassembly

83
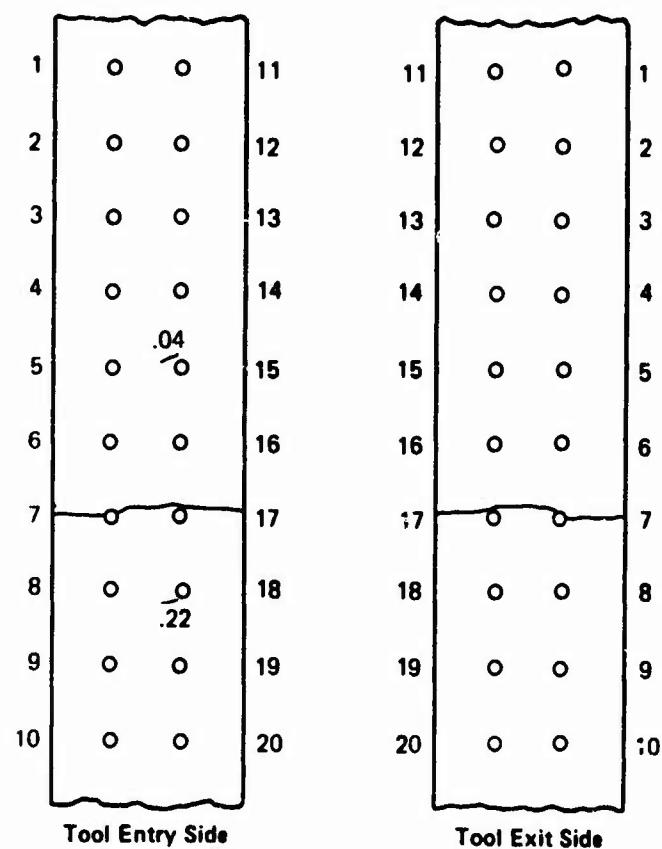
Figure 60.—Fatigue Crack Initiation Sites in Usage Simulation Specimen No. 2A20 (Fig. 2, Load Transfer, Type I) Detected During Testing and After Disassembly
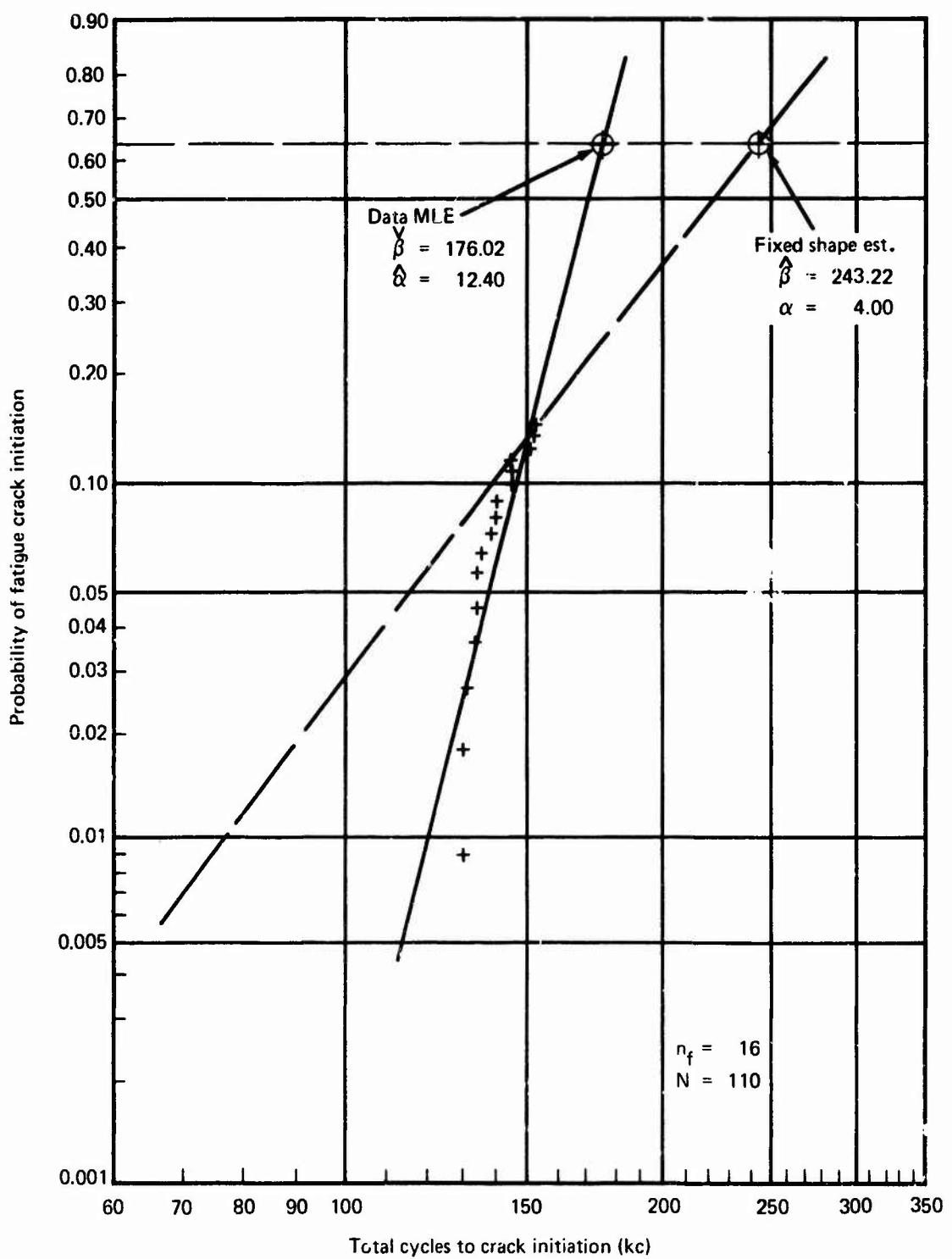
Figure 61.—Weibull Cumulative Probability Representation of Fatigue Crack
Initiation Results on Structural Simulation Specimen A1
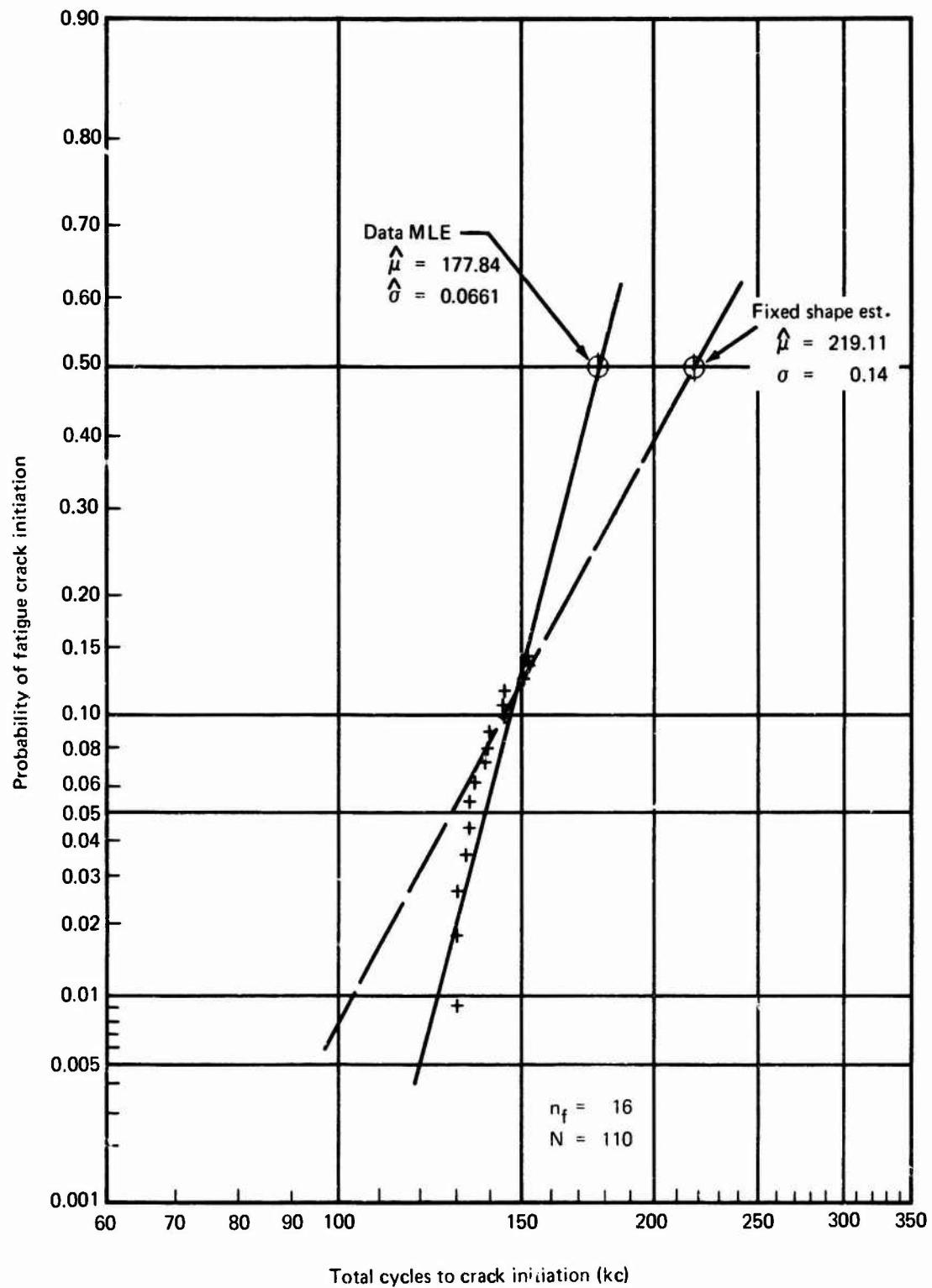
Figure 62. — Log-Normal Cumulative Probability Representation of Fatigue Crack Initiation Results on Structural Simulation Specimen A1
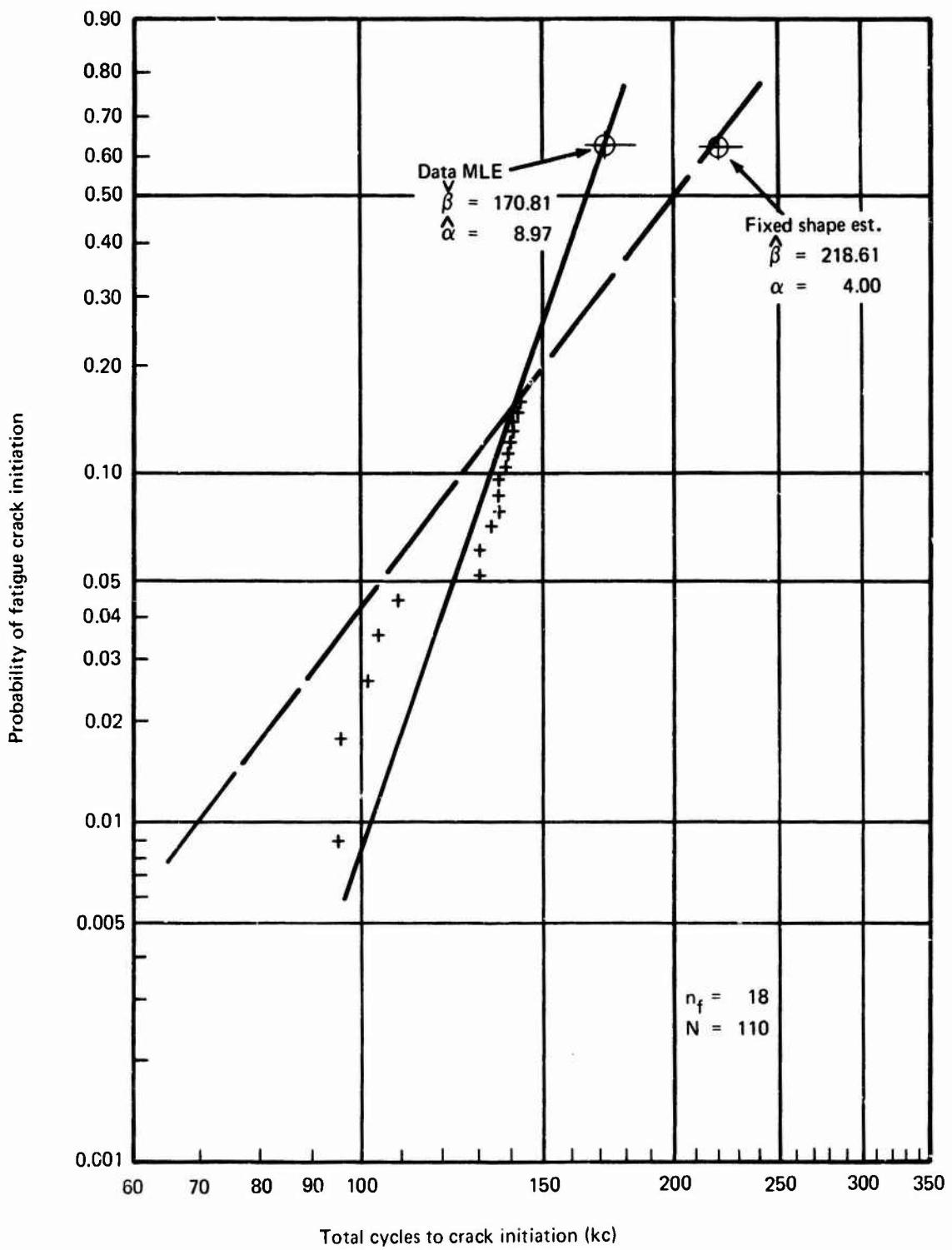
Figure 63.—Weibull Cumulative Probability Representation of Fatigue Crack Initiation Results on Structural Simulation Specimen A2
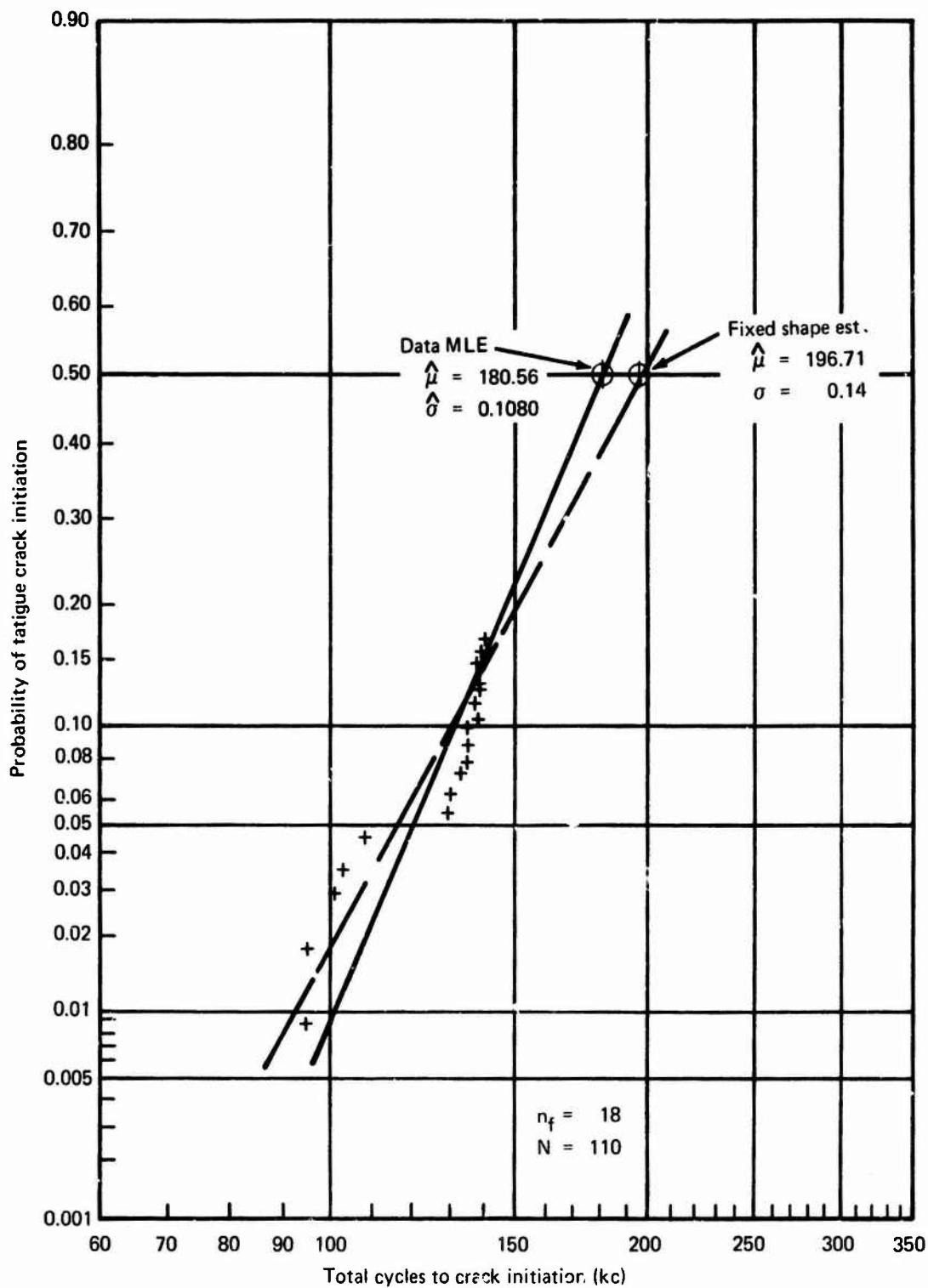
Figure 64. – Log-Normal Cumulative Probability Representation of Fa.igue Crack
Initiation Results on Structural Simulation Specimen A2
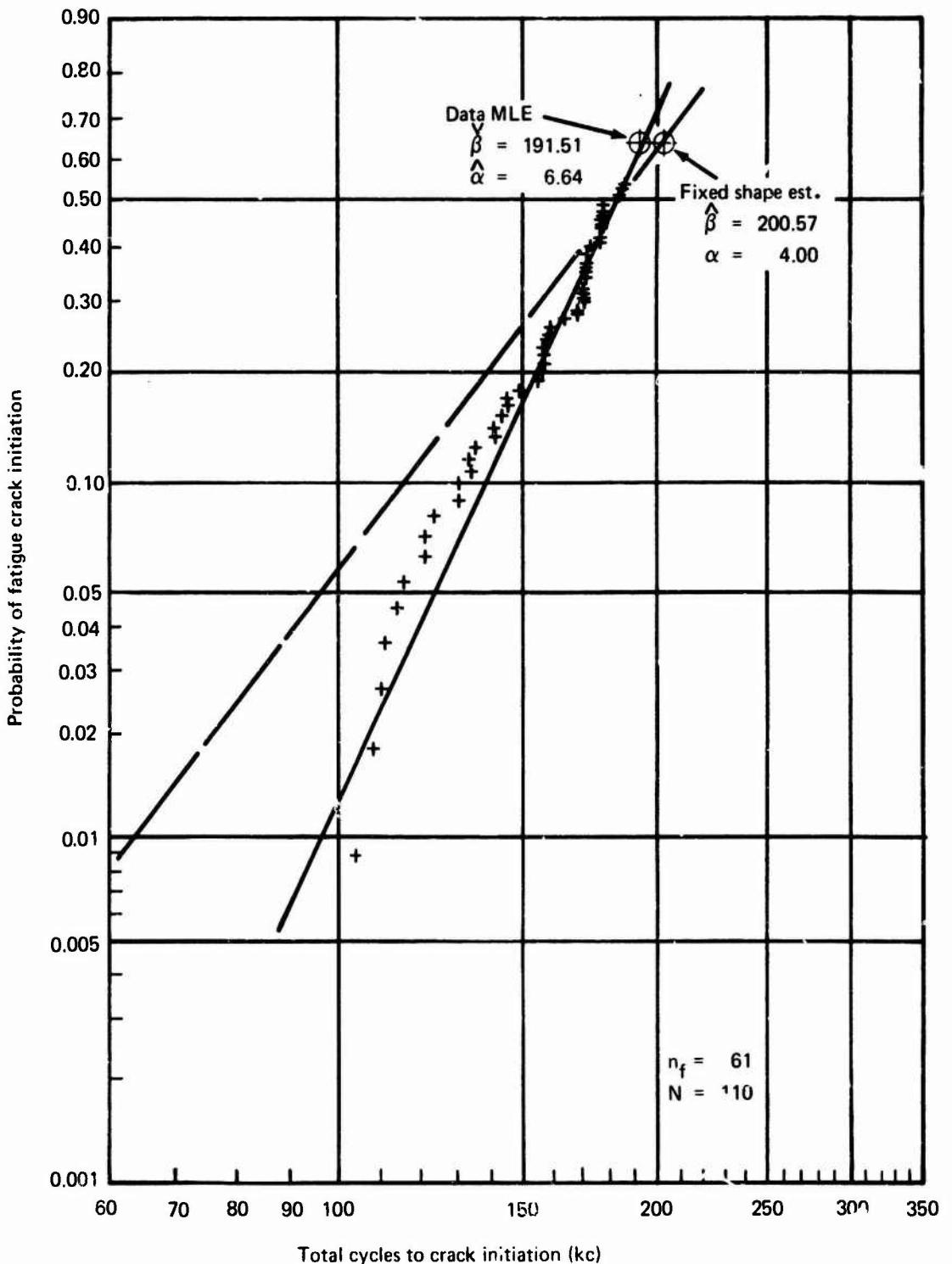
Figure 65. — Weibull Cumulative Probability Representation of Fatigue Crack
Initiation Results From Structural Simulation Specimen A3

89
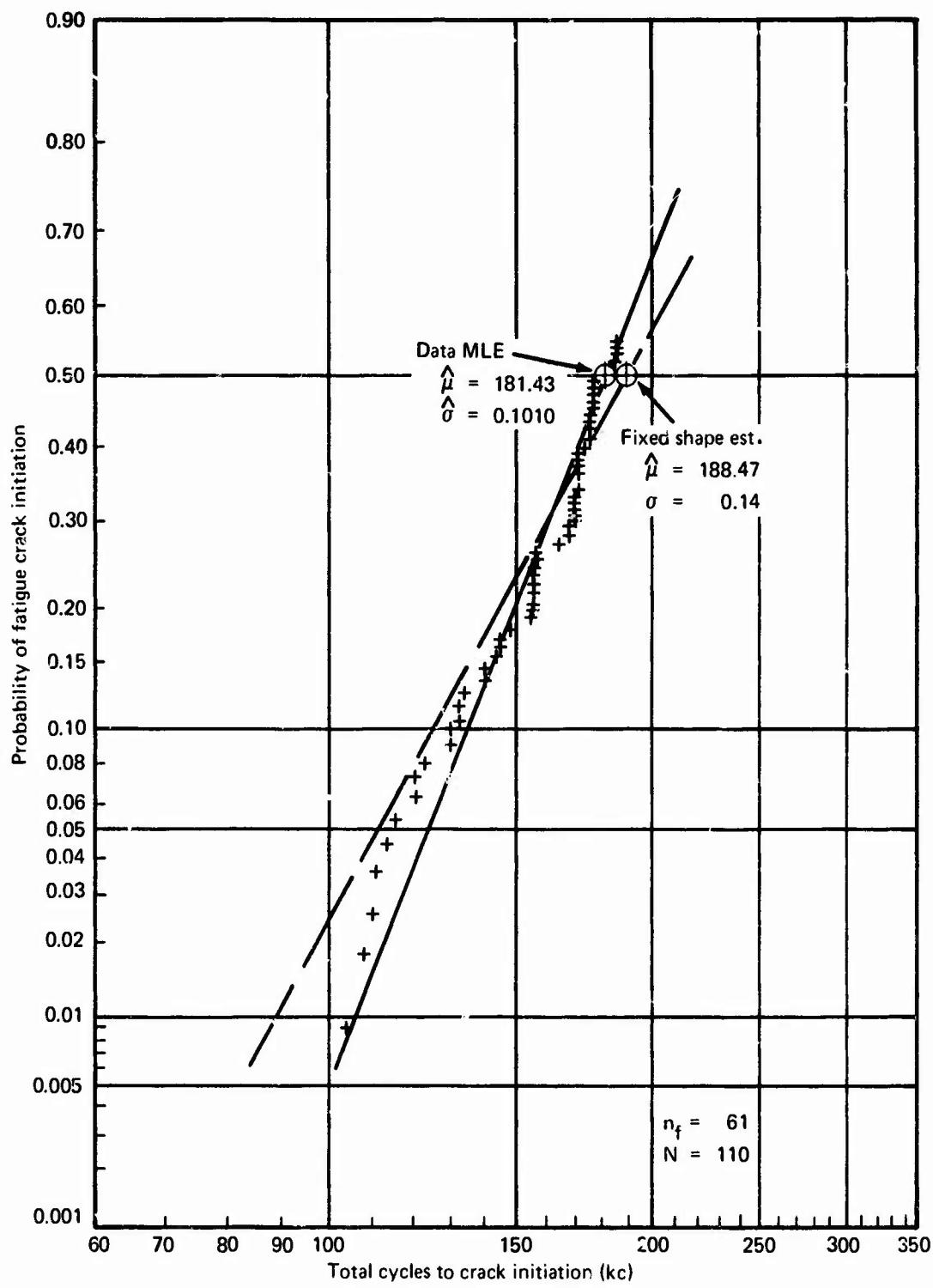
Figure 66.—Log-Normal Cumulative Probability Representation of Fatigue Crack Initiation Results From Structural Simulation Specimen A3

90
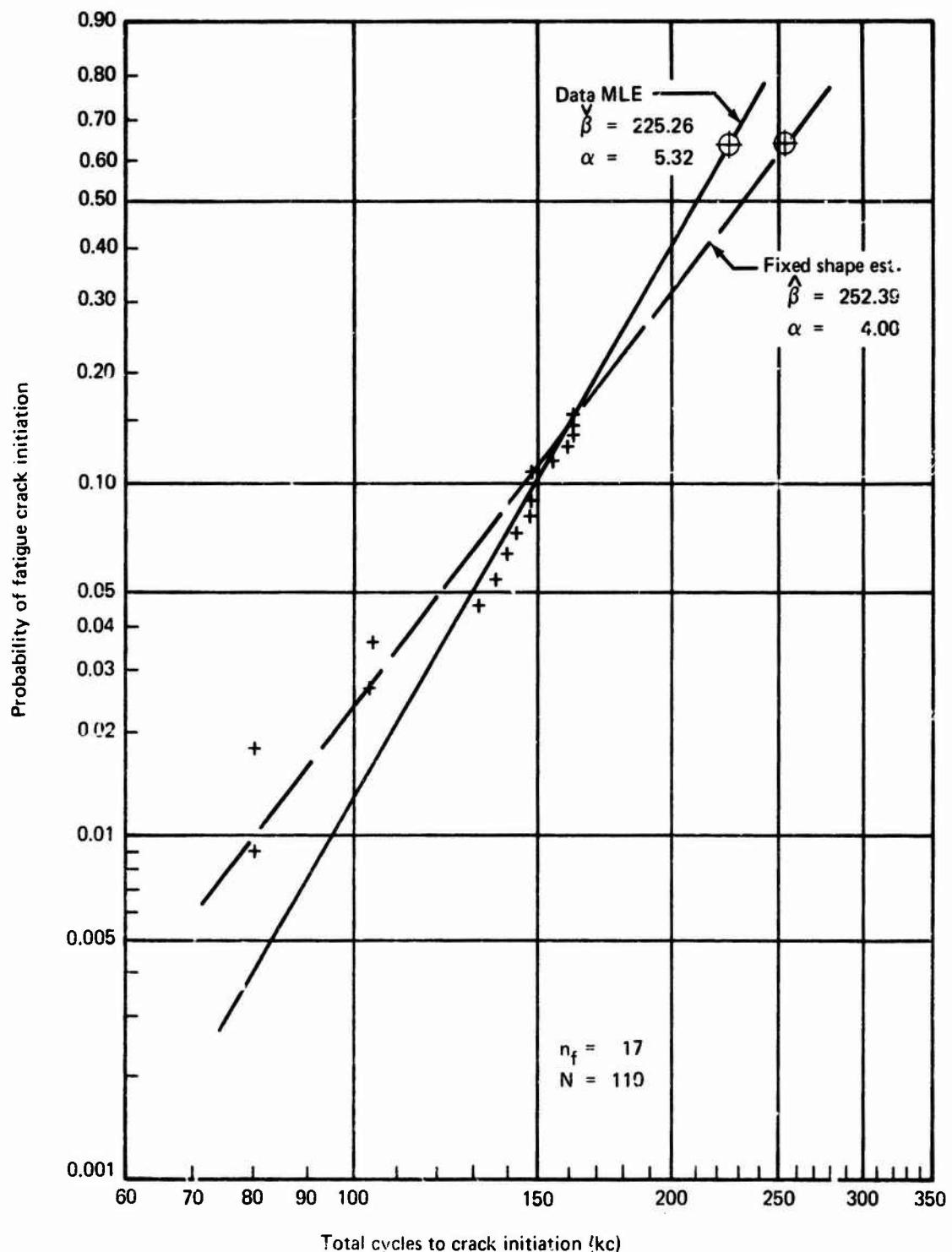
Figure 67. – Weibull Cumulative Probability Representation of Fatigue Crack
Initiation Results From Structural Simulation Specimen A4
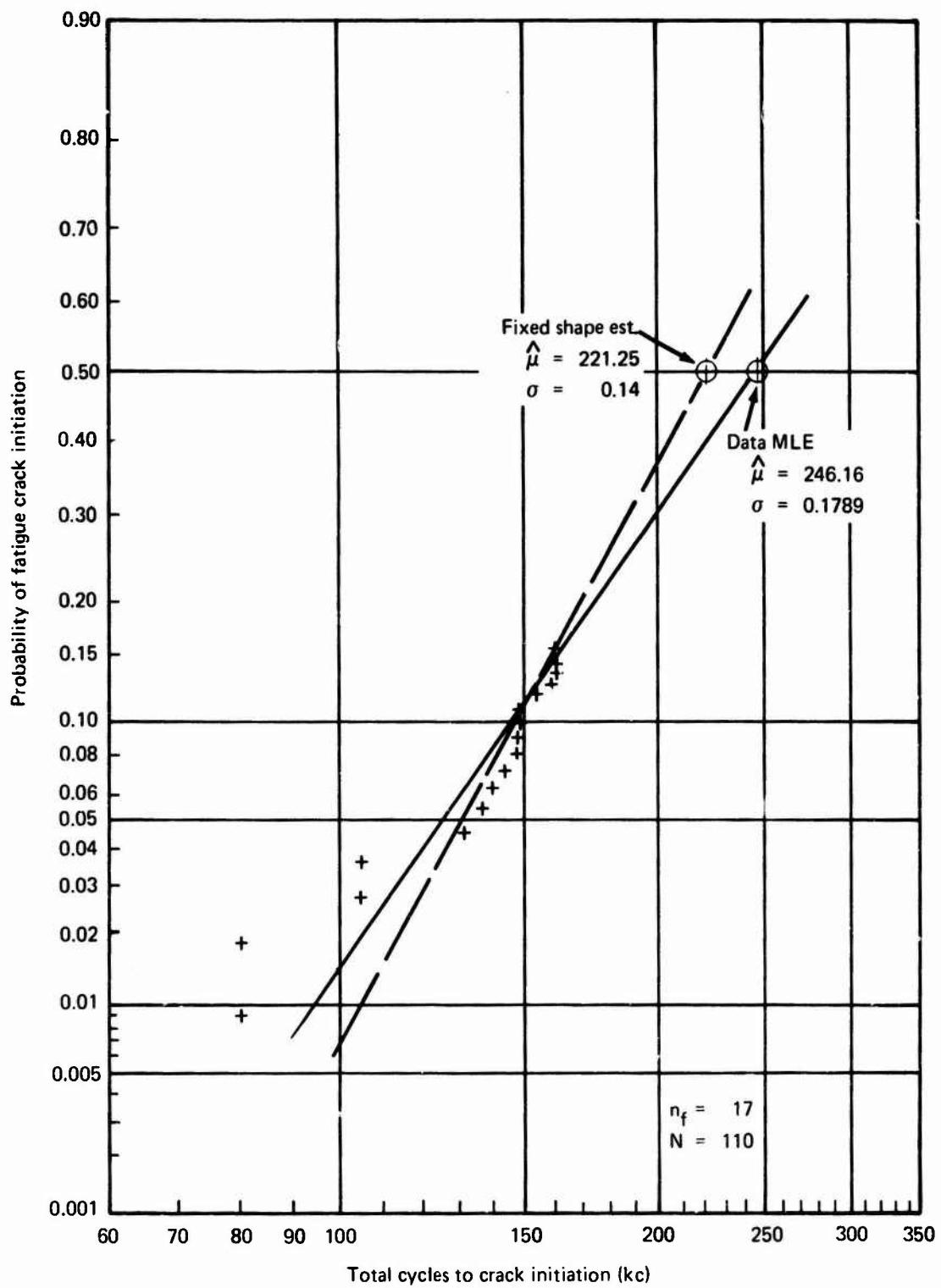
Figure 68.—Log-Normal Cumulative Distribution Representation of Fatigue Crack
Initiation Results From Structural Simulation Specimen A4

92
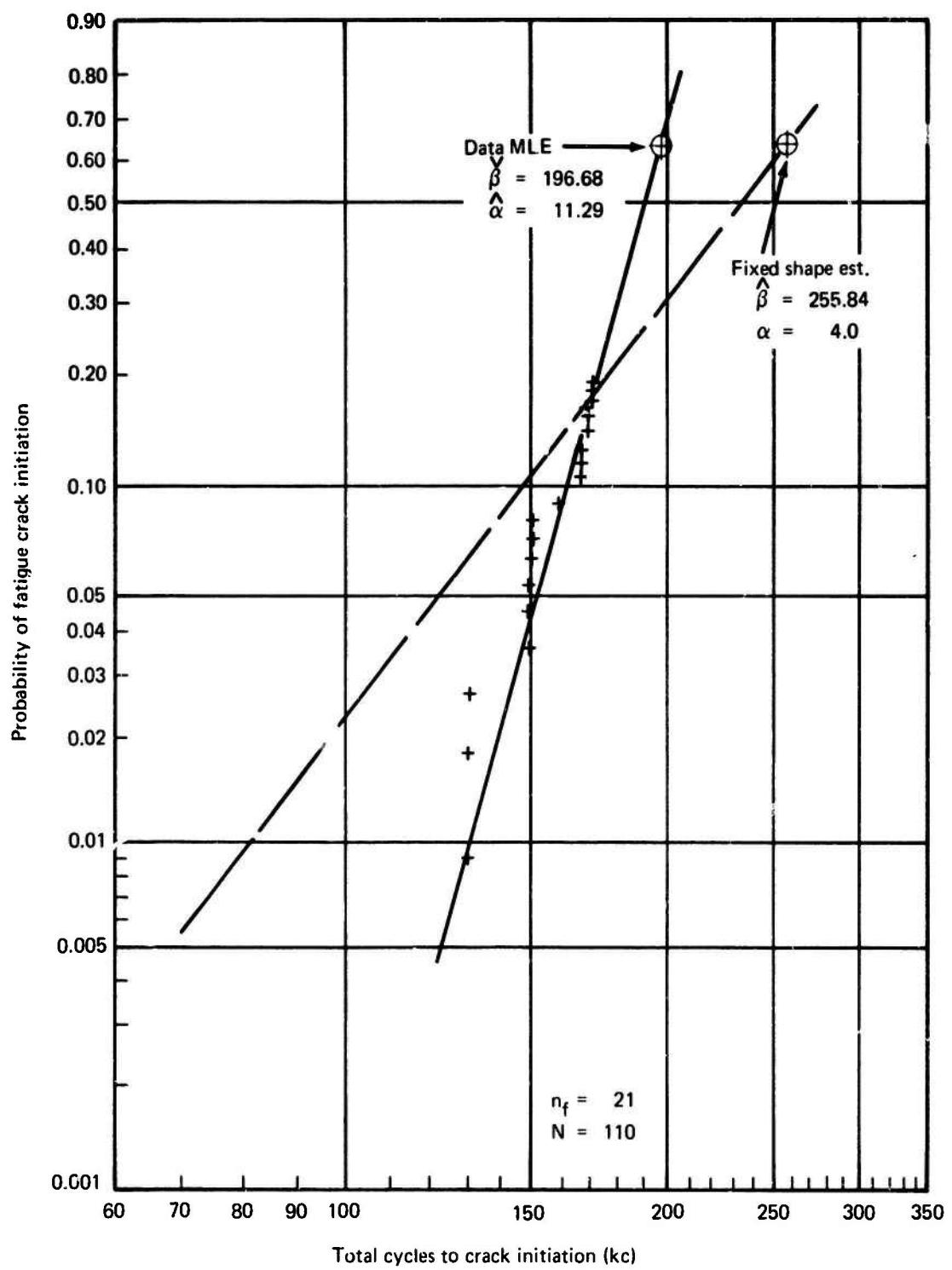
Figure 69. - Weibull Cumulative Probability Representation of Fatigue Crack Initiation Results From Structural Simulation Specimen A5

93
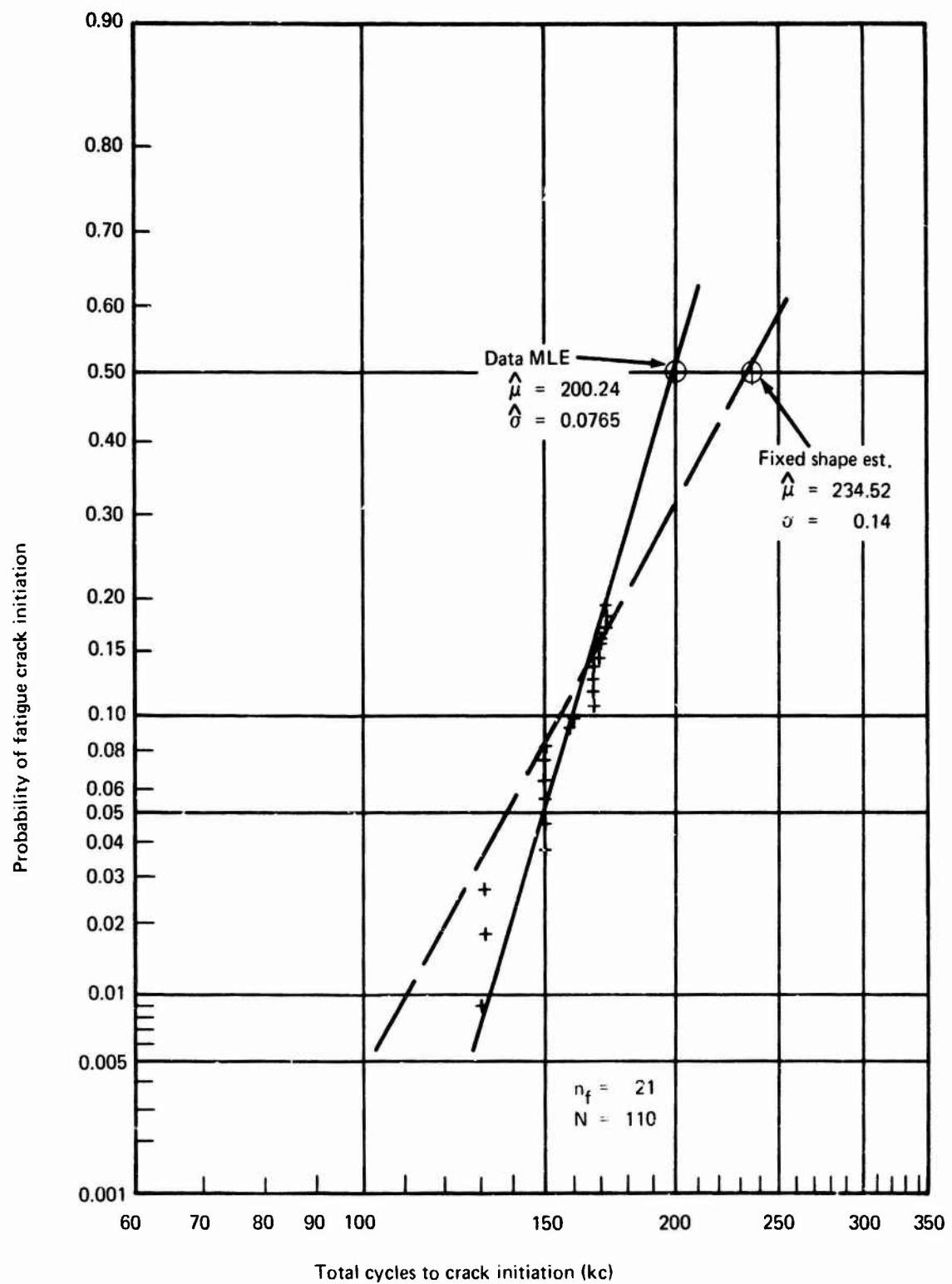
Figure 70. – Log-Normal Cumulative Probability Representation of Fatigue Crack Initiation Results From Structural Simulation Specimen A5
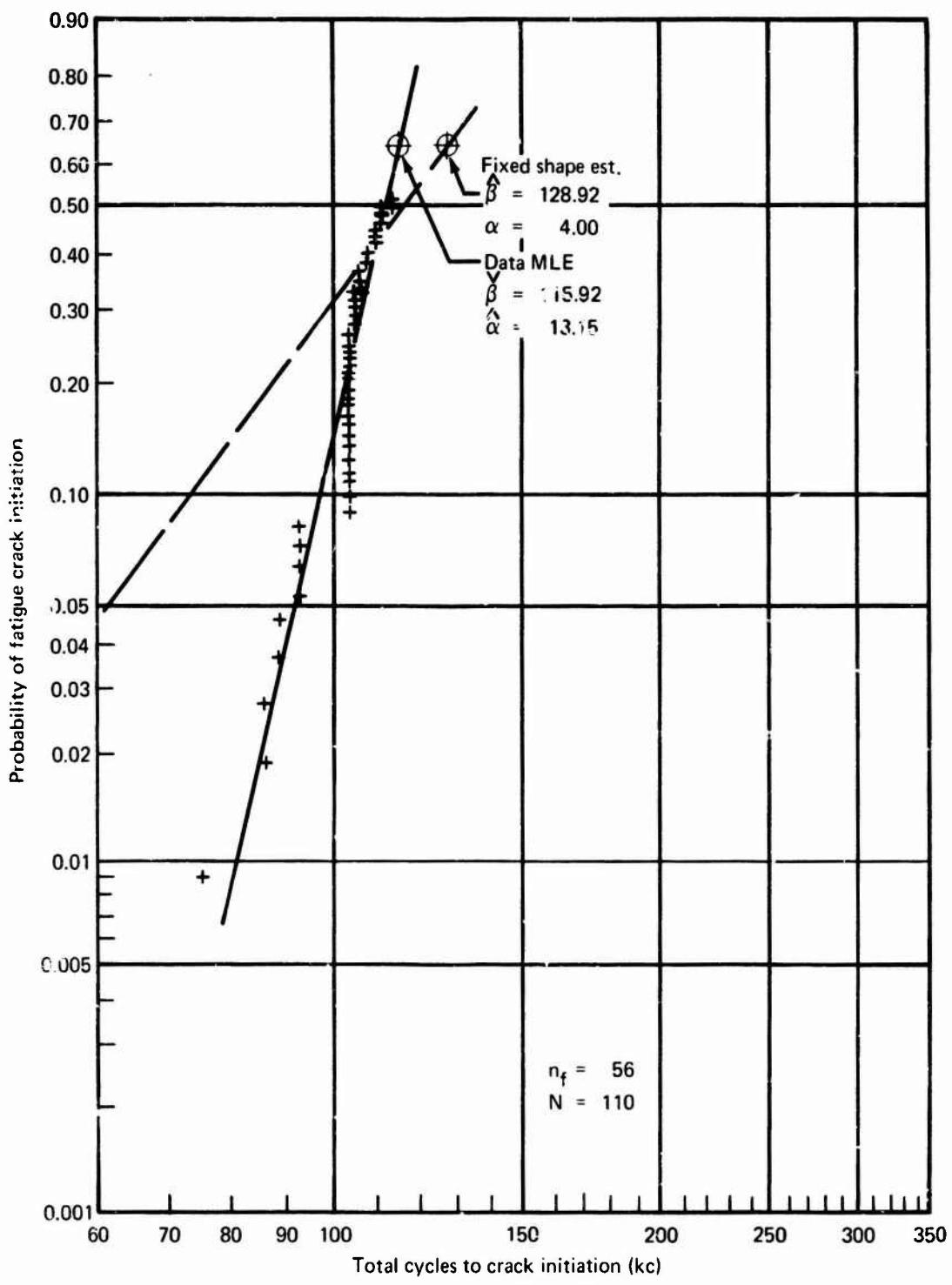
Figure 71. - Weibull Cumulative Probability Representation of Fatigue Crack
Initiation Results From Structural Simulation Specimen A6

95
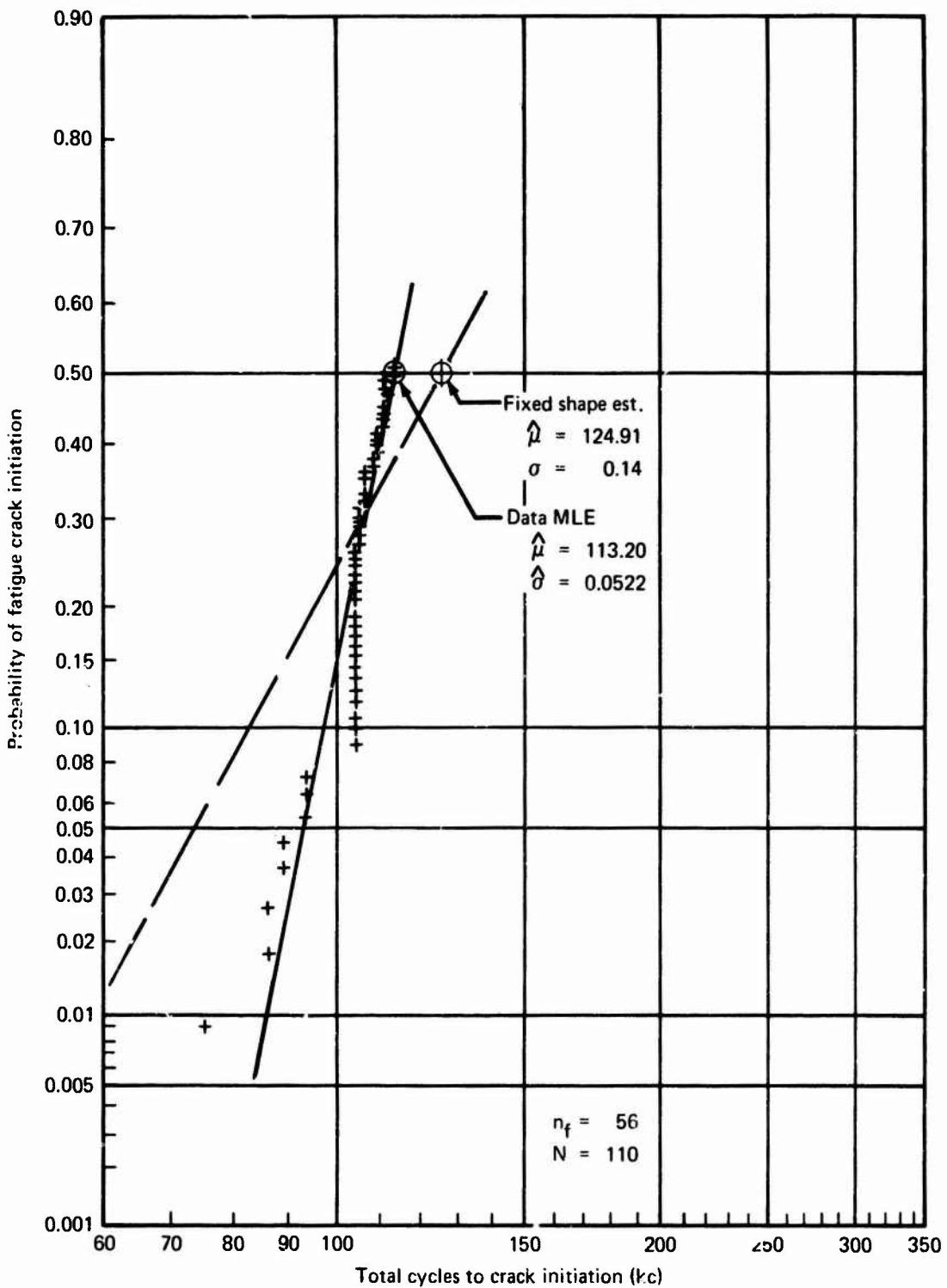
Figure 72. - Log-Normal Cumulative Probability Representation of Fatigue Crack Initiation Results From Structural Simulation Specimen A6

96
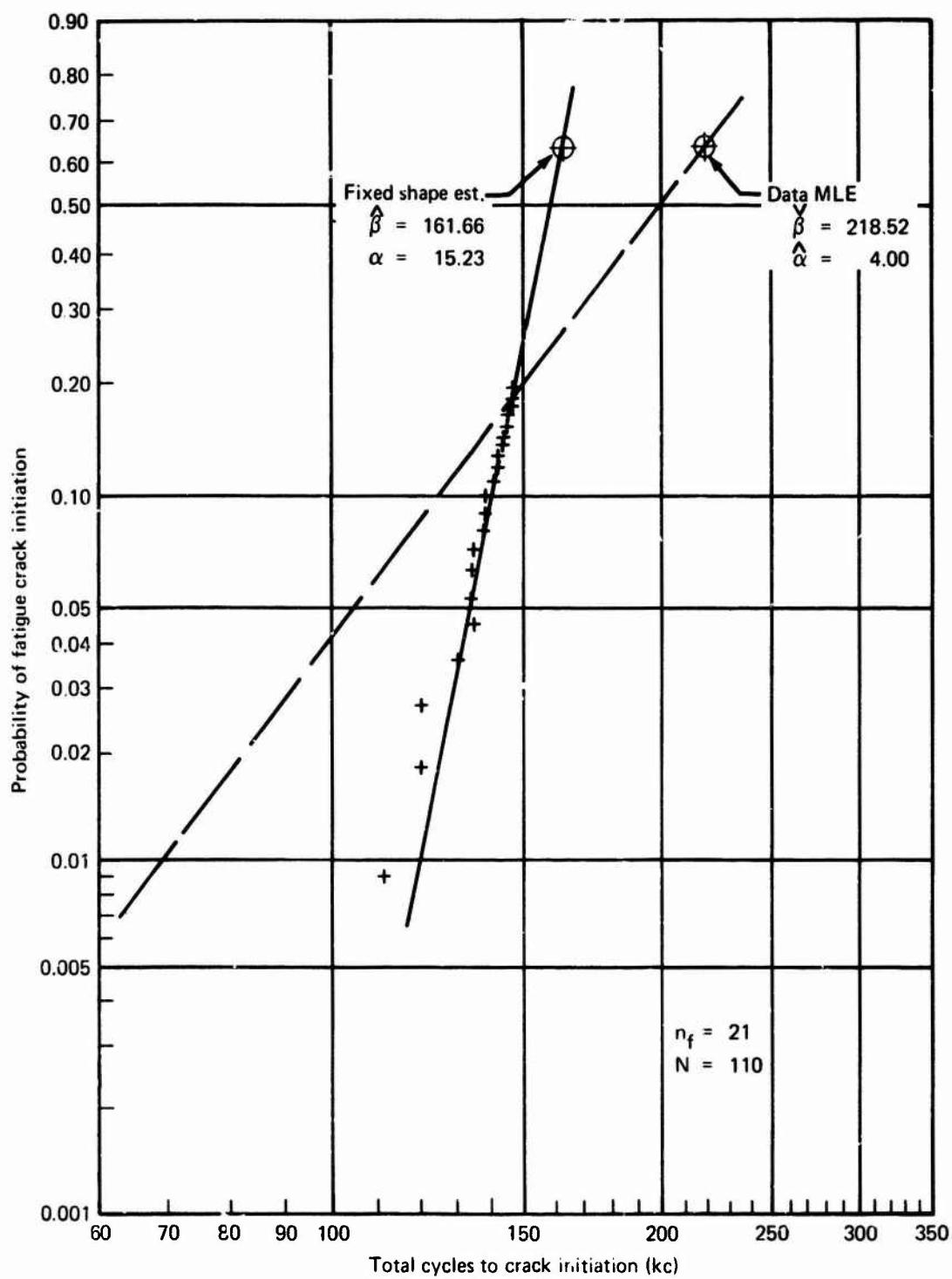
Figure 73. – Weibull Cumulative Probability Representation of Fatigue Crack
Initiation Results From Structural Simulation Specimen A7

97
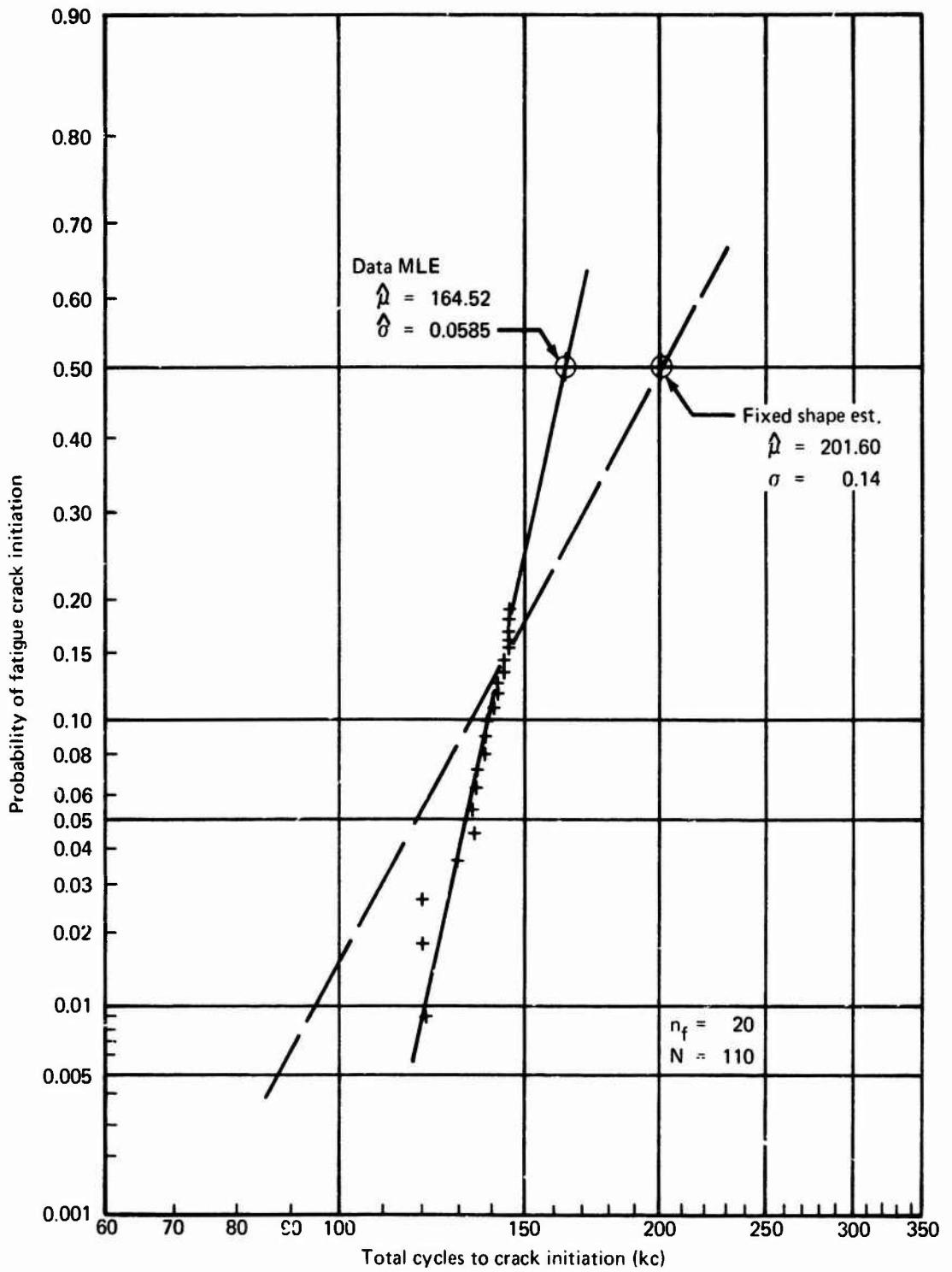
Figure 74. – Log-Normal Cumulative Probability Representation of Fatigue Crack
Initiation Results From Structural Simulation Specimen A7

98
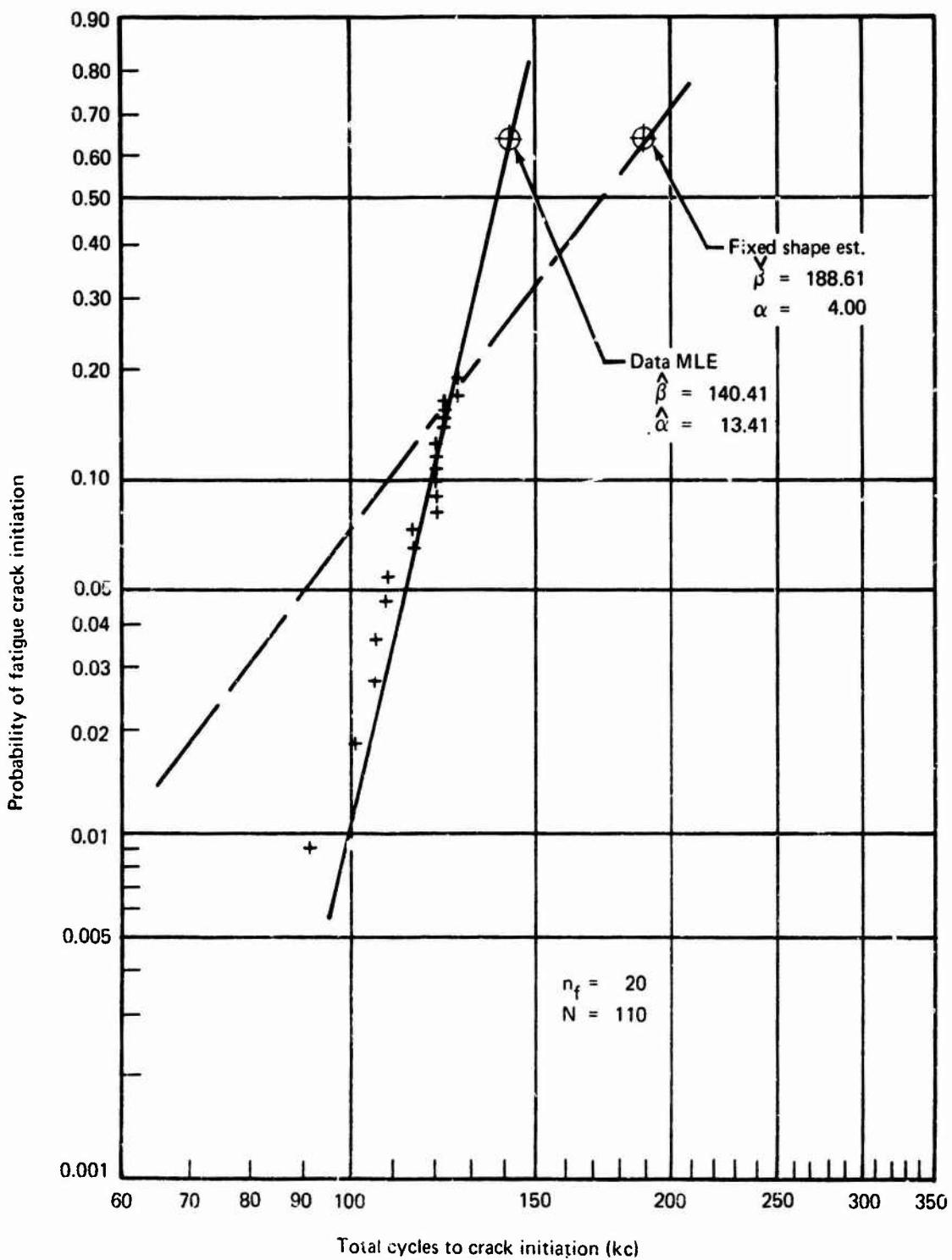
Figure 75. – Weibull Cumulative Probability Representation of Fatigue Crack Initiation Results From Structural Simulation Specimen A8

99
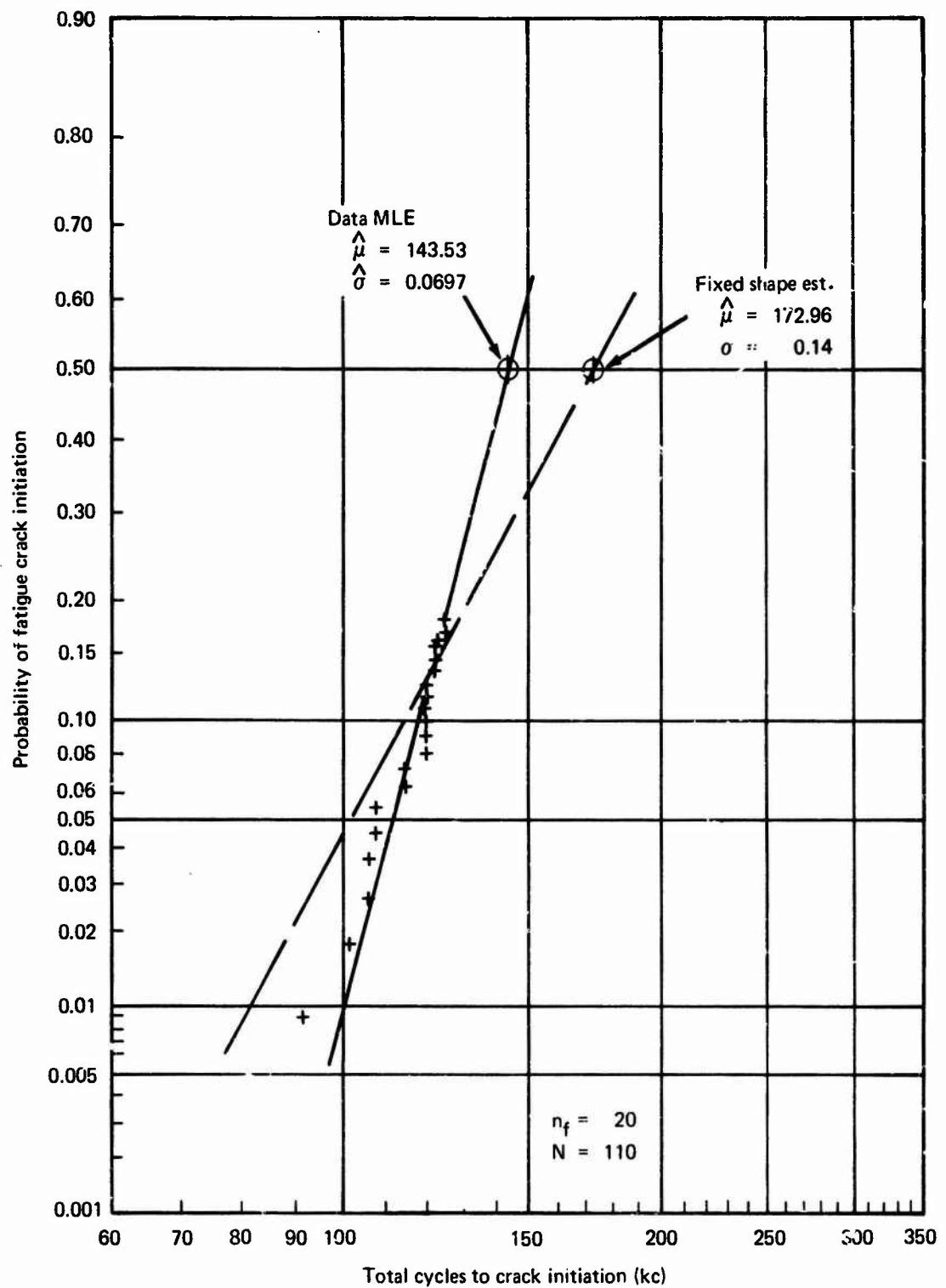
Figure 76.—Log-Normal Cumulative Probability Representation of Fatigue Crack
Initiation Results From Structural Simulation Specimen A8

100
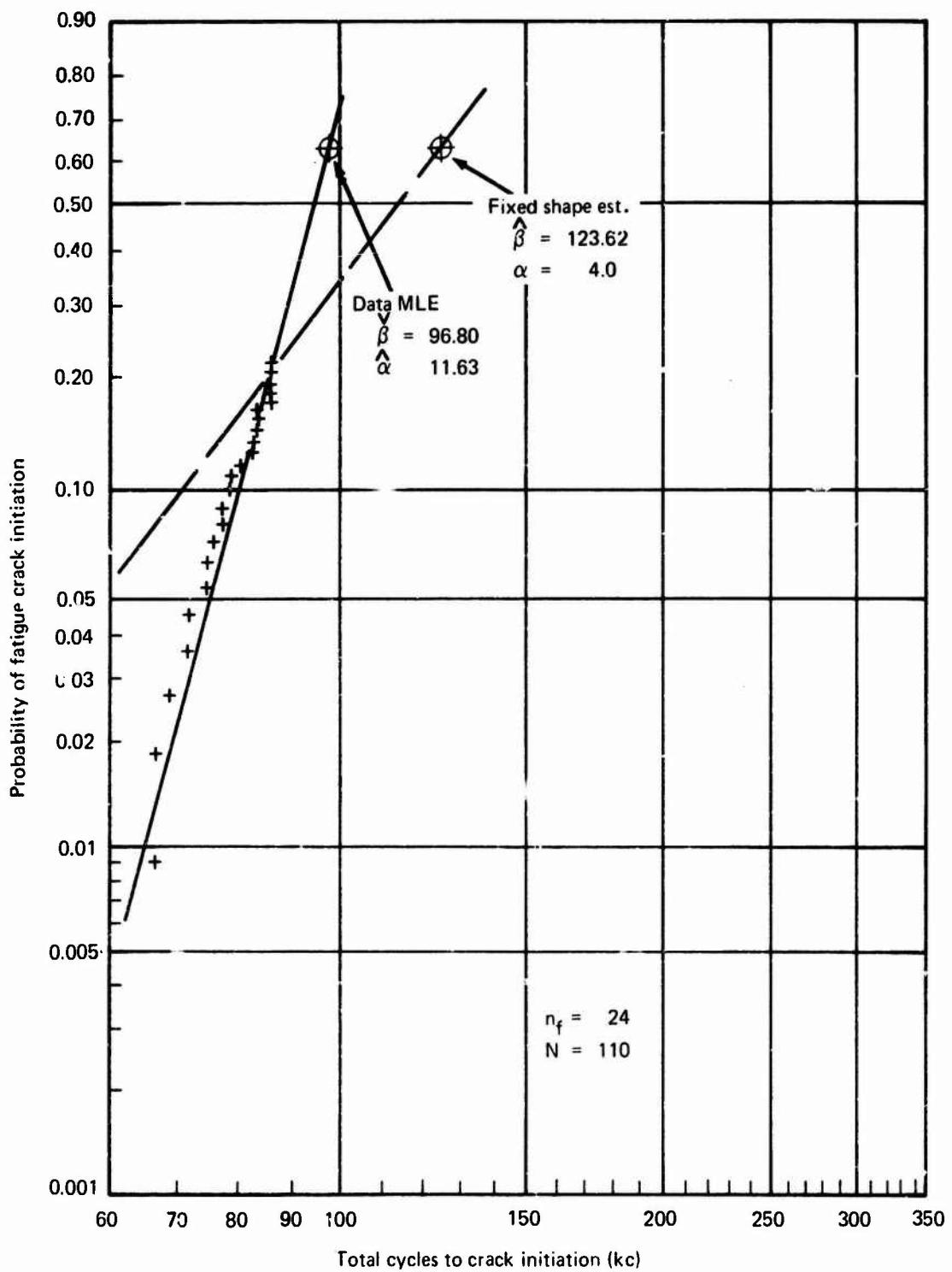
Figure 77. – Weibull Cumulative Probability Representation of Fatigue Crack
Initiation Results From Structural Simulation Specimen A9

101
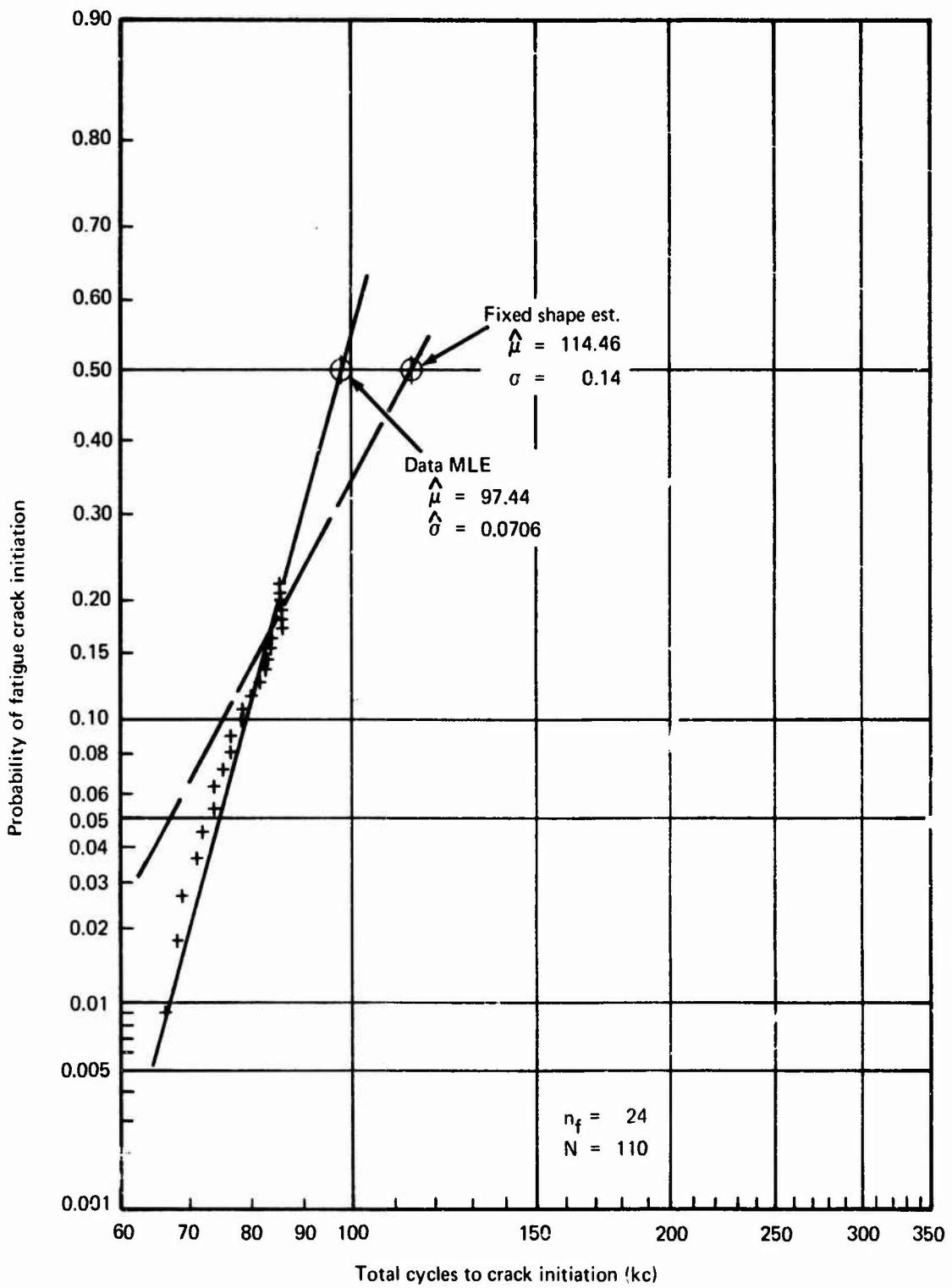
Figure 78. – Log-Normal Cumulative Probability Representation of Fatigue Crack Initiation Results From Structural Simulation Specimen A9
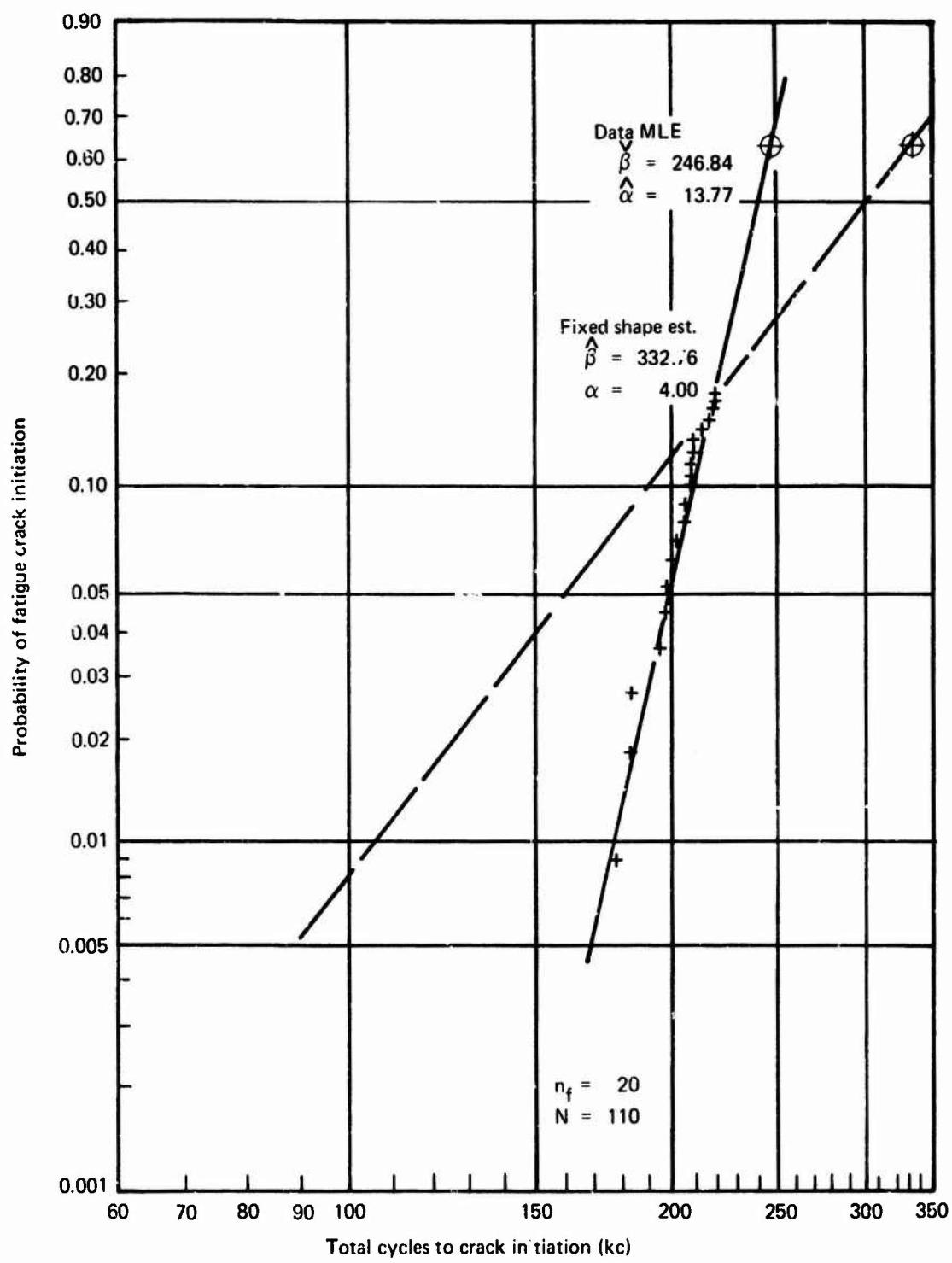
Figure 79. – Weibull Cumulative Probability Representation of Fatigue Crack
Initiation Results From Structural Simulation Specimen A10

103
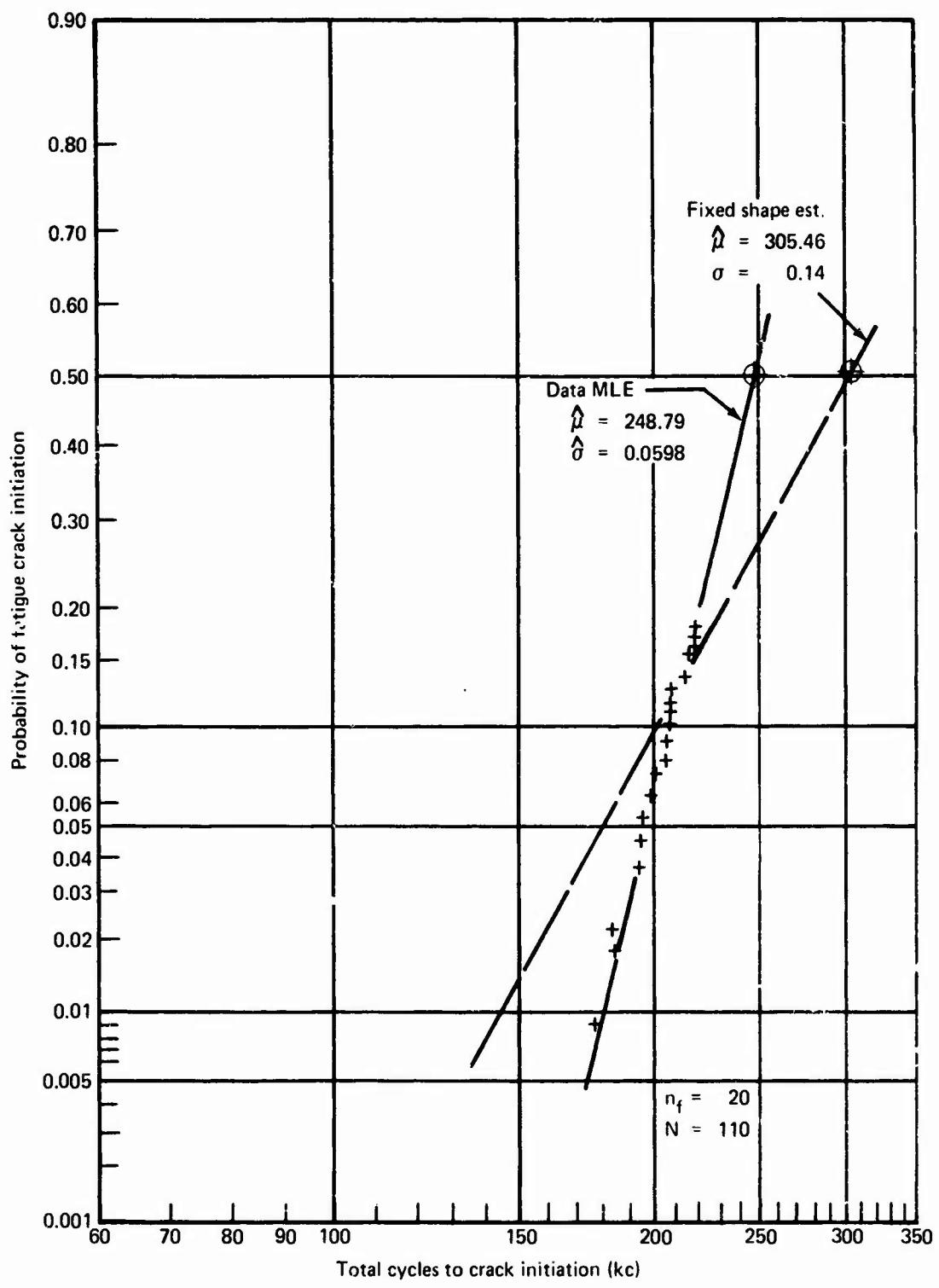
Figure 80.—Log-Normal Cumulative Probability Representation of Fatigue Crack Initiation Results From Structural Simulation Specimen A10

104
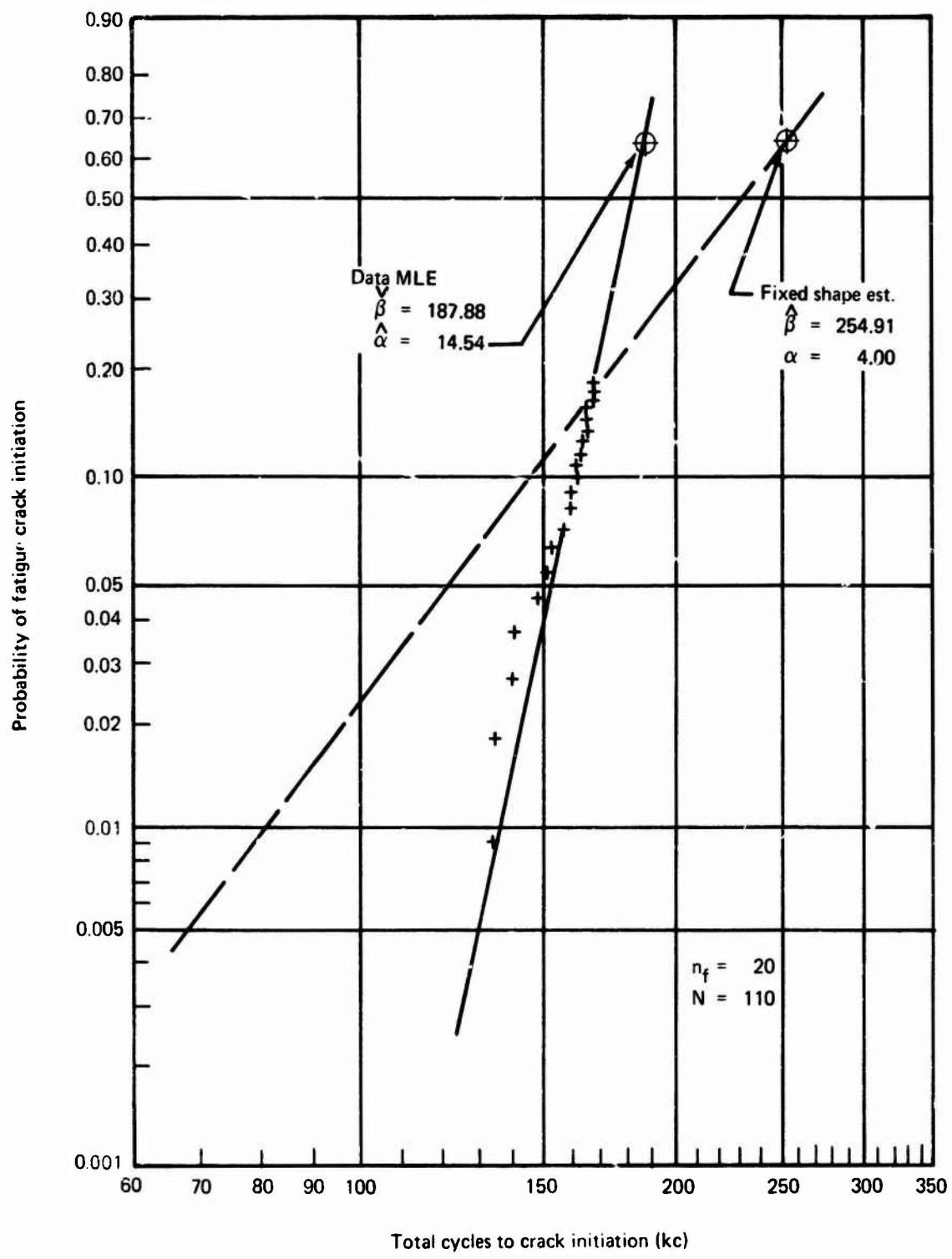
Figure 81. – Weibull Cumulative Probability Representation of Fatigue Crack Initiation Results From Structural Simulation Specimen A11
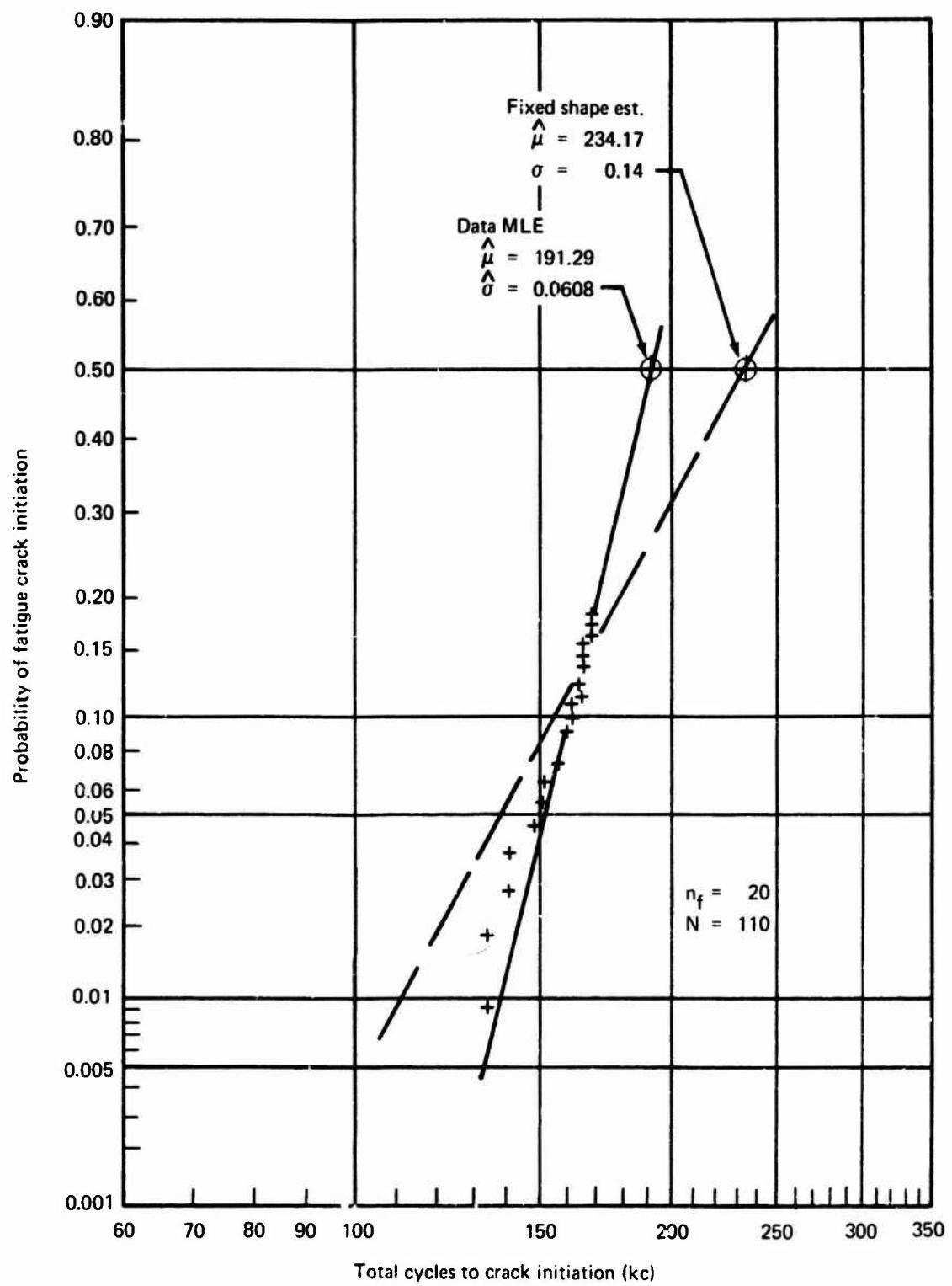
Figure 82. – Log-Normal Cumulative Probability Distribution Representation of Fatigue Crack Initiation Results From Structural Simulation Specimen A11

106
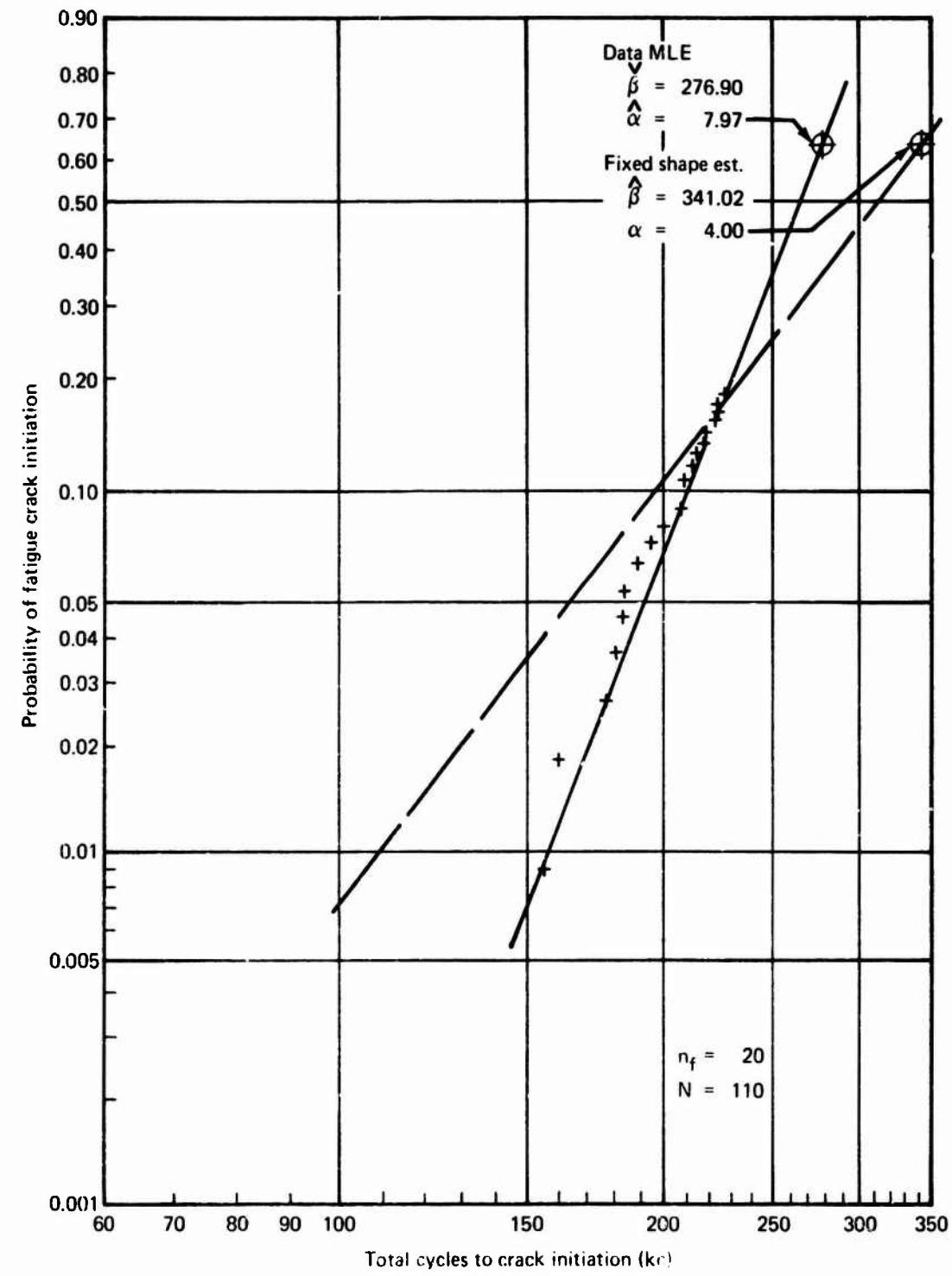
Figure 83. Weibull Cumulative Probability Representation of Fatigue Crack Initiation Results From Structural Simulation. Specimen A12

107
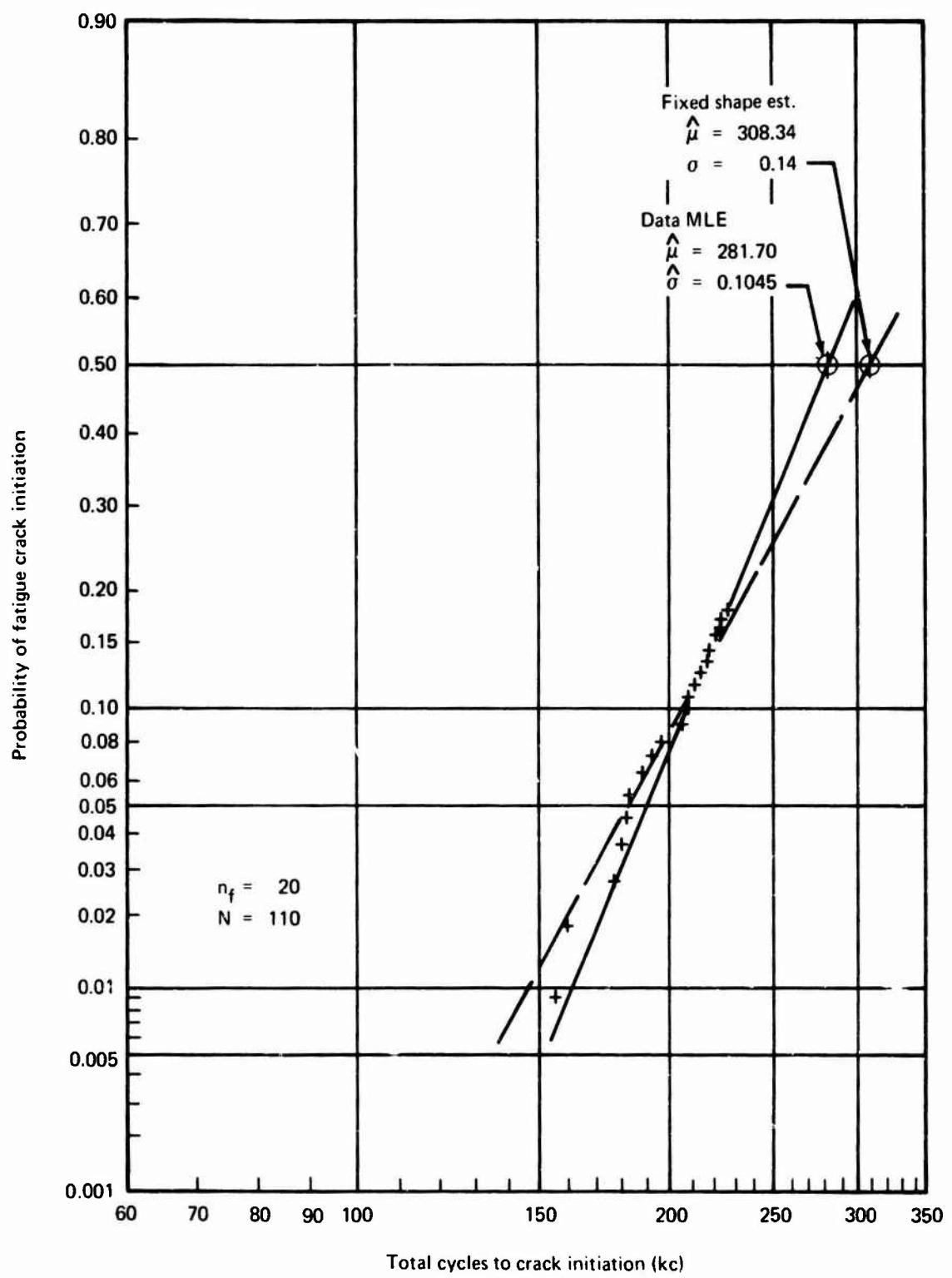
Figure 84. – Log-Normal Cumulative Probability Representation of Fatigue Crack Initiation Results From Structural Simulation Specimen A12

108
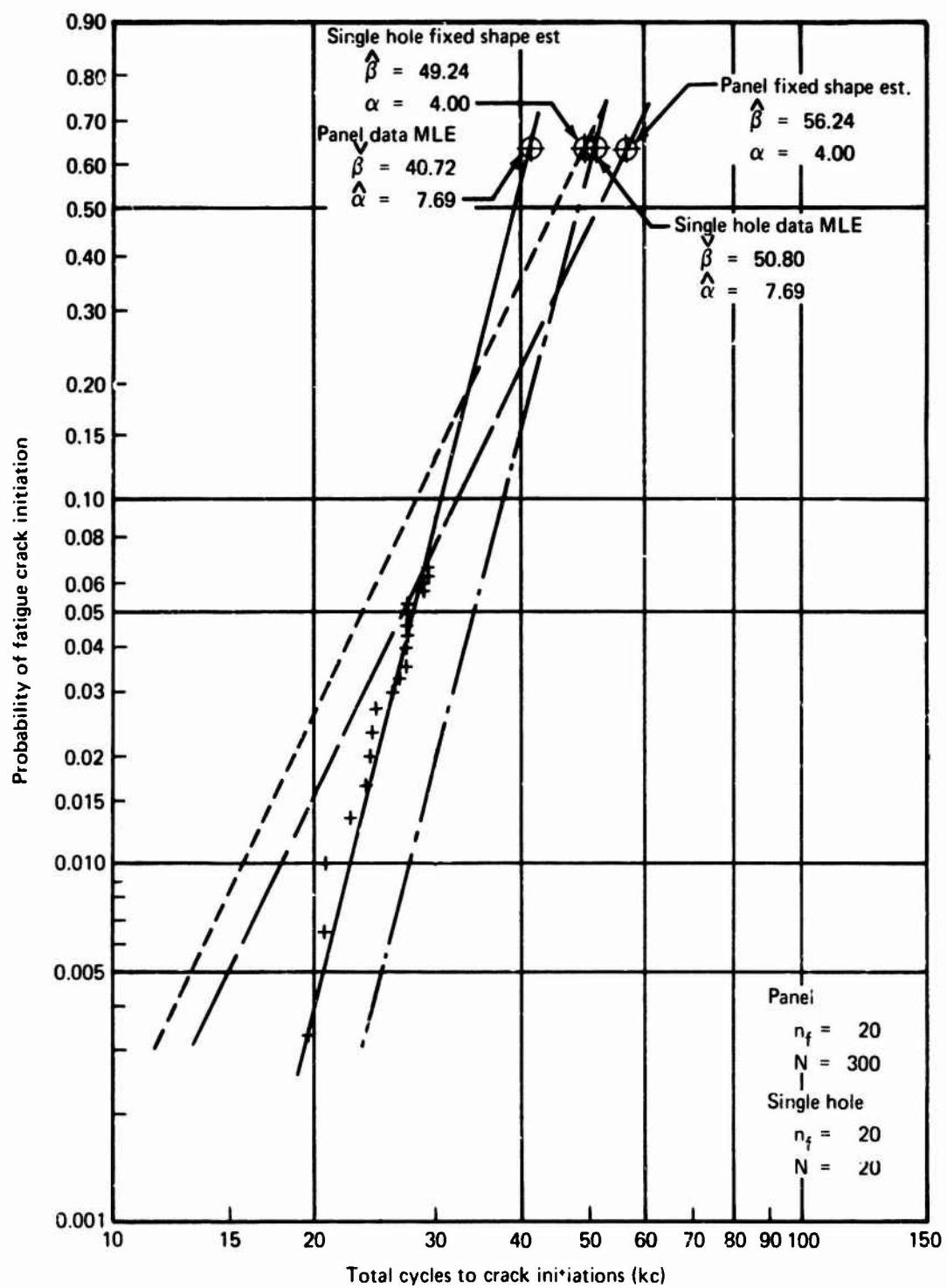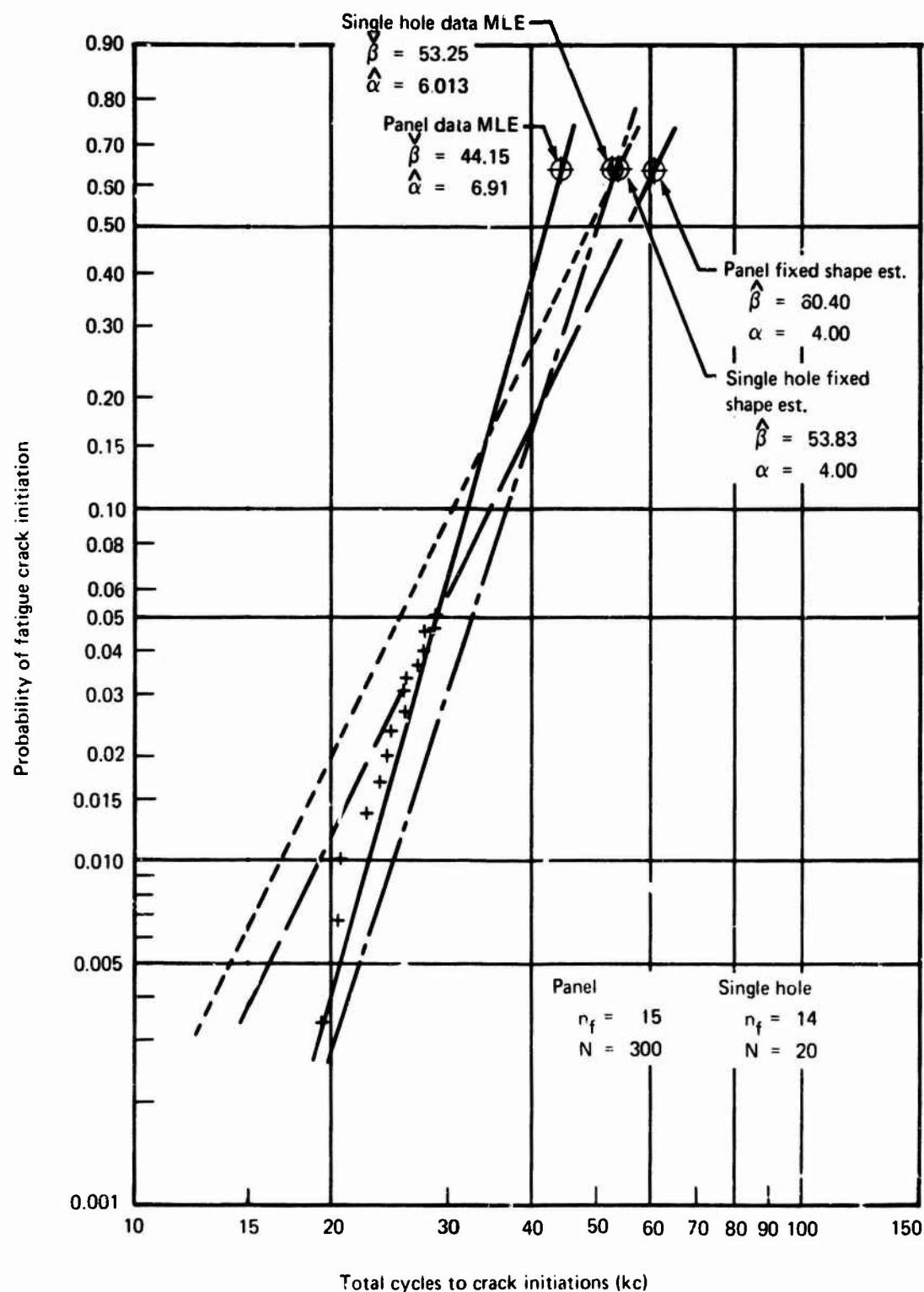
Figure 85. - Weibull Cumulative Probability Representation of Fatigue Crack
Initiation Results From Multihole Test Specimen Panel One (Ref. 2)

109

b. Failures Originating at Tool Exit Face

Figure 85. Continued

110

c. Failures Originating at Tool Entry Face
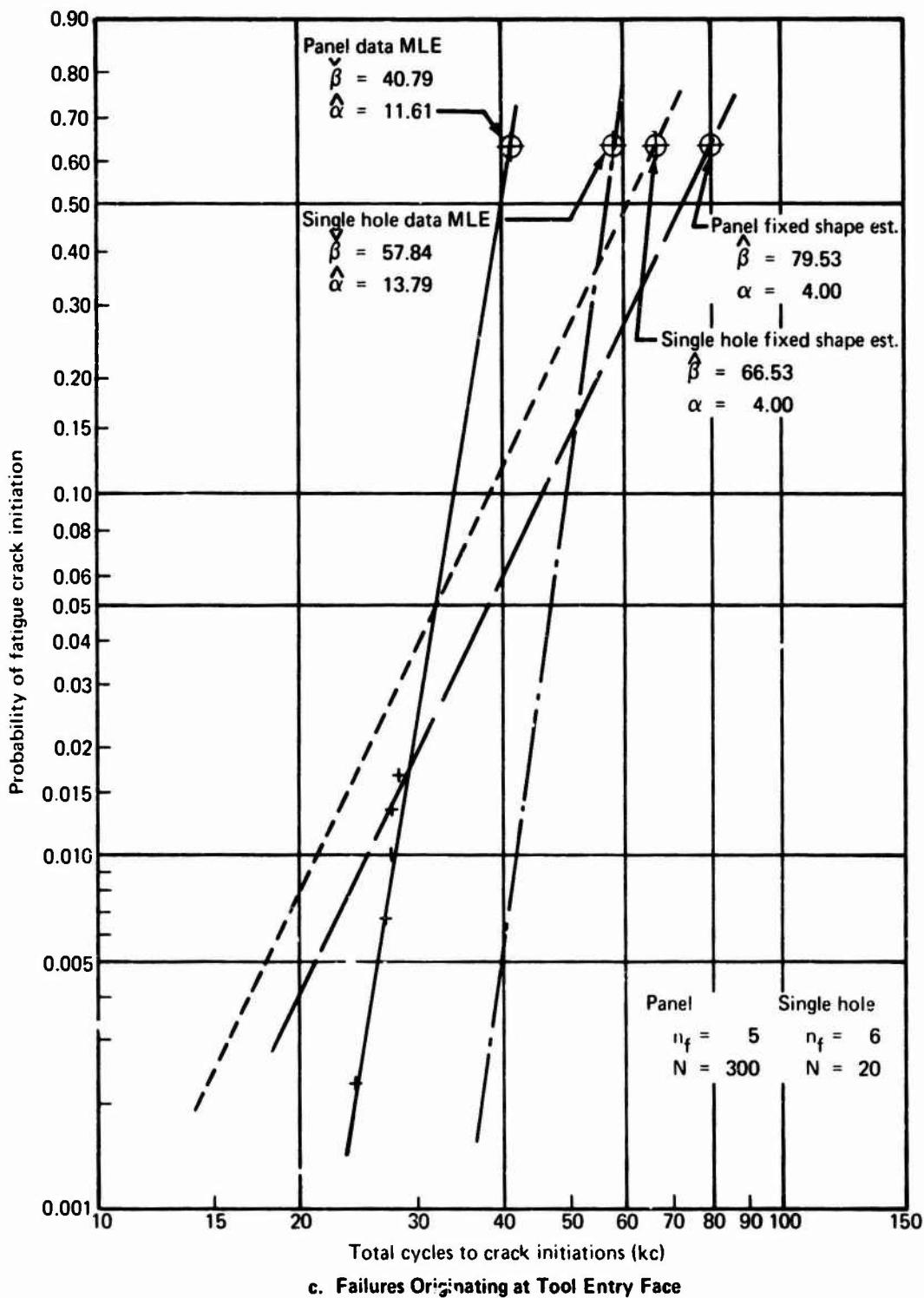
Figure 85.—Concluded

111
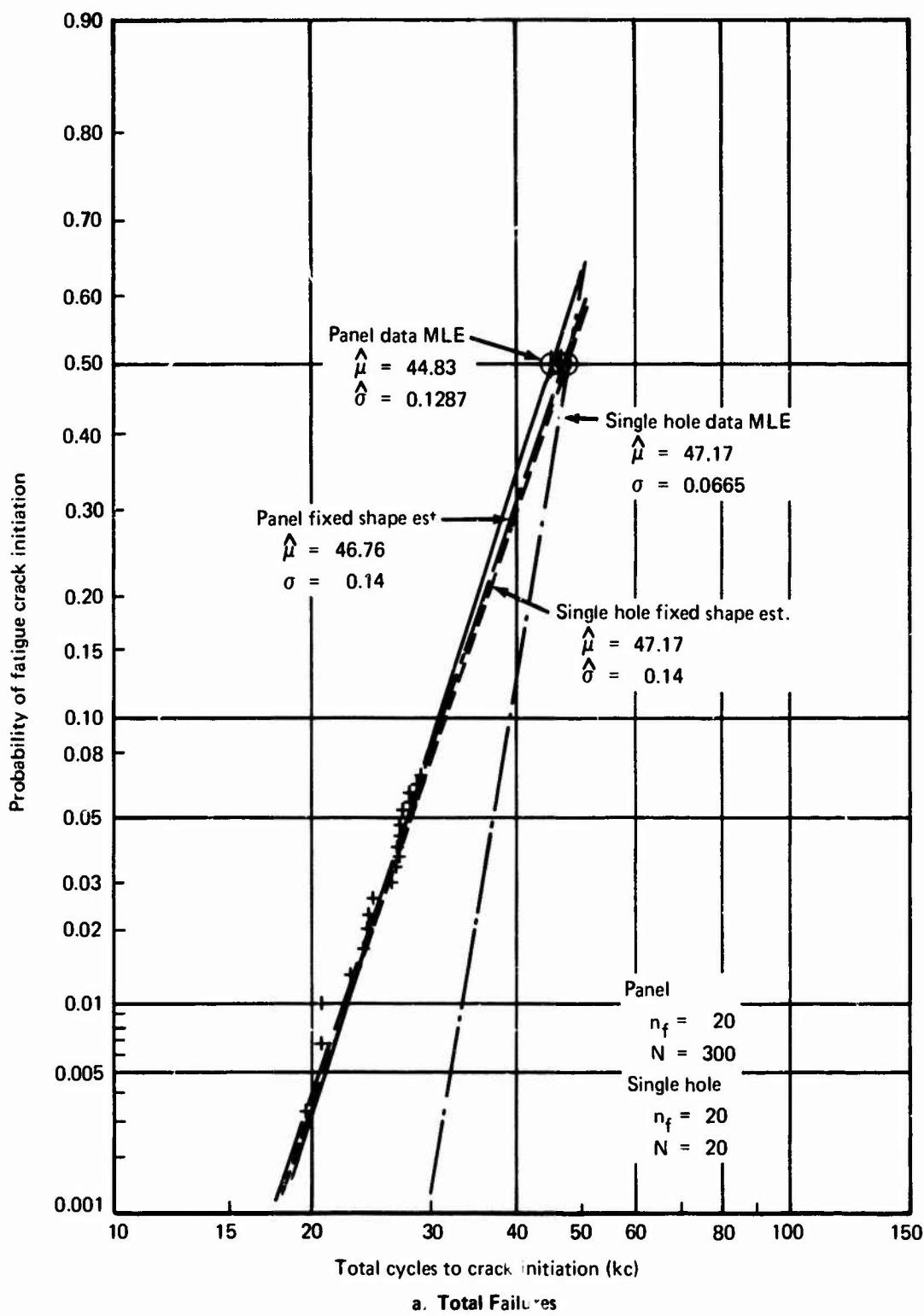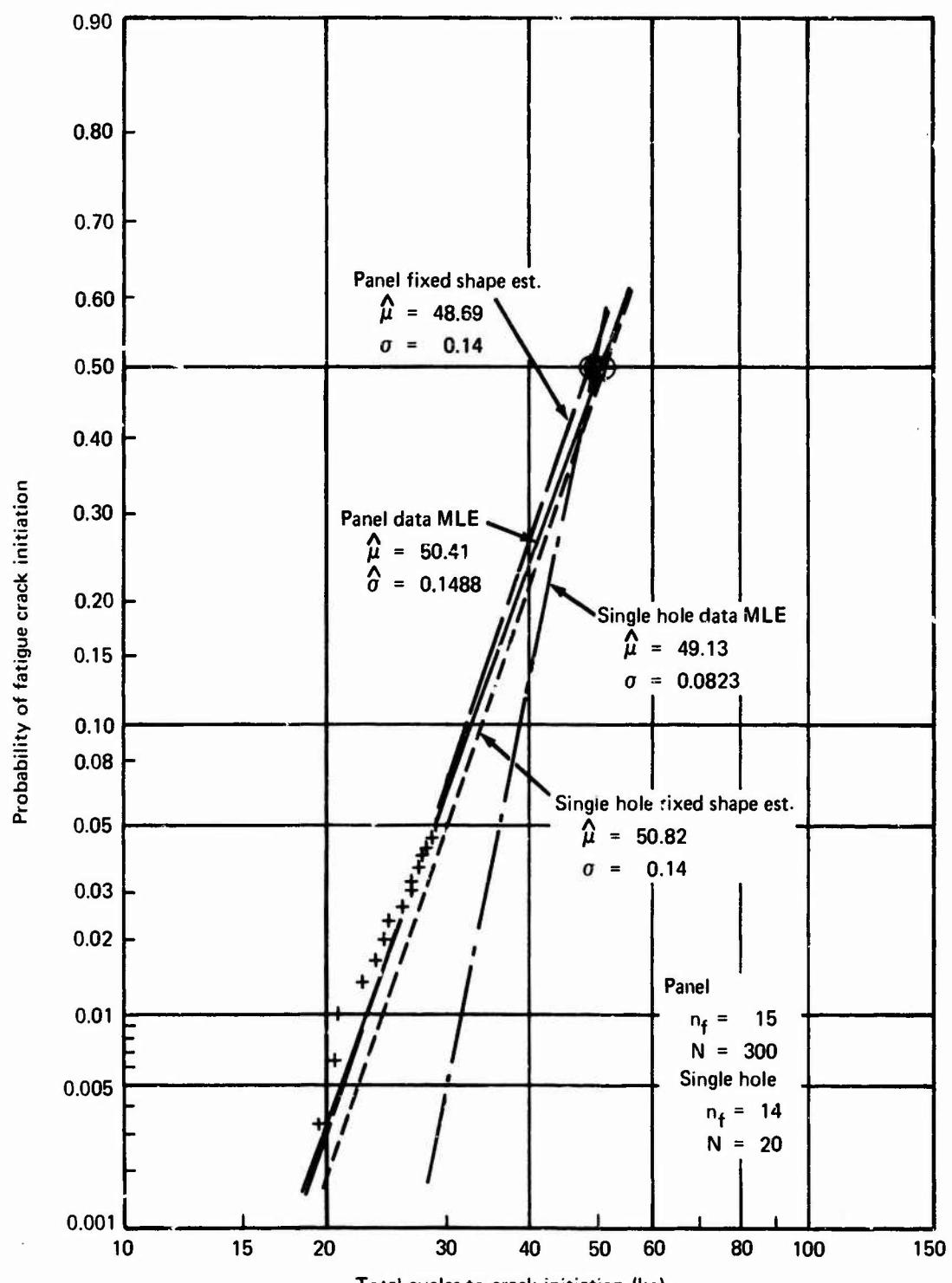
Figure 86. – Log-Normal Cumulative Probability Representation of Fatigue Crack
Initiation Results From Multihole Test Specimen Panel One (Ref. 2)

112

b. Failures Originating at Tool Exit Face

Figure 86.—Continued

113

c. Failures Originating at Tool Entry Face
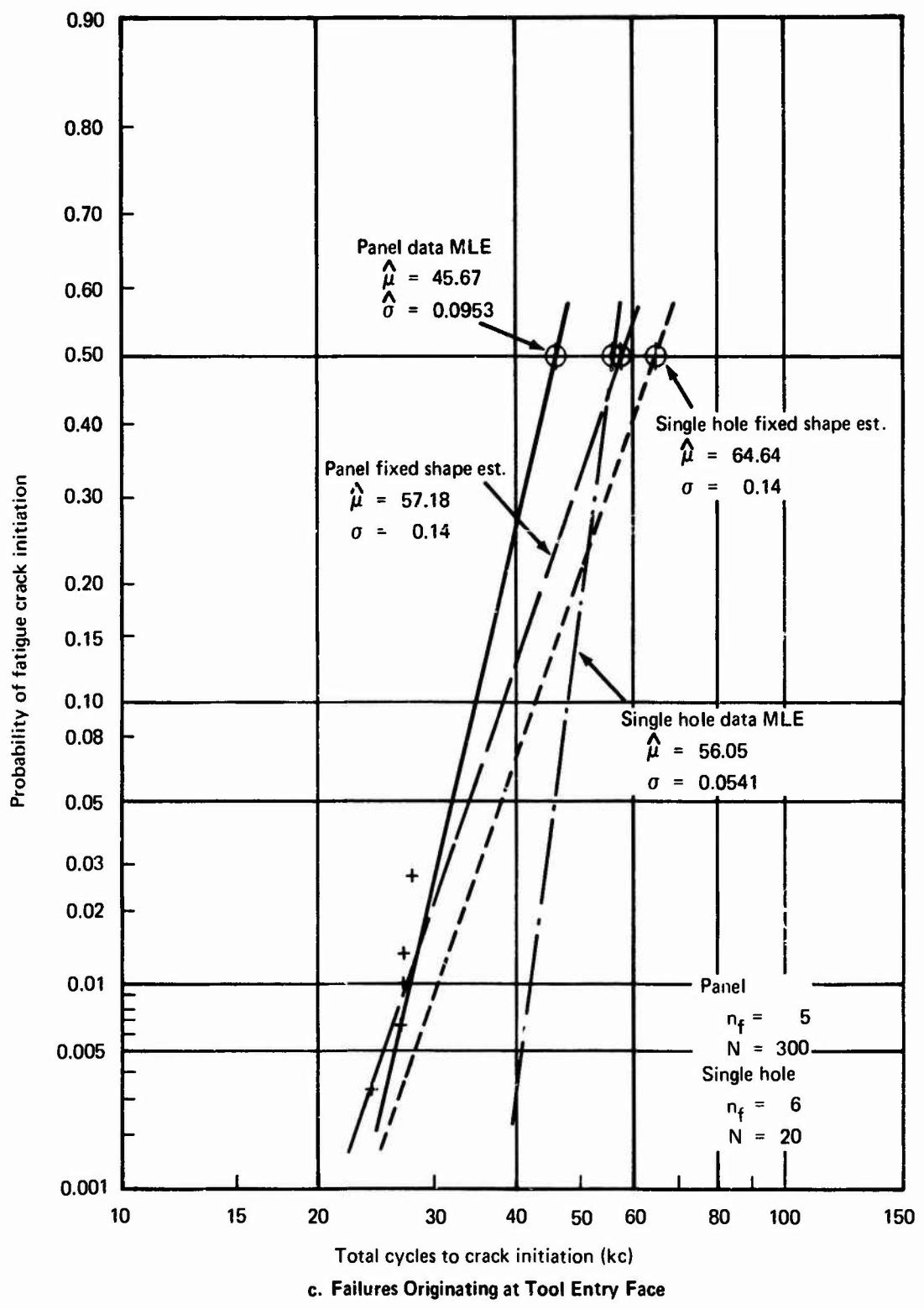
Figure 86. —Concluded

114
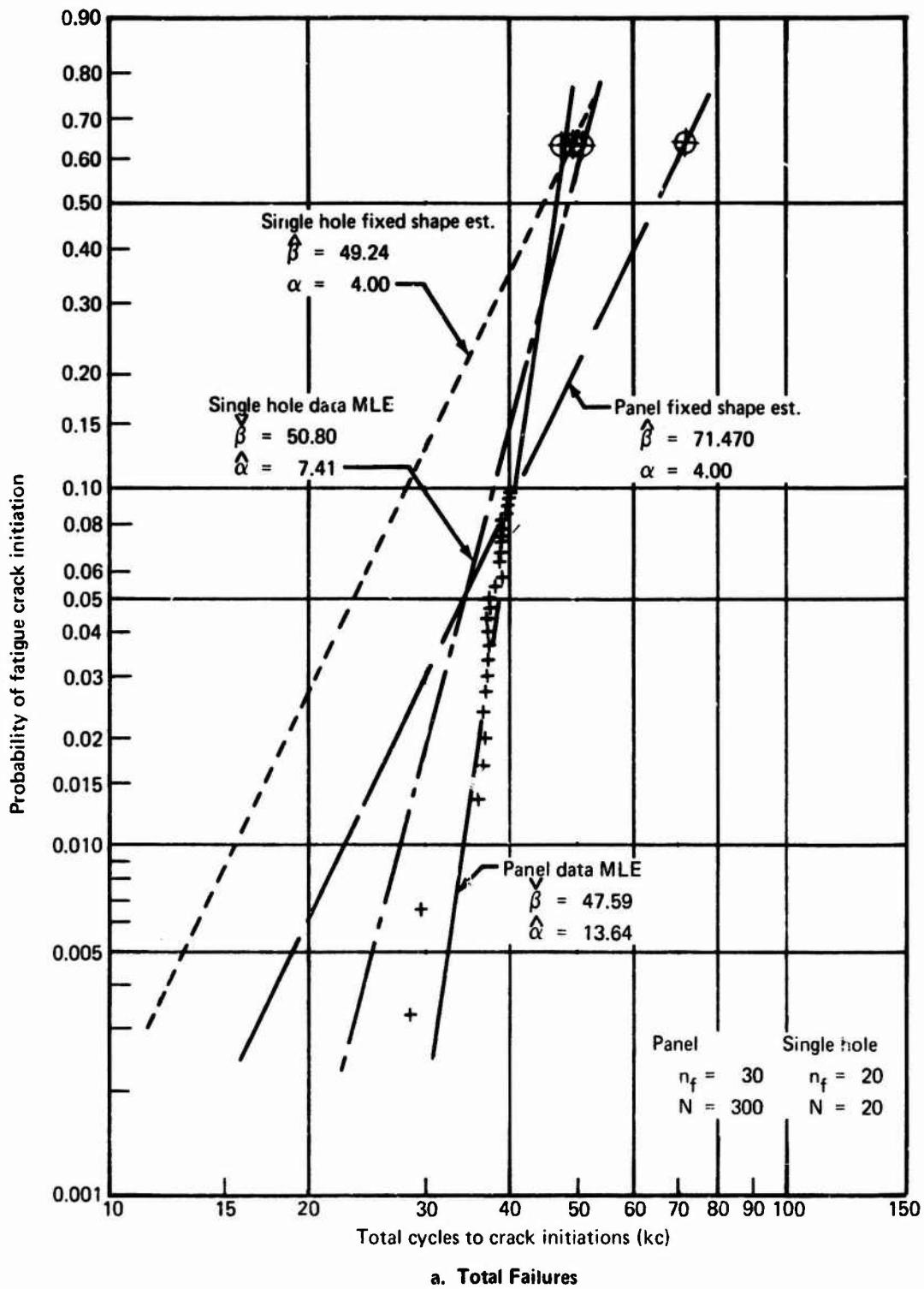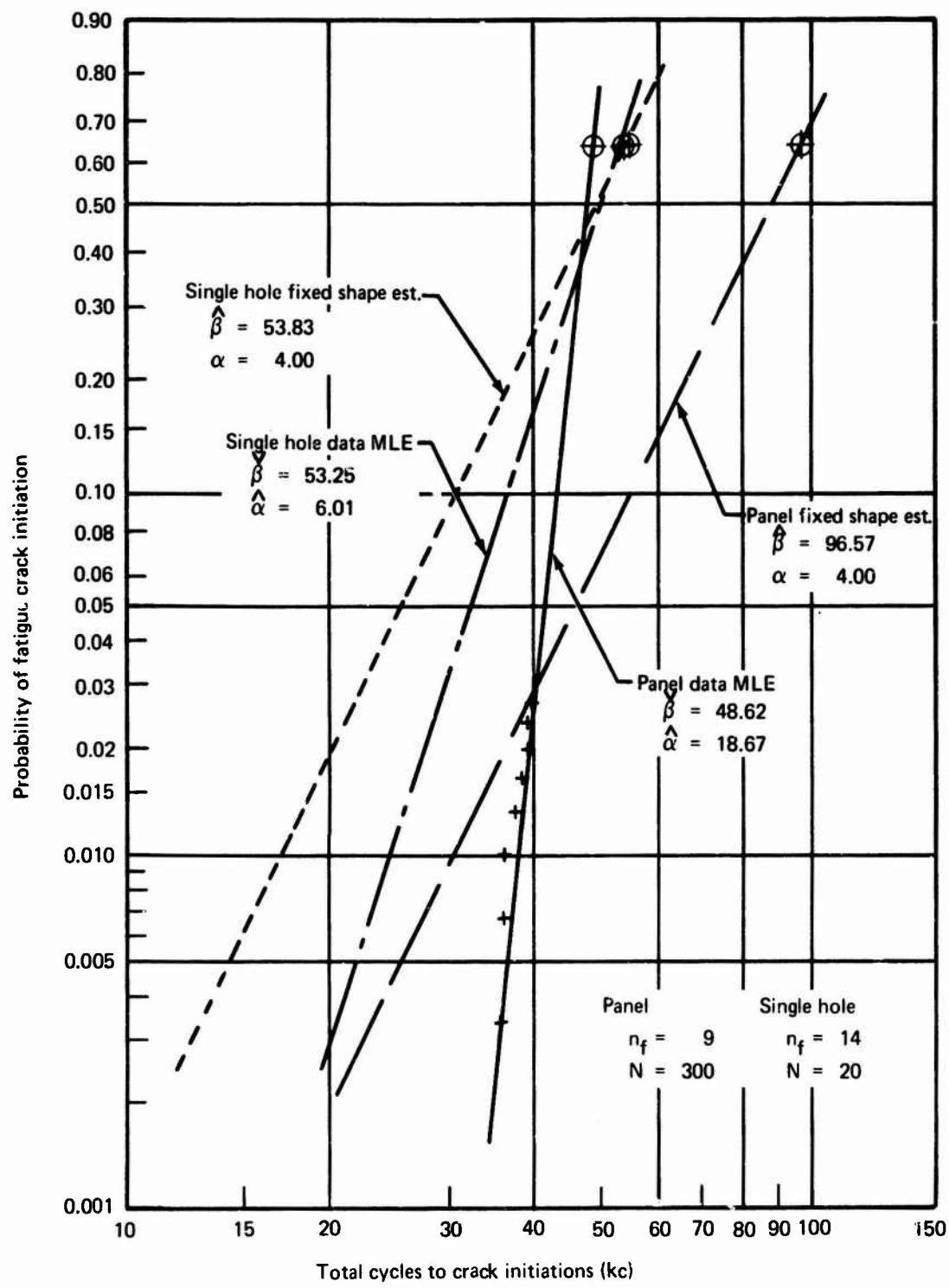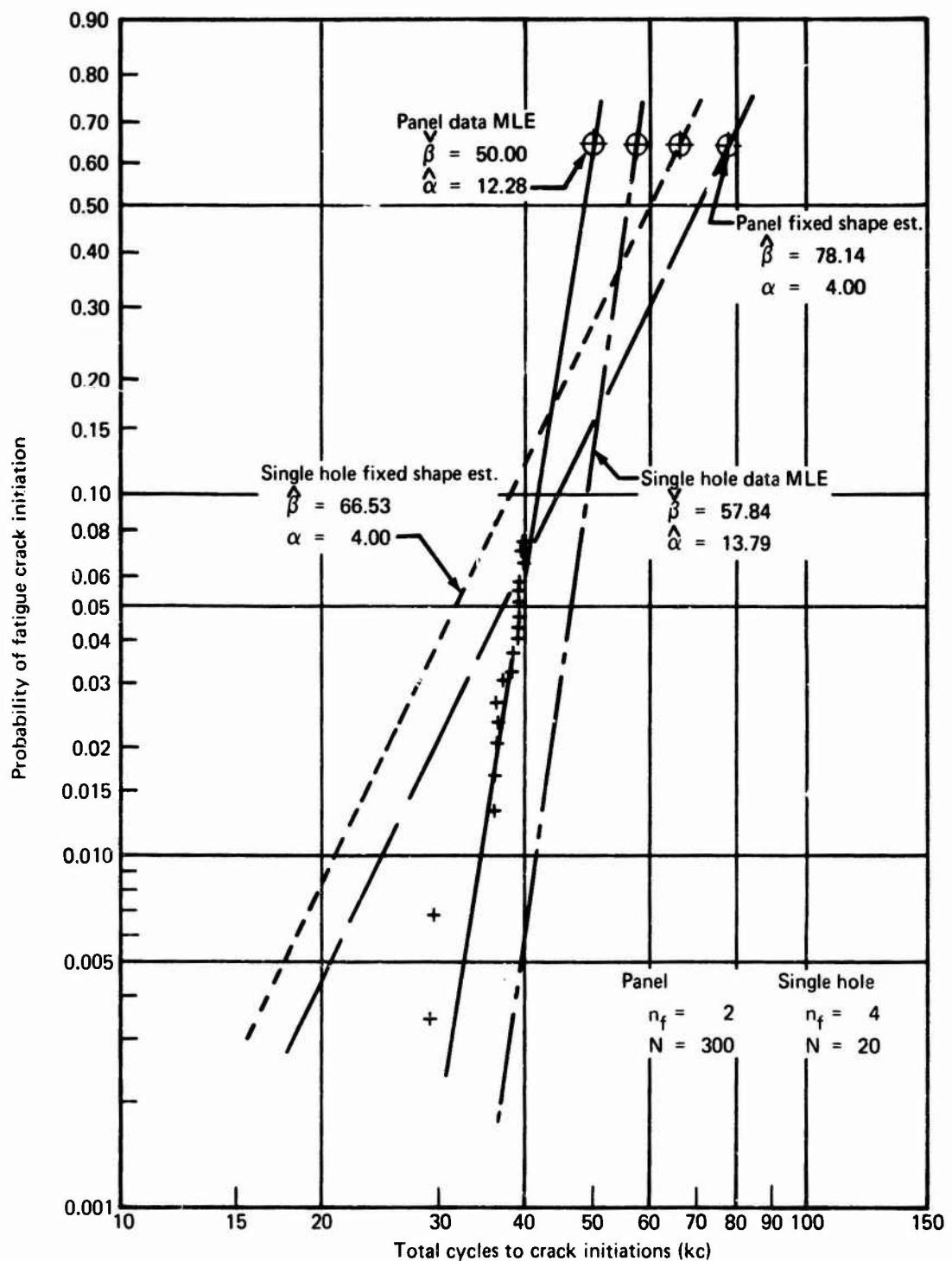
Figure 87. – *Weibull Cumulative Probability Representation of Fatigue Crack Initiation Results From Multihole Test Specimen Panel Two (Ref. 2)*

b. Failures Originating at Tool Exit Face

Figure 87.—Continued

116

c. **Failures Originating at Tool Entry Face**

Figure 87.—Concluded

117
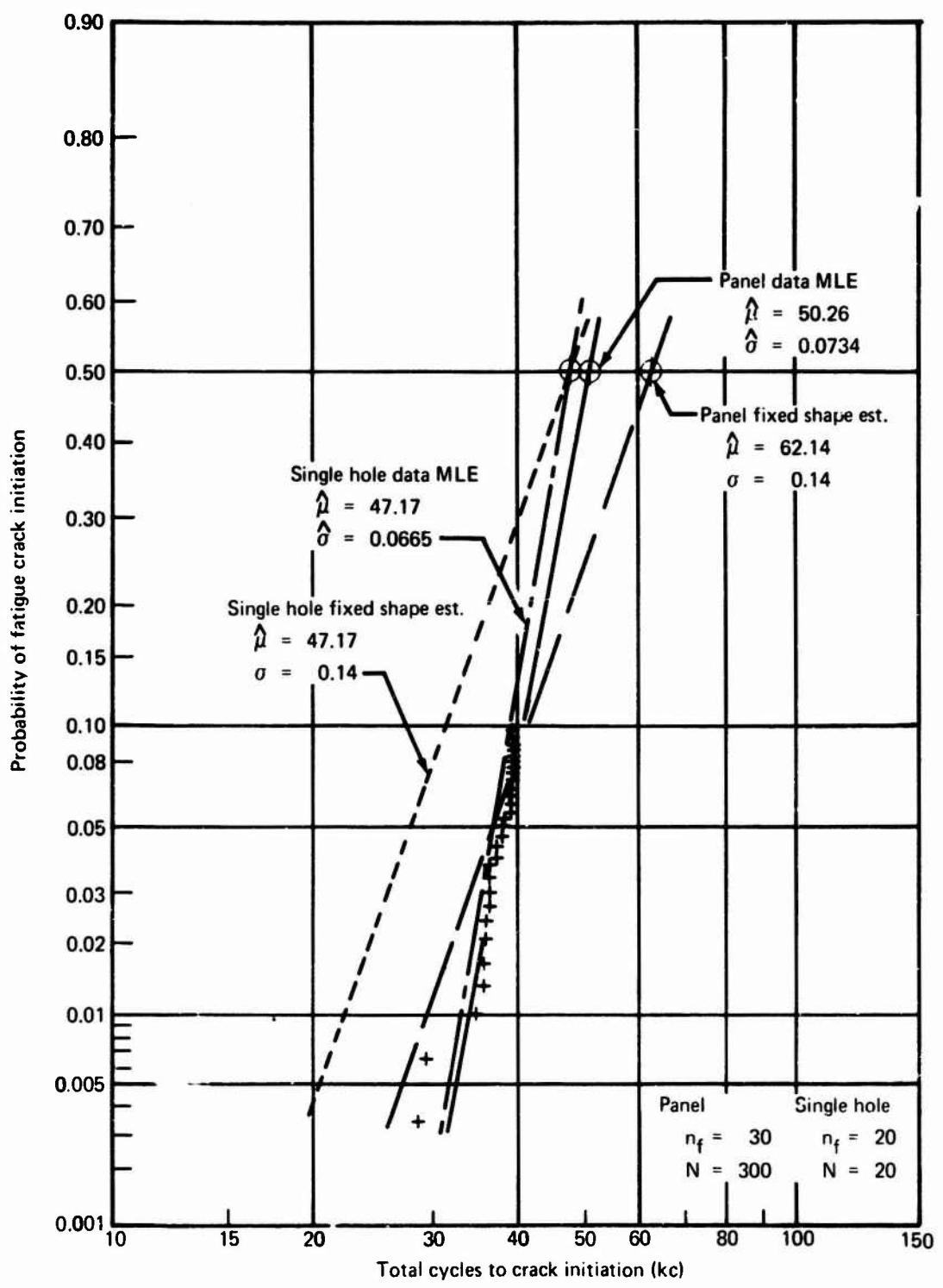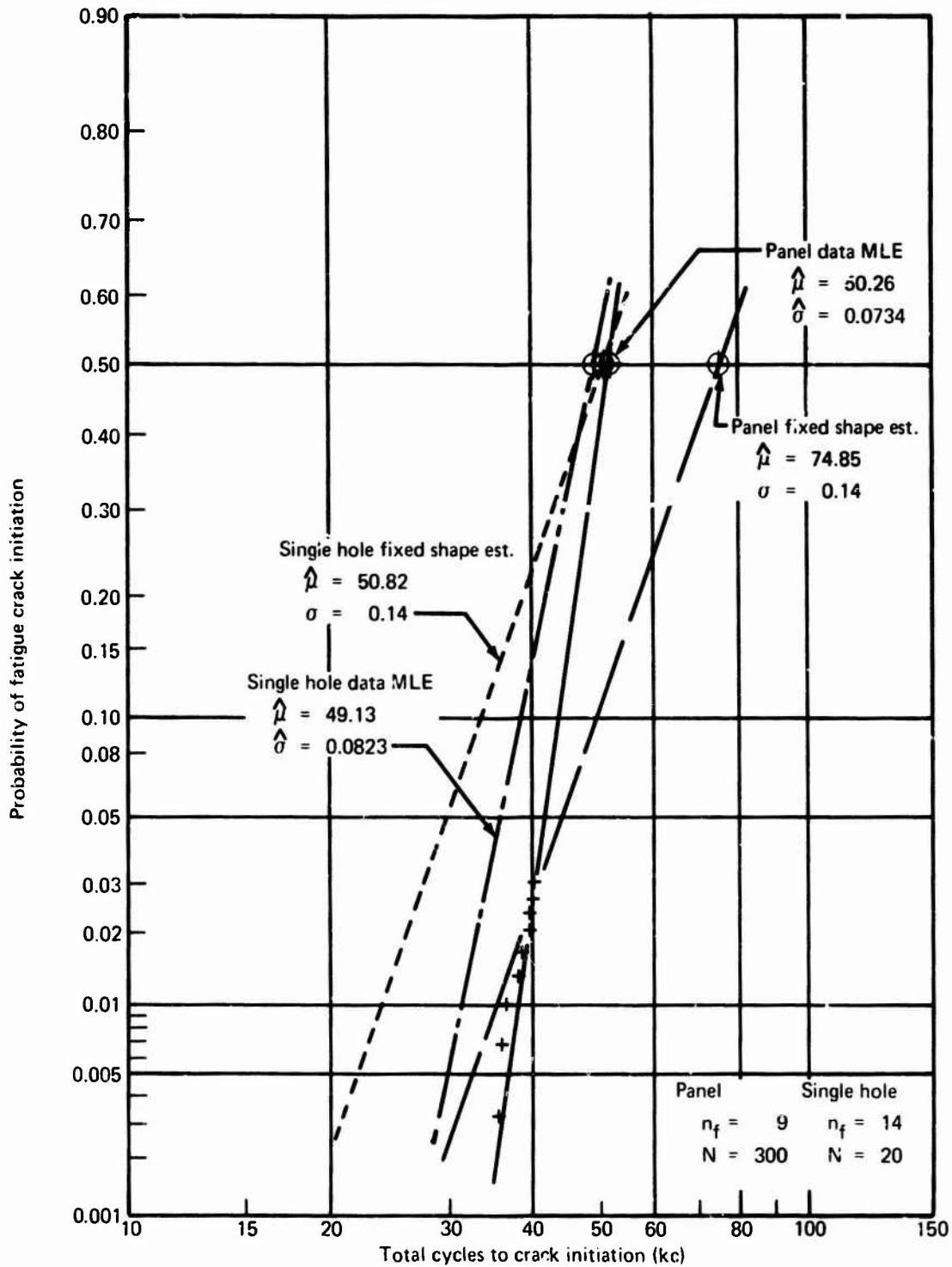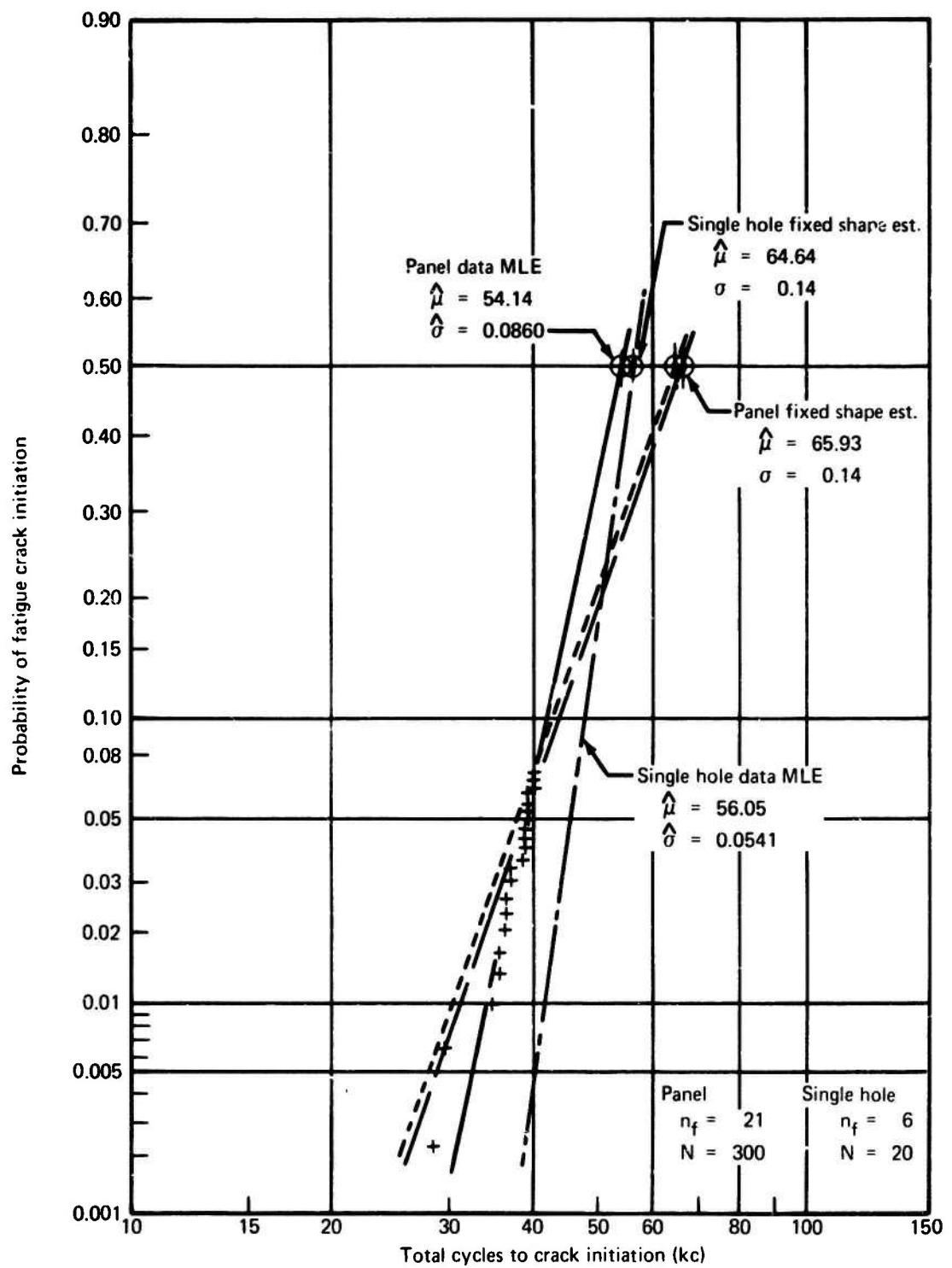
Figure 88.—Log-Normal Cumulative Probability Representation of Fatigue Crack
Initiation Results From Multihole Test Specimen Panel (Ref. 2)

118

b. **Failures Originating at Tool Exit Face**

Figure 88. – Continued

119

c. Failures Originating at Tool Entry Face

Figure 88.--Concluded

120

TABLE 1.–SUMMARY OF TEST PROGRAM AND NUMBER OF SPECIMENS

Test specimen configuration	Test spectrum identification		Material and number of test specimens			Total number of test specimens per configuration
	No.	Description	Heat A	Heat B	Heat C	
Figure 1 Structural simulation	A-1	Gust load	2	1	1	12
	A-2	Gust load	1	–	–	
	A-3	Gust load	1	–	–	
	B-1	Maneuver load	2	1	1	
	B-2	Maneuver load	1	–	–	
	B-3	Maneuver load	1	–	–	
Figure 2a Usage simulation open hole	A-1	Gust load	2[a]	–	1	10
	A-2	Gust load	1	–	–	
	A-3	Gust load	1	–	–	
	B-1	Maneuver load	2[a]	1	–	
	B-2	Maneuver load	1	–	–	
	B-3	Maneuver load	1	–	–	
Figure 2b Usage simulation filled hole	A-1	Gust load	1	–	–	2
	A-2	Gust load	–	–	–	
	A-3	Gust load	–	–	–	
	B-1	Maneuver load	–	1	–	
	B-2	Maneuver load	–	–	–	
	B-3	Maneuver load	–	–	–	
Figure 2c Usage simulation load transfer type I	A-1	Gust load	1	1	1	4
	A-2	Gust load	–	–	–	
	A-3	Gust load	–	–	–	
	B-1	Maneuver load	–	1	–	
	B-2	Maneuver load	–	–	–	
	B-3	Maneuver load	–	–	–	
Figure 2d Usage simulation load transfer type II	A-1	Gust load	1	1	1	4
	A-2	Gust load	–	–	–	
	A-3	Gust load	–	–	–	
	B-1	Maneuver load	–	1	–	
	B-2	Maneuver load	–	–	–	
	B-3	Maneuver load	–	–	–	

[a] One specimen tested under 95% relative humidity

TABLE 2. CORRELATION OF TEST SPECIMEN IDENTIFICATION NUMBER WITH BOEING MANUFACTURING DRAWING NUMBER AND PANEL FABRICATION NUMBER

Test specimen identification number	Material heat number	Drawing number	Drawing title		Panel fabrication number
A1	A	64-22727-1	Multihole Structural Simulation Specimen		1
A2	A	-1			2
A3	B	-2			1
A4	C	-3			1
A5	B	-2			2
A6	A	-1			4
A7	A	-1			5
A8	A	-1			3
A9	A	-1			7
A10	A	-1			6
A11	A	-1			8
A12	C	-3			2
2A1	A	64-22728-1	Usage Simulation Test Specimen	—Open Hole	1
2A2	A	-1		—Open Hole	2
2A3	A	-1		—Open Hole	3
2A4	A	-1		—Open Hole	4
2A5	B	-2		—Open Hole	1
2A6	C	-3		—Open Hole	1
2A7	A	-4		—Filled Hole	1
2A8	B	-5		—Filled Hole	1
2A9	A	-8		—Ld. Trans.—type I	1
2A10	B	-9		—Ld. Trans.—type I	1
2A11	A	-6		—Ld. Trans.—type II	1
2A12	B	-7		—Ld. Trans.—type II	1
2A13	A	-1		—Open Hole	5
2A14	A	-1		—Open Hole	6
2A15	A	-1		—Open Hole	7
2A16	A	-1		—Open Hole	8
2A17	B	-7		—Ld. Trans.—type II	2
2A18	C	-23		—Ld. Trans.—type II	1
2A19	B	-9		—Ld. Trans.—type I	2
2A20	C	-24		—Ld. Trans.—type I	1

TABLE 3. - TYPICAL CHEMISTRY AND MECHANICAL PROPERTIES OF 2024-T3 ALUMINUM ALLOY SHEET, 0.125-IN. THICKNESS (DATA AS SUPPLIED BY VENDOR)

Heat ident.	Heat number and vendor	Typical chemistry (Aluminum is remainder)								Mechanical properties (4 tests)		
		Si (max)	Fe (max)	Cu	Mn	Mg	Cr (max)	Zn (max)	Others	UTS (ksi)	TYS (ksi)	Elong (%)
A	426557 (Vendor X)	0.5	0.5	4.9 to 3.8	0.9 to 0.3	1.8 to 1.2	0.1	0.25	0.05 max each, 0.15 total	68.3 to 67.7	45.3 to 44.9	22.0 to 19.0
B	044731 (Vendor Y)									67.9 to 67.5	45.2 to 43.1	20.0 to 18.0
C	7121015 (Vendor Z)									68.6 to 65.1	45.4 to 43.6	22.0 to 20.0

123

TABLE 4. BASIC TEST LOADS PER FLIGHT FOR LOAD SPECTRUM A-1 (GUST LOADING)

Number of loads per flight	Test loads[a]					
	Nominal stress levels[b]		Structural simulation specimen (fig. 1)		Usage simulation specimen (fig. 2)	
	f_{max} (ksi)	f_{min} (ksi)	P_{max} (kip)	P_{min} (kip)	P_{max} (kip)	P_{min} (kip)
3	-4.8	-7.9	-21.6	-35.7	-6.0	-9.9
14	15.1	5.0	68.1	22.8	18.9	6.3
5	16.3	3.8	73.5	17.1	20.4	4.8
4	16.8	3.1	75.6	14.1	21.4	3.9
3	17.5	2.4	78.9	10.8	21.9	3.0
2	18.7	1.44	84.3	6.6	23.4	1.8
1	19.9	0.24	89.7	1.2	24.9	0.3
1	22.1	-1.9	99.3	-8.7	27.6	-2.4

[a] Test loads are taken at appropriate 300-lb unit of gross load to match test machine load-programming requirements.

[b] Nominal stress level based on nominal gross area of panels:
   $A_1 = 10.00 \times 0.125 = 1.25$ sq in. (usage simulation specimen)

   $A_2 = 36.00 \times 0.125 = 4.50$ sq in. (structural simulation specimen)

   Stresses at nearest 100 psi for usage simulation specimen loads.

124

TABLE 5.—CYCLIC LOAD SEQUENCE AND DISTRIBUTION OF FIVE-FLIGHT BASIC TEST SPECTRUM A-1 FOR STRUCTURAL SIMULATION SPECIMENS (FIG. 1)

Type of loading	Load sequence per flight	Cyclic test load definition per flight (kip)									
		Flight A		Flight B		Flight C		Flight D		Flight E	
		Max	Min	Max	Min	Max	Min	Max	Min	Max	Min
Ground loads	1	-21.6	-35.7	-21.6	-35.7	-21.6	-35.7	-21.6	-35.7	-21.6	-35.7
	2	-21.6	-35.7	-21.6	-35.7	-21.6	-35.7	-21.6	-35.7	-21.6	-35.7
	3	-21.6	-35.7	-21.6	-35.7	-21.6	-35.7	-21.6	-35.7	-21.6	-35.7
Flight gust loads	4	68.1	22.8	68.1	22.8	68.1	22.8	73.5	17.1	68.1	22.8
	5	84.3	6.6	78.9	10.8	73.5	17.1	68.1	22.8	75.6	14.1
	6	73.5	17.1	68.1	22.1	78.9	10.8	84.3	6.6	68.1	22.8
	7	89.7	1.2	68.1	22.8	68.1	22.8	68.1	22.8	68.1	22.8
	8	68.1	22.8	68.1	22.8	73.5	17.1	68.1	22.8	84.3	6.6
	9	73.5	17.1	73.5	17.1	68.1	22.8	89.7	1.2	78.9	10.8
	10	73.5	17.1	89.7	1.2	75.6	14.1	68.1	22.8	75.6	14.1
	11	68.1	22.8	75.6	14.1	78.9	10.8	68.1	22.8	73.5	17.1
	12	75.6	14.1	68.1	22.8	84.3	6.6	68.1	22.8	73.5	17.1
	13	68.1	22.8	68.1	22.8	-.1	22.8	75.6	14.1	68.1	22.8
	14	68.1	22.8	99.3	-8.7	99.3	-8.7	68.1	22.8	89.7	1.2
	15	68.1	22.8	68.1	22.8	73.5	17.1	78.9	10.8	68.1	22.8
	16	68.1	22.8	75.6	14.1	68.1	22.8	73.5	17.1	68.1	22.8
	17	68.1	22.8	84.3	6.6	68.1	22.8	75.6	14.1	73.5	17.1
	18	73.5	17.1	75.6	14.1	75.6	14.1	99.3	-8.7	68.1	22.8
	19	68.1	22.8	68.1	22.8	75.6	14.1	78.9	10.8	75.6	14.1
	20	75.6	14.1	68.1	22.8	73.5	17.1	68.1	22.8	68.1	22.8
	21	68.1	22.8	78.9	10.8	68.1	22.8	68.1	22.8	84.3	6.6
	22	84.3	6.6	73.5	17.1	78.9	10.8	73.5	17.1	73.5	17.1
	23	78.9	10.8	73.5	17.1	84.3	6.6	73.5	17.1	78.9	10.8
	24	78.9	10.8	78.9	10.8	89.7	1.2	75.6	14.1	99.3	-8.7
	25	68.1	22.8	73.5	17.1	68.1	22.8	78.9	10.8	68.1	22.8
	26	68.1	22.8	73.5	17.1	68.1	22.8	68.1	22.8	78.9	10.8
	27	99.3	-8.7	68.1	22.8	68.1	22.8	73.5	17.1	68.1	22.8
	28	68.1	22.8	68.1	22.8	68.1	22.8	68.1	22.8	68.1	22.8
	29	68.1	22.8	75.6	14.1	68.1	22.8	75.6	14.1	68.1	22.8
	30	73.5	17.1	68.1	22.8	68.1	22.8	68.1	22.8	75.6	14.1
	31	75.6	14.1	68.1	22.8	68.1	22.8	68.1	22.8	68.1	22.8
	32	78.9	10.8	84.3	6.6	75.6	14.1	84.3	6.6	68.1	22.8
	33	75.6	14.1	68.1	22.8	73.5	17.1	68.1	22.8	73.5	17.1

TABLE 6. CYCLIC LOAD SEQUENCE AND DISTRIBUTION OF FIVE-FLIGHT BASIC TEST SPECTRUM A-1 FOR USAGE SIMULATION SPECIMENS (FIG. 2)

Type of Loading	Load Sequence per Flight	Cyclic test load definition per flight (kip)									
		Flight A		Flight B		Flight C		Flight D		Flight E	
		Max	Min	Max	Min	Max	Min	Max	Min	Max	Min
Ground loads	1	-6.0	-9.9	-6.0	-9.9	-6.0	-9.9	-6.0	-9.9	-6.0	-9.9
	2	-6.0	-9.9	-6.0	-9.9	-6.0	-9.9	-6.0	-9.9	-6.0	-9.9
	3	-6.0	-9.9	-6.0	-9.9	-6.0	-9.9	-6.0	-9.9	-6.0	-9.9
	4	18.9	6.3	18.9	6.3	18.9	6.3	20.4	4.8	18.9	6.3
	5	23.4	1.8	21.9	3.0	20.4	4.8	18.9	6.3	21.0	3.9
	6	20.4	4.8	18.9	6.3	21.9	3.0	23.4	1.8	18.9	6.3
	7	24.9	0.3	18.9	6.3	18.9	6.3	18.9	6.3	18.9	6.3
	8	18.9	6.3	18.9	6.3	20.4	4.8	18.9	6.3	23.4	1.8
	9	20.4	4.8	20.4	4.8	18.9	6.3	24.9	0.3	21.9	3.0
	10	20.4	4.8	24.9	0.3	21.0	3.9	18.9	6.3	21.0	3.9
	11	18.9	6.3	21.0	3.9	21.9	3.0	18.9	6.3	20.4	4.8
	12	21.0	3.9	18.9	6.3	23.4	1.8	18.9	6.3	20.4	4.8
	13	18.9	6.3	18.9	6.3	18.9	6.3	21.9	3.9	18.9	6.3
	14	18.9	6.3	27.6	-2.4	27.6	-2.4	18.9	6.3	24.9	0.3
Flight gust loads	15	18.9	6.3	18.9	6.3	20.4	4.8	21.9	3.0	18.9	6.3
	16	18.9	6.3	21.0	3.9	18.9	6.3	20.4	4.9	18.9	6.3
	17	18.9	6.3	23.4	1.8	18.9	6.3	21.0	3.9	20.4	4.8
	18	20.4	4.8	21.0	3.9	21.0	3.9	27.6	2.4	18.9	6.3
	19	18.9	6.3	18.9	6.3	21.0	3.9	21.9	3.0	21.0	3.9
	20	21.0	3.9	18.9	6.3	20.4	4.8	18.9	6.3	18.9	6.3
	21	18.9	6.3	21.9	3.0	18.9	6.3	18.9	6.3	23.4	1.8
	22	23.4	1.8	20.4	4.8	21.9	3.0	20.4	4.8	20.4	4.8
	23	21.9	3.0	20.4	4.3	23.4	1.8	20.4	4.8	21.9	3.0
	24	21.9	3.0	21.9	3.0	24.9	0.3	21.0	3.9	27.6	-2.4
	25	18.9	6.3	20.4	4.8	18.9	6.3	21.9	3.0	18.9	6.3
	26	18.9	6.3	18.9	4.8	18.9	6.3	18.9	6.3	21.9	3.0
	27	27.6	-2.4	18.9	6.3	18.9	6.3	20.4	4.8	18.9	6.3
	28	18.9	6.3	21.0	6.3	18.9	6.3	18.9	6.3	18.9	6.3
	29	18.9	6.3	18.9	3.9	18.9	6.3	21.0	3.9	18.9	6.3
	30	20.4	4.8	18.9	6.3	18.9	6.3	18.9	6.3	21.0	3.9
	31	21.0	3.9	18.9	6.3	18.9	6.3	18.9	6.3	18.9	6.3
	32	21.9	3.0	23.4	1.8	21.0	3.9	23.4	1.8	18.9	6.3
	33	21.0	3.9	18.9	6.3	20.4	4.8	18.9	6.3	20.4	4.8

126

Number of loads per flight	Nominal stress levels[b]		Test loads[a]			
			Structural simulation specimen (fig. 1)		Usage simulation specimen (fig. 2)	
	f_{max} (ksi)	f_{min} (ksi)	P_{max} (kip)	P_{min} (kip)	P_{max} (kip)	P_{min} (kip)
30	-4.8	-7.9	-21.6	-35.7	-6.0	-9.9
70	15.1	5.0	68.1	22.8	18.9	6.3
25	16.3	3.8	73.5	17.1	20.4	4.8
20	16.8	3.1	75.6	14.1	21.4	3.9
15	17.5	2.4	78.9	10.8	21.9	3.0
10	18.7	1.44	84.3	6.6	23.4	1.8
5	19.9	0.24	89.7	1.2	24.9	0.3
5	22.1	-1.9	99.3	-8.7	27.6	-2.4

[a] Test loads are taken at appropriate 300-lb unit of gross load to match test machine load-programming requirements.

[b] Nominal stress level based on nominal gross area of panels:
$A_1 = 10.00 \times 0.125 = 1.25$ sq in. (usage simulation specimen)

$A_2 = 36.00 \times 0.125 = 4.50$ sq in. (structural simulation specimen)

Stresses at nearest 100 psi for usage simulation specimen loads.

TABLE 7.—BASIC TEST LOADS PER 10-FLIGHT LOAD SPECTRUM A-2 (GUST LOADING)

TABLE 8.- CYCLIC LOAD SEQUENCE AND DISTRIBUTION OF 10-FLIGHT BASIC TEST SPECTRUM A-2 FOR STRUCTURAL SIMULATION SPECIMENS (FIG. 1)

Cyclic test load definition per spectrum (kip)

Type of loading	Load sequence per flight	Flight A Max	Flight A Min	Flight B Max	Flight B Min	Flight C Max	Flight C Min	Flight D Max	Flight D Min	Flight E Max	Flight E Min	Flight F Max	Flight F Min	Flight G Max	Flight G Min	Flight H Max	Flight H Min	Flight I Max	Flight I Min	Flight J Max	Flight J Min
Ground loads	1	-21.6	-35.7	-21.6	-35.7	-21.6	-35.7	-21.6	-35.7	-21.6	-35.7	-21.6	-35.7	-21.6	-35.7	-21.6	-35.7	-21.6	-35.7	-21.6	-35.7
	2	-21.6	-35.7	-21.6	-35.7	-21.6	-35.7	-21.6	-35.7	-21.6	-35.7	-21.6	-35.7	-21.6	-35.7	-21.6	-35.7	-21.6	-35.7	-21.6	-35.7
	3	-21.6	-35.7	-21.6	-35.7	-21.6	-35.7	-21.6	-35.7	-21.6	-35.7	-21.6	-35.7	-21.6	-35.7	-21.6	-35.7	-21.6	-35.7	-21.6	-35.7
Flight gust loads	4	68.1	22.8	68.1	22.8	68.1	22.8	68.1	22.8	68.1	22.8	75.6	14.1	73.5	17.1	78.9	10.8	68.1	22.8	75.6	14.1
	5	84.3	6.6	75.6	14.1	78.9	10.8	68.1	22.8	73.5	17.1	73.5	17.1	68.1	22.8	68.1	22.8	75.6	14.1	68.1	22.8
	6	73.5	17.1	68.1	22.8	68.1	22.8	78.9	10.8	78.9	10.8	68.1	22.8	84.3	6.6	68.1	6.6	68.1	22.8	84.3	6.6
	7	89.7	1.2	84.3	6.6	68.1	22.8	73.5	17.1	68.1	22.8	78.9	10.8	68.1	22.8	73.5	17.1	68.1	22.8	73.5	17.1
	8	68.1	22.8	78.9	10.8	68.1	22.8	73.5	17.1	73.5	17.1	84.3	6.6	68.1	22.8	73.5	17.1	84.3	6.6	78.9	10.8
	9	73.5	17.1	78.9	10.8	89.7	1.2	78.9	10.8	68.1	22.8	89.7	1.2	89.7	1.2	75.6	14.1	78.9	10.8	99.3	-8.7
	10	73.5	17.1	68.1	22.8	75.6	14.1	73.5	17.1	75.6	14.1	68.1	22.8	68.1	22.8	78.9	10.8	75.6	14.1	68.1	22.8
	11	68.1	22.8	68.1	22.8	68.1	22.8	73.5	17.1	78.9	10.8	68.1	22.8	68.1	22.8	68.1	22.8	73.5	17.1	78.9	10.8
	12	75.6	14.1	99.3	-8.7	68.1	22.8	68.1	22.8	84.3	6.6	68.1	22.8	68.1	22.8	73.5	17.1	73.5	17.1	68.1	22.8
	13	68.1	22.8	68.1	22.8	99.3	-8.7	68.1	22.8	68.1	22.8	68.1	22.8	75.6	14.1	68.1	22.8	68.1	22.8	68.1	22.8
	14	68.1	22.8	68.1	22.8	68.1	22.8	75.6	14.1	99.3	-8.7	68.1	22.8	68.1	22.8	75.6	14.1	68.1	1.2	68.1	22.8
	15	68.1	22.8	73.5	17.1	68.1	22.8	68.1	22.8	73.5	17.1	68.1	22.8	78.9	10.8	68.1	22.8	68.1	22.8	75.6	14.1
	16	68.1	22.8	75.6	14.1	75.6	14.1	68.1	22.8	68.1	22.8	68.1	22.8	73.5	17.1	68.1	22.8	68.1	22.8	68.1	22.8
	17	68.1	22.8	78.9	10.8	84.3	6.6	84.3	6.6	68.1	22.8	75.6	14.1	75.6	14.1	84.3	6.6	73.5	17.1	68.1	22.8
	18	73.5	17.1	75.6	14.1	75.6	14.1	68.1	22.8	75.6	14.1	73.5	17.1	99.3	-8.7	68.1	22.8	68.1	22.8	73.5	17.1
	19	0	-	0	-	0	-	0	-	0	-	0	-	0	-	0	-	0	-	0	-

128

TABLE 9.—CYCLIC LOAD SEQUENCE AND DISTRIBUTION OF 10-FLIGHT BASIC TEST SPECTRUM A-2 FOR USAGE SIMULATION SPECIMENS (FIG. 2)

Cyclic test load definition per spectrum (kip)

Type of loading	Load sequence per flight	Flight A		Flight 8		Flight C		Flight D		Flight E		Flight F		Flight G		Flight H		Flight I		Flight J	
		Max	Min	Max	Min	Max	Min	Max	Min	Max	Min	Max	Min	Max	Min	Max	Min	Max	Min	Max	Min
Ground loads	1	-6.0	-9.9	-6.0	-9.9	-6.0	-9.9	-6.0	-9.9	-6.0	-9.9	-6.0	-9.9	-6.0	-9.9	-6.0	-9.9	-6.0	-9.9	-6.0	-9.9
	2	-6.0	-9.9	-6.0	-9.9	-6.0	-9.9	-6.0	-9.9	-6.0	-9.9	-6.0	-9.9	-6.0	-9.9	-6.0	-9.9	-6.0	-9.9	-6.0	-9.9
	3	-6.0	-9.9	-6.0	-9.9	-6.0	-9.9	-6.0	-9.9	-6.0	-9.9	-6.0	-9.9	-6.0	-9.9	-6.0	-9.9	-6.0	-9.9	-6.0	-9.9
Flight gust loads	4	18.9	6.3	18.9	6.3	18.9	6.3	18.9	6.3	18.9	6.3	21.0	3.9	20.4	4.8	21.9	3.0	18.9	6.3	21.0	3.9
	5	23.4	1.8	21.0	3.9	21.9	3.0	18.9	6.3	20.4	4.8	20.4	4.8	18.9	6.3	18.9	6.3	21.0	3.9	18.9	6.3
	6	20.4	4.8	18.9	6.3	18.9	6.3	21.9	3.0	21.9	3.0	18.9	6.3	23.4	1.8	18.9	6.3	18.9	6.3	23.4	1.8
	7	24.9	0.3	23.4	1.8	18.9	6.3	20.4	4.6	18.9	6.3	21.9	3.0	18.9	5.3	20.4	4.8	18.9	6.3	20.4	4.3
	8	18.9	6.3	21.9	3.0	18.9	6.3	20.4	4.8	20.4	4.8	23.4	1.8	18.9	6.3	20.4	4.8	23.4	1.8	21.0	3.0
	9	20.4	4.8	21.9	3.0	20.4	4.8	21.9	3.0	18.9	6.3	24.9	0.3	21.9	0.3	21.0	3.9	21.3	3.0	27.6	-2.4
	10	20.4	4.8	18.9	6.3	24.9	0.3	20.4	4.8	21.0	3.9	18.9	6.3	18.9	6.3	21.9	3.0	21.0	3.9	18.9	6.3
	11	18.9	6.3	18.9	6.3	21.0	3.9	20.4	4.8	21.9	3.0	18.9	6.3	18.9	6.3	18.9	6.3	20.4	4.8	21.9	3.0
	12	21.0	3.9	27.6	-2.4	18.9	6.3	18.9	6.3	23.4	1.8	18.9	6.3	18.9	4.8	20.4	4.6	20.4	4.8	18.9	6.3
	13	18.9	6.3	18.9	6.3	18.9	6.3	18.9	6.3	18.9	6.3	18.9	6.3	21.0	3.9	18.9	6.3	18.9	6.3	18.9	6.3
	14	18.9	6.3	18.9	6.3	27.6	-2.4	21.0	3.9	27.6	-2.4	18.9	6.3	18.9	6.3	21.0	3.9	24.9	0.3	18.9	6.3
	15	18.9	6.3	20.4	4.8	18.9	6.3	18.9	6.3	20.4	4.8	18.9	6.3	21.9	3.0	18.9	6.3	9.9	6.3	21.0	3.9
	16	18.9	6.3	21.0	3.9	21.0	3.9	18.9	6.3	18.9	6.3	16.9	6.3	20.4	4.8	18.9	6.3	-.9	6.3	18.9	6.3
	17	18.9	6.3	21.9	3.0	22.4	1.8	23.4	1.9	18.9	6.3	21.0	3.9	21.9	3.9	23.4	1.8	20.4	4.8	18.9	6.3
	18	20.4	4.8	21.0	3.9	21.0	3.9	18.9	6.3	21.0	3.9	20.4	4.6	27.6	-2.4	18.9	6.3	15.9	6.3	20.4	4.8
	19	0	-	0	-	0	-	0	-	0	-	0	-	0	-	0	-	0	-	0	-

129

TABLE 10.—BASIC TEST LOADS PER FLIGHT FOR LOAD SPECTRUM A-3 (GUST LOADING)

Number of loads per flight	Nominal test stress levels[a]		Test loads[b]			
			Structural simulation specimen (fig. 1)		Usage simulation specimen (fig. 2)	
	f_{max} (ksi)	f_{min} (ksi)	P_{max} (kip)	P_{min} (kip)	P_{max} (kip)	P_{min} (kip)
3	-4.8	-7.9	-21.6	-35.7	-6.0	-9.9
14	12.9	4.1	58.2	18.6	16.2	5.1
5	13.9	3.1	62.7	14.1	17.4	3.9
4	14.4	2.6	64.8	11.7	18.0	3.3
3	14.9	2.2	67.2	9.9	18.6	2.7
2	15.8	1.2	71.1	5.4	19.8	1.5
1	16.8	0.24	75.6	0.9	21.0	0.3
1	18.7	-1.7	84.6	-7.5	23.4	-2.1

[a] Nominal test stress level based on nominal cross-sectional area:

$A_1 = 36.00 \times 0.125 = 4.50$ sq in. (structural simulation specimen)

$A_2 = 10.00 \times 0.125 = 1.25$ sq in. (usage simulation specimen)

[b] Test loads are taken at appropriate 300-pound unit of load to match test machine load-programming requirements and the nominal test stress.

TABLE 11.–CYCLIC LOAD SEQUENCE AND DISTRIBUTION OF FIVE-FLIGHT BASIC TEST SPECTRUM A-3 FOR STRUCTURAL SIMULATION SPECIMEN (FIG. 1)

Type of loading	Load sequence per flight	Cyclic test load definition per spectrum (kip)									
		Flight A		Flight B		Flight C		Flight D		Flight E	
		Max	Min	Max	Min	Max	Min	Max	Min	Max	Min
Ground loads	1	-21.6	-35.7	-21.6	-35.7	-21.6	-35.7	-21.6	-35.7	-21.6	-35.7
	2	-21.6	-35.7	-21.6	-35.7	-21.6	-35.7	-21.6	-35.7	-21.6	-35.7
	3	-21.6	-35.7	-21.6	-35.7	-21.6	-35.7	-21.6	-35.7	-21.6	-35.7
Flight gust loads	4	58.2	18.6	58.2	18.6	58.2	18.6	62.7	14.1	58.2	18.6
	5	71.1	5.4	67.2	9.9	62.7	14.1	58.2	18.6	64.8	11.7
	6	62.7	14.1	58.2	18.6	67.2	9.9	71.1	5.4	58.2	18.6
	7	75.6	0.9	58.2	18.6	58.2	18.6	58.2	18.6	58.2	18.6
	8	58.2	18.6	58.2	18.6	62.7	14.1	58.2	18.6	71.1	5.4
	9	62.7	14.1	62.7	14.1	58.2	18.6	75.6	0.9	67.2	9.9
	10	62.7	14.1	75.6	0.9	64.8	11.7	58.2	18.6	64.8	11.7
	11	58.2	18.6	64.8	11.7	67.2	9.9	58.2	18.6	62.7	14.1
	12	64.8	11.7	58.2	18.6	71.1	5.4	58.2	18.6	62.7	14.1
	13	58.2	18.6	58.2	18.6	58.2	18.6	64.8	11.7	58.2	18.6
	14	58.2	18.6	84.3	-7.5	84.3	-7.5	58.2	18.6	75.6	0.9
	15	58.2	18.6	58.2	18.6	62.7	14.1	67.2	9.9	58.2	18.6
	16	58.2	18.6	64.8	11.7	58.2	18.6	62.7	14.1	58.2	18.6
	17	58.2	18.6	71.1	5.4	58.2	18.6	64.8	11.7	62.7	14.1
	18	62.7	14.1	64.8	11.7	64.9	11.7	84.3	-7.5	58.2	18.6
	19	58.2	18.6	58.2	18.6	64.8	11.7	67.2	9.9	64.8	11.7
	20	64.8	11.7	58.2	18.6	62.7	14.1	58.2	18.6	58.2	18.6
	21	58.2	18.6	67.2	9.9	58.2	18.6	58.2	18.6	71.1	5.4
	22	71.1	5.4	62.7	14.1	67.2	9.9	62.7	14.1	62.7	14.1
	23	67.2	9.9	62.7	14.1	71.1	5.4	62.7	14.1	67.2	9.9
	24	67.2	9.9	67.2	9.9	75.6	0.9	64.8	11.7	84.3	-7.5
	25	58.2	18.6	62.7	14.1	58.2	18.6	67.2	9.9	58.2	18.6
	26	58.2	18.6	62.7	14.1	58.2	18.6	58.2	18.6	67.2	9.9
	27	84.3	-7.5	58.2	18.6	58.2	18.6	62.7	14.1	58.2	18.6
	28	58.2	18.6	58.2	18.6	58.2	18.6	58.2	18.6	58.2	18.6
	29	58.2	18.6	64.8	11.7	58.2	18.6	64.8	11.7	58.2	18.6
	30	62.7	14.1	58.2	18.6	58.2	18.6	58.2	18.6	64.8	11.7
	31	64.8	11.7	58.2	18.6	58.2	18.6	58.2	18.6	58.2	18.6
	32	67.2	9.9	71.1	5.4	64.8	11.7	71.1	5.4	58.2	18.6
	33	64.8	11.7	58.2	18.6	62.7	14.1	58.2	18.6	62.7	14.1

131

TABLE 12.–CYCLIC LOAD SEQUENCE AND DISTRIBUTION OF FIVE-FLIGHT BASIC TEST SPECTRUM A-3 FOR USAGE SIMULATION SPECIMEN (FIG. 2)

Type of loading	Load sequence per flight	Cyclic test load definition per spectrum (kip)									
		Flight A		Flight B		Flight C		Flight D		Flight E	
		Max	Min	Max	Min	Max	Min	Max	Min	Max	Min
Ground loads	1	-6.0	-9.9	-6.0	-9.9	-6.0	-9.9	-6.0	-9.9	-6.0	-9.9
	2	-6.0	-9.9	-6.0	-9.9	-6.0	-9.9	-6.0	-9.9	-6.0	-9.9
	3	-6.0	-9.9	-6.0	-9.9	-6.0	-9.9	-6.0	-9.9	-6.0	-9.9
Flight gust loads	4	16.2	5.1	16.2	5.1	16.2	5.1	17.4	3.9	16.2	5.1
	5	19.8	1.5	18.6	2.7	17.4	3.9	16.2	5.1	18.0	3.3
	6	17.4	3.9	16.2	5.1	18.6	2.7	19.8	1.5	16.2	5.1
	7	21.0	0.3	16.2	5.1	16.2	5.1	16.2	5.1	16.2	5.1
	8	16.2	5.1	16.2	5.1	17.4	3.9	16.2	5.1	19.8	1.5
	9	17.4	3.9	17.4	3.9	16.2	5.1	21.0	0.3	18.6	2.7
	10	17.4	3.9	21.0	0.3	18.0	3.3	16.2	5.1	18.0	3.3
	11	16.2	5.1	18.0	3.3	18.6	2.7	16.2	5.1	17.4	3.9
	12	18.0	3.3	16.2	5.1	19.8	1.5	16.2	5.1	17.4	3.9
	13	16.2	5.1	16.2	5.1	16.2	5.1	18.0	3.3	16.2	5.1
	14	16.2	5.1	23.4	-2.1	23.4	-2.1	16.2	5.1	21.0	0.3
	15	16.2	5.1	16.2	5.1	17.4	3.9	18.6	2.7	16.2	5.1
	16	16.2	5.1	18.0	3.3	16.2	5.1	17.4	3.9	16.2	5.1
	17	16.2	5.1	19.8	1.5	16.2	5.1	18.0	3.3	17.4	3.9
	18	17.4	3.9	18.0	3.3	18.0	3.3	23.4	-2.1	16.2	5.1
	19	16.2	5.1	16.2	5.1	18.0	3.3	18.6	2.7	18.0	3.3
	20	18.0	3.3	16.2	5.1	17.4	3.9	16.2	5.1	16.2	5.1
	21	16.2	5.1	18.6	2.7	16.2	5.1	16.2	5.1	19.8	1.5
	22	19.8	1.5	17.4	3.9	18.6	2.7	17.4	3.9	17.4	3.9
	23	18.6	2.7	17.4	3.9	19.8	1.5	17.4	3.9	18.6	2.7
	24	18.6	2.7	18.6	2.7	21.0	0.3	18.0	3.3	23.4	-2.1
	25	16.2	5.1	17.4	3.9	16.2	5.1	18.6	2.7	16.2	5.1
	26	16.2	5.1	17.4	3.9	16.2	5.1	16.2	5.1	18.6	2.7
	27	23.4	-2.1	16.2	5.1	16.2	5.1	17.4	3.9	16.2	5.1
	28	16.2	5.1	16.2	5.1	16.2	5.1	16.2	5.1	16.2	5.1
	29	16.2	5.1	18.0	3.3	16.2	5.1	18.0	3.3	16.2	5.1
	30	17.4	3.9	16.2	5.1	16.2	5.1	16.2	5.1	18.0	3.3
	31	18.0	3.3	16.2	5.1	16.2	5.1	16.2	5.1	16.2	5.1
	32	18.6	2.7	19.8	1.5	18.0	3.3	19.8	1.5	16.2	5.1
	33	18.0	3.3	16.2	5.1	17.4	3.9	16.2	5.1	17.4	3.9

132

TABLE 13. –BASIC TEST LOADS PER FLIGHT FOR LOAD SPECTRUM B-1 (MANEUVER LOADING)

Number of loads per flight	Test loads[a]					
	Nominal stress levels[b]		Structural simulation specimen (fig. 1)		Usage simulation specimen (fig. 2)	
	f_{max} (ksi)	f_{min} (ksi)	P_{max} (kip)	P_{min} (kip)	P_{max} (kip)	P_{min} (kip)
3	-0.24 (-0.27)[c]	-0.96 (-1.00)[c]	-0.3	-1.2	-1.2	-4.5
15	19.0	3.8	23.7	4.8	85.5	17.1
9	21.1	3.8	26.4	4.8	94.8	17.1
4	23.0	3.8	28.8	4.8	103.5	17.1
2	25.9	3.8	32.4	4.8	116.7	17.1

[a]Test loads are taken at appropriate 300-lb unit of load to match test machine load-programming requirements.

[b]Nominal stress level based on nominal gross area of panels:

$A_1 = 10.00 \times 0.125 = 1.25$ sq in. (usage simulation specimen)

$A_2 = 36.00 \times 0.125 = 4.50$ sq in. (structural simulation specimen)

Stresses at nearest 100 psi for usage simulation specimen loads.

[c]Calculated nominal stress for large panel

133

TABLE 14. CYCLIC LOAD SEQUENCE AND DISTRIBUTION OF FIVE-FLIGHT BASIC TEST SPECTRUM B-1 FOR STRUCTURAL SIMULATION SPECIMENS (FIG. 1)

Type of loading	Load sequence per flight	Cyclic test load definition per flight (kip)									
		Flight A		Flight B		Flight C		Flight D		Flight E	
		Max	Min	Max	Min	Max	Min	Max	Min	Max	Min
Ground loads	1	-1.2	-4.5	-1.2	-4.5	-1.2	-4.5	-1.2	-4.5	-1.2	-4.5
	2	-1.2	-4.5	-1.2	-4.5	-1.2	-4.5	-1.2	-4.5	-1.2	-4.5
	3	-1.2	-4.5	-1.2	-4.5	-1.2	-4.5	-1.2	-4.5	-1.2	-4.5
	4	85.5	17.1	85.5	17.1	85.5	17.1	85.5	17.1	85.5	17.1
	5	103.5	17.1	103.5	17.1	94.8	17.1	85.5	17.1	94.8	17.1
	6	94.8	17.1	85.5	17.1	103.5	17.1	103.5	17.1	85.5	17.1
	7	116.7	17.1	85.5	17.1	85.5	17.1	85.5	17.1	85.5	17.1
	8	85.5	17.1	85.5	17.1	94.8	17.1	116.7	17.1	103.5	17.1
	9	94.8	17.1	94.8	17.1	85.5	17.1	85.5	17.1	94.8	17.1
	10	94.8	17.1	116.7	17.1	94.8	17.1	85.5	17.1	94.8	17.1
	11	85.5	17.1	94.8	17.1	94.8	17.1	85.5	17.1	94.8	17.1
	12	94.8	17.1	85.5	17.1	103.5	17.1	94.8	17.1	85.5	17.1
	13	85.5	17.1	85.5	17.1	85.5	17.1	85.5	17.1	116.7	17.1
Flight gust loads	14	85.5	17.1	116.7	17.1	116.7	17.1	85.5	17.1	85.5	17.1
	15	85.5	17.1	85.5	17.1	94.8	17.1	103.5	17.1	85.5	17.1
	16	85.5	17.1	94.8	17.1	85.5	17.1	94.8	17.1	94.8	17.1
	17	85.5	17.1	103.5	17.1	85.5	17.1	94.8	17.1	85.5	17.1
	18	85.5	17.1	94.8	17.1	94.8	17.1	116.7	17.1	94.8	17.1
	19	85.5	17.1	85.5	17.1	94.8	17.1	103.5	17.1	85.5	17.1
	20	94.8	17.1	85.5	17.1	94.8	17.1	85.5	17.1	103.5	17.1
	21	85.5	17.1	103.5	17.1	85.5	17.1	103.5	17.1	94.8	17.1
	22	103.5	17.1	94.8	17.1	103.5	17.1	94.8	17.1	103.5	17.1
	23	103.5	17.1	94.8	17.1	103.5	17.1	94.8	17.1	116.7	17.1
	24	103.5	17.1	94.8	17.1	116.7	17.1	85.5	17.1	85.5	17.1
	25	85.5	17.1	85.5	17.1	85.5	17.1	94.8	17.1	103.5	17.1
	26	85.5	17.1	94.8	17.1	85.5	17.1	85.5	17.1	85.5	17.1
	27	116.7	17.1	85.5	17.1	85.5	17.1	94.8	17.1	85.5	17.1
	28	85.5	17.1	85.5	17.1	85.5	17.1	85.5	17.1	85.5	17.1
	29	85.5	17.1	94.8	17.1	85.5	17.1	94.8	17.1	94.8	17.1
	30	94.8	17.1	85.5	17.1	94.8	17.1	85.5	17.1	85.5	17.1
	31	94.8	17.1	85.5	17.1	85.5	17.1	103.5	17.1	85.5	17.1
	32	94.8	17.1	103.5	17.1	94.8	17.1	85.5	17.1	85.5	17.1
	33	94.8	17.1	85.5	17.1	85.5	17.1	85.5	17.1	85.5	17.1

134

TABLE 15. CYCLIC LOAD SEQUENCE AND DISTRIBUTION OF FIVE-FLIGHT BASIC TEST SPECTRUM B-1 FOR USAGE SIMULATION SPECIMENS (FIG. 2)

Type of loading	Load sequence per flight	Cyclic test load definition per flight (kip)									
		Flight A		Flight B		Flight C		Flight D		Flight E	
		Max	Min	Max	Min	Max	Min	Max	Min	Max	Min
Ground loads	1	-0.3	-1.2	-0.3	-1.2	-0.3	-1.2	-0.3	-1.2	-0.3	-1.2
	2	-0.3	-1.2	-0.3	-1.2	-0.3	-1.2	-0.3	-1.2	-0.3	-1.2
	3	-0.3	-1.2	-0.3	-1.2	-0.3	-1.2	-0.3	-1.2	-0.3	-1.2
	4	23.7	4.8	23.7	4.8	23.7	4.8	23.7	4.8	23.7	4.8
	5	28.8	4.8	28.8	4.8	26.4	4.8	23.7	4.8	26.4	4.8
	6	26.4	4.8	23.7	2.8	28.8	4.8	28.8	4.8	23.7	4.8
	7	32.4	4.8	23.7	4.8	23.7	4.8	23.7	4.8	23.7	4.8
	8	23.7	4.8	23.7	4.8	26.4	4.8	23.7	4.8	28.8	4.8
	9	26.4	4.8	26.4	4.8	23.7	4.8	32.4	4.8	26.4	4.8
	10	26.4	4.8	32.4	4.8	26.4	4.8	23.7	4.8	26.4	4.8
	11	23.7	4.8	26.4	4.8	26.4	4.8	23.7	4.8	26.4	4.8
Flight gust loads	12	26.4	4.8	23.7	4.8	28.8	4.8	23.7	4.8	26.4	4.8
	13	23.7	4.8	23.7	4.8	23.7	4.8	26.4	4.8	26.4	4.2
	14	23.7	4.8	32.4	4.8	32.4	4.8	23.7	4.8	32.4	4.8
	15	23.7	4.8	23.7	4.8	26.4	4.8	28.8	4.8	23.7	4.8
	16	23.7	4.8	26.4	4.8	23.7	4.8	26.4	4.8	23.7	4.8
	17	23.7	4.8	28.8	1.8	23.7	4.8	26.4	4.8	26.4	4.8
	18	23.7	4.8	26.4	4.8	26.4	4.8	32.4	4.8	23.7	4.8
	19	23.7	4.8	23.7	4.8	26.4	4.8	28.8	4.8	26.4	4.8
	20	26.4	4.8	23.7	4.8	26.4	4.8	23.7	4.8	23.7	4.8
	21	23.7	4.8	28.8	4.8	23.7	4.8	23.7	4.8	28.8	4.8
	22	28.8	4.8	26.4	4.8	28.8	4.8	26.4	4.8	26.4	4.8
	23	28.8	4.8	26.4	4.8	28.8	4.8	26.4	4.8	28.8	4.8
	24	28.8	4.8	26.4	4.8	32.4	4.8	26.4	4.8	32.4	4.8
	25	23.7	4.8	23.7	4.8	23.7	4.8	26.4	4.8	23.7	4.8
	26	23.7	4.8	26.4	4.8	23.7	4.8	23.7	4.8	28.8	4.8
	27	32.4	4.8	23.7	4.8	23.7	4.8	26.4	4.8	23.7	4.8
	28	23.7	4.8	23.7	4.8	23.7	4.8	23.7	4.8	23.7	4.8
	29	23.7	4.8	26.4	4.8	23.7	4.8	26.4	4.8	23.7	4.8
	30	26.4	4.8	23.7	4.8	23.7	4.8	23.7	4.8	26.4	4.8
	31	26.4	4.8	23.7	4.8	23.7	4.8	23.7	4.8	23.7	4.8
	32	26.4	4.8	28.8	4.8	26.4	4.8	28.8	4.8	23.7	4.8
	33	26.4	4.8	23.7	4.8	23.7	4.8	23.7	4.8	23.7	4.8

TABLE 16. – BASIC TEST LOADS PER 10-FLIGHT LOAD SPECTRUM B-2 (MANEUVER LOADING)

Number of loads per flight	Test loads[a]							
	Nominal stress levels[b]		Structural simulation specimen (fig. 1)		Usage simulation specimen (fig. 2)			
	f_{max} (ksi)	f_{min} (ksi)	P_{max} (kip)	P_{min} (kip)	P_{max} (kip)	P_{min} (kip)		
30	-0.24 (-0.27)[c]	-0.96 (-1.00)[c]	-0.3	-1.2	-1.2	-4.5		
75	19.0	3.8	23.7	4.8	85.5	17.1		
45	21.1	3.8	26.4	4.8	94.8	17.1		
20	23.0	3.8	28.8	4.8	103.5	17.1		
10	25.9	3.8	32.4	4.8	116.7	17.1		

[a]Test loads are taken at appropriate 300-lb unit of load to match test machine load-programming requirements.

[b]Nominal stress level based on nominal gross area of panels:

A_1 = 10.00 x 0.125 = 1.25 sq in. (usage simulation specimen)

A_2 = 36.00 x 0.125 = 4.50 sq in. (structural simulation specimen)

Stresses at nearest 100 psi for usage simulation specimen loads.

[c]Calculated nominal stress for large panel

136

TABLE 17. CYCLIC LOAD SEQUENCE AND DISTRIBUTION OF 10-FLIGHT BASIC TEST SPECTRUM B-2 FOR STRUCTURAL SIMULATION SPECIMENS (FIG. 1)

Type of loading	Load sequence per flight	Cyclic test load definition per spectrum (kip)																			
		Flight A		Flight B		Flight C		Flight D		Flight E		Flight F		Flight G		Flight H		Flight I		Flight J	
		Max	Min	Max	Min	Max	Min	Max	Min	Max	Min	Max	Min	Max	Min	Max	Min	Max	Min	Max	Min
Ground loads	1	-1.2	-4.5	-1.2	-4.5	-1.2	-4.5	-1.2	-4.5	-1.2	-4.5	-1.2	-4.5	-1.2	-4.5	-1.2	-4.5	-1.2	-4.5	-1.2	-4.5
	2	-1.2	-4.5	-1.2	-4.5	-1.2	-4.5	-1.2	-4.5	-1.2	-4.5	-1.2	-4.5	-1.2	-4.5	-1.2	-4.5	-1.2	-4.5	-1.2	-4.5
	3	-1.2	-4.5	-1.2	-4.5	-1.2	-4.5	-1.2	-4.5	-1.2	-4.5	-1.2	-4.5	-1.2	-4.5	-1.2	-4.5	-1.2	-4.5	-1.2	-4.5
Flight maneuver loading	4	85.5	17.1	85.5	17.1	85.5	17.1	85.5	17.1	85.5	17.1	94.8	17.1	85.5	17.1	103.5	17.1	85.5	17.1	94.8	17.1
	5	103.5	17.1	94.8	17.1	103.5	17.1	85.5	17.1	94.8	17.1	94.8	17.1	85.5	17.1	85.5	17.1	94.8	17.1	85.5	17.1
	6	94.8	17.1	85.5	17.1	85.5	17.1	103.5	17.1	103.5	17.1	85.5	17.1	103.5	17.1	85.5	17.1	85.5	17.1	103.5	17.1
	7	116.7	17.1	103.5	17.1	85.5	17.1	94.8	17.1	85.5	17.1	103.5	17.1	85.5	17.1	94.8	17.1	85.5	17.1	94.8	17.1
	8	85.5	17.1	103.5	17.1	85.5	17.1	94.8	17.1	94.8	17.1	103.5	17.1	85.5	17.1	94.8	17.1	103.5	17.1	103.5	17.1
	9	94.8	17.1	103.5	17.1	94.8	17.1	94.8	17.1	85.5	17.1	116.7	17.1	116.7	17.1	94.8	17.1	94.8	17.1	116.7	17.1
	10	94.8	17.1	85.5	17.1	116.7	17.1	85.5	17.1	94.8	17.1	85.5	17.1	85.5	17.1	85.5	17.1	94.8	17.1	85.5	17.1
	11	85.5	17.1	85.5	17.1	94.8	17.1	94.8	17.1	94.8	17.1	85.5	17.1	85.5	17.1	85.5	17.1	94.8	17.1	103.5	17.1
	12	94.8	17.1	116.7	17.1	85.5	17.1	85.5	17.1	103.5	17.1	85.5	17.1	85.5	17.1	94.8	17.1	94.8	17.1	85.5	17.1
	13	85.5	17.1	85.5	17.1	35.5	17.1	85.5	17.1	85.5	17.1	85.5	17.1	94.8	17.1	85.5	17.1	85.5	17.1	85.5	17.1
	14	85.5	17.1	35.5	17.1	116.7	17.1	94.8	17.1	116.7	17.1	85.5	17.1	85.5	17.1	94.8	17.1	116.7	17.1	85.5	17.1
	15	85.5	17.1	94.8	17.1	85.5	17.1	85.5	17.1	94.8	17.1	103.5	17.1	103.5	17.1	85.5	17.1	85.5	17.1	94.8	17.1
	16	85.5	17.1	94.8	17.1	94.8	17.1	85.5	17.1	85.5	17.1	85.5	17.1	94.8	17.1	85.5	17.1	85.5	17.1	85.5	17.1
	17	85.5	17.1	94.8	17.1	103.5	17.1	103.5	17.1	85.5	17.1	94.8	17.1	94.8	17.1	103.5	17.1	94.8	17.1	85.5	17.1
	18	85.5	17.1	94.8	17.1	94.8	17.1	85.5	17.1	94.8	17.1	85.8	17.1	116.7	17.1	85.5	17.1	85.5	17.1	85.5	17.1
	19	0	-	0	-	0	-	0	-	0	-	0	-	0	-	0	-	0	-	0	-

137

TABLE 18.– CYCLIC LOAD SEQUENCE AND DISTRIBUTION OF 10-FLIGHT BASIC TEST SPECTRUM B-2 FOR USAGE SIMULATION SPECIMENS (FIG. 2)

Cyclic test load definition per spectrum (kip)

Type of loading	Load sequence per flight	Flight A		Flight B		Flight C		Flight D		Flight E		Flight F		Flight G		Flight H		Flight I		Flight J	
		Max	Min	Max	Min	Max	Min	Max	Min	Max	Min	Max	Min	Max	Min	Max	Min	Max	Min	Max	Min
Ground loads	1	-0.3	-1.2	-0.3	-1.2	-0.3	-1.2	-0.3	-1.2	-0.3	-1.2	-0.3	-1.2	-0.3	-1.2	-0.3	-1.2	-0.3	-1.2	-0.3	-1.2
	2	-0.3	-1.2	-0.3	-1.2	-0.3	-1.2	-0.3	-1.2	-0.3	-1.2	-0.3	-1.2	-0.3	-1.2	-0.3	-1.2	-0.3	-1.2	-0.3	-1.2
	3	-0.3	-1.2	0.3	-1.2	-0.3	-1.2	-0.3	-1.2	-0.3	-1.2	-0.3	-1.2	-0.3	-1.2	-0.3	-1.2	-0.3	-1.2	-0.3	-1.2
Flight maneuver loads	4	23.7	4.8	23.7	4.8	23.7	4.8	23.7	4.8	23.7	4.8	26.4	4.8	23.7	4.8	28.8	4.8	23.7	4.8	26.4	4.8
	5	28.8	4.8	26.4	4.8	28.8	4.8	23.7	4.8	26.4	4.8	26.4	4.8	23.7	4.8	23.7	4.8	26.4	4.8	23.7	4.8
	6	26.4	4.8	23.7	4.8	23.7	4.8	28.8	4.8	28.8	4.8	23.7	4.8	28.8	4.8	23.7	4.8	23.7	4.8	28.8	4.8
	7	32.4	4.8	28.8	4.8	23.7	4.8	26.4	4.8	23.7	4.8	28.8	4.8	23.7	4.8	26.4	4.8	23.7	4.8	26.4	4.8
	8	23.7	4.8	28.8	4.8	23.7	4.8	26.4	4.8	26.4	4.8	28.8	4.8	23.7	4.8	26.4	4.8	28.8	4.8	28.8	4.9
	9	26.4	4.8	28.8	4.8	26.4	4.8	26.4	4.8	23.7	4.8	32.4	4.8	32.4	4.8	26.4	4.8	26.4	4.8	32.4	4.8
	10	26.4	4.8	23.7	4.8	32.4	4.8	23.7	4.6	26.4	4.8	23.7	4.8	23.7	4.8	23.7	4.8	26.4	4.8	23.7	4.8
	11	23.7	4.8	23.7	4.8	26.4	4.8	26.4	4.8	26.4	4.8	23.7	4.8	23.7	4.8	23.7	4.8	26.4	4.8	23.7	4.8
	12	26.4	4.8	32.4	4.8	23.7	4.8	23.7	4.8	23.7	4.8	23.7	4.8	23.7	4.8	23.7	4.8	26.4	4.8	23.7	4.8
	13	23.7	4.8	23.7	4.8	23.7	4.8	23.7	4.8	23.7	4.9	23.7	4.8	26.4	4.8	23.7	4.8	23.7	4.8	23.7	4.8
	14	23.7	4.8	23.7	4.8	32.4	4.8	26.4	4.8	32.4	4.8	23.7	4.8	23.7	4.8	26.4	4.8	32.4	4.8	23.7	4.8
	15	23.7	4.6	26.4	4.8	23.7	4.8	23.7	4.8	26.4	4.8	23.7	4.8	28.8	4.8	23.7	4.8	23.7	4.8	26.4	4.8
	16	23.7	4.8	26.4	4.8	26.4	4.8	23.7	4.8	23.7	4.9	23.7	4.8	26.4	4.8	23.7	4.8	23.7	4.8	23.7	4.8
	17	23.7	4.8	26.4	4.8	28.8	4.8	28.8	4.8	23.7	4.8	26.4	4.8	26.4	4.8	28.8	4.8	26.4	4.8	23.7	4.8
	18	23.7	4.8	26.4	4.8	26.4	4.8	23.7	4.8	26.4	4.8	23.7	4.8	32.4	4.8	23.7	4.8	23.7	4.8	23.7	4.8
	19	0	–	0	–	0	–	0	–	0	–	0	–	0	–	0	–	0	–	0	–

138

TABLE 19.—BASIC TEST LOADS PER FLIGHT FOR LOAD SPECTRUM B-3 (MANEUVER LOADING)

Number of loads per flight	Nominal test stress levels[a]		Test loads[b]			
			Structural simulation specimen (fig. 1)		Usage simulation specimen (fig. 2)	
	f_{max} (ksi)	f_{min} (ksi)	P_{max} (kip)	P_{min} (kip)	P_{max} (kip)	P_{min} (kip)
3	-0.27	-1.00	-1.2	-4.5	-0.3	-1.2
15	16.3	3.3	72.9	15.3	20.4	4.2
9	18.0	3.3	81.0	15.3	22.5	4.2
4	19.5	3.3	87.9	15.3	24.3	4.2
2	22.1	3.3	99.6	15.3	27.6	4.2

[a]Nominal stress level based on nominal area of panels:

A_1 = 36.00 x 0.125 = 1.25 sq in. (structural simulation specimen)

A_2 = 10.00 x 0.125 = 4.50 sq in. (usage simulation specimen)

[b]Test loads are taken at appropriate 300-pound unit of load to match test machine load programming requirements.

Type of loading	Load sequence per flight	Cyclic test load definition per spectrum (kip)									
		Flight A		Flight B		Flight C		Flight D		Flight E	
		Max	Min	Max	Min	Max	Min	Max	Min	Max	Min
Ground loads	1	-1.2	-4.5	-1.2	-4.5	-1.2	-4.5	-1.2	-4.5	-1.2	-4.5
	2	-1.2	-4.5	-1.2	-4.5	-1.2	-4.5	-1.2	-4.5	-1.2	-4.5
	3	-1.2	-4.5	-1.2	-4.5	-1.2	-4.5	-1.2	-4.5	-1.2	-4.5
Flight maneuver loads	4	72.9	15.3	72.9	15.3	72.9	15.3	72.9	15.3	72.9	15.3
	5	87.9	15.3	87.9	15.3	81.0	15.3	72.9	15.3	81.0	15.3
	6	81.0	15.3	72.9	15.3	87.9	15.3	87.9	15.3	72.9	15.3
	7	99.6	15.3	72.9	15.3	72.9	15.3	72.9	15.3	72.9	15.3
	8	72.9	15.3	72.9	15.3	81.0	15.3	72.9	15.3	87.9	15.3
	9	81.0	15.3	81.0	15.3	72.9	15.3	99.6	15.3	81.0	15.3
	10	81.0	15.3	99.6	15.3	81.0	15.3	72.9	15.3	81.0	15.3
	11	72.9	15.3	81.0	15.3	81.0	15.3	72.9	15.3	81.0	15.3
	12	81.0	15.3	72.9	15.3	87.9	15.3	72.9	15.3	81.0	15.3
	13	72.9	15.3	72.9	15.3	72.9	15.3	81.0	15.3	72.9	15.3
	14	72.9	15.3	99.6	15.3	99.6	15.3	72.0	15.3	99.6	15.3
	15	72.9	15.3	72.9	15.3	81.0	15.3	87.9	15.3	72.9	15.3
	16	72.9	15.3	81.0	15.3	72.9	15.3	81.0	15.3	72.9	15.3
	17	72.9	15.3	87.9	15.3	72.9	15.3	81.0	15.3	81.0	15.3
	18	72.9	15.3	81.0	15.3	81.0	15.3	99.6	15.3	72.9	15.3
	19	72.9	15.3	72.9	15.3	81.0	15.3	87.9	15.3	81.0	15.3
	20	81.0	15.3	72.9	15.3	81.0	15.3	72.9	15.3	72.9	15.3
	21	72.9	15.3	87.9	15.3	72.9	15.3	72.9	15.3	87.9	15.3
	22	87.9	15.3	81.0	15.3	87.9	15.3	81.0	15.3	81.0	15.3
	23	87.9	15.3	81.0	15.3	87.9	15.3	81.0	15.3	87.9	15.3
	24	87.9	15.3	81.0	15.3	99.6	15.3	81.0	15.3	99.6	15.3
	25	72.9	15.3	72.9	15.3	72.9	15.3	81.0	15.3	72.9	15.3
	26	72.9	15.3	81.0	15.3	72.9	15.3	72.9	15.3	87.9	15.3
	27	99.6	15.3	72.9	15.3	72.9	15.3	81.0	15.3	72.9	15.3
	28	72.9	15.3	72.9	15.3	72.9	15.3	72.9	15.3	72.9	15.3
	29	72.9	15.3	81.0	15.3	72.9	15.3	81.0	15.3	72.9	15.3
	30	81.0	15.3	72.9	15.3	72.9	15.3	72.9	15.3	81.0	15.3
	31	81.0	15.3	72.9	15.3	72.9	15.3	72.9	15.3	72.9	15.3
	32	81.0	15.3	87.9	15.3	81.0	15.3	87.9	15.3	72.9	15.3
	33	81.0	15.3	72.9	15.3	72.9	15.3	72.9	15.3	72.9	15.3

TABLE 21.—CYCLIC LOAD SEQUENCE AND DISTRIBUTION OF FIVE-FLIGHT BASIC TEST SPECTRUM B-3 FOR USAGE SIMULATION SPECIMEN (FIG. 2)

Type of loading	Load sequence per flight	Cyclic test load definition per spectrum (kip)									
		Flight A		Flight B		Flight C		Flight D		Flight E	
		Max	Min	Max	Min	Max	Min	Max	Min	Max	Min
Ground loads	1	-0.3	-1.2	-0.3	-1.2	-0.3	-1.2	-0.3	-1.2	-0.3	-1.2
	2	-0.3	-1.2	-0.3	-1.2	-0.3	-1.2	-0.3	-1.2	-0.3	-1.2
	3	-0.3	-1.2	-0.3	-1.2	-0.3	-1.2	-0.3	-1.2	-0.3	-1.2
Flight maneuver loads	4	20.4	4.2	20.4	4.2	20.4	4.2	20.4	4.2	20.4	4.2
	5	24.3	4.2	24.3	4.2	22.5	4.2	20.4	4.2	22.5	4.2
	6	22.5	4.2	20.4	4.2	24.3	4.2	24.3	4.2	20.4	4.2
	7	27.6	4.2	20.4	4.2	20.4	4.2	20.4	4.2	20.4	4.2
	8	20.4	4.2	20.4	4.2	22.5	4.2	20.4	4.2	24.3	4.2
	9	22.5	4.2	22.5	4.2	20.4	4.2	27.6	4.2	22.5	4.2
	10	22.5	4.2	27.6	4.2	22.5	4.2	20.4	4.2	22.5	4.2
	11	20.4	4.2	22.5	4.2	22.5	4.2	20.4	4.2	22.5	4.2
	12	22.5	4.2	20.4	4.2	24.3	4.2	20.4	4.2	22.5	4.2
	13	20.4	4.2	20.4	4.2	20.4	4.2	22.5	4.2	20.4	4.2
	14	20.4	4.2	27.6	4.2	27.6	4.2	20.4	4.2	27.6	4.2
	15	20.4	4.2	20.4	4.2	22.5	4.2	24.3	4.2	20.4	4.2
	16	20.4	4.2	22.5	4.2	20.4	4.2	22.5	4.2	20.4	4.2
	17	20.4	4.2	24.3	4.2	20.4	4.2	22.5	4.2	22.5	4.2
	18	20.4	4.2	22.5	4.2	22.5	4.2	27.6	4.2	20.4	4.2
	19	20.4	4.2	20.4	4.2	22.5	4.2	24.3	4.2	22.5	4.2
	20	22.5	4.2	20.4	4.2	22.5	4.2	20.4	4.2	20.4	4.2
	21	20.4	4.2	24.3	4.2	20.4	4.2	20.4	4.2	24.3	4.2
	22	24.3	4.2	22.5	4.2	24.3	4.2	22.5	4.2	22.5	4.2
	23	24.3	4.2	22.5	4.2	24.3	4.2	22.5	4.2	24.3	4.2
	24	24.3	4.2	22.5	4.2	27.6	4.2	22.5	4.2	27.6	4.2
	25	20.4	4.2	20.4	4.2	20.4	4.2	22.5	4.2	20.4	4.2
	26	20.4	4.2	22.5	4.2	20.4	4.2	20.4	4.2	24.3	4.2
	27	27.6	4.2	20.4	4.2	20.4	4.2	22.5	4.2	20.4	4.2
	28	20.4	4.2	20.4	4.2	20.4	4.2	20.4	4.2	20.4	4.2
	29	20.4	4.2	22.5	4.2	20.4	4.2	22.5	4.2	20.4	4.2
	30	22.5	4.2	20.4	4.2	20.4	4.2	20.4	4.2	22.5	4.2
	31	22.5	4.2	20.4	4.2	20.4	4.2	20.4	4.2	20.4	4.2
	32	22.5	4.2	24.3	4.2	22.5	4.2	24.3	4.2	20.4	4.2
	33	22.5	4.2	20.4	4.2	20.4	4.2	20.4	4.2	20.4	4.2

TABLE 22.—STRAIN GAGE SURVEY ON USAGE SIMULATION SPECIMEN (FIG. 2a, OPEN HOLE) WITHOUT BUCKLING RESTRAINT FIXTURE

Gage no.	Lower end free	Lower end bolted	Installed specimen zero load	Strain gage data at no-ad load condition (0.000001 in./in.)						
				4.0 kip	8.0 kip	12.0 kip	16.0 kip	18.9 kip	Zero load
1	0	-8	0	303	595	889	1183	1394	3
2	0	-9	0	297	589	883	1178	1389	-3
3	0	0	0	294	598	903	1211	1433	-1
4	0	-2	0	294	597	900	1208	1428	0
5	0	11	0	311	614	919	1227	1449	-1
6	0	12	0	314	616	920	1227	1451	2

142

TABLE 23. -STRAIN GAGE SURVEY ON USAGE SIMULATION SPECIMEN
FIG. 2a, OPEN HOLE) WITH BUCKLING RESTRAINT FIXTURE

Gage no.	Strain gage data at noted load condition (0.000001 in./in.)						
	Installed specimen zero load	4.0 kip	8.0 kip	12.0 kip	16.0 kip	18.9 kip	Zero load
1	0	29	583	875	1171	1384	1
2	0	290	584	878	1171	1384	0
3	0	301	607	913	1218	1442	1
4	0	301	608	912	1218	1439	1
5	0	299	604	907	1214	1434	-2
6	0	301	606	909	1216	1438	-1

TABLE 24.—STRAIN GAGE SURVEY ON USAGE SIMULATION SPECIMEN (FIG. 2a, OPEN HOLE) WITH BUCKLING RESTRAINT FIXTURE AND LOAD REVERSAL

Gage no.	Strain gage data at noted load condition (0.000001 in./in.)											
	Initial zero load	4.0 kip	8.0 kip	12.0 kip	16.0 kip	18.9 kip	Zero load	Initial zero load	-3.3 kip	-6.6 kip	-9.9 kip	Zero load
1	0	290	583	875	1171	1384	1	0	-242	-482	-723	-1
2	0	290	584	878	1171	1384	0	0	-241	-483	-724	-2
3	0	301	607	913	1218	1442	1	0	-252	-502	-753	-3
4	0	301	608	912	1218	1439	1	0	-251	-502	-750	-1
5	0	299	604	907	1214	1434	-2	0	-251	-501	-747	0
6	0	301	606	909	1216	1438	-1	0	-249	-500	-747	-2

TABLE 25. – STRAIN GAGE SURVEY ON USAGE SIMULATION SPECIMEN (FIG. 2c. LOAD TRANSFER TYPE I) WITH BUCKLING RESTRAINT FIXTURE AND LOAD REVERSAL

Gage no.	Strain gage data at noted load condition (0.000001 in./in.)											
	Initial zero load	4.0 kip	8.0 kip	12.0 kip	15.0 kip	18.9 kip	Zero load	Initial zero load	-3.3 kip	-6.6 kip	-9.9 kip	Zero load
1	0	324	642	960	1273	1497	6	0	-266	-532	-798	4
2	0	324	642	953	1263	1484	7	0	-271	-535	-799	2
3	0	311	619	931	1241	1466	2	0	-256	-510	-765	3
4	0	311	620	931	1243	1468	1	0	-256	-507	-760	3
5	0	307	615	926	1237	1460	0	0	-251	-501	-750	8
6	0	306	611	920	1232	1455	2	0	-245	-492	-737	8

145

TABLE 26. – STRAIN GAGE SURVEY ON USAGE SIMULATION SPECIMEN (FIG. 2d. LOAD TRANSFER TYPE II) WITH BUCKLING RESTRAINT FIXTURE AND LOAD REVERSAL

Gage no.	Initial zero load	4.0 kip	8.0 kip	12.0 kip	16.0 kip	18.9 kip	Zero load	Initial zero load	-3.3 kip	-6.6 kip	-9.9 kip	Zero load
						Strain gage data at noted load condition (0.000001 in./in.)						
1	0	343	678	999	1316	1544	7	0	-277	-555	-827	4
2	0	363	707	1033	1357	1589	8	0	-292	-584	-871	5
3	0	319	631	942	1252	1478	6	0	-257	-519	-774	2
4	0	321	636	948	1263	1490	5	0	-257	-515	-773	5
5	0	315	623	933	1246	1472	5	0	-254	-506	-757	5
6	0	311	621	926	1233	1457	4	0	-251	-498	-747	5

146

TABLE 27.—STRAIN GAGE SURVEY ON STRUCTURAL SIMULATION TEST SPECIMEN (FIG. 1) WITHOUT BUCKLING RESTRAINT FIXTURE

Gage no.	Strain gage data at noted load condition (0.000001 in./in.)						
	Installed specimen zero load	14.0 kip	28.0 kip	42.0 kip	56.0 kip	68.1 kip	Zero load
1	0	290	582	876	1176	1426	2
2	0	303	597	892	1190	1448	2
3	0	292	587	885	1184	1445	-1
4	0	311	611	909	1213	1472	4
5	0	288	575	868	1162	1420	6
6	0	305	601	898	1196	1454	4
7	0	289	576	868	1156	1410	3
8	0	292	585	878	1172	1426	0
9	0	298	591	888	1183	1442	3
10	0	291	582	876	1168	1423	1
11	0	291	582	874	1167	1420	3
12	0	291	580	872	1164	1416	3

TABLE 28.—STRAIN GAGE SURVEY ON STRUCTURAL SIMULATION TEST SPECIMEN (FIG. 1) WITH BUCKLING RESTRAINT FIXTURE AND LOAD REVERSAL

		Strain gage data at noted load condition (0.000001 in./in.)										
Gage no.	Initial zero load	14.0 kip	28.0 kip	42.0 kip	56.0 kip	68.1 kip	Zero load	Initial zero load	-12.0 kip	-24.0 kip	-35.7 kip	Zero load
1	0	295	592	885	1180	1436	—	0	-251	-500	-746	7
2	0	295	593	888	1183	1442	—	0	-255	-506	-741	6
3	0	297	596	895	1192	1454	—	0	-256	-506	-752	4
4	0	301	603	904	1202	1465	—	0	-258	-510	757	3
5	0	290	580	874	1164	1422	—	0	-246	-492	-726	2
6	0	301	599	898	1192	1451	—	0	-260	-506	-752	4
7	0	290	580	871	1159	1414	—	0	-245	-487	-734	5
8	0	294	587	879	1172	1427	—	0	-253	-502	-734	4
9	0	296	593	889	1185	1442	—	0	-253	-502	-745	7
10	0	293	586	878	1171	1427	—	0	-247	-492	-733	8
11	0	287	578	870	1161	1415	—	0	-244	-484	-713	5
12	0	295	587	879	1171	1425	—	0	-251	-501	-750	7

148

TABLE 29. STRAIN GAGE SURVEY ON USAGE SIMULATION SPECIMEN AND LOAD STRAPS (FIG. 2d, LOAD TRANSFER TYPE II) WITH BUCKLING RESTRAINT FIXTURE

Gage no.	Initial zero load	4.0 kip	8.0 kip	12.0 kip	16.0 kip	18.9 kip	Zero load	Initial zero load	-3.3 kip	-6.6 kip	-9.9 kip	Zero load
						Strain gage data at noted load condition (0.000001 in./in.)						
1	0	343	672	991	1305	1533	0	0	-284	-560	-835	+3
2	0	351	693	1025	1352	1595	-3	0	-290	-575	-851	7
3	0	307	617	929	1240	1466	-1	0	-255	-516	-768	2
4	0	306	616	926	1236	1464	-4	0	-261	-518	-767	2
5	0	310	620	931	1245	1471	-3	0	-255	-523	-774	3
6	0	313	628	942	1259	1487	-5	0	-259	-523	-780	4
7	0	132	253	381	505	581	-11	0	-79	-108	-108	7
8	0	139	268	399	525	607	-5	0	-94	-152	-187	6
9	0	128	249	374	493	570	-5	0	-81	-121	-130	5
10	0	139	268	400	525	607	-5	0	-98	-164	-205	5
11	0	128	254	379	496	571	-6	0	-75	-107	-109	5
12	0	137	272	401	523	604	-5	0	-93	-153	-189	4

149

TABLE 30. – SUMMARY OF STRUCTURAL SIMULATION SPECIMEN (FIG. 1) TEST RESULTS

Specimen no.	Heat	Test environment	Test load	Crack initiation sequence	Hole no.	Tool entry face Left	Tool entry face Right	Tool exit face Left	Tool exit face Right	Estimated crack origin face	Total load points to crack detection	Total equivalent load cycles to crack detection
A1	A	Air	A-1	1	I10	—	—	—	0.02	Exit	259,817	129,908
				2	E9	—	0.03	—	—	Entry	260,038	130,019
				3	F9	—	0.03	—	—	Entry	261,783	130,891
				4	C3	—	0.03	—	0.03	Exit	266,567	133,283
				5	A3	—	0.01	—	0.03	Exit	266,863	133,431
				6	G8	—	0.04	—	0.05	Entry	269,000	134,500
				7	A1	—	0.01	—	0.03	Exit	272,964	136,482
				8	B7	0.05	0.02	—	0.03	Exit	277,226	138,613
				9	F8	—	0.03	—	0.04	Entry	279,109	139,554
				10	G3	—	0.03	—	0.03	Exit	281,176	140,588
				11	C10	—	0.03	—	0.05	Exit	288,776	144,388
				12	B2	—	0.05	—	0.04	Exit	288,776	144,388
				13	G7	—	0.04	—	0.04	Exit	289,117	144,558
				14	E4	—	0.05	—	0.02	Entry	301,005	150,502
				15	D9	—	0.08	—	0.03	Entry	303,431	151,715
				16	C7	—	0.02	—	0.03	Exit	303,431	151,715
A2	A	Air	A-1	1	H8	—	—	0.025	—	Exit	189,344	94,672
				2	I8	—	—	—	0.02	Exit	190,264	95,132
				3	K8	—	0.01	0.03	0.03	Exit	202,350	101,175
				4	D5	—	—	—	—	Exit	207,162	103,581
				5	C7	—	0.01	—	0.03	Exit	217,717	108,858
				6	D7	—	0.05	—	0.04	Exit	260,620	130,310
				7	E7	—	0.02	—	0.05	Exit	260,620	130,310
				8	D2	—	0.04	—	0.04	Entry	265,291	132,645
				9	A7	—	—	—	0.03	Exit	270,984	135,492
				10	F6	—	—	—	0.035	Exit	272,559	136,279
				11	F7	—	—	—	0.03	Exit	272,559	136,279
				12	G6	—	0.02	—	0.025	Exit	276,501	138,250
				13	C2	—	0.01	—	0.04	Exit	276,501	138,250
				14	J10	—	—	—	0.03	Exit	277,501	138,750
				15	E5	—	0.01	—	0.04	Exit	278,000	139,000
				16	H6	—	0.01	—	0.03	Exit	278,000	139,000
				17	D6	—	0.02	—	0.03	Exit	281,384	140,692
				18	K7	—	0.03	—	0.04	Exit	281,384	140,692

TABLE 30. – CONTINUED

Specimen no.	Heat	Test environment	Test load	Crack initiation sequence	Hole no.	Crack location and size (in.)				Estimated crack origin face	Total load points to crack detection	Total equivalent load cycles to crack detection
						Tool entry face		Tool exit face				
						Left	Right	Left	Right			
A3	B	Air	B-1	1	F8	0.04	–	0.01	–	Entry	207,579	103,789
				2	I5	0.01	–	0.03	–	Exit	215,797	107,898
				3	G8	0.01	–	0.03	0.01	Exit	221,470	110,735
				4	F1	–	0.02	–	–	Entry	222,367	111,183
				5	A10	0.02	–	0.03	–	Exit	226,100	113,050
				6	G1	0.02	0.04	–	0.04	Entry	231,900	115,950
				7	G7	–	–	0.02	–	Exit	241,600	120,800
				8	E8	–	–	–	0.04	Exit	241,600	120,800
				9	K8	–	0.03	–	0.03	Exit	245,273	122,636
				10	C9	0.02	–	0.07	–	Exit	260,504	130,252
				11	E4	–	–	0.02	0.08	Exit	260,504	130,252
				12	I7	–	0.04	–	–	Entry	265,884	132,942
				13	I4	0.03	–	–	–	Entry	265,884	132,942
				14	K2	–	0.04	–	–	Entry	268,500	134,250
				15	G3	–	0.04	–	–	Exit	281,900	140,950
				16	J6	–	–	0.03	–	Exit	281,900	140,950
				17	J4	–	0.02	–	–	Entry	285,916	142,958
				18	E7	–	0.03	–	–	Entry	287,086	143,543
				19	C7	–	0.03	–	–	Exit	288,298	144,149
				20	A1	0.02	–	0.03	–	Entry	296,539	148,269
				21	I10	–	–	0.02	–	Exit	307,159	153,579
				22	J1	0.03	–	0.04	0.03	Exit	308,000	154,000
				23	D10	0.04	–	–	–	Entry	311,002	155,501
				24	K5	0.05	0.02	–	–	Entry	311,002	155,501
				25	G4	0.02	–	0.02	0.02	Exit	311,999	155,999
				26	J7	0.02	–	0.03	–	Exit	311,999	155,999
				27	I2	–	–	0.03	0.03	Exit	313,000	156,500
				28	H10	0.04	–	–	–	Entry	316,670	158,335
				29	E6	–	0.05	–	–	Entry	316,670	158,335
				30	G2	–	0.04	–	–	Entry	327,819	163,909
				31	E10	0.04	–	0.02	0.03	Entry	336,530	168,265
				32	H4	–	0.05	0.02	–	Entry	336,530	168,265
				33	E1	0.02	0.04	–	–	Entry	339,829	169,914
				34	F2	0.04	0.01	–	–	Entry	339,829	169,914
				35	J3	0.05	–	–	–	Entry	339,829	i69,914
				36	E9	–	0.03	0.04	–	Exit	339,829	169,914
				37	G10	0.02	0.04	0.02	–	Entry	339,829	169,914
				38	F9	–	–	0.04	–	Exit	342,001	171,000

TABLE 30. - CONTINUED

Specimen no.	Heat	Test environment	Test load	Crack initiation sequence	Hole no.	Crack location and size (in.)				Estimated crack origin face	Total load points to crack detection	Total equivalent load cycles to crack detection
						Tool entry face		Tool exit face				
						Left	Right	Left	Right			
A3 (concluded)	B	Air	B-1	39	I6	–	0.03	–	–	Entry	342,001	171,000
				40	F10	0.02	–	–	–	Entry	342,001	171,000
				41	A5	0.03	–	–	–	Entry	342,999	171,499
				42	K3	0.03	–	–	–	Entry	342,999	171,499
				43	K4	–	–	–	0.04	Exit	342,999	171,499
				44	I3	0.04	–	–	–	Entry	345,401	172,700
				45	J9	–	0.03	0.02	–	Entry	345,401	172,700
				46	K7	0.04	–	0.01	–	Entry	350,004	175,002
				47	K6	–	–	0.02	0.01	Exit	350,004	175,002
				48	I9	0.03	–	0.01	–	Entry	352,230	175,115
				49	H8	0.02	0.03	–	–	Entry	352,230	175,115
				50	D9	0.02	–	–	–	Entry	353,476	176,738
				51	B6	0.04	–	–	0.04	Exit	354,186	177,094
				52	D2	–	0.03	–	–	Entry	354,188	177,094
				53	K9	–	0.03	–	0.02	Entry	354,188	177,094
				54	H3	0.05	0.04	–	–	Entry	355,981	177,990
				55	C6	0.02	0.04	0.04	–	Entry	363,717	181,858
				56	H2	–	0.03	0.01	0.02	Exit	363,717	181,858
				57	I1	0.04	–	0.04	–	Entry	367,032	183,516
				58	F5	–	–	–	0.02	Exit	367,032	183,516
				59	B7	0.05	0.02	0.02	–	Entry	370,432	185,216
				60	H5	0.05	–	0.04	–	Entry	370,432	185,216
				61	K10	–	–	0.02	–	Exit	370,432	185,216
A4	C	Air	B-1	1	K10	–	0.03	–	–	Entry	160,738	80,369
				2	C10	–	0.03	–	0.05	Entry	160,802	80,401
				3	B3	–	–	–	0.05	Exit	206,956	103,478
				4	I1	–	–	0.04	–	Exit	209,612	104,806
				5	J1	–	0.03	–	0.03	Entry	263,040	131,520
				6	E6	–	–	–	0.03	Exit	273,142	136,571
				7	K1	–	–	–	0.04	Exit	279,239	139,619
				8	A5	0.04	–	0.02	–	Entry	285,103	142,551
				9	E1	–	0.08	–	0.06	Entry	293,248	146,624
				10	B5	0.03	–	0.02	0.02	Entry	293,248	146,624
				11	G1	–	0.04	0.04	–	Entry	293,508	146,754
				12	K3	–	0.03	–	–	Exit	293,508	146,754
				13	H1	–	0.04	0.04	–	Exit	307,056	153,528
				14	D10	0.04	–	0.02	0.02	Entry	318,133	159,066

152

TABLE 30.– CONTINUED

Specimen no.	Heat	Test environment	Test load	Crack initiation sequence	Hole no.	Tool entry face Left	Tool entry face Right	Tool exit face Left	Tool exit face Right	Estimated crack origin face	Total load points to crack detection	Total equivalent load cycles to crack detection
A4 (Concluded)	C	Air	B-1	15	A6	–	0.03	–	0.01	Entry	321,598	160,799
				16	I2	0.04	–	–	–	Entry	321,598	160,799
				17	A7	–	0.01	–	0.05	Exit	321,598	160,799
A5	B	Air	A-1	1	A7	–	–	0.030	–	Exit	260,690	130,345
				2	B3	–	–	0.030	–	Exit	260,690	130,345
				3	F5	–	–	0.020	–	Exit	261,038	130,519
				4	G6	–	–	0.050	–	Exit	298,800	149,400
				5	A1	–	–	0.040	–	Exit	298,800	149,400
				6	H5	0,040	–	0.030	–	Entry	298,800	149,400
				7	F3	–	–	0.025	–	Exit	299,512	149,756
				8	J6	–	–	0.030	–	Exit	299,512	149,756
				9	B8	–	0.030	–	0.020	Entry	299,512	149,756
				10	I7	–	0.015	–	–	Exit	317,043	158,522
				11	C8	0.030	–	0.030	–	Exit	321,641	160,820
				12	K10	–	–	0.040	–	Exit	332,018	166,009
				13	D5	0.10	–	0.030	–	Exit	332,018	166,009
				14	E2	–	–	0.040	–	Exit	332,226	166,113
				15	I4	–	–	0.040	–	Exit	332,226	166,113
				16	H3	–	–	–	0.040	Exit	337,850	168,925
				17	I3	–	–	–	0.040	Exit	337,850	168,925
				18	K3	0.010	–	0.030	–	Exit	337,850	168,925
				19	J7	–	–	0.050	–	Exit	342,703	171,352
				20	B9	–	–	–	0.030	Exit	342,703	171,352
				21	K6	–	–	0.040	–	Exit	342,703	171,352
A6	A	Air	B-1	1	G8	0.050	–	–	0.050	Exit	150,000	75,000
				2	G6	–	0.050	–	–	Entry	172,000	86,000
				3	K6	–	–	0.030	–	Entry	172,000	86,000
				4	C4	0.030	0.030	0.030	–	Exit	178,246	89,123
				5	H4	0.050	–	0.025	–	Exit	178,246	89,123
				6	D8	0.025	–	–	–	Entry	186,506	93,253
				7	K3	–	0.030	0.030	–	Entry	186,506	93,253
				8	E7	–	–	–	0.035	Exit	186,506	93,253
				9	I5	–	0.030	0.030	–	Exit	186,506	93,253
				10	A2	0.040	–	–	0.040	Entry	207,525	103,762
				11	B9	–	0.030	–	0.010	Exit	207,525	103,762
				12	D2	0.030	–	–	0.040	Entry	207,525	103,762
				13	D4	–	0.040	–	0.040	Exit	207,525	103,762

TABLE 30.–CONTINUED

Specimen no.	Heat	Test environment	Test load	Crack initiation sequence	Hole no.	Crack location and size (in.)				Estimated crack origin face	Total load points to crack detection	Total equivalent load cycles to crack detection
						Tool entry face		Tool exit face				
						Left	Right	Left	Right			
A6 (continued)	A	Air	B-1	14	E8	0.025	–	–	0.020	Entry	207,525	103,762
				15	G1	0.030	0.030	–	0.020	Entry	207,525	103,762
				16	G4	0.030	–	0.020	0.030	Entry	207,525	103,762
				17	H1	–	0.025	0.050	0.020	Exit	207,525	103,762
				18	I1	–	0.040	0.010	–	Entry	207,525	103,762
				19	I2	0.040	–	0.060	0.030	Entry	207,525	103,762
				20	J3	0.050	0.030	–	0.025	Entry	207,525	103,762
				21	K4	0.050	–	–	0.030	Entry	207,525	103,762
				22	K9	0.030	0.020	–	0.030	Exit	207,525	103,762
				23	K10	0.040	–	0.070	–	Exit	207,525	103,762
				24	B6	0.020	0.030	0.020	0.030	Exit	207,525	103,762
				25	C9	0.020	–	–	0.030	Exit	207,525	103,762
				26	F10	–	0.010	–	0.030	Exit	207,525	103,762
				27	J4	0.010	–	–	.030	Exit	207,525	103,762
				28	J5	0.010	–	0.060	0.030	Exit	207,525	103,762
				29	K5	–	0.060	–	0.060	Exit	207,525	103,762
				30	A7	–	–	–	0.030	Exit	209,000	104,500
				31	D7	0.030	0.010	0.040	–	Exit	209,000	104,500
				32	E2	0.030	–	0.040	–	Exit	209,000	104,500
				33	F2	0.040	–	0.020	0.040	Exit	209,000	104,500
				34	C6	0.030	–	–	0.030	Exit	209,000	104,500
				35	I9	0.020	–	–	–	Exit	209,000	104,500
				36	A6	–	0.040	–	–	Exit	212,000	106,000
				37	B4	–	0.040	0.010	–	Entry	212,000	106,000
				38	C7	–	–	–	–	Exit	212,000	106,000
				39	E9	–	0.020	0.010	–	Exit	212,000	106,000
				40	G7	0.020	–	0.040	–	Exit	212,000	106,000
				41	D9	–	–	–	–	Exit	216,000	108,000
				42	J9	0.030	0.030	0.040	–	Exit	216,000	108,000
				43	A3	–	0.050	–	–	Entry	218,000	109,000
				44	A4	–	0.020	–	0.060	Exit	219,000	109,000
				45	B7	–	–	0.010	0.030	Entry	219,000	109,000
				46	E5	0.030	–	0.020	–	Exit	219,000	109,000
				47	F8	0.030	–	0.020	–	Entry	221,000	110,500
				48	J10	–	0.060	–	0.060	Entry	221,000	110,500
				49	A8	–	0.040	–	0.030	Exit	221,000	110,500
				50	C8	–	–	–	–	Exit	221,000	110,500
				51	F7	0.030	–	–	0.040	Entry	222,276	111,138
				52	H8	0.030	–	0.010	0.039	Entry	222,276	111,138

154

TABLE 30.—CONTINUED

Specimen no.	Heat	Test environment	Test load	Crack initiation sequence	Hole no.	Tool entry face Left	Tool entry face Right	Tool exit face Left	Tool exit face Right	Estimated crack origin face	Total load points to crack detection	Total equivalent load cycles to crack detection
A6 (concluded)	A	Air	B-1	53	F4	0.030	0.030	0.010	0.020	Entry	222,276	111,138
				54	K1	–	0.030	0.020	0.030	Exit	222,276	111,138
				55	H5	0.040	0.020	0.020	–	Entry	226,334	113,167
				56	F3	–	0.050	0.020	0.070	Exit	226,334	113,167
A7	A	Air	A-2	1	K5	0.010	–	0.040	–	Exit	228,077	110,956
				2	F3	–	0.035	–	–	Entry	246,602	119,969
				3	I6	0.035	–	0.030	–	Exit	246,602	119,969
				4	I8	–	–	0.010	0.020	Entry	266,082	129,445
				5	E1	–	–	–	0.030	Exit	275,424	133,990
				6	F2	–	–	0.030	–	Exit	275,424	133,990
				7	A9	–	0.040	–	–	Entry	276,500	134,514
				8	G2	0.040	–	–	–	Entry	277,000	134,757
				9	D8	–	–	–	0.030	Entry	282,000	137,189
				10	H2	–	–	0.030	–	Exit	284,000	138,162
				11	J10	0.060	–	0.030	–	Entry	284,000	138,162
				12	B3	0.040	–	–	–	Entry	289,000	140,595
				13	G7	–	–	–	0.030	Exit	291,000	141,568
				14	J5	0.030	–	0.040	–	Exit	291,000	141,568
				15	J6	0.030	–	0.030	0.020	Exit	294,000	143,027
				16	D1	–	–	–	0.030	Exit	295,000	143,514
				17	I10	0.030	0.010	0.010	–	Entry	298,000	144,973
				18	D7	0.040	–	0.010	0.010	Entry	299,000	145,459
				19	B1	–	0.020	–	–	Entry	300,000	145,946
				20	B6	–	–	–	0.020	Entry	300,000	145,946
				21	C1	–	0.030	–	0.030	Exit	300,000	145,946
A8	A	Air	B-1	1	K6	–	–	–	0.020	Exit	183,000	91,600
				2	C4	0.040	0.050	–	–	Entry	201,567	100,784
				3	K10	0.040	–	0.050	–	Entry	211,094	105,547
				4	B2	–	–	–	–	Entry	211,094	105,547
				5	E9	–	–	–	0.030	Exit	216,663	108,332
				6	G9	–	–	0.040	–	Exit	216,663	108,332
				7	D7	–	–	–	0.040	Exit	229,382	114,691
				8	F10	–	–	–	0.030	Exit	229,382	114,691
				9	B4	0.025	0.035	–	–	Entry	240,712	120,356
				10	C3	0.025	0.030	–	0.035	Entry	240,712	120,356
				11	D5	–	0.040	–	–	Entry	240,712	120,356
				12	F5	–	–	–	–	Entry	240,712	120,356

155

TABLE 30.– CONTINUED

Specimen no.	Heat	Test environment	Test load	Crack initiation sequence	Hole no.	Crack location and size (in.)				Estimated crack origin face	Total load points to crack detection	Total equivalent load cycles to crack detection
						Tool entry face		Tool exit face				
						Left	Right	Left	Right			
A8 (Concluded)	A	Air	B-1	13	C1	–	–	0.040	–	Exit	241,000	120,500
				14	B6	–	0.050	0.010	–	Entry	241,000	120,500
				15	K7	–	–	0.060	–	Exit	244,000	122,000
				16	A1	–	–	0.030	–	Exit	245,000	122,500
				17	E2	–	0.040	–	0.010	Entry	245,000	122,500
				18	B10	–	0.030	–	–	Exit	246,000	123,000
				19	A2	–	0.020	0.050	–	Exit	249,000	124,500
				20	I4	–	0.030	–	–	Entry	249,000	124,500
A9	A	Air	B-2	1	D2	–	–	0.025	0.035	Exit	136,149	66,235
				2	K5	–	–	–	0.025	Exit	137,654	66,967
				3	J8	–	0.020	0.020	0.020	Exit	141,229	68,706
				4	D3	–	0.030	–	0.010	Entry	146,691	71,363
				5	C3	0.030	0.030	0.020	–	Entry	146,863	71,449
				6	J6	0.030	0.020	0.020	–	Entry	152,789	74,330
				7	G3	0.010	0.020	0.040	–	Exit	152,789	74,330
				8	F3	–	–	0.030	–	Exit	155,000	75,405
				9	H2	–	–	0.030	–	Exit	155,000	76,865
				10	I7	–	–	0.040	–	Exit	158,000	76,865
				11	B2	–	0.030	0.040	0.030	Exit	161,000	78,324
				12	A1	0.040	–	–	–	Entry	162,003	78,811
				13	B10	0.040	–	–	–	Entry	165,000	80,270
				14	A3	–	0.030	0.030	0.020	Entry	168,000	81,730
				15	C1	–	0.030	–	–	Exit	169,000	82,216
				16	A8	–	0.030	–	–	Entry	170,000	82,703
				17	D9	0.030	–	0.030	–	Exit	171,000	83,189
				18	K10	–	–	0.040	–	Exit	172,000	83,676
				19	A10	–	0.040	–	0.010	Entry	176,301	85,768
				20	G2	–	0.020	–	–	Entry	176,301	85,768
				21	H6	–	0.020	–	–	Exit	176,301	85,763
				22	H7	0.030	0.020	0.030	0.020	Exit	176,301	85,768
				23	G1	–	–	0.040	0.040	Exit	176,301	85,768
				24	K1	–	–	0.040	–	Exit	176,301	85,768
A10	A	Air	A-3	1	A3	–	0.040	–	–	Entry	354,000	177,000
				2	D1	–	0.030	–	–	Entry	366,000	183,000
				3	A10	0.040	–	–	–	Entry	366,000	183,000
				4	H9	–	0.030	–	–	Entry	387,000	193,500
				5	A8	0.030	–	–	–	Entry	393,000	196,500

TABLE 30. CONTINUED

Specimen no.	Heat	Test environment	Test load	Crack initiation sequence	Hole no.	Crack location and size (in.) Tool entry face Left	Tool entry face Right	Tool exit face Left	Tool exit face Right	Estimated crack origin face	Total load points to crack detection	Total equivalent load cycles to crack detection
A10 (Continued)	A	Air	A-3	6	H7	—	0.030	—	—	Entry	393,000	196,500
				7	E1	—	—	0.030	0.020	Exit	399,000	199,500
				8	J9	—	0.030	—	—	Entry	403,939	201,970
				9	A6	0.020	0.030	0.020	0.020	Entry	413,892	206,946
				10	F5	—	0.020	—	0.030	Exit	413,892	206,946
				11	A2	0.020	—	0.030	0.040	Exit	415,632	207,866
				12	E4	0.030	0.010	0.040	—	Exit	417,962	208,981
				13	J7	0.020	0.020	0.020	—	Entry	417,962	208,981
				14	E7	0.020	0.020	0.030	—	Exit	419,554	209,777
				15	J4	—	—	0.030	—	Exit	419,554	209,777
				16	C5	0.030	0.030	0.040	0.020	Entry	428,404	214,202
				17	F8	—	—	0.030	—	Exit	433,293	216,646
				18	G5	—	—	0.050	—	Exit	438,263	219,132
				19	J2	—	—	0.040	—	Exit	439,000	219,500
				20	E3	0.030	—	0.040	—	Exit	439,500	219,750
A11	A	Air	B-3	1	B3	—	—	—	0.040	Exit	268,000	134,000
				2	E2	—	—	—	0.040	Exit	269,000	134,500
				3	F9	0.030	—	0.030	0.020	Exit	282,000	141,000
				4	D2	0.030	—	—	0.040	Entry	283,000	141,500
				5	B9	—	0.040	—	—	Exit	297,000	148,500
				6	E1	0.020	—	0.040	—	Exit	303,653	151,826
				7	C3	—	—	—	0.030	Exit	315,402	152,701
				8	I9	—	—	—	0.030	Exit	315,402	157,701
				9	A7	—	0.030	—	0.040	Exit	319,267	159,634
				10	G2	—	0.030	—	0.040	Exit	319,267	159,634
				11	F1	0.060	0.040	—	0.050	Entry	323,623	161,812
				12	C4	0.030	—	—	0.020	Exit	323,623	161,812
				13	C10	0.030	—	—	0.020	Entry	326,216	163,108
				14	K3	0.030	—	0.020	0.040	Entry	327,259	163,630
				15	A4	—	—	—	—	Exit	331,670	165,835
				16	B7	0.030	0.030	—	—	Entry	331,670	165,835
				17	F3	0.020	0.020	—	0.030	Entry	331,670	165,835
				18	B10	—	0.030	—	—	Entry	336,344	168,172
				19	G7	—	0.040	—	—	Exit	336,344	168,172
				20	J9	—	—	0.030	—	Exit	336,344	168,172

157

TABLE 30.—CONCLUDED

Specimen no.	Heat	Test environment	Test load	Crack initiation sequence	Hole no.	Crack location and size (in.)				Estimated crack origin face	Total load points to crack detection	Total equivalent load cycles to crack detection
						Tool entry face		Tool exit face				
						Left	Right	Left	Right			
A12	C	Air	A-1	1	K1	–	–	0.025	–	Exit	310,035	150,018
				2	A1	–	–	–	0.025	Exit	319,359	109,580
				3	E9	–	–	0.020	0.030	Exit	354,198	177,099
				4	A9	–	–	–	0.030	Exit	360,277	180,138
				5	B4	0.030	–	0.005	0.010	Exit	364,672	182,336
				6	K7	–	–	0.010	0.010	Entry	366,412	183,206
				7	J3	–	–	0.040	–	Exit	377,732	188,866
				8	G2	0.040	–	0.040	0.010	Exit	386,269	193,134
				9	F2	0.010	–	–	–	Entry	397,347	198,674
				10	H6	–	–	0.030	–	Exit	412,268	206,134
				11	A8	–	–	0.025	–	Exit	416,295	208,148
				12	B2	0.015	0.010	–	0.030	Exit	416,295	208,148
				13	A7	–	–	0.025	0.030	Exit	421,643	210,822
				14	K2	–	–	0.030	–	Exit	426,010	213,005
				15	A3	–	–	0.030	–	Exit	434,478	217,239
				16	J9	–	0.020	0.030	–	Exit	436,450	218,225
				17	H9	0.010	–	–	0.015	Entry	442,857	221,428
				18	E2	–	–	0.035	–	Exit	444,352	222,176
				19	G3	–	–	–	0.030	Exit	445,285	222,642
				20	B8	–	–	–	0.025	Exit	452,939	226,470

158

TABLE 31. - SUMMARY OF MULTIHOLE TEST SPECIMEN PANEL ONE RESULTS
(FROM REF. 3, TABLE 5: CONSTANT AMPLITUDE AT 12.5 + 11.5 KSI).

Failure	Hole location		Life to crack		Crack location		Remarks
	Row	Column	Crack length (in.)	Cycles	Drill entry or exit side	Hole side	
—	2	15	0.02	18,768	Entry	Right	Hole with fabrication gouge
1	15	4	0.02	19,504	Exit	Left	
—	3	14	0.06	20,500	Entry	Right	Hole with fabrication gouge
2	10	11	0.02	20,576	Exit	Left	
3	14	1	0.02	20,604	Exit	Left	
4	4	2	0.02	22,548	Exit	Left	
5	11	15	0.02	23,624	Exit	Right	
6	1	8	0.02	24,060	Entry	Right	
7	8	14	0.02	24,390	Exit	Right	
8	7	11	0.02	24,690	Exit	Right	
9	9	5	0.02	26,060	Exit	Left	
10	13	1	0.02	26,400	Entry	Left	Adjacent to hole 14-1
11	19	5	0.02	26,760	Exit	Right	
12	19	2	0.04	26,780	Exit	Left	
13	3	1	0.03	26,901	Entry	Left	Adjacent to hole 4-2
14	9	15	0.02	26,901	Entry	Right	Adjacent to hole 8-14
—	1	8	0.06	26,901			Reworked hole at 24,060
15	20	1	0.02	27,205	Exit	Right	Adjacent to hole 19-2
16	13	12	0.05	27,385	Exit	Left	
17	3	5	0.02	27,750	entry	Left	
18	7	12	0.02	27,815	Exit	Right	Adjacent to hole 7-11
19	19	4	0.02	28,636	Exit	Left	Adjacent to hole 19-5
20	13	9	0.02	28,788	Exit	Right	

TABLE 32.—SUMMARY OF MULTIHOLE TEST SPECIMEN PANEL TWO RESULTS (FROM REF. 3, TABLE 6: CONSTANT AMPLITUDE AT 12.5 + 11.5 KSI)

Failure	Hole location		Life to crack		Crack location		Remarks
	Row	Column	Crack length (in.)	Cycles	Drill entry or exit side	Hole side	
1	8	3	0.02	28,615	Entry	Right	
2	15	6	0.02	29,498	Entry	Right	
3	12	6	0.03	34,850	Entry	Right	
4	4	1	0.02	35,688	Exit	Left	
5	10	1	0.02	36,160	Exit	Left	
6	9	1	0.02	36,228	Entry	Right	Adjacent to hole 10-1
7	10	3	0.02	36,320	Entry	Right	
8	1	13	0.02	36,480	Entry	Left	
9	9	6	0.02	36,555	Exit	Right	
10	11	1	0.02	36,572	Entry	Left	Adjacent to hole 10-1
11	15	12	0.02	36,597	Entry	Right	
12	10	14	0.02	37,035	Entry	Left	
13	14	8	0.02	37,246	Entry	Right	
14	14	5	0.02	37,930	Exit	Left	Adjacent to hole 15-6
15	3	1	0.02	37,972	Entry	Left	Adjacent to hole 4-1
16	6	2	0.02	38,394	Exit	Right	
17	7	14	0.02	38,900	Entry	Right	
18	3	11	0.02	39,295	Entry	Left	
19	13	7	0.02	39,368	Entry	Left	Adjacent to hole 12-6
20	6	12	0.02	39,410	Entry	Right	
21	9	14	0.02	39,480	Entry	Right	Adjacent to hole 10-14
22	5	11	0.02	39,518	Exit	Left	Adjacent to hole 6-12
23	17	3	0.02	39,610	Exit	Left	
24	15	15	0.02	39,626	Entry	Right	
25	6	15	0.02	39,658	Entry	Right	Adjacent to hole 7-14
26	13	4	0.02	39,996	Entry	Right	Adjacent to hole 14-5
27	17	1	0.02	40,152	Exit	Left	
28	11	9	0.02	40,212	Exit	Left	
29	13	1	0.02	40,333	Entry	Right	
30	8	2	0.02	40,423	Entry	Left	Adjacent to hole 8-3

TABLE 33. SUMMARY OF SINGLE HOLE TEST SPECIMEN RESULTS (FROM REF. 3, TABLE 4: CONSTANT AMPLITUDE AT 12.5 + 11.5 KSI)

Test	Hole location		Life to crack		Crack location		Life to failure (cycles
	Row	Column	Crack length (in.)	Cycles	Drill entry or exit side	Hole side	
1	3	2	0.02	50,000	Exit	Left	71,000
2	13	8	0.02	43,000	Exit	Left	67,000
3	13	10	0.02	56,000	Entry	Left	74,000
4	8	3	0.02	50,000	Entry	Right	73,000
5	8	7	0.02	59,000	Entry	Right	73,000
6	8	9	0.02	45,000	Exit	Right	61,000
7	8	11	0.02	54,000	Exit	Right	76,000
8	18	13	0.02	42,000	Exit	Left	64,000
9	3	6	0.02	39,000	Exit	Left	58,000
10	3	8	0.02	46,000	Exit	Left	61,000
11	18	5	0.02	48,000	Exit	Left	67,000
12	13	14	0.02	46,000	Exit	Right	59,000
13	13	6	0.02	51,000	Exit	Left	68,000
14	3	10	0.02	40,000	Exit	Right	54,000
15	3	4	0.02	61,000	Entry	Right	72,000
16	13	12	0.02	41,000	Entry	Right	61,000
17	18	11	0.02	54,000	Entry	Left	67,000
18	18	7	0.02	37,000	Exit	Right	57,000
19	18	9	0.02	37,000	Exit	Left	58,000
20	3	12	0.02	55,000	Exit	Left	68,000

TABLE 34. SUMMARY OF USAGE SIMULATION SPECIMEN (FIG. 2) TEST RESULTS

No.	Description	Heat	Test environment	Test load	Hole no.	Crack location and size (in.)[a] Tool entry face Left	Tool entry face Right	Tool exit face Left	Tool exit face Right	Total load points to crack detection	Total equivalent load cycles to crack detection
2A1	Fig. 2a. Open Hole	A	Air	A-1	4	:	-	:	-	182,016	91,008
					6	:	-	2	0.06	182,016	91,008
					10	:	-		0.025	182,016	91,008
2A2	Fig. 2a. Open Hole	A	Air	B-1	19	0.03	-	0.03	-	84,078	42,039
					3	-	-	-	-	87,282	43,641
2A3	Fig. 2a. Open Hole	A	95% RH	A-1	2	0.15	-	0.10	-	165,863	82,931
					7	0.22	-	0.17	-	165,863	82,931
					11	0.06	-	-	-	165,863	82,931
2A4	Fig. 2a. Open Hole	A	95% RH	B-1	11	0.10	0.13	0.11	0.17	99,000	49,500
					20	0.10	0.09	0.04	0.09	111,000	55,500
					1	-	-	0.05	0.03	115,551	57,775
					4	0.03	-	-	-		
					5	0.03	-	-	-		
					6	0.02	-	-	-	↓	↓
					8	0.13	-	0.15	-		
					13	-	0.07	-	-		
					14	-	-	0.06	0.06		
					15	0.02	-	0.08	0.08		
					17	0.02	-	-	0.06		
					18	0.08	-	0.05	-		
					19	0.10	-	0.05	-	115,551	57,775
2A5	Fig. 2a. Open Hole	B	Air	B-1	3	-	-	-	0.03	163,284	81,642
					1	-	0.04	-	-	166,744	83,372
2A6	Fig. 2a. Open Hole	C	Air	A-1	2	-	-	0.03	-	190,569	95,284
						-	-	0.02	-	196,619	98,309
2A7	Fig. 2b. Filled Hole	A	Air	B-1	19	-	-	0.04	-	1,351,520[b]	
					10	-	-	0.03	-	1,360,803[c]	
2A8	Fig. 2b. Filled Hole	B	Air	B-1	4	-	-	-	0.03	1,113,653[d]	556,826
2A9	Fig. 2c. Load Transfer Type 1	A	Air	A-1	2	-	0.12	-	0.08	1,192,821[e]	596,410
2A10	Fig. 2c. Load Transfer Type 1	B	Air	B-1	20	0.06	-	0.06	-	905,128[e]	452,564

162

TABLE 34. CONCLUDED

Specimen identification		Heat	Test environment	Test load	Hole no	Crack location and size (in.)[a]				Total load points to crack detection	Total equivalent load cycles to crack detection
No.	Description					Tool entry face		Tool exit face			
						Left	Right	Left	Right		
2A11	Fig 2c Load Transfer Type II	A	Air	A-1	12	-	-	-	0.06	851,191[e]	452,595
2A12	Fig 2d Load Transfer	B	Air	B-1	15	(3 4 failure; test stopped)		0.03		996,485[e] 998,529	483,242 449,714
2A13	Fig 2a Open Hole	A	Air	A-2	9 13	0.03	0.04 -	-	0.02 -	215,000 223,300	104,595 108,632
2A14	Fig 2a Open Hole	A	Air	A-3	13 14	0.03 0.04	-	-	-	199,000 304,962	99,500 152,481
2A15	Fig 2a Open Hole	A	Air	B-2	9 1	0.040 -	- 0.03	-	-	102,000 106,800	49,622 51,957
2A16	Fig 2a Open Hole	A	Air	B-3	15 5	- -	- 0.03	- 0.01	0.03 0.03	193,013 208,045	96,596 104,022
2A17	Fig 2d Load Transfer Type II	B	Air	A-1	20 20	0.03	0.03 (failure)	0.03	0.03	1,091,872 1,129,749	545,936 564,874
2A18	Fig 2d Load Transfer Type II	C	Air	A-1	7 5	0.05	0.05 (failure)	-	-	1,170,765 1,253,432	585,382 626,716
2A19	Fig 2c Load Transfer Type I	8	Air	A-1	-	(crack initiated at edge)				(1,245,734)	(622,867)
2A20	Fig 2c Load Transfer Type I	C	Air	A-1	17 17	-	- (failure)	0.06	-	1,147,000 1,183,831	573,500 591,916

[a]See figure 3 for definition of crack location and direction of propagation.

[b]Crack propagating upward at about 45 angle above net section at this stage. (Testing terminated at 1,432,289 load points; at disassembly cracks not detectable and believed in paint.)

[c]Crack propagating downward at about 30 angle below net section. (See parenthetical note of b above.)

[d]Crack propagating in section about 1/4 of fastener diameter above net section.

[e]Crack lengths on load transfer specimens are measured from edge of straps.

163

	Test specimen fatigue performance					Weibull distribution estimates parameters						Log normal distribution estimated parameters					
Panel no	Spectrum and heat	Failure origin face	No of fatigue cracked holes	Minimum initiation life	Maximum initiation life	Characteristic life (kc)	Shape parameter	Shape 2% lower bound	Shape 5% lower bound	Shape 95% upper bound	Shape 98% upper bound	Mean life (kc)	Shape parameter	Shape 2% lower bound	Shape 5% lower bound	Shape 95% upper bound	Shape 98% upper bound
A1	A1	Entry	7	130.02	151.71	186.39	12.956	20.276	18.274	5.935	4.908	196.45	0.0751	0.0474	0.0518	0.1438	0.1727
	(A)	Exit	9	129.91	151.71	183.59	12.668	19.050	17.378	6.682	5.76.	190.18	0.0720	0.0474	0.0517	0.1231	0.1428
		Total	16	129.91	151.71	176.02	12.396	17.145	15.994	8.075	7.322	177.84	0.0661	0.0482	0.0512	0.0950	0.1047
A2	A1	Entry	1	135.49													
	(A)	Exit	17	94.67	140.69	113.29	8.625	11.848	11.072	5.712	5.196	183.99	0.1124	0.0826	0.0877	0.1594	0.1748
		Total	18	94.67	140.69	170.81	8.966	12.215	11.436	6.030	5.501	180.56	0.1080	0.0800	0.0848	0.1513	0.1654
A3	B1	Entry	37	103.79	185.22	202.07	7.894	9.930	9.476	6.127	5.763	198.35	0.0974	0.0783	0.0818	0.1211	0.1282
	(B)	Exit	24	107.90	185.22	232.03	5.318	7.006	6.606	3.820	3.536	231.28	0.1477	0.1135	0.1195	0.1958	0.2108
		Total	61	103.79	185.22	191.51	6.641	7.992	7.691	5.507	5.252	181.43	0.1009	0.0850	0.0879	0.1190	0.1241
A4	B1	Entry	11	80.37	160.80	239.78	5.574	8.126	7.482	3.207	2.827	284.59	0.1932	0.1328	0.1428	0.3078	0.3493
	(C)	Exit	6	103.48	160.80	286.73	4.906	7.876	7.039	2.014	1.600	340.95	0.2065	0.1262	0.1388	0.4316	0.5325
		Total	17	80.37	160.80	225.26	5.319	7.306	6.828	3.522	3.204	246.16	0.1789	0.1315	0.1395	0.2536	0.2782
A5	A1	Entry	2	149.40	149.76												
	(B)	Exit	19	130.34	171.35	196.99	11.873	16.066	15.067	8.094	7.407	202.40	0.0763	0.0569	0.0602	0.1056	0.1151
		Total	21	130.34	171.35	196.68	11.292	15.101	14.213	7.877	7.245	200.24	0.0765	0.0578	0.0611	0.1039	0.1126
A6	B1	Entry	22	86.00	113.17	123.67	13.945	18.544	17.475	9.834	9.067	124.60	0.0601	0.0457	0.0482	0.0809	0.0874
	(A)	Exit	34	75.00	113.17	120.82	12.586	15.972	15.201	9.637	9.042	119.69	0.0603	0.0481	0.0503	0.0758	0.0805
		Total	56	75.00	113.17	115.92	13.150	15.940	15.309	10.797	10.274	113.20	0.0522	0.0436	0.0452	0.0620	0.0648
A7	A2	Entry	9	119.97	145.95	169.21	16.251	24.437	22.292	8.571	7.390	176.70	0.0608	0.0403	0.0437	0.1040	0.1206
	(A)	Exit	12	110.96	145.95	168.62	14.678	21.119	19.519	8.726	7.750	176.75	0.0681	0.0475	0.0509	0.1056	0.1189
		Total	21	110.96	145.95	161.66	15.230	20.374	19.169	10.624	9.772	164.52	0.0585	0.0442	0.0467	0.0794	0.0861
A8	B1	Entry	10	100.78	124.50	141.19	18.220	26.953	24.689	10.083	8.802	148.03	0.0572	0.0387	0.0417	0.0941	0.1078
	(A)	Exit	10	91.50	124.50	154.90	10.602	15.683	14.365	5.867	5.1216	164.19	0.0911	0.0616	0.0664	0.1498	0.1717
		Total	20	91.50	124.50	140.41	13.410	18.049	16.953	9.255	8.493	143.53	0.0671	0.0530	0.0532	0.0918	0.0997
A9	B2	Entry	10	71.36	85.77	100.79	14.082	20.831	19.081	7.792	6.803	105.14	0.0683	0.0462	0.0498	0.1123	0.1287
	A	Exit	14	66.24	86.55	103.59	10.391	14.514	13.535	6.475	5.819	107.22	0.0868	0.0620	0.0662	0.1290	0.1434
		Total	24	66.24	85.77	96.80	11.631	15.323	14.448	8.355	7.733	97.36	0.0706	0.0542	0.0571	0.0936	0.1008
A10	A3	Entry	10	177.00	216.65	282.80	9.181	13.581	1.244	5.080	4.435	293.72	0.0962	0.0650	0.0701	0.1582	0.1813
	(A)	Exit	10	199.50	219.75												
		Total	20	177.00	266.65	246.84	13.774	18.538	17.413	9.506	8.723	249.12	0.0615	0.0452	0.0478	0.0824	0.0896
A11	B3	Entry	7	141.50	157.70	187.28	24.525	38.380	34.590	11.234	9.290	196.99	0.0459	0.0290	0.0317	0.0880	0.1056
	(A)	Exit	13	134.00	168.17	199.76	11.919	16.954	15.703	7.285	6.513	206.83	0.0766	0.0541	0.0579	0.1161	0.1298
		Total	20	134.00	168.17	187.88	14.451	19.571	18.384	10.036	9.209	191.29	0.0608	0.0483	0.0534	0.0906	0.0906
A12	A1	Entry	3	183.21	221.43	339.63	8.627	15.460	15.459	1.449	0.938	349.55	0.1253	0.0634	0.0724	0.1996	0.2190
	(C)	Exit	17	155.02	226.47	294.62	6.740	9.259	8.652	4.464	4.060	315.72	0.1408	0.1035	0.1098	0.1996	0.2190
		Total	20	155.02	226.47	276.90	7.971	10.728	10.077	5.501	5.048	281.70	0.1045	0.0785	0.0830	0.1432	0.1556
Panel one	12 5	Entry	5	22.06	27.75	40.79	11.607	19.217	16.895	4.120	3.030	47.67	0.0953	0.0558	0.0619	0.2260	0.2910
	+11 5	Exit	15	19.50	28.79	44.15	6.912	9.653	8.976	4.419	3.991	50.40	0.1488	0.1074	0.1144	0.2172	0.2403
	ks(a)	Total	20	19.50	28.79	40.72	7.690	10.350	9.722	5.307	4.870	44.83	0.1287	0.0967	0.1022	0.1764	0.1917
Panel two	12 5	Entry	21	28.62	40.42	50.00	12.282	16.431	15.459	8.547	7.880	54.14	0.0860	0.0650	0.0686	0.1188	0.1266
	+11 5	Exit	9	35.69	40.21	48.62	18.667	28.067	25.605	9.845	8.488	51.98	0.0587	0.0397	0.0422	0.1005	0.1185
	ks(a)	Total	30	28.62	40.42	47.69	13.614	17.498	18.602	10.205	9.527	50.26	0.0734	0.0578	0.0606	0.0939	0.1001
Single hole	12 5	Entry	6	41.00	61.00	57.83	13.790	22.14	19.790	5.662	4.497	56.05	0.0541	0.0330	0.0363	0.1130	0.1394
	+11 5	Exit	14	37.00	55.00	53.25	6.013	8.469	7.871	3.785	3.354	49.13	0.0923	0.0588	0.0628	0.1223	0.1360
	ks(a)	Total	20	37.00	61.00	50.80	7.412	9.975	9.370	5.115	4.694	47.17	0.0665	0.0499	0.0528	0.0911	0.0990

(a) From same unidentified heat

TABLE 36.— SUMMARY OF STATISTICAL FATIGUE FAILURE CHARACTERISTICS OF ALUMINUM ALLOY 2024-T3 STRUCTURAL SIMULATION SPECIMENS AT 0.50 RELIABILITY LEVEL ON ESTIMATED LOG-MEAN OR CHARACTERISTIC CYCLIC LIFE

Structure simulation specimen test no with (spectrum) and (heat)	Distribution	Test cyclic life at selected number of failures (kc)					Cyclic life at selected number of failures for MLE and fixed shape parameters (kc)									
							MLE parameters					Fixed shape parameter (σ = 0.14, α = 4.00)				
		One failure	Two failures	Three failures	Four failures	Five failures	One failure	Two failures	Three failures	Four failures	Five failures	One failure	Two failures	Three failures	Four failures	Five failures
A1 (A1) (Ht A)	Test	129.91	130.02	130.89	133.28	133.43	–	–	–	–	–	–	–	–	–	–
	Log-normal						121.62	127.91	131.63	134.49	136.78	98.00	109.05	115.99	121.28	125.68
	Weibull						116.96	125.66	130.51	133.95	136.62	68.53	85.58	96.26	104.32	110.92
A2 (A1) (Ht A)	Test	94.67	95.13	101.18	103.58	108.86	–	–	–	–	–	–	–	–	–	–
	Log-normal						97.05	105.39	110.52	114.39	117.58	87.98	97.90	104.13	108.88	112.83
	Weibull						97.07	107.18	112.95	117.09	120.33	61.59	76.92	86.52	93.77	99.69
A3 (B1) (Ht B)	Test	103.79	107.90	110.34	111.18	113.05	–	–	–	–	–	–	–	–	–	–
	Log-normal						101.56	109.69	114.68	118.43	121.53	84.3	93.80	95.77	104.32	108.10
	Weibull						89.29	102.08	109.58	115.02	119.34	56.51	70.57	79.38	86.03	91.47
A4 (B1) (Ht C)	Test	172.70	172.70	175.00	175.00	175.12	–	–	–	–	–	–	–	–	–	–
	Log-normal						88.05	100.93	109.20	115.61	120.99	98.96	110.12	117.12	122.47	126.91
	Weibull						86.89	102.69	112.19	119.19	124.81	71.11	88.80	99.89	108.26	115.10
A5 (A1) (Ht B)	Test	130.34	130.34	130.52	149.40	149.40	–	–	–	–	–	–	–	–	–	–
	Log-normal						128.98	136.74	141.42	144.92	147.77	104.89	116.72	124.14	129.81	134.52
	Weibull						126.38	135.85	141.63	145.72	148.92	72.08	90.02	101.25	109.74	116.78
A6 (B1) (Ht A)	Test	75.00	86.00	86.00	89.12	89.12	–	–	–	–	–	–	–	–	–	–
	Log-normal						83.87	87.28	89.31	90.81	92.02	55.87	62.17	66.12	69.14	71.65
	Weibull						78.85	84.37	87.44	89.64	91.29	36.32	45.36	51.02	55.30	58.79
A7 (A2) (Ht A)	Test	110.96	119.97	119.97	129.44	133.99	–	–	–	–	–	–	–	–	–	–
	Log-normal						117.55	122.91	126.12	128.49	130.42	90.17	100.34	106.72	111.59	115.64
	Weibull						115.91	122.87	126.73	129.43	131.54	61.57	76.89	86.48	93.73	99.65
A8 (B1) (Ht A)	Test	91.50	100.78	105.55	105.55	108.33	–	–	–	–	–	–	–	–	–	–
	Log-normal						99.67	102.80	105.87	108.16	110.02	77.36	86.08	91.56	95.74	99.21
	Weibull						96.23	102.82	106.49	109.08	111.09	53.14	66.34	74.65	81.90	86.01

165

TABLE 36. CONCLUDED

Structure simulation specimen test no. with (spectrum) and (heat)	Distribution	Test cyclic life at selected number of failures (kc)					Cyclic life at selected number of failures for MLE and fixed shape parameters (kc)									
							MLE parameters					Fixed shape parameter (σ = 0.14; α = 4.00)				
		One failure	Two failures	Three failures	Four failures	Five failures	One failure	Two failures	Three failures	Four failures	Five failures	One failure	Two failures	Three failures	Four failures	Five failures
A9 (B2) (Ht A)	Test	66.24	66.97	68.71	71.36	71.45										
	Log normal						69.94	68.54	70.70	72.31	73.62	51.19	56.96	60.58	63.35	65.65
	Weibull						62.61	67.59	70.37	72.35	73.89	34.93	43.50	48.93	53.02	56.38
A10 (A3) (Ht A)	Test	177.00	183.00	183.00	193.50	196.50										
	Log normal						176.46	184.70	189.61	193.26	196.24	136.62	152.03	161.70	169.13	175.21
	Weibull						170.86	182.25	188.59	193.04	196.51	93.75	117.08	131.70	142.73	151.75
A11 (B3) (Ht A)	Test	134.00	134.50	141.00	146.50	148.50										
	Log normal						134.86	141.27	145.10	147.94	150.26	104.74	116.55	123.96	129.62	134.32
	Weibull						132.60	140.96	145.60	148.85	151.38	71.82	89.69	100.89	109.34	116.78
A12 (A1) (Ht C)	Test	155.02	159.68	177.10	180.14	182.34										
	Log normal						154.51	167.34	175.21	181.16	186.03	137.91	153.46	163.22	170.67	176.86
	Weibull						147.05	163.94	173.91	181.09	186.73	96.08	119.99	134.97	146.27	155.52
Panel one data[a] (300 details)	Test	19.50	20.58	20.60	22.55	23.62										
	Log normal						19.36	21.14	22.21	23.01	23.66	18.76	20.64	21.78	22.64	23.34
	Weibull						18.49	20.75	22.05	22.98	23.76	12.33	15.38	17.30	18.73	19.90
Panel two data[a] (300 details)	Test	28.62	29.50	34.85	35.69	36.16										
	Log normal						31.15	32.74	33.68	34.37	34.92	25.06	27.57	29.10	30.24	31.18
	Weibull						30.47	32.52	33.65	34.45	35.07	15.67	19.55	21.98	23.80	25.29
Single hole data[a] (20 details)	Test	37.00	37.00	39.00	40.00	41.00										
	Log normal						35.67	38.14	39.74	41.01	42.12	26.20	30.15	32.88	35.14	37.16
	Weibull						32.27	36.49	39.00	40.86	42.38	21.30	26.67	30.17	32.99	35.99
Single hole data[a] (300 details)	Test															
	Log normal						30.57	31.98	32.81	33.42	33.91	14.87	17.71	19.26	20.36	21.21
	Weibull						22.40	25.24	26.88	28.06	29.00	5.63	9.14	11.26	12.81	14.04

[a] Data from reference 3, constant amplitude testing at 12.5 ± 11.5 ksi at 200 cpm.

166

TABLE 37. SUMMARY OF STATISTICAL FATIGUE FAILURE CHARACTERISTICS OF ALUMINUM ALLOY 2024-T3 STRUCTURAL SIMULATION SPECIMENS AT 0.50 RELIABILITY LEVEL WITH 0.95 CONFIDENCE (BASED ON NUMBER OF FAILURES ONLY) ON ESTIMATED LOG-MEAN AND CHARACTERISTIC LIFE

Structure simulation specimen test no. with (spectrum) and (heat)	Distribution	Test cyclic life at selected number of failures (kc)					Cyclic life at selected number of failures for MLE and fixed shape parameters (kc)									
							MLE parameters					Fixed shape parameter (σ = 0.14, α = 4.00)				
		One failure	Two failures	Three failures	Four failures	Five failures	One failure	Two failures	Three failures	Four failures	Five failures	One failure	Two failures	Three failures	Four failures	Five failures
A1 (A-1) (Ht. A)	Test	129.10	130.02	130.89	133.28	133.43	–	–	–	–	–	–	–	–	–	–
	Log-normal	–	–	–	–	–	114.23	120.15	123.70	126.33	128.48	85.83	95.51	101.58	106.22	110.07
	Weibull	–	–	–	–	–	112.97	121.36	126.06	129.37	131.96	?1.53	76.84	86.43	93.67	99.59
A2 (A-1) (Ht. A)	Test	94.67	95.13	101.18	103.58	108.86	–	–	–	–	–	–	–	–	–	–
	Log-normal	–	–	–	–	–	88.12	95.69	100.36	103.88	106.77	77.64	86.40	91.89	96.09	99.67
	Weibull	–	–	–	–	–	92.73	102.39	107.91	111.85	114.95	55.59	69.42	78.09	84.83	89.98
A3 (B-1) (Ht. B)	Test	103.79	107.90	110.34	111.18	113.05	–	–	–	–	–	–	–	–	–	–
	Log-normal	–	–	–	–	–	96.71	104.46	109.20	112.78	115.71	78.76	87.65	93.22	97.48	101.01
	Weibull	–	–	–	–	–	86.13	98.46	105.89	110.94	115.11	53.22	66.46	74.76	81.02	86.15
A4 (B-1) (Ht. C)	Test	172.70	172.70	175.00	175.00	175.12	–	–	–	–	–	–	–	–	–	–
	Log-normal	–	–	–	–	–	74.70	85.64	92.65	98.09	102.65	87.02	96.83	102.98	107.69	111.59
	Weibull	–	–	–	–	–	80.29	94.89	103.67	110.13	115.33	64.02	79.95	89.93	97.46	103.63
A5 (A-1) (Ht. B)	Test	130.34	130.34	130.52	149.40	149.40	–	–	–	–	–	–	–	–	–	–
	Log-normal	–	–	–	–	–	121.07	128.36	132.75	136.04	138.71	93.43	103.97	110.58	115.63	119.82
	Weibull	–	–	–	–	–	121.36	131.30	136.89	140.85	143.94	85.48	81.77	91.98	99.89	105.99
A6 (B-1) (Ht. A)	Test	75.00	86.00	86.00	89.12	89.12	–	–	–	–	–	–	–	–	–	–
	Log-normal	–	–	–	–	–	81.69	85.01	85.80	88.44	89.62	52.05	57.92	61.60	64.41	66.75
	Weibull	–	–	–	–	–	77.37	82.78	86.98	87.92	89.58	34.13	42.62	47.94	51.96	55.24
A7 (A-2) (Ht. A)	Test	110.96	119.97	119.97	129.44	133.99	–	–	–	–	–	–	–	–	–	–
	Log-normal	–	–	–	–	–	112.00	117.11	120.77	122.53	124.26	80.32	89.37	95.05	99.40	103.00
	Weibull	–	–	–	–	–	113.02	119.81	123.57	126.21	128.26	55.93	69.84	78.56	85.14	90.53
A8 (B-1) (Ht. A)	Test	91.50	100.78	105.55	105.55	108.33	–	–	–	–	–	–	–	–	–	–
	Log-normal	–	–	–	–	–	92.29	97.13	100.04	102.20	103.95	68.71	76.46	81.32	85.63	88.11
	Weibull	–	–	–	–	–	93.45	99.86	103.42	105.90	107.89	48.18	60.16	67.67	73.34	77.96
A9 (B-2) (Ht. A)	Test	66.24	66.97	68.71	71.36	71.45	–	–	–	–	–	–	–	–	–	–
	Log-normal	–	–	–	–	–	61.49	64.89	66.94	68.47	69.70	45.94	51.12	54.31	56.86	58.91
	Weibull	–	–	–	–	–	60.69	65.51	68.21	70.12	71.62	31.81	39.72	44.68	48.42	51.49

167

TABLE 37. — CONCLUDED

Structure simulation specimen test no with (spectrum) and (heat)	Distribution	Test cyclic life at selected number of failures (kc)					Cyclic life at selected number of failures for MLE and fixed shape parameters (kc) MLE parameters					Fixed shape parameter (σ = 0 14, α = 4.00)				
		One failure	Two failures	Three failures	Four failures	Five failures	One failure	Two failures	Three failures	Four failures	Five failures	One failure	Two failures	Three failures	Four failures	Five failures
A10 (A-3) (Ht. A)	Test	177.00	183.00	183.00	193.50	196.50	-	-	-	-	-	-	-	-	-	-
	Log-normal	-	-	-	-	-	167.55	177.13	180.13	183.62	186.45	121.35	135.03	143.61	150.17	150.17
	Weibull	-	-	-	-	-	166.06	175.43	183.29	187.62	190.99	85.00	106.15	119.39	129.40	137.58
A11 (3-3) (Ht. A)	Test	134.C0	134.50	141.00	141.50	148.50	-	-	-	-	-	-	-	-	-	-
	Log-normal	-	-	-	-	-	128.09	134.18	137.82	140.52	142.71	93.02	103.52	110.10	115.13	119.30
	Weibull	-	-	-	-	-	129.07	137.21	141.72	144.89	147.36	65.11	81.31	91.46	99.12	105.39
A12 (A-1) (Ht. C)	Test	155.02	159.68	177.10	180.14	182.34	-	-	-	-	-	-	-	-	-	-
	Log-normal	-	-	-	-	-	141.42	153.16	160.37	165.81	170.27	122.49	136.31	144.97	151.59	157.09
	Weibull	-	-	-	-	-	139.60	156.07	165.56	172.38	177.76	87.10	108.78	122.36	132.61	140.99
Panel one data[a] (300 details)	Test	19.50	20.58	20.60	22.55	23.62	-	-	-	-	-	-	-	-	-	-
	Log-normal	-	-	-	-	-	17.36	18.95	19.62	20.64	21.22	16.66	18.30	19.35	20.10	20.73
	Weibull	-	-	-	-	-	17.57	19.72	20.95	21.84	22.54	11.78	13.95	15.68	16.98	18.04
Panel two data[a] (300 details)	Test	28.62	29.50	34.85	35.69	36.16	-	-	-	-	-	-	-	-	-	-
	Log-normal	-	-	-	-	-	29.81	31.12	32.01	32.67	34.31	22.75	25.02	26.41	27.45	28.30
	Weibull	-	-	-	-	-	29.60	31.81	32.92	33.70	31.19	14.43	18.01	20.24	21.92	23.29
Single hole data[d] (20 details)	Test	37.00	37.00	39.00	40.00	41.00	-	-	-	-	-	-	-	-	-	-
	Log-normal	-	-	-	-	-	33.72	36.05	37.56	38.77	39.81	23.27	26.78	29.21	31.21	33.01
	Weibull	-	-	-	-	-	30.61	34.61	36.99	38.75	40.19	19.26	24.18	27.35	29.82	31.90
Single hole data[a] (300 details)	Test	-	-	-	-	-	-	-	-	-	-	-	-	-	-	-
	Log-normal	-	-	-	-	-	28.90	30.23	31.02	31.59	32.05	16.81	18.49	19.52	20.29	20.91
	Weibull	-	-	-	-	-	21.24	23.94	25.50	26.61	27.50	9.79	12.21	13.73	14.87	15.80

[a] Data from reference 3, constant amplitude testing at 12.5 + 11.5 ksi at 200 cpm

168

TABLE 38 - SUMMARY OF STATISTICAL FATIGUE FAILURE CHARACTERISTICS OF ALUMINUM ALLOY 2024-T3 STRUCTURAL SIMULATION SPECIMENS AT 0.90 RELIABILITY LEVEL ON ESTIMATED LOG-MEAN OR CHARACTERISTIC CYCLIC LIFE

| Structure simulation specimen test no with (spectrum) and (heat) | Distribution | Test cyclic life at selected number of failures (kc) | | | | | Cyclic life at selected number of failures for MLE and fixed shape parameters (kc) | | | | | | | | | |
| | | One failure | Two failures | Three failures | Four failures | Five failures | MLE parameters | | | | | Fixed shape parameter (σ = 0.14; α = 4.00) | | | | |
							One failure	Two failures	Three failures	Four failures	Five failures	One failure	Two failures	Three failures	Four failures	Five failures
A1 (A-1) (Ht. A)	Test	129.91	130.02	130.89	133.28	133.43										
	Log-normal						110.87	119.94	124.84	128.27	130.98	98.00	109.05	115.99	121.28	125.68
	Weibull						100.47	114.53	121.51	126.14	129.62	68.53	85.58	96.26	104.32	110.92
A2 (A-1) (Ht. A)	Test	94.67	95.13	101.18	103.58	108.86										
	Log-normal						78.67	94.29	102.32	107.76	113.37	72.34	85.45	93.00	98.50	102.94
	Weibull						83.44	94.68	101.28	105.89	109.55	38.46	57.71	69.22	78.02	84.69
A3 (B-1) (Ht. B)	Test	103.79	107.90	110.34	111.18	113.05										
	Log-normal						88.19	99.44	105.70	110.18	113.80	69.57	81.87	89.10	94.38	98.62
	Weibull						67.24	85.96	95.88	102.82	108.18	35.28	52.95	63.60	71.43	77.70
A4 (B-1) (Ht. C)	Test	172.70	172.70	175.00	175.00	175.12										
	Log-normal						68.56	84.82	94.51	101.72	107.60	81.37	96.11	104.60	110.79	115.78
	Weibull						60.97	82.74	94.97	103.62	110.40	44.40	66.63	80.03	89.88	97.78
A5 (A-1) (Ht. B)	Test	130.34	130.34	130.52	149.40	149.40										
	Log-normal						115.89	126.94	132.95	137.20	140.54	96.25	101.87	110.87	117.44	122.72
	Weibull						106.27	122.71	130.94	136.43	140.57	45.01	67.54	81.13	91.11	99.12
A6 (B-1) (Ht. A)	Test	75.00	86.00	86.00	89.12	89.12										
	Log-normal						77.97	82.97	85.62	87.48	88.92	45.94	54.26	59.05	62.55	65.36
	Weibull						68.33	77.31	81.74	84.67	86.88	22.68	34.03	40.88	45.91	49.95
A7 (A-2) (Ht. A)	Test	110.96	119.97	119.97	129.44	133.99										
	Log-normal						108.32	116.12	120.30	123.23	125.51	74.14	84.61	95.31	100.95	105.49
	Weibull						102.42	113.94	119.56	123.26	126.02	38.44	57.69	69.29	77.82	84.66
A8 (B-1) (Ht. A)	Test	91.50	100.78	105.5	105.55	108.33										
	Log-normal						88.94	96.32	100.30	103.10	105.29	63.61	75.13	81.77	86.61	90.51
	Weibull						83.62	94.38	99.68	103.19	105.82	33.18	49.79	59.81	67.17	73.07

[a]Data from reference 3: constant amplitude testing a. 12.5 + 11.5 ksi at 200 cpm.

TABLE 38.— CONCLUDED

Structure simulation specimen test no. with (spectrum) and (heat)	Distribution	Test cyclic life at selected number of failures (kc)					Cyclic life at selected number of failures for MLE and fixed shape parameters (kc) — MLE parameters					Fixed shape parameter (σ = 0.14; α = 4.00)				
		One failure	Two failures	Three failures	Four failures	Five failures	One failure	Two failures	Three failures	Four failures	Five failures	One failure	Two failures	Three failures	Four failures	Five failures
A9 (B-2) (Ht. A)	Test	66.24	86.97	88.71	71.36	71.45	–	–	–	–	–	–	–	–	–	–
	Log-normal						58.84	83.99	86.78	68.75	70.29	42.09	49.72	54.11	57.31	59.89
	Weibull						53.25	81.23	85.21	67.87	89.86	21.75	32.64	39.20	44.02	47.89
A10 (A-3) (Ht. A)	Test	177.00	183.00	183.00	193.50	196.50	–	–	–	–	–	–	–	–	–	–
	Log-normal						182.31	174.27	180.69	185.18	188.69	112.33	132.89	144.41	152.96	159.84
	Weibull						149.02	167.87	178.83	182.89	187.?	58.54	87.85	105.52	118.50	128.92
A11 (B-3) (Ht. A)	Test	134.00	134.50	141.00	146.50	148.50	–	–	–	–	–	–	–	–	–	–
	Log-normal						123.87	133.15	138.15	141.64	144.38	86.12	101.72	110.71	117.26	122.54
	Weibull						116.49	130.27	136.99	141.42	147.01	44.84	87.30	80.83	90.78	98.78
A12 (A-1) (Ht. C)	Test	155.02	159.68	177.70	180.14	182.34	–	–	–	–	–	–	–	–	–	–
	Log-normal						133.50	151.17	161.04	168.10	173.72	113.39	133.94	145.77	154.40	181.35
	Weibull						115.72	141.93	155.61	164.93	172.05	59.99	90.03	103.14	121.44	132.12
Panel one data[a] (300 details)	Test	19.50	20.58	20.60	22.55	23.62	–	–	–	–	–	–	–	–	–	–
	Log-normal						16.42	18.89	20.26	21.23	21.99	15.68	18.27	19.71	20.74	21.55
	Weibull						14.47	17.87	19.85	20.86	21.79	7.70	11.55	13.86	15.55	18.91
Panel two data[a] (300 details)	Test	28.62	29.50	34.85	35.69	36.16	–	–	–	–	–	–	–	–	–	–
	Log-normal						28.36	30.71	31.96	32.82	33.49	20.95	24.40	26.33	27.70	28.79
	Weibull						26.53	29.89	31.53	32.62	33.43	9.78	14.67	17.61	19.78	21.48
Single hole data[a] (20 details)	Test	37.00	37.00	39.00	40.00	41.00	–	–	–	–	–	–	–	–	–	–
	Log-normal						31.88	35.11	37.00	38.42	39.81	20.87	25.34	28.29	30.63	32.85
	Weibull						25.03	31.25	34.60	36.95	38.80	19.13	24.01	27.04	29.41	31.44
Single hole data[a] (300 details)	Test	–	–	–	–	–	–	–	–	–	–	–	–	–	–	–
	Log-normal						28.07	30.18	31.29	32.06	32.65	15.82	18.43	19.88	20.92	21.74
	Weibull						17.37	21.62	23.85	25.38	28.56	8.74	10.11	12.13	13.61	14.90

[a] Data from reference 3: constant amplitude testing at 12.5 + 11.5 ksi at 200 cpm.

170

TABLE 39. *SUMMARY OF STATISTICAL FATIGUE FAILURE CHARACTERISTICS OF ALUMINUM ALLOY 2024-T3 STRUCTURAL SIMULATION SPECIMENS AT 0.95 RELIABILITY LEVEL ON ESTIMATED LOG-MEAN OR CHARACTERISTIC CYCLIC LIFE*

Structure simulation specimen test no with (spectrum) and (heat)	Distribution	Test cyclic life at selected number of failures (kc)					Cyclic life at selected number of failures for MLE and fixed shape parameters (kc) MLE parameters					Fixed shape parameter (σ = 0.14, α = 4.00)				
		One failure	Two failures	Three failures	Four failures	Five failures	One failure	Two failures	Three failures	Four failures	Five failures	One failure	Two failures	Three failures	Four failures	Five failures
A1 (A1) (Ht A)	Test	129.91	130.02	130.89	133.28	133.43										
	Log-normal						107.43	117.49	122.77	126.43	129.26	75.37	91.10	99.99	106.40	115.77
	Weibull						94.79	110.86	118.62	123.68	127.43	35.73	58.05	71.58	81.48	89.39
A2 (A1) (Ht A)	Test	94.67	95.13	101.18	103.58	108.86										
	Log-normal						79.25	91.73	98.36	103.40	107.22	67.67	81.79	89.77	95.52	100.12
	Weibull						72.60	90.14	98.97	104.86	109.29	32.12	52.18	64.34	73.23	80.34
A3 (B1) (Ht B)	Test	103.79	107.90	110.34	111.18	113.05										
	Log-normal						84.04	96.35	103.04	107.76	111.48	64.83	78.36	86.01	91.52	95.92
	Weibull						60.33	80.81	91.67	99.57	104.80	29.47	47.79	59.03	87.19	73.71
A4 (B1) (Ht C)	Test	172.70	172.70	175.00	175.00	175.12										
	Log-normal						62.95	80.21	90.34	97.80	103.86	76.11	91.99	100.97	107.44	112.61
	Weibull						53.25	76.70	89.78	98.97	106.11	37.08	60.24	74.28	84.25	92.76
A5 (A1) (Ht B)	Test	130.34	130.34	130.52	149.40	149.40										
	Log-normal						111.73	123.93	130.50	134.91	138.42	80.67	97.51	107.02	113.88	119.36
	Weibull						99.70	118.40	127.52	133.51	137.96	37.59	61.06	75.29	85.71	94.03
A6 (B1) (Ht A)	Test	75.00	86.00	86.00	89.12	89.12										
	Log-normal						76.05	81.62	84.50	86.33	88.01	42.97	51.94	56.96	66.66	63.57
	Weibull						64.68	74.97	79.91	83.11	85.49	18.94	30.77	37.94	43.19	47.38
A7 (A2) (Ht A)	Test	110.96	119.97	119.97	129.44	133.99										
	Log-normal						105.33	114.23	118.54	121.65	124.06	69.35	83.82	92.00	97.90	102.61
	Weibull						97.69	110.97	117.24	121.30	124.29	32.10	52.16	64.31	73.20	80.31
A8 (B1) (Ht A)	Test	91.50	100.78	105.55	105.55	108.33										
	Log-normal						86.15	94.32	98.62	101.59	103.90	59.50	71.91	78.93	83.99	88.03
	Weibull						79.24	91.58	97.49	101.33	104.17	27.71	45.02	55.51	63.18	36.75

171

TABLE 39. CONCLUDED

Structure simulation specimen test no with (spectrum) and (heat)	Distribution	Test cyclic life at selected number of failures (kc)					Cyclic life at selected number of failures for MLE and fixed shape parameters (kc)										
							MLE parameters					Fixed shape parameter (σ = 0.14, α = 4.00)				
		One failure	Two failures	Three failures	Four failures	Five failures	One failure	Two failures	Three failures	Four failures	Five failures	One failure	Two failures	Three failures	Four failures	Five failures
A9 (B 2) (Ht A)	Test	66.24	66.97	54.71	71.36	71.45										
	Log-normal						56.89	62.59	65.60	67.69	69.31	39.47	47.59	52.23	55.58	58.25
	Weibull						50.05	59.14	63.56	66.46	68.61	18.16	29.51	36.38	41.41	45.43
A10 (A-3) (Ht A)	Test	177.00	183.00	183.00	193.50	196.50										
	Log-normal						157.74	171.04	177.97	182.76	186.47	105.07	127.01	139.40	148.33	155.47
	Weibull						141.42	162.82	173.04	179.68	184.57	48.89	79.42	97.93	111.47	122.30
A11 (B 3) (Ht A)	Test	134.00	134.50	141.00	146.50	148.50										
	Log-normal						120.32	130.64	136.04	139.76	142.65	80.55	97.36	106.86	113.71	119.18
	Weibull						110.86	126.69	134.20	139.07	142.66	37.45	60.84	75.02	85.31	93.69
A12 (A 1) (Ht C)	Test	155.02	159.68	177.10	180.14	182.34										
	Log-normal						127.01	146.30	156.84	164.29	170.15	106.06	128.02	140.71	149.73	156.93
	Weibull						105.77	134.90	149.89	159.95	167.56	50.10	81.39	100.36	114.24	125.33
Panel one data[a] (300 details)	Test	19.50	20.58	20.30	22.55	25.62										
	Log-normal						15.51	18.21	19.68	20.70	21.50	14.74	17.55	19.09	20.18	21.03
	Weibull						13.18	16.89	18.90	20.21	21.20	6.43	10.44	12.36	14.63	16.04
Panel two data[a] (300 details)	Test	28.62	29.50	34.85	35.69	36.16										
	Log-normal						27.45	30.08	31.43	32.35	33.07	19.69	23.45	25.50	26.95	28.09
	Weibull						25.16	29.01	30.85	32.04	32.92	8.17	13.26	16.34	18.59	20.38
Single hole data[a] (20 details)	Test	37.00	37.30	39.00	40.00	41.00										
	Log-normal						30.73	34.22	36.21	37.69	38.90	19.13	24.01	27.04	29.41	31.44
	Weibull						22.71	29.59	33.24	35.75	37.71	11.08	18.09	22.43	25.68	28.35
Single hole data[a] (300 details)	Test															
	Log-normal						27.26	29.62	30.82	31.64	32.27	14.87	17.71	19.26	20.36	21.21
	Weibull						15.76	20.46	22.91	24.56	25.81	5.63	9.14	11.26	12.81	14.04

[a] Data from reference 3, constant amplitude testing at 12.5 ± 11.5 ks; at 200 cpm

172

REFERENCES

1. Whittaker, I. C., and Besumer, P. M. *A Reliability Analysis Approach to Fatigue Life Variability of Aircraft Structures*, AFML-TR-69-65, Air Force Materials Laboratory, March 1969.

2. Whittaker, I. C., and Gerharz, J. J., *A Feasibility Study for Verification of Fatigue Reliability Analysis*, AFML-TR-70-157, Air Force Materials Laboratory, September 1970.

3. Weibull, W., *Fatigue Testing and Analysis of Results*, Pergamon Press, New York 1961.

LIST OF ABBREVIATIONS AND SYMBOLS

ABBREVIATIONS

exp   exponential function

kc   kilocycles

ln   natural logarithm

log   common logarithm

log-normal   normal cumulative distribution with variable taken as log of cyclic life to crack initiation:

$$F(X) = \frac{1}{\sqrt{2\pi}\,\sigma} \int_{-\infty}^{+X} \exp\left[-(X_i - \bar{X})^2/\sigma^2\right] dX$$

MLE   maximum likelihood estimate or estimator

RH   relative humidity

Weibull   Weibull cumulative distribution:

$$F(X) = 1 - \exp[-(X/\beta)^\alpha]$$

SYMBOLS

α shape parameter for two-parameter Weibull distribution

$\hat{\alpha}$ maximum likelihood estimate of two-parameter Weibull distribution shape parameter which is implicitly defined as follows:

$$\frac{\sum_{i=1}^{n_f} X_i^{\hat{\alpha}} \ln X_i + \sum_{i=1}^{n_g} G_i^{\hat{\alpha}} \ln G_i}{\sum_{i=1}^{n_f} X_i^{\hat{\alpha}} + \sum_{i=1}^{n_g} G_i^{\hat{\alpha}}} - \frac{1}{\hat{\alpha}} = \frac{1}{n_f}\sum_{i=1}^{n_f} \ln X_i$$

175   **Preceding page blank**

β scale parameter or characteristic life for two-parameter Weibull distribution

$\hat{\beta}$ maximum likelihood estimate of two-parameter Weibull distribution scale parameter or characteristic life; for a censored sample with known α this is

$$\hat{\beta} = \left[\frac{1}{n_f}\left(\sum_{i=1}^{n_f} X_i^\alpha + \sum_{i=1}^{n_g} G_i^\alpha\right)\right]^{1/\alpha}$$

$\check{\beta}$ maximum likelihood estimate of two-parameter Weibull scale parameter or characteristic life when it depends upon an estimate of the shape parameter; for a censored sample with an estimated shape parameter this is

$$\check{\beta} = \left[\frac{1}{n_f}\left(\sum_{i=1}^{n_f} X_i^{\hat{\alpha}} + \sum_{i=1}^{n_g} G_i^{\hat{\alpha}}\right)\right]^{1/\hat{\alpha}}$$

μ mean or log-mean cyclic life to crack initiation for log-normally distributed population

$\hat{\mu}$ maximum likelihood estimate of the mean cyclic life of a log-normally distributed variable; its estimate is

$$\bar{X}_L = \hat{\mu} - \frac{1}{n_f}\sum_{i=1}^{n_g} h_i$$

ξ_i standardized log-normal variate, $(G_i - \hat{\mu})/\hat{\sigma}$, for detail with testing terminated for reasons other than failure

σ log-normal distribution shape parameter; i.e., the standard deviation of a normally distributed population with the variable transposed to base 10 logarithms

$\hat{\sigma}$ maximum likelihood estimate of log-normal distribution shape parameter; for uncensored test groups the estimate is

$$\hat{\sigma} = \sum_{i=1}^{n}\left[\frac{\left(X_{L_i} - \bar{X}_L\right)^2}{n}\right]^{1/2}$$

176

for censored data, the estimate is determined from this relationship

$$s^2 = \hat{\sigma}^2 \left[1 - \frac{1}{n_f} \sum_{i=1}^{n_g} \xi_i h_i - \left(\frac{1}{n_f} \sum_{i=1}^{n_g} h_i \right)^2 \right]$$

$\hat{\sigma}$ unbiased maximum likelihood estimate of log-normal distribution shape parameter; for uncensored test groups the estimate is

$$\sigma = \sum_{i=1}^{n} \left[\frac{\left(X_{L_i} - \bar{X}_L \right)^2}{n-1} \right]^{1/2}$$

$\sum$ summation symbol

$\phi(t)$ $\frac{1}{\sqrt{2\pi}} \exp\left[-\frac{t^2}{2} \right]$, frequency distribution for log-normal distribution

$\Phi(t)$ $\int_{-\infty}^{\xi_i} \phi(t)dt$, cumulative distribution for log-normal distribution

G_i cyclic life (log) when test has been terminated for reasons other than failure

h_i $h(\xi_i) = \frac{\phi(\xi_i)}{1 - \Phi(\xi_i)}$, hazard function

n total number of details in sample or ordered detail in sample

N total number of details in sample or fleet

n_f number of failures in sample

n_g number of nonfailures in sample

s^2 $\displaystyle \sum_{i=1}^{n_f} \left(X_{L_i} - X_L \right)^2 / n_f = \hat{\sigma}^2 \left[1 - \frac{i}{n_f} \sum_{i=1}^{n_g} \xi_i h_i - \left(\frac{1}{n_f} \sum_{i=1}^{n_g} h_i \right)^2 \right]$

t	standard normal variate
X	continuous random time-to-failure variable usually referring to tests useful in estimating fatigue scatter
X_i	cyclic life to crack initiation of a detail
$\bar{X}$	average cyclic life or $\dfrac{1}{n}\displaystyle\sum_{i=1}^{n}(X_i)$
X_L	log X or log of cyclic life to crack initiation
$\bar{X}_L$	$\hat{\mu} - \dfrac{1}{n_f}\displaystyle\sum_{i=1}^{n_g}(h_i)$

178